

Starch-based Films Incorporated with Different Bioactive Compounds for Food Packaging Using
Pressurized Hot Water Technology

by

Yujia Zhao

A thesis submitted in partial fulfillment of the requirements for the degree of

Doctor of Philosophy
in
Bioresource and Food Engineering

Department of Agriculture, Food and Nutritional Science
University of Alberta

© Yujia Zhao, 2019

Abstract

In recent years, biodegradable polymers, like starch, have been studied as potential packaging materials to deal with the increasing concern on plastic disposal/degradation and to extend food products shelf-life. This objective of this thesis was to develop bioactive starch-based films using pressurized hot water technology, with the incorporation of various bioactive compounds (e.g. gallic acid, chitosan and carvacrol essential oil), to investigate the potential application of such films on ready-to-eat (RTE) ham. All films produced were characterized by mechanical, physico-chemical, structural, optical and functional properties. First, cassava starch and chitosan behaviors in pressurized hot water media were studied at 75-150 °C and 50-155 bar to understand depolymerization and interactions between them. Then, bioactive films composed of chitosan, gallic acid and cassava starch were developed in pressurized hot water media. The tensile strength and hydrophobicity of films improved as chitosan ratio increased up to 0.15 g/g starch, due to the cross-linking of electrostatic interaction, ester bonds and hydrogen bonds. Further addition of cellulose nanofibers (63.1% purity) improved tensile strength from 0.83 to 10.51 MPa. Also, films prepared from potato by-products showed high tensile strength (0.9-7.8 MPa) with the increasing ratio of potato peel. Furthermore, carvacrol essential oil was incorporated to chitosan-cassava starch films to improve antimicrobial activity. Antimicrobial tests performed on RTE ham showed that chitosan and carvacrol added cassava starch films inactivated *L. monocytogenes* ($\log \text{cfu/cm}^2 < 2$) and extended ham shelf-life up to 25 days. In addition, the biodegradability tests demonstrated the complete degradation of such films in compost (< 85 days). Finally, essential oil nanogels and film grafting opens new alternatives in packaging. All these results suggested that pressurized hot water technology is a promising green method to develop bioactive starch-based films with enhanced mechanical and water barrier

properties. The incorporation of various bioactive compounds provided starch-based films with unique antioxidant/antimicrobial activities that were applied on ham, suggesting potential use on a wide variety of food products.

Preface

Chapter 3 of this thesis has been published as “Zhao, Y. and Saldaña, M.D.A. (2018). Hydrolysis of Cassava Starch, Chitosan and Their Mixtures in Pressurized Hot Water Media. *The Journal of Supercritical Fluids*. doi.org/10.1016/j.supflu.2018.11.013”. I was responsible for the experimental design, performing experiments, data collection and analysis, and drafting the manuscript. My supervisor Dr. Saldaña provided the topic research area, discussed the experimental design and data obtained, and revised the manuscript.

Chapter 4 of this thesis has been published as “Zhao, Y. and Saldaña, M.D.A. (2019). Use of Potato By-products and Gallic Acid for Development of Bioactive Film Packaging by Subcritical Water Technology. *The Journal of Supercritical Fluids*. 143, 97-106”. I was responsible for the experimental design, performing experiments, data collection and analysis, and drafting the manuscript. Dr. Saldaña provided the topic research area, helped with experimental design, data discussion, and revision of the manuscript.

Chapter 5 of this thesis has been published as “Zhao, Y., Teixeira, J. S., Gänzle, M. G., & Saldaña, M.D.A. (2018). Development of antimicrobial films based on cassava starch, chitosan and gallic acid using subcritical water technology. *The Journal of Supercritical Fluids*, 137, 101-110.” I was responsible for the experimental design, performing experiments, data collection and analysis, and drafting the manuscript. Dr. Saldaña provided the topic research area, helped with experimental design. Dr. Teixeira assisted with the antimicrobial data collection. Dr. Saldaña, Dr. Gänzle and Dr. Teixeira revised the manuscript.

Chapter 6 of this thesis has been submitted to the journal of Food Packaging and Shelf Life as “Zhao, Y. and Saldaña, M.D.A. (2019). Bioactive Cassava Starch Films Incorporated with Chitosan and Carvacrol Essential Oil for Packaging Produced by Subcritical Water

Technology”. I was responsible for the experimental design, performing experiments, data collection and analysis, and drafting the manuscript. Dr. Saldaña provided the topic research area, helped with experimental design, data discussion, and revision of the manuscript.

Chapter 7 of this thesis has been submitted to the Journal of Supercritical Fluids as “Zhao, Y., Huerta R. R., Saldaña, M.D.A. (2019). Use of Subcritical Water Technology to Develop Cassava Starch/Chitosan Bioactive Films Reinforced with Cellulose Nanofibers From Canola Straw”. Dr. Saldaña provided the research topic. The experimental design was discussed with Raquel and Dr. Saldaña. Raquel provided the cellulose nanofibers and assisted with film characterization. I was responsible for data collection and analysis, and drafting the manuscript. Dr. Saldaña and Raquel helped with data discussion, and revision of the manuscript.

Chapter 8 of this thesis will be submitted to the International Journal of Food Microbiology as “Zhao, Y., Teixeira, J. S., Gänzle, M. G., and Saldaña, M. D. A. (2019). Antimicrobial Activity of Bioactive Starch Films Against *L. monocytogenes* and Reconstituted Meat Microbiota on Ham”. Dr. Saldaña provided the research topic. Experimental design was discussed with all authors. I was responsible for performing experiments, data collection and analysis, and drafting the manuscript. Dr. Teixeira provided the ham and performed all PCR experiments., Dr. Saldaña, Dr. Gänzle and Dr. Teixeira helped with data discussion, and revision of the manuscript.

Chapter 9 of this thesis has been published as “Zhao, Y., Sun W. and Saldaña, M.D.A. (2018). Nanogels of poly-N-isopropylacrylamide, poly-N,N-diethylacrylamide and acrylic acid for controlled release of thymol. *The Journal of Polymer Research*. 12 pp. <https://doi.org/10.1007/s10965-018-1644-x>”. Topic and the experimental design were discussed with Dr. Saldaña and Dr. Sun. I was responsible for performing experiments, data collection and

analysis, and drafting the manuscript. Dr. Saldaña and Dr. Sun helped with data discussion, and revision of the manuscript.

Acknowledgements

First, I would like to express my sincere gratitude to my supervisor, Dr. Marleny D.A. Saldaña for the continuous support of my PhD studies, for her patience, motivation, and immense knowledge. Her guidance and the time she spent with me during research and writing of my thesis helped me to grow as a scientist and expand my knowledge.

Besides, I would like to thank my committee members, Dr. Michael Gänzle and Dr. Thava Vasanthan, for their comments, which incited me to widen my research during the past four years.

I am grateful to my colleagues Dr. Januana Teixeira, Raquel Huerta and Dr. Wenxiu Sun, who assisted me with some characterizations in three of my PhD thesis chapters. I would also like to thank my labmates: Carla Valdivieso, Idaresit Ekaette, Angelica Chourio Chavez, Azadeh Aghashahi, Alaleh Boroomand, Eduardo Rodriguez and Junchao Zhang for sharing their knowledge and collaborative environment in the sub/supercritical fluid and high pressure processing laboratory.

My thanks and appreciation also goes to my parents and friends for their constant encouragement and belief that helped me finalize my PhD thesis and survive stressful times. You have all helped me to focus on what has been a hugely rewarding and enriching process.

Finally, I would like to thank to the Natural Sciences and Engineering Research Council of Canada (NSERC) for funding this project. I am also grateful for my PhD scholarship from China Scholarship Council-CSC at the University of Alberta.

Table of Contents

Abstract	ii
Preface	iv
Acknowledgements	vii
List of Tables	xiii
List of Figures	xv
Nomenclature	xx
Chapter 1: Introduction	1
1.1 Rationale	1
1.2 Hypothesis	5
1.3 Thesis objectives	6
Chapter 2: Literature review	8
2.1 Subcritical water and properties	8
2.1.1 Ionic strength	8
2.1.2 Dielectric constant	9
2.1.3 Viscosity and mass transfer	10
2.1.4 Reactions in subcritical water: model and real systems.....	11
2.2 Starch reactions	20
2.2.1 Starch	20
2.2.2 Starch film formation techniques.....	22
2.2.2.1 Wet process.....	23
2.2.2.2 Dry process	23
2.2.3 Incorporation of polymers in starch-based films	25
2.2.3.1 Chitosan	25
2.2.3.2 Cellulose and derivatives	27
2.2.3.3 Other biopolymers	29
2.2.3.4 Synthetic polymers.....	30
2.2.4 Incorporation of bioactive compounds in starch-based films	33
2.2.4.1 Phenolic acid and phenolic compounds from plant extract	33
2.2.4.2 Essential oils	41
2.2.5 Food systems used to determine film functionality	48
2.2.5.1 Food simulants	48
2.2.5.2 Disk diffusion for antimicrobial test.....	49
2.2.5.3 Application of starch-based films on food products	50
2.2.6 Commercial biodegradable plastics	55
2.2.7 Film Biodegradability	58
2.3 Thermosensitive micro/nanogels	61
2.3.1 N-Isopropylacrylamide copolymers.....	62
2.3.2 Natural polymers.....	64
2.4 Future perspectives	65

Chapter 3: Hydrolysis of Cassava Starch, Chitosan and Their Mixtures in Pressurized Hot Water Media*	70
3.1 Introduction	70
3.2 Materials and methods	72
3.2.1 Materials	72
3.2.2 Methods.....	73
3.2.2.1 Production of hydrolysates	73
3.2.2.2 Hydrodynamic diameter, zeta potential and molecular weight	74
3.2.2.3 Reducing end	75
3.2.2.4 Reducing sugar.....	75
3.2.2.5 Amylose content	75
3.2.2.6 Color	75
3.2.2.7 X-Ray diffraction (XRD) and relative crystallinity	76
3.2.2.8 Differential scanning calorimetry (DSC).....	76
3.2.2.9 Fourier transform infrared (FT-IR) spectroscopy	77
3.2.2.10 Statistical analysis.....	77
3.3 Results and discussion	77
3.3.1 Amylose production of cassava starch hydrolysates and its effect on starch retrogradation and crystallinity	77
3.3.2 Reducing end yield of cassava starch and chitosan hydrolysates	86
3.3.3 Molecular weight and particle size of cassava starch and chitosan hydrolysates.....	88
3.3.4 Color performance of pressurized hot water treated cassava starch, chitosan and starch-chitosan complexes	91
3.3.5 Cross-linking of chitosan-starch complexes after pressurized hot water treatment	94
3.4. Conclusions	98
Chapter 4: Use of Potato By-products and Gallic Acid for Development of Bioactive Film Packaging by Pressurized Hot Water Technology*	99
4.1. Introduction	99
4.2. Materials and methods	101
4.2.1 Materials	101
4.2.2 Bioactive film development.....	102
4.2.3 Film characterization	103
4.2.3.1 Structural properties.....	103
4.2.3.2 Mechanical properties.....	104
4.2.3.3 Physico-chemical properties	104
4.2.3.4 Optical and morphological properties.....	105
4.2.3.5 Functional properties	107
4.2.3.5.1 Determination of total phenolic compound content.....	107
4.2.3.5.2 Ferric Reducing Antioxidant Power (FRAP) Assay.....	107
4.2.3.5.3 Inhibition of the 2,2'-azinobis (3-ethyl-benzothiazoline-6-sulfonic acid) (ABTS) Assay.....	108
4.3 Results and discussion	108
4.3.1 Structural properties.....	109
4.3.2 Mechanical properties.....	112
4.3.3 Physico-chemical properties	114

4.3.4 Optical and morphological properties.....	119
4.3.5 Antioxidant activity and total phenolic content of potato by-product films.....	124
4.4 Conclusions.....	126
Chapter 5: Development of Antimicrobial Films Based on Cassava Starch, Chitosan and Gallic Acid Using Pressurized Hot Water Technology*	127
5.1 Introduction.....	127
5.2 Materials and methods	129
5.2.1 Materials	129
5.2.2 Preparation of bioactive films.....	129
5.2.3 Film characterization	130
5.2.4 Statistical analysis.....	130
5.3 Results and discussion	130
5.3.1 Chemical properties of bioactive starch films	131
5.3.2 Mechanical properties of bioactive starch films	135
5.3.3 Water activity, solubility and water vapor permeability of bioactive starch films....	137
5.3.4 Optical and morphological properties.....	142
5.3.5 Antioxidant activity of bioactive films	144
5.3.6 Antimicrobial activity of bioactive films.....	146
5.4 Conclusions.....	148
Chapter 6: Bioactive Cassava Starch Films Incorporated with Chitosan and Carvacrol Essential Oil for Packaging Produced by Pressurized Hot Water Technology*	150
6.1 Introduction.....	150
6.2 Materials and methods	153
6.2.1 Materials	153
6.2.2 Bioactive film preparation	153
6.2.3 Film characterization	154
6.2.5 Biodegradability test.....	154
6.2.4 Statistical analysis.....	155
6.3 Results and discussion	155
6.3.1 Structural properties.....	156
6.3.2 Mechanical properties.....	160
6.3.3 Physico-chemical properties	161
6.3.4 Optical properties.....	166
6.3.5 Functional properties	169
6.3.6 Biodegradability test.....	170
6.4. Conclusions.....	174
Chapter 7: Use of Pressurized Hot Water Technology to Develop Cassava Starch/Chitosan Bioactive Films Reinforced with Cellulose Nanofibers From Canola Straw*	177
7.1 Introduction.....	177
7.2 Materials and methods	179
7.2.1 Materials	179
7.2.2 Preparation of cellulose nanofibers (CNFs) from canola straw.....	180
7.2.3 Preparation of bioactive films.....	181
7.2.4 Film characterization	182

7.3. Results and discussion	182
7.3.1 Mechanical properties	182
7.3.2 Structural properties	184
7.3.3 Physico-chemical properties	186
7.3.4 Thermal properties	191
7.3.5 Morphological properties	192
7.3.6 Optical properties	195
7.3.7 Antioxidant activity	198
Chapter 8: Antimicrobial Activity of Bioactive Starch Films Against <i>L. monocytogenes</i> and Reconstituted Meat Microbiota on Ham*	201
8.1. Introduction.....	201
8.2. Material and Methods	203
8.2.1. Bacterial strains and growth conditions	203
8.2.2 Antimicrobial preparation	205
8.2.3 Determination of the combined activity of gallic acid or carvacrol and chitosan with the checkerboard method	205
8.2.4 Sample preparation and inoculation.....	206
8.2.5 Detection of surviving cells	206
8.2.6 Extraction of total DNA and PCR	207
8.3 Results	209
8.3.1 Inhibitory activity of gallic acid or carvacrol as a function of chitosan concentration against <i>L. monocytogenes</i> and reconstituted meat microbiota	209
8.3.2 Bioactive starch films on inhibition of individual <i>L. monocytogenes</i> or reconstituted meat microbiota on ham.....	211
8.3.3 Bioactive starch films on inhibition of combined <i>L. monocytogenes</i> and reconstituted meat microbiota on ham.....	214
8.3.4 Individual strains of reconstituted meat microbiota detection on ham using PCR....	215
8.4. Discussion.....	218
8.5 Conclusions	222
Chapter 9: Nanogels of Poly-N-isopropylacrylamide, Poly-N,N-diethylacrylamide and Acrylic Acid for Controlled Release of Thymol*	223
9.1. Introduction.....	223
9.2 Materials and methods	226
9.2.1 Materials	226
9.2.2 Synthesis of homopolymers and copolymers	226
9.2.3 Preparation of thymol-loaded nanogels and self-assembly on chitosan film	227
9.2.4 Thymol release from nanogels.....	228
9.2.5 Nanogel characterization	229
9.2.5.1 Particle size measurement.....	229
9.2.5.2 Zeta potential measurement	229
9.2.5.3 Fourier transform infrared spectroscopy analysis.....	230
9.2.5.4. Thermogravimetric analysis (TGA).....	230
9.2.5.5 Nuclear magnetic resonance (NMR) measurement	230
9.2.5.6 Turbidity or transmittance measurement	231
9.2.5.7 Scanning electron microscopy	231

9.2.6 Antimicrobial activity measurement.....	231
9.2.6.1 Endospores preparation.....	232
9.2.6.2 Agar well diffusion method	232
9.3 Results and discussion	233
9.3.1 PNIPAM-co-PNDEA-co-PAA polymer nanogels.....	233
9.3.2 Thymol loading and release from copolymer nanogels.....	246
9.3.3 Antimicrobial activity of thymol loaded polymer nanogels	248
9.4. Conclusions.....	250
Chapter 10: Conclusions and Recommendations	251
10.1 Conclusions.....	251
10.1.1 Pressurized hot water hydrolysis of starch and chitosan.....	251
10.1.2 Potato by-product film with(out) gallic acid	252
10.1.3 Cassava starch/chitosan film loaded with gallic acid.....	253
10.1.4 Cassava starch/chitosan film loaded with carvacrol essential oil and biodegradability	253
10.1.5 Cassava starch/chitosan film loaded with gallic acid and cellulose nanofiber	254
10.1.6 Film antimicrobial activity against <i>Listeria monocytogenes</i> and reconstructed meat microbiota	255
10.1.7 Nanoparticles loaded with essential oil for film grafting.....	255
10.2 Recommendations	256
References	260

List of Tables

Table 2.1 Reactions of model and real systems in subcritical water.....	14
Table 2.2 Conversion pathway of model systems in SCW media.	16
Table 2.3 Bioactive starch-based films containing different phenolic acids or plant extracts.	36
Table 2.4 Bioactive starch-based films containing different essential oils.....	44
Table 2.5 Bioactive starch-based films used on various food products.	53
Table 2.6 Commercial bioplastics brands for food-related packaging applications.	56
Table 3.1 Retrogradation characteristics of pure cassava starch after pressurized hot water treatment during storage for 0, 1, 3, 7, 11 and 14 days.	85
Table 3.2 Color performance of cassava starch and chitosan hydrolysates and their complex hydrolysates after pressurized hot water treatment	93
Table 3.3 Molecular weight and zeta potential values of chitosan-starch complexes after pressurized hot water treatment at 100 °C and 85 bar for 10 min.....	97
Table 4.1 Formulations of bioactive films based on potato by-products.	103
Table 4.2 Moisture content, water activity and water vapour permeability of bioactive films based on potato by-products.	116
Table 4.3 Color performance, transparency, and gloss of top and bottom surfaces of bioactive films based on potato by-products.....	121
Table 5.1 Parameters evaluated for bioactive starch film formation.	130
Table 5.2 Physical properties of bioactive cassava starch films.	140
Table 6.1 Process parameters evaluated for carvacrol incorporated chitosan-cassava starch film formation.....	153
Table 6.2 Elongation of carvacrol incorporated chitosan-cassava starch films using a fractional factorial design.....	156
Table 6.3 Physico-chemical properties of carvacrol incorporated chitosan-cassava starch films produced at 75 °C and 120 bar.	165
Table 6.4 Optical properties of carvacrol incorporated chitosan-cassava starch films produced at 75 °C and 120 bar.	168
Table 7.1 Process parameters evaluated for CNFs reinforced cassava starch/chitosan/gallic acid film formation.....	182
Table 7.2. Mechanical properties of CNFs reinforced cassava starch/chitosan/gallic acid films.....	184
Table 7.3 Physico-chemical properties of CNFs reinforced cassava starch/chitosan/gallic acid films produced at 100 °C and 85 bar.	190
Table 7.4 Optical properties of CNFs reinforced cassava starch/chitosan/gallic acid films produced at 100 °C and 85 bar.....	197
Table 8.1. Bacterial strains and growth conditions used in this study.	205
Table 8.2. Primers and conditions.....	208
Table 9.1 Polymers used for synthesis of nanogels	227
Table 9.2 Hydrodynamic diameter of nanogels as a function of temperature (nm).....	242
Table 9.3 Encapsulation efficiency and loading capacity of thymol-loaded homopolymer and copolymer nanogels.	247

Table 9.4 Antibacterial activity of thymol loaded nanogels, thymol and thymol-free nanogels against tested microorganisms 249

List of Figures

Fig. 2.1 Starch granule conformation and linkages.	21
Fig. 2.2 Starch film formation techniques.	22
Fig. 2.3 Classification of packaging materials.	32
Fig. 2.4 Common antioxidants incorporated in starch-based films.	35
Fig. 2.5 Starch-based films incorporated with antimicrobials.	42
Fig. 2.6 Starch based-films for food and non-food applications.	57
Fig. 2.7 Bioactive starch-based film development and application.	66
Fig. 2.8 A) Number of scientific publications on bioactive starch packaging and B) graphical representation of bioactive food packaging by research area.	67
Fig. 3.1 Subcritical fluid reaction system: (1) Solvent reservoir, (2) Pump, (3) One-way valve, (4) Pressure gauge, (5) Band heaters, (6) Pressurised fluid reaction vessel, (7) Motor stirrer controlled by the control panel, (8) Stirrer, (9) Thermocouple, (10) Temperature controller, (11) Safety valve, (12) Back pressure regulator, and (13) Sample collection.	74
Fig. 3.2 A) Amylose content of pure cassava starch after pressurized hot water treatment at 75-150 °C and 50-155 bar for 10 min, and B) hydrolysis scheme of cassava starch.	80
Fig. 3.3 XRD patterns and relative crystallinity (RC, %) of: a) native cassava starch, b) pure cassava starch gelatinized at 90 °C, c-f) pure cassava starch after pressurized hot water treatment at 75-150 °C and 85 bar, and g-j) pure cassava starch after pressurized hot water treatment at 50-155 bar and 100 °C for 10 min.	82
Fig. 3.4 Reducing end yield of: A) pure cassava starch, and B) chitosan after pressurized hot water treatment at 75-150 °C and 50-155 bar for 10 min.	88
Fig. 3.5 Molecular weight of: A) pure cassava starch, and B) chitosan, and hydrodynamic diameter of: C) chitosan after pressurized hot water treatment at 75-150 °C and 50-155 bar for 10 min, and D) chitosan hydrolysis scheme.	91
Fig. 3.6 FT-IR spectra of pure cassava starch, pure chitosan and starch-chitosan complexes after pressurized hot water treatment at 100 °C and 85 bar for 10 min.	95
Fig. 4.1 FT-IR spectra of pure gallic acid (GA) and bioactive films based on potato by-products at different GA/potato cull starch ratios of 0-0.3 g/g and constant glycerol/starch ratio of 1 g/g at 120 bar and 125 °C.	110
Fig. 4.2 XRD patterns and relative crystallinity (RC, %) of: a) freeze dried potato cull and bioactive films based on potato by-products: b) 0 g GA/g potato cull starch, c) 0.1 g GA/g potato cull starch, d) 0.2 g GA/g potato cull starch, and e) 0.3g GA/g potato cull starch produced with constant glycerol/starch ratio of 1 g/g at 120 bar and 125 °C.	112
Fig. 4.3 Tensile strength and elongation at break for bioactive films based on potato by-products of: A) potato peel/cull ratios (0-1.3 g/g) and glycerol/potato cull starch ratio (0.5 g/g), B) glycerol/potato cull starch ratios (0.5-2 g/g) and potato peel/cull ratios (1.3 g/g), and C) GA/potato cull starch ratios (0-0.3 g/g) and glycerol/potato cull starch ratio (1 g/g) produced at 120 bar and 125 °C.	114
Fig. 4.4 A) Film solubility in water at 4, 25 and 50 °C, and B) top and bottom surfaces contact angle of bioactive films based on potato by-products with different potato	

peel/cull ratios (0-1.3 g/g) and constant glycerol/potato cull starch ratio (0.5 g/g) or GA/potato cull starch ratios (0-0.3 g/g) and constant glycerol/potato cull starch ratio (1 g/g) at 120 bar and 125 °C.	119
Fig. 4.5 SEM images of: a) ground potato cull, and bioactive films based on potato by-products: b) 0 g peel/g cull, c) 0.5 g peel/g cull, d) 1.0 g peel/g cull, and e) 1.3 g peel/g cull with constant glycerol/potato cull starch ratio of 0.5 g/g produced at 120 bar and 125 °C.	123
Fig. 4.6 SEM images of: a) pure gallic acid, and bioactive films based on potato by-products: b) 0 g GA/g potato cull starch, c) 0.1 g GA/g potato cull starch, d) 0.2 g GA/g potato cull starch, e) 0.3g GA/g potato cull starch, and f-g) 0.4 GA/g potato cull starch with constant glycerol/potato cull starch ratio of 1 g/g produced at 120 bar and 125 °C.	123
Fig. 4.7 Total phenolic content, and antioxidant activity by ABTS and FRAP methods of bioactive films based on potato by-products with different: A) potato peel/cull ratios (0-1.3 g/g) and constant glycerol/potato cull starch ratio of 0.5 g/g, and B) GA/potato cull starch ratios (0-0.3 g/g) and constant glycerol/potato cull starch ratio of 1 g/g produced at 120 bar and 125 °C.	125
Fig. 5.1 FTIR spectra of: A) pure gallic acid, cassava starch and chitosan, B) cassava starch film, gallic acid+starch film (0.1 g gallic acid/g starch, 0.5 g glycerol/g starch) and gallic acid+chitosan starch film produced at a chitosan/starch ratio of 0.15 g/g starch, gallic acid/starch ratio of 0.1 g/g and glycerol/starch ratio of 0.5 g/g at 85 bar and 100 °C.	133
Fig. 5.2 XRD patterns and relative crystallinity (RC) of pure chitosan, native cassava starch and bioactive cassava starch films with different chitosan/starch ratios of 0-0.15 g/g, constant gallic acid/starch ratio of 0.1 g/g and glycerol/starch ratio of 0.5 g/g at 85 bar and 100 °C.	135
Fig. 5.3 Mechanical properties of bioactive cassava starch films with different chitosan/starch ratios of 0-0.15g/g, constant gallic acid/starch ratio of 0.1 g/g and glycerol/starch ratio of 0.5 g/g at 85 bar and 100 °C.	137
Fig. 5.4 A) Film solubility in water at 4, 25 and 50°C, B) top and bottom surfaces contact angle of bioactive cassava starch films with different chitosan/starch ratios of 0-0.15g/g, constant gallic acid/starch ratio of 0.1 g/g and glycerol/starch ratio of 0.5 g/g at 85 bar and 100 °C.	141
Fig. 5.5 A) Color performance (total color difference, whiteness index and yellowness index), B) transparency, and C) top and bottom surfaces gloss of bioactive starch films with different chitosan/starch ratios of 0-0.15 g/g, constant gallic acid/starch ratio of 0.1g/g and glycerol/starch ratio of 0.5 g/g at 85 bar and 100 °C.	144
Fig. 5.6 Total phenolic content, antioxidant activity (ABTS and FRAP methods) of bioactive starch films with different chitosan/starch ratios of 0-0.15 g/g, constant gallic acid/starch ratio of 0.1 g/g and glycerol/starch ratio of 0.5 g/g at 85 bar and 100 °C.	146
Fig. 5.7 Growth of a 5 strain cocktail of meat spoilage microbiota containing <i>Brochothrix thermosphacta</i> FUA3558, <i>Carnobacterium maltaromaticum</i> FUA3559, <i>Leuconostoc gelidum</i> FUA3560 and FUA3561, and <i>Lactobacillus sakei</i> FUA3562 on the surface of cooked ham during storage at 4°C. The ham was covered with a	

starch film (control, squares), or with starch films containing 25 mg (circles) or 150 mg chitosan (triangles)/g starch and bacterial cell counts were enumerated over 28 d of storage. Cell counts of un-inoculated ham remained below the detection limit throughout the 4 weeks of storage.....	148
Fig. 6.1 FT-IR spectra of: a) pure cassava starch film, and bioactive films produced at a constant chitosan/starch ratio of 0.025g/g, glycerol/starch ratio of 0.5 g/g, and different carvacrol/starch ratios: b) 0 g/g, c) 0.049 g/g, d) 0.098 g/g, e) 0.147 g/g, and f) 0.195 g/g produced at 75 °C and 120 bar.....	158
Fig. 6.2 XRD patterns and relative crystallinity (RC) of: a) native cassava starch, and bioactive films produced at a constant chitosan/starch ratio of 0.025g/g , glycerol/starch ratio of 0.5 g/g and different carvacrol/starch ratios: b) 0 g/g, c) 0.049 g/g, d) 0.098 g/g, e) 0.147 g/g, and f) 0.195 g/g produced at 75 °C and 120 bar.	159
Fig. 6.3 Mechanical properties of bioactive starch films produced at different carvacrol/starch ratios of 0-0.195 g/g, constant chitosan/starch ratio of 0.025 g/g and glycerol/starch ratio of 0.5 g/g produced at 75 °C and 120 bar.....	161
Fig. 6.4 Total phenolic content, total antioxidant activity (ABTS and FRAP methods) of bioactive starch films with different carvacrol/starch ratios of 0-0.195 g/g, constant chitosan/starch ratio of 0.025 g/g and glycerol/starch ratio of 0.5 g/g produced at 75 °C and 120 bar.	170
Fig. 6.5 Weight loss curves of: a) potato peel/cull films, b) potato cull/gallic acid films, c) cassava starch/gallic acid/chitosan films, and d) cassava starch/chitosan/carcacrol films during biodegradation in compost as a function of time.....	174
Fig. 7.1 FT-IR spectra of: a) pressurized aqueous ethanol (20%) treated canola straw, and b-d) CNFs reinforced cassava starch/chitosan/gallic acid films with different CNFs/starch ratios, constant chitosan/starch ratio (0.15 g/g) and gallic acid/starch ratio (0.1 g/g) produced at 100 °C and 85 bar.	186
Fig. 7.2 (A) TG, and (B) DTG curves of pressurized aqueous ethanol (20%) treated canola straw and CNFs reinforced cassava starch/chitosan/gallic acid films with different CNFs/starch ratios and constant glycerol/g starch ratio of 0.5 g/g, chitosan/starch ratio of 0.15 g/g and gallic acid/starch ratio of 0.1 g/g produced at 85 bar and 100 °C.	192
Fig. 7.3 TEM image of: a) CNFs from canola straw after ultrasonication, and SEM images of: b-f) top surfaces and g-k) fractured surfaces of CNFs reinforced cassava starch/chitosan/gallic acid films with 0-0.1 g CNFs/g starch, constant chitosan/starch ratio (0.15 g/g) and gallic acid/starch ratio (0.1 g/g) produced at 100 °C and 85 bar.	194
Fig. 7.4 Total phenolic content, and total antioxidant activity of CNFs reinforced cassava starch/chitosan/gallic acid films with different CNFs/starch ratios, constant chitosan/starch ratio (0.15 g/g) and gallic acid/starch ratio (0.1 g/g) produced at 100 °C and 85 bar. ABTS: 6-Dydroxy-2,5,7,8-tetramethylchroman-2-carboxylic acid, and FRAP: Ferric reducing antioxidant power. ^{a-d} Different lowercase letters in the same pattern indicate significant differences ($p < 0.05$).	199
Fig. 8.3 Growth of a 5 strain cocktail of <i>L. monocytogenes</i> strains: FSL J1-177, FSL C1-056, FSL N3-013, FSL R2-499, and FSL N1-227 on the surface of cooked ham	

during storage at 4 °C, bacteria were counted on A) TSB and B) PALCAM agar. The ham was covered with a potato starch film (Potato control), or with a cassava starch film (Cassava control), or potato films containing 0.1 g or 0.3 g gallic acid/g starch, or with cassava starch films containing 0.1 g gallic acid/g starch and 0.025 g or 0.15 g chitosan /g starch, or with cassava starch films containing 0.025 g chitosan /g starch and 0.048 g or 0.195 g carvacrol /g starch. Bacterial cell counts were enumerated over 28 d of storage. Cell counts of un-inoculated ham remained below the detection limit throughout the 4 weeks of storage. Data are means ± standard deviations of triplicate independent experiments. Symbols crossing the dot line indicate cell counts below the detection limit of 2 log CFU/cm²..... 212

Fig. 8.4 Growth of a 5 strain cocktail of reconstituted meat microbiota containing *Brochothrix thermosphacta* FUA3558, *Carnobacterium maltaromaticum* FUA3559, *Leuconostoc gelidum* FUA3560 and FUA3561, and *Lactobacillus sakei* FUA3562 on the surface of cooked ham during storage at 4 °C, bacteria were counted on APT agar. The ham was covered with a potato starch film (Potato control), or with a cassava starch film (Cassava control), or potato starch films containing 0.1 g or 0.3 g gallic acid/g starch, or with cassava starch films containing 0.1 g gallic acid/g starch and 0.025 g or 0.15 g chitosan /g starch, or with cassava starch films containing 0.025 g chitosan /g starch and 0.048 g or 0.195 g carvacrol /g starch. Bacterial cell counts were enumerated over 28 d of storage. Cell counts of un-inoculated ham remained below the detection limit throughout the 4 weeks of storage. Data are means ± standard deviations of triplicate independent experiments. Symbols crossing the dot line indicate cell counts below the detection limit of 2 log CFU/cm²..... 213

Fig. 8.5 Growth of the mixture of a 5 strain cocktail of reconstituted meat microbiota containing *Brochothrix thermosphacta* FUA3558, *Carnobacterium maltaromaticum* FUA3559, *Leuconostoc gelidum* FUA3560 and FUA3561, and *Lactobacillus sakei* FUA3562 and a 5 strain cocktail of *L. monocytogenes* strains: FSL J1-177, FSL C1-056, FSL N3-013, FSL R2-499, and FSL N1-227 on the surface of cooked ham during storage at 4 °C, bacteria were counted on A) APT and B) PALCAM agar. The ham was covered with a potato starch film (Potato control), or with a cassava starch film (Cassava control), or potato films containing 0.1 g or 0.3 g gallic acid/g starch, or with cassava starch films containing 0.1 g gallic acid/g starch and 0.025 g or 0.15 g chitosan /g starch, or with cassava starch films containing 0.025 g chitosan /g starch and 0.048 g or 0.195 g carvacrol /g starch. Cell counts of un-inoculated ham remained below the detection limit throughout the 4 weeks of storage. Data are means ± standard deviations of triplicate independent experiments. Symbols crossing the dot line indicate cell counts below the detection limit of 2 log CFU/cm². 215

Fig. 9.1 FTIR spectra of polymer nanogels 234

Fig. 9.2 Thermal gravity and derivation analysis (TG-DTG) of nanogel polymers. 236

Fig. 9.3 ¹H NMR spectra of: (a) PID 100/0, and (b) PID 50/50 in D₂O. Hydrogen is indicated as “A-F” in the inset and spectra..... 237

Fig. 9.4 SEM images of nanogels and their self-assembly onto chitosan films: (a) Dried PNIPAM nanogels, (b) Dried PNDEA nanogels, (c) Dried nanogels of PID85/15, (d)

Dried nanogels of PID75/25, (e) Dried nanogels of PID65/35, (f) Dried nanogels of PID50/50, (g) Plain chitosan film, and (h) Self-assembled chitosan film with PID 50/50 nanogels.....	238
Fig. 9.5 The influence of polymer composition on nanogel transition temperature: (a) Transmittance of polymer nanogels in water as a function of temperature, and (b) LCST of polymer nanogels	240
Fig. 9.6 Effect of different salt ions on the LCST of copolymer nanogels in aqueous solutions: (a) anions, and (b) cations.....	244
Fig. 9.7 Effect of pH on the diameter of polymer nanogels in aqueous solutions: (a) PNIPAM, (b) PNDEA, (c) PID85/15, (d) PID75/25, (e) PID65/35, and (f) PID50/50	245
Fig. 9.8 Thymol release behavior of polymer nanogels: (a) PID50/50 at 4 °C, (b) PID50/50 at 25 °C, and (c) PID50/50 at pH 6	248

Nomenclature

ΔE	Total color difference
ΔH_r	Retrogradation enthalpy change
ΔP	Partial water vapor pressure difference
A	Hunter color index a
a_w	Water activity
ABTS	6-Dihydroxy-2,5,7,8-tetramethylchroman-2-carboxylic acid
APT	All purpose tween agar
B	Hunter color index b
CFU	Colony-forming unit
CMC	Carboxymethyl cellulose
CNF	Cellulose nanofiber
DSC	Differential scanning calorimetry
DTG	Derivative thermo-gravimetric analysis
E%	Percent elongation at break
EO	Essential oil
FRAP	Ferric reducing antioxidant power
FT-IR	Fourier transform infrared spectroscopy
GA	Gallic acid
GU	Gloss unit
HMF	Hydroxymethyl furfural
HPC	Hydroxypropyl cellulose
HPLC	High performance liquid chromatography
HPMC	Hydroxypropylmethyl cellulose
K_w	Water autoionization constant
L	Hunter color index L
LCST	Low critical solution temperature
MIC	Minimum inhibitory concentration
PAA	Poly acrylic acid

PAE	Pressurized aqueous ethanol
PBAT	Poly butylene adipate co-terephthalate
PCL	Polycaprolactone
PLA	Poly(lactic acid)
PNDEA	Poly (N, N-diethylacrylamide)
PNIPAM	Poly-N-isopropylacrylamide
PVOH	Poly vinylalcohol
RC	Relative crystallinity
RH	Relative humidity
RTE	Ready-to-eat
SCW	Subcritical water
SEM	Scanning electron microscopy
T_c	Conclusion temperature of retrogradation
TEAC	Trolox equivalent antioxidant capacity
TEM	Transmission electron microscopy
TGA	Thermogravimetric analysis
T_o	Onset temperature of retrogradation
T_p	Peak temperature of retrogradation
TS	Tryptic soy agar
TSB	Tryptic soy broth
WI	Whiteness index
WVP	Water vapor permeability
WVTR	Water vapor transmission rate
XRD	X-Ray diffraction
YI	Yellowness index

Chapter 1: Introduction

1.1 Rationale

Concerns with non-biodegradable petroleum-based packaging disposal and consumers demand for safe food products has caused an increasing interest in developing biodegradable and bioactive packaging materials using renewable biopolymers. Among biopolymers, starch is abundant, renewable, inexpensive and can be chemically modified (Shah, Naqash, Gani & Masoodi, 2016). Starch modification by physical methods such as pre-gelatinization, hydrothermal treatment, annealing, heat-moisture treatment, ultrasonication, high hydrostatic pressure and microwave treatment enhances starch heat resistance, texture, adhesion, and solubility. On the other hand, chemical modification by acetylation, cationization, cross-linking and oxidation, aims to functionalize starch to provide specific characteristics (Masina et al., 2017; Zia-ud-Din, Xiong & Fei, 2017). For example, acetylation increased the hydrophobicity of cassava starch (Colivet & Carvalho, 2017). Other modified cationic starches are applied as an additive, adhesive and coating binder in the paper industry (Kettle, Lamminmäki & Gane, 2010). Cross-linking of cassava starch film by citric acid improved hydrophobicity and mechanical strength (Seligra, Jaramillo, Famá & Goyanes, 2016). These modifications make starch an attractive and promising biopolymer for packaging applications.

Root and tuber crops are the second major source of starch after cereals, including potato, cassava, yam and taro. Among the two major components existing in starch, amylose provides starch film rigidity, whereas the branched structure of amylopectin leads to a decreased tensile stress (Tharanathan, 2003). Although starch-based materials are known to have excellent oxygen barrier properties (Forssell, Lahtinen, Lahelin & Myllärinen, 2002), their applications are limited due to the poor moisture barrier properties, brittleness and low tensile strength (Laohakunjit &

Noomhorm, 2004; Sun et al., 2009). To overcome these shortcomings, biopolymers such as chitosan and cellulose have been incorporated into the starch matrix (Babae, Jonoobi, Hamzeh & Ashori, 2015; Ren, Yan, Zhou, Tong & Su, 2017). Chitosan was used due to its good film forming property and miscibility with starch at concentrations of 1:2-1:0.5 w/w chitosan/starch, where chitosan was dissolved in acid solution (Bourtoom & Chinnan, 2008). Chitosan-starch films have shown reduced water absorption and improved mechanical and barrier properties (Bonilla, Talón, Atarés, Vargas & Chiralt, 2013; Pelissari et al., 2012; Ren et al., 2017). Moreover, the addition of chitosan inactivated Gram-positive and Gram-negative bacteria (Kong, Chen, Xing & Park, 2010) yeasts and molds (Liu, Du, Wang & Sun, 2004).

Another abundant biopolymer, cellulose can improve mechanical strength and film hydrophobicity due to interactions between cellulose and starch molecules by hydrogen bonds (Slavutsky & Bertuzzi, 2014). Also, bioactive compounds like phenolic acids (ferulic acid, tannic acid and gallic acid) were incorporated into starch-based films to improve film antioxidant/antimicrobial activities (Pyla, Kim, Silva & Jung, 2010; Rui et al., 2017; Woranuch, Yoksan & Akashi, 2015). Another approach to improve film functionality is to add essential oils to enhance microorganism inactivation of starch-based films. Various studies have demonstrated that carvacrol had the highest antibacterial activity among thymol, menthol and streptomycin (Sánchez-González, Vargas, González-Martínez, Chiralt & Cháfer, 2011; Soković, Glamočlija, Marin, Brkić & van Griensven, 2010). Earlier, Ravishankar et al. (2012) reported the use of carvacrol (0.5-3 wt%) in pectin-based films to control *L. monocytogenes* growth on ham, showing decreased cell counts more than 3 log cfu/g when ham was covered with a film containing 3% carvacrol stored under 4 °C at day 7. Moreover, carvacrol up to 625 µg/mL exhibited complete inactivation of lactic acid bacteria, including *Lactobacillus spp.* and

Leuconostoc spp. (Bellés, Alonso, Roncalés & Beltrán, 2018; Chan, Gan, Shah & Corke, 2018). However, essential oils are volatile, easily oxidize and might have a strong pungent smell. To overcome these challenges, some studies have evaluated essential oil encapsulation (Santos, Kamimura, Hill & Gomes, 2015; Wen et al., 2016). Santos et al. (2015) encapsulated carvacrol into beta-cyclodextrin, which significantly inhibited *Escherichia coli* and *Salmonella enterica* growth at lower carvacrol concentrations of 300-350 µg/mL compared to free carvacrol (≥ 1000 µg/mL). Thus, essential oil encapsulation can be a promising approach for active food packaging. Also, intelligent polymers have attracted interest to encapsulate bioactive compounds (Esfanjeni & Jafari, 2016). Among them, poly-N-isopropyl acrylamide (PNIPAM) is a temperature-responsive polymer, which undergoes a phase transition at around 32°C, unique for bioactive control release. But, PNIPAM nanogels have only been used in the bio-medical area (Najafi, Hebels, Hennink & Vermonden, 2018). The application of this nanogel in food packaging is yet to be explored.

As a carrier for bioactive compounds, starch-based films are produced traditionally through casting, extrusion blowing, and thermo-compression. Among them, the most commonly used is the casting method. Using this method, after the gelatinization and homogenization steps, film-forming dispersions must be poured or cast on dishes and allowed to dry at controlled conditions. However, a heterogeneous film could be produced if the additive (antioxidant/antimicrobial) has poor compatibility with the starch (Acosta et al., 2016). Extrusion usually includes two steps, where the starch is mixed with plasticizers and extruded to disrupt the starch granules, thus obtaining a thermoplastic starch, followed by thermo-molded to form films. Once the starch is in the amorphous state, it can be extruded using a film-blowing die (Jiménez, Fabra, Talens & Chiralt, 2012a). In this case, gelatinization is achieved at low moisture content

due to the high-shear and high-pressure conditions used, which breaks down the starch granules, allowing fast water transfer into the starch molecules. However, the intense shear can break down the molecule chain and cause poor film mechanical properties (Liu, Xie, Yu, Chen & Li, 2009). Therefore, investigation of new technologies on bioactive starch-based film development is of great interest, due to the requirement for a green process to enhance film properties with an active response to storage environment.

Subcritical water (SCW), also known as “pressurized hot water” or “near critical water” is defined as the water at temperatures above 100 °C and below its critical point of 374 °C and pressure high enough to maintain in the liquid state (Brunner, 2009). SCW has been attracting growing interest as a solvent and reaction medium for biomass conversion and bioactive extraction (Plaza & Turner, 2015; Saldaña & Valdivieso-Ramirez, 2015). Changes in temperature and pressure lead to unique variations of physico-chemical properties of SCW compared to those of normal water. At SCW conditions, water dissociates into acidic hydronium ions (H_3O^+) and basic hydroxide ions (OH^-), accelerating acid- or base-catalyzed reactions (Brunner, 2009; Toor, Rosendahl & Rudolf, 2011). Also, the reduced dielectric constant decreased from 78 F m^{-1} at 25 °C/1 bar to 14.07 F m^{-1} at 350 °C/200 bar, improving solubility of non-polar compounds in SCW and favoring their extraction (Uematsu & Frank, 1980). Furthermore, the high diffusion rate due to the reduced surface tension and low viscosity improves mass transfer, enabling SCW as a promising medium for homogeneous, fast, and efficient reactions (Ramos, Kristenson & Brinkman, 2002). Consequently, SCW is an attractive green reaction media. Numerous studies have been conducted to investigate the application of SCW on extraction and biomass transformation to produce hydrolyzed liquid products. For example, bioactives like phenolic compounds, essential oils, polysaccharides (hemicellulose,

pectin) have been extracted from various plant resources and agriculture biomass (Saldaña & Valdivieso-Ramirez, 2015). SCW conversion of carbohydrates (lignocellulosic biomass, starch), lipids and proteins produced fermentable sugars, free fatty acids and amino acids, respectively (Machmudah, Wahyudiono, Kanda & Goto, 2017; Toor et al., 2011). Recently, one study reported the use of SCW technology for bioactive potato starch film formation, where SCW acts as a catalyst or reaction medium to improve loading of phenolic acids (Zhang, 2015). But, more studies are needed to understand biopolymer behavior, bioactive addition and interactions on starch film formation and the effect on mechanical, physico-chemical and functional properties of films.

1.2 Hypothesis

- Pressurized hot water will hydrolyse cassava starch and chitosan to promote network formation.
- Pressurized hot water will promote reactions of gallic acid and biopolymers (e.g. chitosan and starch) to enhance cross-linking within the film.
- The addition of carvacrol will modify film properties and enhance film antimicrobial activity.
- The incorporation of cellulose nanofiber with 63.1% purity will improve film mechanical strength and water barrier property.
- Starch-based films developed in this thesis will be biodegradable.
- Functional starch films produced using pressurized hot water technology will extend ham shelf-life.
- Nanoparticles loaded with thymol essential oil for film grafting will improve film functionality by controlling essential oil release.

1.3 Thesis objectives

The main objective of this thesis was to understand mechanisms of bioactive starch-based film formation using pressurized hot water technology, and the effect of different bioactives addition on film structure/property/functionality to extend ham shelf-life. To achieve this main objective, some specific objectives were:

- Understand starch and chitosan hydrolysis mechanisms under pressurized hot water conditions to form starch-chitosan complexes.
- Study the influence of potato peel/cull ratio or gallic acid/cull starch ratio, and glycerol/starch ratio in pressurized hot water media to improve film cross-linking and antioxidant activity.
- Understand the effect of gallic acid and chitosan addition on mechanical and antimicrobial properties of bioactive cassava starch-based films developed by pressurized hot water technology.
- Investigate the addition of carvacrol essential oil on chitosan-cassava starch films by pressurized hot water technology, and its effect on film mechanical, optical, structural, water barrier properties and antioxidant activity.
- Compare the biodegradability in soil compost of bioactive starch-based films incorporated with gallic acid, chitosan and carvacrol essential oil as a function of time.
- Investigate the influence of cellulose nanofiber (63.1% purity) addition on starch/chitosan films, especially on structural and mechanical properties.
- Investigate and compare the antimicrobial efficiency of bioactive starch films incorporated with different bioactive compounds of gallic acid, chitosan and carvacrol essential oil for ready-to-eat ham to control the growth of *L. monocytogenes* and reconstituted meat microbiota.

- Develop thermosensitive nanogels using N-isopropylacrylamide with the copolymerization of N, N-diethylacrylamide and acrylic acid to evaluate thymol control release of the nanogels to prevent microbial contamination.

Chapter 2: Literature review

2.1 Subcritical water and properties

Subcritical water (SCW) refers to the water at temperatures between 100 and 374 °C under pressure to maintain water in the liquid state (Brunner, 2009). The major changes of SCW properties are mainly described as increased ionization (OH^- and H_3O^+), thermal conductivity and diffusion coefficient, and decreased dielectric constant and viscosity (NIST, 2008; Kruse & Gawlik, 2003). SCW is used to promote hydrolysis reactions and facilitate extraction.

2.1.1 Ionic strength

As the ion product of water (K_w) increases by three orders of magnitude from $K_w=10^{-14}$ mol^2/L^2 at 25 °C to 10^{-11} mol^2/L^2 at 300 °C under subcritical conditions, reactivity of water molecules is enhanced (Akiya & Savage, 2002; Hunter & Savage, 2004). Therefore, the ionic product can be tuned or modulated by changing mainly temperature. All ionic reactions are triggered due to the stabilization of the charged transition state from equilibrium molecules to contact ion pairs (Westacott, Johnston & Rossky, 2001). Due to these advantages, SCW has been widely studied for conversion of biomass into valuable compounds that generally exhibit low molecular weight at temperatures below 300 °C within a short reaction time. For example, reducing sugars (glucose, xylose, arabinose, fructose and galactose) yield of 0.346 g/g rice straw was obtained using SCW at 280 °C and 200 bar ($\text{Log } K_w \approx -11$ mol^2/L^2) (Lin et al., 2015). Also, alginate (28.12%) and fucoidan (14.93%) were obtained from brown seaweed at optimal conditions of 150 °C ($\text{Log } K_w \approx -11.7$ mol^2/L^2), 20 bar, and liquid/solid ratio of 36.81 mL/g (Saravana, Cho, Woo & Chun, 2018). A study conducted in Dr. Saldaña's laboratory to isolate cellulose from barley and canola straws showed that 54% and 45% of total lignin were removed using pressurized aqueous ethanol (20%) at 180 °C ($\text{Log } K_w \approx -11.5$ mol^2/L^2) and 50 bar during

40 min of treatment (Huerta & Saldaña, 2018b). In addition, a semi-batch SCW system reported a higher lignin removal of > 75% from corn stover compared to the batch extraction (<30%) due to lignin tendency to form insoluble compounds when left in the reactor. Moreover, lignin removal increased from 35% to 75% with increasing water flow rate from 1 to 10 mL/min (Liu & Wyman, 2003; Liu & Wyman, 2005).

On the other hand, the catalytic effect of the addition of acids or bases in SCW results in increased H^+ and OH^- ion concentration and elevated ionic strength (Jin & Enomoto, 2008; Salak Asghari & Yoshida, 2006). As such, a batch SCW conversion process of fructose as a function of reaction temperature in the presence of formic and acetic acid (10.8 mg/mL) was reported by Li et al. (2009). Results showed that the addition of formic acid (10.8 mg/mL) led to increased decomposition rate constants from 0.0205-0.3096 to 0.0682-0.6615 at temperatures of 180-220 °C under a constant pressure of 100 bar (Li et al., 2009). Also, it is possible to enhance SCW reaction capability by adding carbon dioxide as it forms carbonic acid ($K_w=2.43-2.54 \times 10^{-9}$), which acts as an acid catalyst (Zhou et al., 2018). Prado et al. (2017) reported that SCW hydrolysis assisted by CO_2 (2.8% mol/mol water, 250 °C, 200 bar for 30 min) increased total reducing sugar by 15% and 56% compared with SCW hydrolysis alone for sugarcane bagasse and pressed palm, respectively.

2.1.2 Dielectric constant

As a result of the breakdown of intermolecular hydrogen bonds, the dielectric constant of water decreases under subcritical conditions (Möller, Nilges, Harnisch & Schröder, 2011). Water at ambient conditions (25 °C and 1 bar) has a high polarity and a dielectric constant close to 80, while SCW at 250 °C and 50 bar has a reduced dielectric constant of 27, which is similar to that of ethanol (Bröll et al., 1999). Therefore, SCW is considered as a promising green alternative

solvent able to selectively extract polar or slightly non-polar compounds by adjusting temperature.

Extraction of a wide diverse range of antioxidants, proteins and anti-inflammatory agents have been obtained from various plants/herbs and food by-products. For example, thyme essential oil from *Thymbra spicate* showed the best extraction yield of 3.7% at 150 °C and 60 bar, using a flow rate of 2 mL/min for 30 min (Ozel, Gogus & Lewis, 2003). Phenolic compounds extraction, mainly gallic acid (29.56 mg/g dry weight), chlorogenic acid (14.59 mg/g dry weight), protocatechuic acid (13.58 mg/g dry weight) and caffeic acid (9.23 mg/g dry weight) from potato peel were maximized at 180 °C, 60 bar and 60 min using SCW (Singh & Saldaña, 2011). The yields of myricetin (568 mg/kg dry weight), quercetin (1179 mg/kg dry weight), and kaempferol (2770 mg/kg dry weight) from black tea were maximal at 170 °C and 200 °C and 101 bar for 15 min (Cheigh, Yoo, Ko, Chang & Chung, 2015). More recently, glycogen (6.48 g glucose/100 g dried weight), protein (22.48 g/100 g dried weight) and phenolic content (0.72 g gallic acid/100 dried weight) extracted from the oyster powder were optimized at 225 °C and 100 bar. Conversely, the maximum yield of total amino acid from oyster powder was obtained at 175 °C and 60 bar in SCW (Lee, Saravana, Cho, Haq & Chun, 2018). Overall, the precise use of treatment conditions, especially temperature is crucial to maximize the extraction yield and maintain the bioactivity of these compounds.

2.1.3 Viscosity and mass transfer

The reduced viscosity of SCW leads to an increased mass transfer that accelerates various chemical reactions (Möller et al., 2011). In general, mass transfer during extraction of a bioactive compound from a single plant/herb/crop particle can be divided into three main steps: 1) the transportation of bioactive compound from the inner solid matrix to the particle surface or pores

(intra-particle diffusion), 2) diffusion of the bioactive compound from the particle surface to water film around the solid plant particle (external diffusion), and 3) transfer of the bioactive compound into the flowing solvent through thermodynamic partitioning. Based on these three main dominant factors, different strategies can be used to optimize the extraction yield. For example, increasing the water flow rate leads to a high extraction yield when the extraction process is dominated by the external diffusion (Gilbert-López, Plaza, Mendiola, Ibáñez & Herrero, 2018). A high flow rate decreases the residence time, consequently, lowering the extraction yield. Therefore, the simultaneous counter effects of high water flow rate can determine the final extraction yield (Ghoreishi & Shahrestani, 2009).

2.1.4 Reactions in subcritical water: model and real systems

To better understand the reaction pathways of biomass conversion, some model systems have been proposed for lignin (model system guaiacol) (Sasaki & Goto, 2011; Yong & Yukihiro, 2013), carbohydrates (model system glucose, starch, chitosan) (Saito, Sasaki, Kawanabe, Yoshino & Goto, 2009; Yu & Wu, 2011) and phenolic acid (caffeic acid) (Khuwijitjaru, Suaylam & Adachi, 2014). Table 2.1 summarizes typical examples of model and real systems in subcritical water reaction.

Guaiacol as a model compound for lignin decomposition in SCW media (210-290 °C/120 min) underwent only slight degradation (9.62% converted) to form catechol as the main product. Also, products with molecular weight of 110-246 kDa were formed as a result of cross-linking between the active sites and the phenolic structure of guaiacol decomposition (Sasaki & Goto, 2011; Yong & Yukihiro, 2013).

In addition, the conversion pathway of glucose in SCW media has been reported by Saito et al. (2009). Main conversion/decomposition products include D-Fructose (isomerized from D-

glucose), furfural (dehydrated product of D-fructose) and aldehydes such as glyceraldehyde and glycolaldehyde obtained by retro-aldol condensation of D-glucose. Further reaction of aldehydes produced organic acids, such as formic acid and acetic acid (Saito et al., 2009, Table 2.2). It is also noticeable that D-fructose is not stable in SCW and was dehydrated to form 5-HMF within a few seconds at 240 °C and 200 bar (Saito et al., 2009). The yield of 2-furfural also increased with residence time from 40 to 120 s at 240 °C and 200 bar with an initial glucose concentration of 3 wt %. Furthermore, Yu & Wu (2011) reported that at glucose concentration below 10 mg/L, SCW promoted isomerization and retro-aldol condensation reactions of glucose, while high glucose concentrations (> 10 mg/L) led to the increased 5-HMF conversion from 5 to 20%.

Specifically, starch hydrolysis in SCW media was scarce, mainly targeting glucose as a final product (Nagamori & Funazukuri, 2004; Orozco et al., 2012; Rogalinski, Liu, Albrecht & Brunner, 2008, Table 2.2). Then, temperatures > 180 °C were used to produce glucose monomers, further degradation resulted in 5-HMF, furfural formation (0.09-0.21 g/g carbon basis) from glucose at temperatures > 220 °C. The maximum yield of glucose obtained from starch was 632 g/kg on the carbon basis at 200 °C and 30 min (Nagamori & Funazukuri, 2004). Also, with the assistance of CO₂, where the formation of carbonic acid dissociates to increase the hydronium ion concentration of the solution (30 bar), a glucose yield of 548 g/kg carbon basis was obtained at 200°C in a shorter reaction time of 15 min (Orozco et al., 2012). However, SCW hydrolysis using mild temperatures (100-150 °C) is yet to explore to investigate the starch chain behavior based on amylose and amylopectin association. Moreover, to form a continuous network using starch as the matrix needs accurate control of starch hydrolysis, as high temperatures tend to reduce the chain length, making it challenging for starch molecules to react and cross-link. More

studies are needed to understand and optimize starch hydrolysis and cross-linking effect of starch and bioactives in SCW media.

Another model biopolymer studied by SCW hydrolysis is chitin. The reaction mechanism and hydrolysis rate of chitin are affected by its crystallinity. Aida et al. (2014) reported that high crystallinity (95%) prevented the hydrolysis process of raw chitin, due to the highly ordered structure that is less accessible to water attack. The major hydrolysis products of chitin in SCW are acetic acid and 5-HMF, but glucosamine was not obtained because of its deamination to produce glucose (Quitain, Sato, Daimon & Fujie, 2001). These products were produced above 283 °C, showing significantly higher resistance to hydrothermal degradation than starch (180 °C), due to *N*-acetyl group that can stabilize chitin crystallite structure by the additional hydrogen bond between -OH group and *N*-acetyl group (Yang, Wang, Zhou & Wu, 2018b).

In terms of phenolic acids, caffeic acid was selected as a model compound and subjected to degradation under SCW conditions within 160-240 °C (Khuwijitjaru et al., 2014). Depending on the degree of hydrolysis, main degradation products of hydroxytyrosol, protocatechonic aldehyde and 4-vinylcatechol were detected in the hydrolysates (Khuwijitjaru et al., 2014, Table 2.2). Interestingly, degradation products of caffeic acid contain the phenol structure and were stable in SCW even after treatment at 250°C for 120 min, further contributing to high antioxidant activity. Therefore, caffeic acid may be used in a high temperature process with preserved antioxidant activity.

Table 2.1 Reactions of model and real systems in subcritical water.

Compound/biomass	Treatment conditions	Reaction pathway and degradation products	Ref
Model systems			
Guaiacol (model system for lignin)	210-290 °C, unspecified pressure, 7200 s	Cleavage of the ether bonds connecting structural units to produce catechol as the main product.	Sasaki & Goto (2011)
Guaiacol (model system for lignin)	300-450 °C, 250 bar, 0.5-40 s	-Phenol radicals formed first, which could further react with hydrogen from another guaiacol to form phenol. - Minimal formation of catechol in the subcritical region compared to the supercritical region.	Yong & Yukihiro (2013)
Glucose (model system for carbohydrates)	200-240 °C, 150-200 bar, 40-120 s	-D-fructose from glucose isomerization. -Glyceraldehydes from glucose retro-aldol condensation. -5-HMF and 2-furfural through from glucose dehydration.	Saito et al. (2009)
Glucose (model system for carbohydrates)	175-275 °C, 100 bar, 0-60 s	-Isomerization and retro-aldol condensation reactions to produce fructose, glyceraldehydes and/or glycolaldehyde at glucose concentration < 10 mg/L. -Dehydration reactions to produce 5-HMF at glucose concentration < 10 mg/L.	Yu & Wu (2011)
Starch (model system for carbohydrates)	180-240 °C, unspecified pressure, 600-1800 s	-Glucose as the main product (632 g/kg on carbon basis) produced at 200 °C and 30 min. -Further dehydrated products of 5-HMF and furfural detected at >220 °C.	Nagamori & Funazukuri (2004)
Chitin (model system for carbohydrates)	220 °C, unspecified pressure, 60-1200 s	-Deacetylation and dehydration of glucosamine to form 5-HMF. -Deacetylation of glucosamine to form acetic acid.	Aida et al. (2014)
Chitin (model system for carbohydrates)	280-366 °C, unspecified pressure, 0-1190s	Hydrolysis kinetics of chitin followed first-order model, yielding activation energies of 215.4 kJ mol ⁻¹ (283-323 °C), 153.7 kJ mol ⁻¹ (323-344 °C) and 297.4 kJ mol ⁻¹ (344-366 °C).	Yang et al., (2018b)

Table 2.1 (Continued)

Compound/biomass	Treatment conditions	Reaction pathway and degradation products	Ref
Caffeic acid (model system for phenolic acids)	160-240 °C, 50 bar, 30-1080 s	Decarboxylation of caffeic acid to form hydroxytyrosol (~ 14-34 mol%), protocatechuic aldehyde (~ 9 mol%), and 4-vinylcatechol (~ 38-57 mol%).	Khuwijitjaru et al. (2014)
Real systems			
Corn stalk	Supercritical water (380 °C, 230-240 bar, 9-10 s) + subcritical water hydrolysis (240 °C, 80-90 bar, 45-50 s)	Hexoses yields of 20.6-29.4 g/100 raw material.	Zhao et al. (2012)
Lupin hull	180-260 °C, 100-200 bar, 2-10 mL/min	Optimum hemicellulosic sugar yield of 85.5 wt% at 180 °C, 50 bar, 5 mL/min.	Ciftci & Saldaña (2015)
Palm fiber and coconut husk	208-257 °C, 200 bar, 30 min	-Maximum total reducing sugars recovered from coconut husk (11.7 g/100 g raw material) and palm fiber (11.9 g/100 g raw material). - Maximum xylose production of 1.58 g/100 g coconut husk and 0.87 g/100 g palm fiber.	Prado et al. (2014)
Sugarcane straw	190-260 °C, 90-160 bar, 480 s	The highest yield of glucose, xylose, galactose and arabinose were 2.1, 2.3, 0.7 and 1.0g/g straw at 200 °C and 100 bar.	Lachos-Perez et al. (2017)
Shrimp shell	90-373 °C, unspecified pressure, 5-60 min	-Maximum amino acid yield of 70 mg/g of dry shrimp shell at 250 °C and 60 min. -No glucosamine produced due to deacetylation and deamination of glucosamine, forming acetic acid and ammonia.	Quitain et al. (2001)
Shrimp cephalothorax waste	230-280 °C, 28-202 bar, 5-30 min	Maximum protein removal of 96% and chitin yield of 82.2 wt% based on raw material at 260 °C and 50 bar for 30 min.	Espíndola-Cortés et al. (2017)

Table 2.2 Conversion pathway of model systems in SCW media.

Compounds	Treatment	Conversion pathway	Ref
Glucose (Initial feed concentration: 15-100 mg/mL water)	Continuous system; 200-240 °C, 150-200 bar, 40-120 s	<p>The diagram illustrates the conversion pathway of glucose in supercritical water (SCW) media. It starts with Glucose, which can undergo retro-aldol cleavage to form Glycolaldehyde and Glycerinaldehyde. Alternatively, Glucose can isomerize to Fructose. Fructose then undergoes dehydration, losing three water molecules (-3H₂O), to form 5-HMF and Furfural. Finally, 5-HMF and Furfural are converted to Formic acid and Acetic acid under acidic conditions (H⁺), with the conversion of 5-HMF also involving the addition of two water molecules (2H₂O).</p>	Saito et al. (2009)

Table 2.2 (Continued)

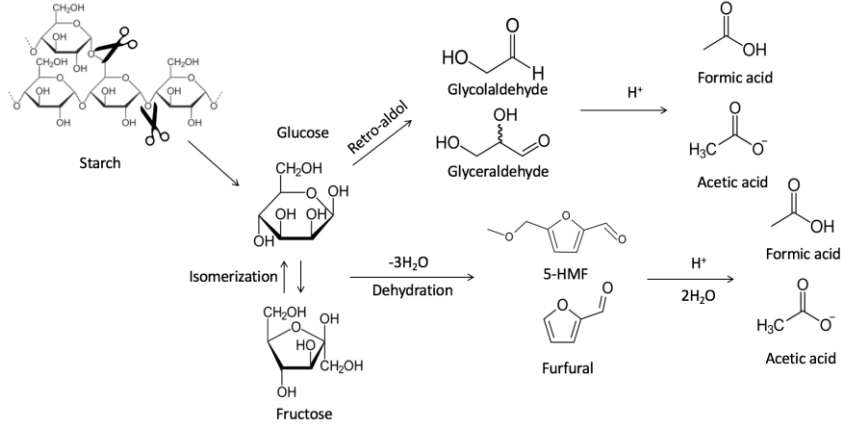
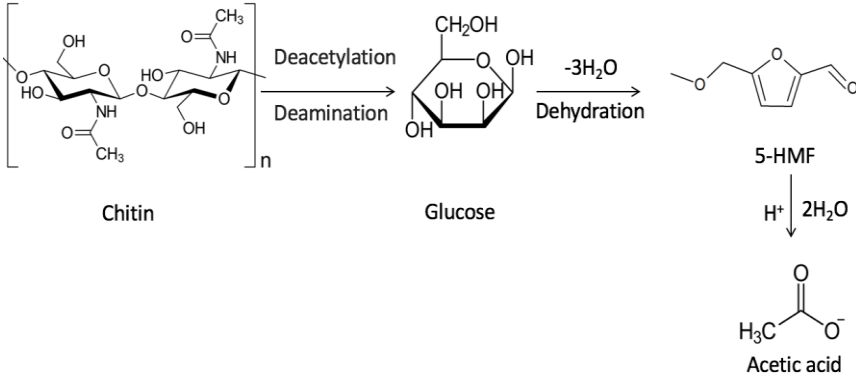
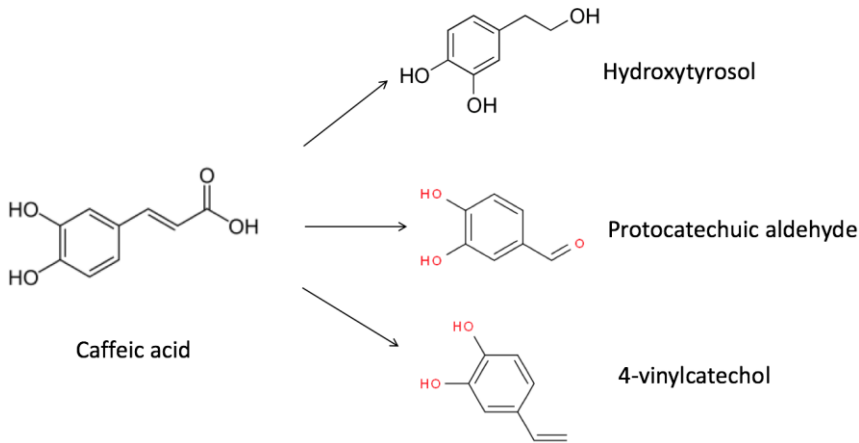
Compounds	Treatment	Conversion pathway	Ref
<p>Starch (100 mg/mL water)</p>	<p>Batch system; 180-240 °C, Unspecified pressure, 300-2400 s</p>	 <p>Starch</p> <p>Glucose</p> <p>Retro-aldol</p> <p>Glycolaldehyde</p> <p>Glyceraldehyde</p> <p>Formic acid</p> <p>Acetic acid</p> <p>Isomerization</p> <p>Fructose</p> <p>Dehydration</p> <p>5-HMF</p> <p>Furfural</p> <p>Formic acid</p> <p>Acetic acid</p>	<p>Nagamori & Funazukuri (2004); Saito et al. (2009)</p>
<p>Chitin (33.3 mg/mL in water)</p>	<p>Batch system; 220-400 °C, Unspecified pressure, 60-1200 s</p>	 <p>Chitin</p> <p>Deacetylation</p> <p>Deamination</p> <p>Glucose</p> <p>Dehydration</p> <p>5-HMF</p> <p>Acetic acid</p>	<p>Aida et al. (2014); Quitain et al. (2001)</p>

Table 2.2 (Continued)

Compounds	Treatment	Conversion pathway	Ref
<p>Caffeic acid (Initial feed concentration: 100 mg/mL water)</p>	<p>Continuous system; 160-240 °C, 50 bar, 30-1080 s</p>	 <p>The diagram illustrates the conversion pathway of Caffeic acid. Caffeic acid (3,4-dihydroxycinnamic acid) is shown on the left. Three arrows point to the products: Hydroxytyrosol (3,4-dihydroxyphenylethanol), Protocatechuic aldehyde (3,4-dihydroxybenzaldehyde), and 4-vinylcatechol (3,4-dihydroxyphenylacetylene). The hydroxyl groups in the products are highlighted in red.</p>	<p>Khuwijitjaru et al. (2014)</p>

Compared to model systems, biomass hydrolysis is a complex and extremely substrate-dependent process. The data acquired from model systems provided a good basis to understand the behavior of biomass hydrolysis. However, more studies are needed to investigate optimization of hydrolysis process with high desired product yield and low degradation product content due to complexity of raw biomass. Hydrolysis of biopolymers from lignocellulosic residues in SCW, such as sugarcane straw (Lachos-Perez et al., 2017), palm fiber, coconut husk (Prado et al., 2014), lupin hull (Ciftci & Saldaña, 2015) and corn stalk (Zhao et al., 2012) have been investigated for production of fermentable sugars or liquefaction products. These lignocellulosic biomass are rich in cellulose, hemicellulose and lignin, which are closely associated through hydrogen and covalent cross-linkages. Hence, the selective hydrolysis of hemicellulose has been conducted to acquire valuable hemicellulosic sugars and purify cellulose.

In the study by Ciftci & Saldaña (2015), lupin hull was subjected to SCW hydrolysis to obtain hemicellulosic sugars, with the optimum yield of 85.5% at conditions of 180 °C, 50 bar, 5 mL/min, and pH 6.2. Among hemicellulosic sugars hydrolyzed from palm fiber and coconut husk, xylose exhibited the highest yield with 0.77 and 1.58 g/100g raw material, respectively (Prado et al., 2014). Other biomass from marine source studied was shrimp/crab shells that are rich in chitin. The purification of chitin from shrimp waste by thermochemical methods (acid or alkali) involves deproteinization as the crucial step due to the restricted hydrolysis of the fraction embedded in the complex chitin-protein matrix network. A high protein removal up to 96% was obtained for the 0.17 chitin:H₂O (w/w) ratio for 30 min treatment at 260 °C and 50 bar, reaching chitin yield of 82.2 wt% based on raw material (Espíndola-Cortés et al., 2017). It is noticeable that no glucosamine was produced at >320 °C due to deacetylation and deamination of glucosamine to acetic acid and ammonia (Quitain et al., 2001).

To understand biopolymer (starch and chitosan) reaction in SCW, additional review on starch structure is provided.

2.2 Starch reactions

2.2.1 Starch

Starch is a homo-polysaccharide with repeating units of glucose linked through α -1,4 and α -1,6 glycosidic bonds. It is a biopolymer due to its natural origin. Commercial starches are obtained mainly from maize, potato, wheat, rice, and cassava. Starch is constituted by two main components: the linear polymer of amylose and branched amylopectin joined by α -1,4 bonds in the linear sections, and by α -1,6 bonds in the branch points. Further arrangement of amylose and amylopectin contribute to the formation of amorphous and crystalline regions, generating the concentric layers that contribute to the “growth rings” that are visible by light microscopy (Fig. 2.1). It is suggested that amylose and the branching point of amylopectin form the amorphous regions while the linear sections in the amylopectin contribute to the main crystallinity of granular starch (Cheetham & Tao, 1998). The ratio of amylose/amylopectin depends on the source and maturity of the plant. Generally, regular starch has 25-30% amylose and 70-75% amylopectin (Brown & Poon, 2005). However, waxy starches had amylopectin content as high as 98-99%, while others had high amylose content of 50-80% (Liu, 2005).

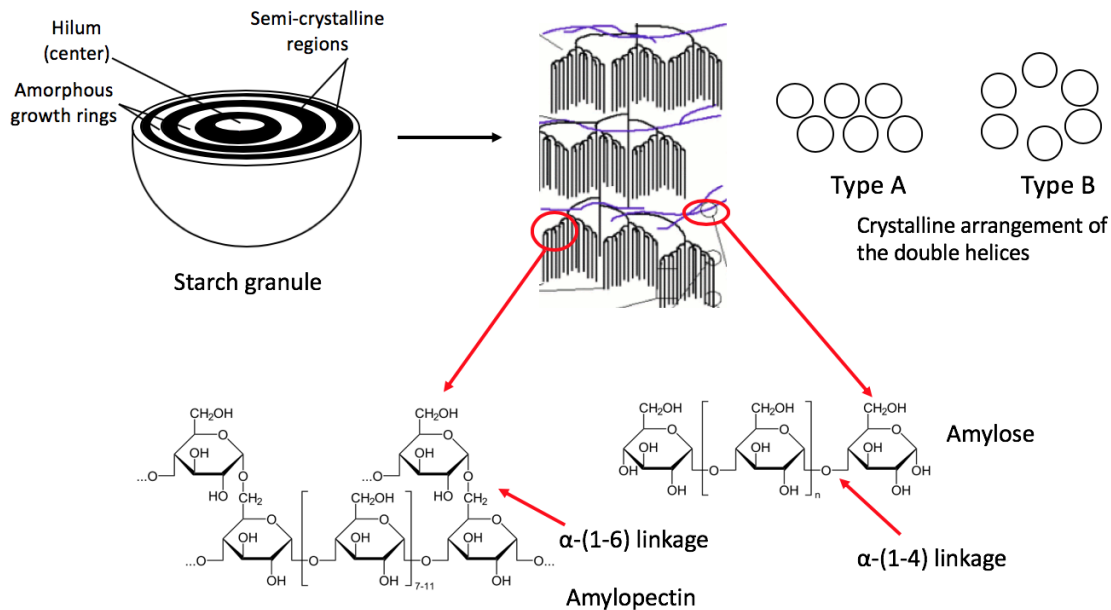


Fig. 2.1 Starch granule conformation and linkages.

Starches from different botanical sources have characteristic X-ray diffraction patterns of amylopectin. In general, the type-A starch with staggered monoclinic packing is mostly present in cereals, while diffractograms of starches from tubers, rhizomes, and high-amylose maize are designed as hydrated type-B with hexagonal crystallites. Moreover, some seeds and legumes show a type-C pattern that is a mix of type A and B (Parker & Ring, 2001).

Starch is not considered a natural thermoplastic polymer, but in the presence of a plasticizer (water, glycerol or sorbitol), shearing, and high temperatures (90°C-140°C), starch gelatinization can be achieved during extrusion (Vilpoux & Averous, 2004). The starch granules swell, forming a viscous paste, with destruction of most of inter-molecule hydrogen links, enabling its use in injection, extrusion, and blowing equipment, such as those for synthetic plastics (e.g. polyethylene, polypropylene and polyvinyl chloride).

2.2.2 Starch film formation techniques

In general, starch films can be obtained through two main techniques, as shown in Fig. 2.2: solution casting (wet method) and thermoplastic processing (dry method) (Paes, Yakimets & Mitchell, 2008). Using the wet processing method, starch film is formed from a film-forming solution that contains high amount of water (>90%). In contrast, a dry process can be conducted in low water content (20-40%). This method is used for materials with thermoplastic properties where the material goes through reversible solid-gel transition upon heating and cooling, therefore, they can be molded into a determined shape when submitted to a thermal/mechanical process (Jiménez et al., 2012a). However, native starch does not present this thermoplastic property, only when plasticizers such as water or glycerol are added. The crystalline starch structure disappears when it is heated to temperatures above 70-90 °C, leading to the formation of thermoplastic starch (Huneault & Li, 2007).

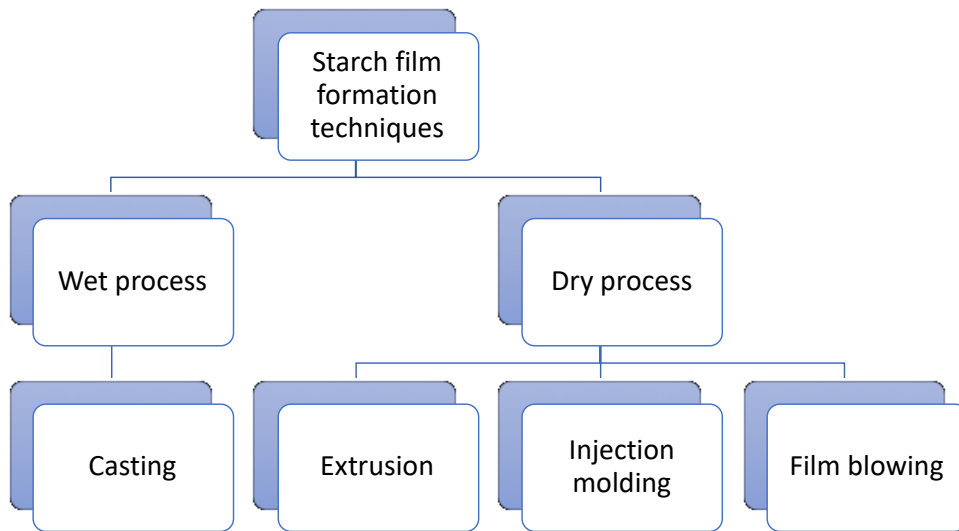


Fig. 2.2 Starch film formation techniques.

2.2.2.1 Wet process

This simple wet process, extensively used by researchers at laboratory scale (Bourtoom, 2008; Dias, Müller, Larotonda & Laurindo, 2010; Nandi & Guha, 2018; Othman, Azahari, & Ismail, 2011; Pyla et al., 2010), mainly consists of gelatinization, mixing, casting and drying. During the starch gelatinization, granules are disrupted in an excess of water by means of a heating step. Once the starch has been gelatinized and other components (e.g. bioactives, plasticizer) have been added to the mixture, the following step is homogenization. This step can be combined with or even conducted prior to the first step, depending on the film formulation. Homogenization is compulsory when non-miscible components are added in order to obtain a stable emulsion and an adequate integration of all components (Souza, Goto, Mainardi, Coelho & Tadini, 2013). In the last stage, the obtained solution is poured or casted on Petri dishes and allowed to dry under controlled conditions of temperature and relative humidity. Recently, Nandi & Guha (2018) dried potato starch/guar gum (3.7:0.4 w/w) films at 37 °C for 24 h (unspecified relative humidity), whereas Jiménez et al. (2012b) obtained corn starch films (unknown amylose content) by drying at room temperature and 45% relative humidity for 60 h. However, the difficulty in scaling-up the production and long drying times used make the solution casting technique challenging at industrial scale.

2.2.2.2 Dry process

As mentioned above, thermoplastic starch can be produced by adding a plasticizer, so that it can be repeatedly softened and hardened, allowing starch to be molded or shaped by the action of heat and shear forces. According to Carvalho (2008), the production of thermoplastic starch is generally conducted at 140-160 °C, high shear up to 120 rpm and high pressure up to 70 bar using an extruder in the presence of a plasticizer. The dry process typically include extrusion,

injection molding and film blowing process (Li et al., 2011; Matzinos, Tserki, Kontoyiannis & Panayiotou, 2002; Yan, Hou, Guo & Dong, 2012; Zullo & Iannace, 2009).

Extrusion usually includes two steps, where the starch is mixed with plasticizers and extruded to disrupt the starch granules, thus obtaining a thermoplastic starch, followed by a slit or flat film die that molds starch into films/sheets (Walenta, Fink, Weigel, Ganster & Schaaf, 2001; Yu & Christie, 2005). In some studies, the thermoplastic starch paste or pellet is produced first and kept at room temperatures for few hours, promoting stress-relaxation and stabilization. Then, these pellets are extruded using a film-blowing die (Leblanc et al., 2008) or injected and molded under high pressure of 1400 bar (Tábi & Kovács, 2007). In this case, gelatinization is achieved at low moisture content due to the high-shear and high-pressure conditions used, which breaks down the starch granules, allowing fast water transfer into the starch molecules. However, the intense shear can break down the molecule chain and cause poor film mechanical properties (Liu et al., 2009).

Film blowing is a method commonly used to produce plastic films, where the material is extruded as an empty tube, then the pressure inside the tube is increased to expand the film. Due to the stretching of film tube by elongation rolls and the circumferential direction by air pressure existing inside the tube, a two-axes molecular orientation is imparted into the materials produced during the film blowing process, influencing film morphological properties (Matzinos et al., 2002). However, the preparation of thermoplastic starch films using film blowing technique is still a challenge. Most film blowing studies conducted on thermoplastic starch blends only use starch at a moderate ratio (<40 wt%), due to the sticky surface and poor adhesiveness to melt without rupture of starch (Thunwall, Kuthanova, Boldizar & Rigdahl, 2008). Also, the large surface to volume ratio of the film during blowing may interfere with the stability of the

solidification process when the film is exposed to surrounding air longer than 40 s, as starch is a hydrophilic polymer and is sensitive to moisture (Janssen & Moscicki, 2006). To overcome these disadvantages, Matzinos et al. (2002) blended thermoplastic starch with polycaprolactone (10-50 wt%) to adjust the rheological properties of the melt before the film blowing process. Other blends such as poly (butylene adipate co-terephthalate)/cassava starch at 6:4 w/w (Reis et al., 2014), linear low-density polyethylene/cassava starch at 6:4 w/w (Khanonkon, Yoksan & Ogale, 2016) and hydroxypropyl starch phosphate/polyhydroxyalkanoate at 4:1 w/w (Sun, Liu, Ji, Hou & Dong, 2018) have also been investigated to improve the film moisture resistance and mechanical properties.

To date, only few publications have reported the preparation of thermoplastic starch/biopolymer films using the film blowing process, where chitosan has been the most studied biopolymer component (Dang & Yoksan, 2015; Dang & Yoksan, 2016; Pelissari, Grossmann, Yamashita & Pineda, 2009; Pelissari et al., 2012). With the addition of chitosan, improved extrusion processability and reduced surface stickiness were observed in composite films compared to the neat thermoplastic starch film (Dang & Yoksan, 2016).

2.2.3 Incorporation of polymers in starch-based films

2.2.3.1 Chitosan

Chitosan, composed of β -(1-4)-linked D-glucosamine and N-acetyl-D-glucosamine, is a deacetylated product of chitin and is considered a non-toxic and biodegradable polymer (Beverly, Janes, Prinyawiwatkula & No, 2008). Chitosan has shown great potential to be used in packaging for food preservation against a wide variety of microorganisms due to its antimicrobial activity. Three models have been proposed with regards to chitosan's antimicrobial mechanism: 1) the electrostatic interaction between positively charged chitosan

molecules and negatively charged microbial cell membranes, resulting in imbalanced internal osmotic environment and leakage of intercellular electrolytes (Raafat, von Bargaen, Haas & Sahl, 2008); and 2) the chelation of metal ions, suppression of spore germination and binding to essential nutrients for microbial growth (Roller & Covill, 1999). Several studies evaluated the effectiveness of chitosan incorporated in starch films. For example, the clear zone on agar plate enlarged significantly from 6.9 to 29.1 mm² when the addition of chitosan into sweet potato starch increased from 5% to 15% on an *E. coli* inoculated media (Shen, Wu, Chen, & Zhao, 2010). In a more recent study, films containing 70% sweet potato starch and 30% chitosan delayed the total aerobic bacteria growth on sliced pork by 1.5 log (CFU/g) during 7-day storage at 10 °C, corresponding to an extension of shelf-life for 3 days, compared to non-coated sliced pork (Valencia-Sullca, Vargas, Atarés & Chiralt, 2018a). A significant antimicrobial effect was reported by Zhao et al. (2018), where bioactive cassava starch-based films with the highest chitosan loading (15 wt% of starch) showed prolonged ham shelf-life up to 25 days compared to the control (7 days).

In addition, chitosan incorporation also enhanced starch film physico-chemical and mechanical properties. Dang & Yoksan (2016) reported that adding chitosan (0.37-1.45 wt%) to cassava starch led to improved film hydrophobicity and oxygen barrier properties, showing increased contact angle from 52° to 76° and oxygen permeability reductions from 6.5×10^{-16} to 3.9×10^{-16} mol/m.s.Pa with respect to pure cassava starch film. The authors also observed a decreased in water vapor permeability (WVP) values by 40%, which was attributed to more hydrogen bond interactions between starch and chitosan molecules that imparted greater hydrophobicity to the films and reduced the interaction of the film matrix with water molecules (Pelissari et al., 2012) . Similarly, Lopez et al. (2014) reported that corn starch-chitosan films

showed a low WVP value (3.1 g.mm/m².h.kPa) at a high chitosan concentration (10 wt% of starch). However, WVP values showed that chitin addition (2.11 g.mm/m².h.kPa) had more pronounced effect than chitosan (3.1 g.mm/m².h.kPa) attributed to the high amount of acetyl groups in its structure. Moreover, the formation of intermolecular hydrogen bonding between NH₃⁺ of the chitosan backbone and -OH of the corn starch was found to improved the film tensile strength, reaching a maximum of 6.5 MPa at 61 wt% of starch (Ren et al., 2017).

2.2.3.2 Cellulose and derivatives

Cellulose, a linear homo-polysaccharide composed of D-glucan units linked by β -1-4-linkages, is considered to be the most abundant renewable biopolymer on earth (Bourtoom, 2008). Due to the linearity of the cellulose backbone, adjacent chains form water-insoluble aggregates through numerous hydrogen bonds, resulting in poor solubility and processability of cellulose, limiting its wide application (Wang, Lu & Zhang, 2016). However, cellulose displays strong mechanical strength, low aqueous solubility, high resistance to moisture permeability and effective resistance to acid hydrolysis due to strong hydrogen bondings within the cellulose microfibrils (Müller, Laurindo & Yamashita, 2009; Slavutsky & Bertuzzi, 2014).

In most studies, cellulose incorporation increases film tensile strength, and decreases elongation capacity. Babae et al. (2015) reported an increased modulus and strength of corn starch composite film with 10 wt% pure cellulose nanofibers compared to the pure corn starch film. The Young's modulus and tensile strength increased from 16.6 and 8.6 MPa to 141 and 38 MPa, respectively. Similarly, the incorporation of 0.1 and 0.5 g cellulose fiber/g cassava starch increased the tensile strength of reinforced films by 6.7 and 18 times, respectively (Müller et al., 2009). In a recent study, potato or cassava starch films showed significant decrease in elongation at break from 13.8% to 2.12% and 4.6% to 2.1%, respectively, after the incorporation

of 20 wt% pure microcrystalline cellulose (El Halal et al., 2018). According to Lu et al. (2005), cellulose fibers interacted strongly with the starch matrix through hydrogen bonds, restricting the movement of the chain of the polymer matrix.

The interaction between starch and cellulose can also contribute to the improvement in film WVP and film solubility in water. According to Slavutsky & Bertuzzi (2014), the permeation process was controlled by the water diffusion and depended on the tortuous pathway formed by cellulose nanocrystals incorporation. The addition of cellulose nanocrystals (3 wt%) reduced the corn starch film solubility from 26.6% to 18.5%, and the WVP from 2.5 to 0.82 g.mm/m².h.kPa. Due to the chemical similarity between starch and cellulose, structural and interface defects decrease, creating a strong resistance to the passage of water molecules. A similar study reported that WVP values decreased significantly from 0.47 to 0.3 g.mm/m².h.kPa when increasing the cellulose nanofibers content from 0 to 15 wt%. The presence of cellulose nanofibers increased the compactness of the film network, voiding space in starch films. Conversely, the greater aggregation and extent of pores in the network structure might facilitate the water vapor permeation at cellulose nanofiber concentrations above 20 wt% (Li, Tian, Jin, & Li, 2018).

Different forms of cellulose have also been utilized, including carboxymethyl cellulose (CMC), methylcellulose (MC), hydroxypropyl cellulose (HPC) and hydroxypropylmethyl cellulose (HPMC). They are produced by etherification of water-insoluble cellulose with monochloroacetate (chloroacetic acid), methyl chloride, propylene oxide, and mixed propylene oxide/methyl chloride, respectively (Khalil et al., 2017; Olivas & Barbosa-Cánovas, 2005). These derivatives have been successfully applied on various food products as coatings, especially for fruits and vegetables. Films based on cellulose derivatives are generally

transparent, flexible, odorless, tasteless, and moderate to oxygen permeability. However, due to their high water solubility after chemical modification, they can impair the film water vapor barrier property. Examples of cellulose derivative films were reported by Ma et al. (2008), who developed composite films from pea starch and CMC (3-12 wt%) through extrusion. The use of microcrystalline cellulose increased the thermal stability. But, the addition of CMC resulted in the decrease of thermal stability, which was ascribed to the poor thermal stability of CMC. In another study performed by Jiménez et al. (2012b), water barrier properties of corn starch films were hardly affected by the addition of HPMC, ranging from 5.21 to 10.3 g.mm/m².h.kPa, although oxygen permeability increased more than 7 times from 4.2 to 31.1 x10¹⁴ cm³ m⁻¹ s⁻¹ Pa⁻¹ when HPMC content increased to 50 wt%, due to its poor oxygen barrier properties. Moreover, the presence of a dispersed phase of HPMC (0-20 wt%) in corn starch matrix led to the decrease of film tensile strength from 10.5 to 8.5 MPa, due to the loss in the cohesion forces between starch and HPMC in the film (Ortega-Toro, Contreras, Talens & Chiralt, 2015).

2.2.3.3 Other biopolymers

Various gums, including gum arabic (Vigneshwaran, Ammayappan & Huang, 2011), κ -carrageenan (Oladzadabbasabadi, Ebadi, Nafchi, Karim & Kiahosseini, 2017), gellan (Sapper, Wilcaso, Santamarina, Roselló & Chiralt, 2018), and xanthan (Arismendi et al., 2013) have been added into starch-based films to improve water solubility and humidity stability. These films are often used in applications that require fast and high water solubility, such as breath films and sore throat films (Embuscado & Huber, 2009). Kim et al. (2015) obtained gum composite cassava starch films with increased film solubility in water, films containing gum arabic or xanthan gum (0.2%) showed closed to 20% solubility compared to pure starch film that exhibited

1% solubility. Chen et al. (2009) reported a significant increase in viscosity of starch/decolorized hsian-tsau leaf gum mixture compared to the gelatinized starch, indicating pronounced interactions between soluble starch and hsian-tsau leaf gum through hydrogen bondings and entanglements of starch and gum molecules. High viscosity of film-forming solutions can prevent sagging by gravity effects and allow capillary leveling when it is used for coating on food product surfaces (Peressini, Bravin, Lapasin, Rizzotti & Sensidoni, 2003). It is still essential to optimize the rheological properties of film-forming solution for the operating process, otherwise, high viscosity solution mixtures can block tubing of equipment.

In addition to gum, proteins have been used as another filler in starch-based films due to its high miscibility with starch. The addition of peanut protein isolate to the pea starch film significantly reduced tensile strength from 5.44 to 3.06 MPa, but increased elongation from 28.56% to 98.12% with the incorporation of protein at 50 wt%. Film solubility decreased from 22.31% to 9.78% with the addition of 50% peanut protein isolate (unspecified purity) (Sun, Sun, & Xiong, 2013). Hence, Basiak et al. (2017b) suggested that film surface properties can be modified according to the starch/whey protein ratio and were mainly related to the polar groups exposed on the film surface. Films composed of 80% starch and 20% whey proteins showed the highest contact angle of 89° than other composite films due to the cross-linkings of starch and protein molecules that reduced the hydrophilic groups available on the film surface.

2.2.3.4 Synthetic polymers

The main purpose of producing combined starch and synthetic polymer films is to improve the barrier or mechanical properties as dictated by the need of a specific application. Commonly used synthetic polymers can be divided into biodegradable and non-biodegradable polymers (Fig. 2.3). Three major challenges should be carefully considered before adding these

polymers: 1) poor adhesion and compatibility between the hydrophilic starch and the hydrophobic synthetic polymer that can result in weak functional properties; 2) minimization of film biodegradability; and 3) restricted amount of starch $\leq 40\%$ in the total composite (Pushpadass, Bhandari & Hanna, 2010). In the low-density polyethylene/linear low-density polyethylene/thermoplastic starch films, tensile strength and elongation at break decreased from 18 to 10.5 MPa and 340 to 200%, respectively, when starch content increased from 5 to 20% (Sabetzadeh, Bagheri & Masoomi, 2015). Other starch/non-biodegradable synthetic polymer composite films included polypropylene/thermoplastic corn starch (70:30 w/w) films and cassava starch/polyvinyl chloride (100:0-50:50 w/w) films (Martins & Santana, 2016; Wang et al., 2018). Results showed that the adhesion between starch and polypropylene (30:70 w/w) was improved by the addition of stearic acids (3 wt%) as a compatibilizer (Martins & Santana, 2016), leading to increased tensile strength from 15.5 to 19.5 MPa. In this case, the compatibilizer reduced the interfacial energy and homogenized the polar starch with synthetic polymer, improving the interfacial tensions between the phases. But, the synthetic polymer (e.g. polyvinyl chloride) still needs to be the main component (> 50 wt%) in order to have a continuous phase to maintain the mechanical strength of the composite film (Wang et al., 2018).

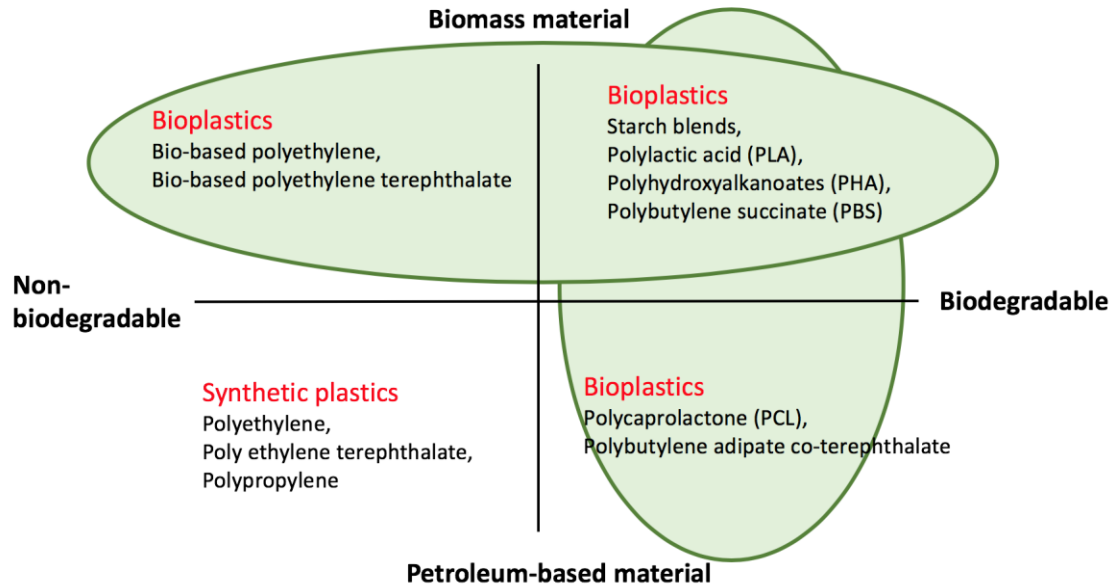


Fig. 2.3 Classification of packaging materials.

To preserve starch composite films biodegradability while improving the mechanical properties, the mixture with other biodegradable synthetic polymers, such as poly butylene adipate co-terephthalate (PBAT), polylactic acid (PLA), poly vinylalcohol (PVOH), and polycaprolactone (PCL) is frequently used (Fourati, Tarrés, Mutjé & Boufi, 2018; Garcia et al., 2011; Muller, González-Martínez & Chiralt, 2017; Olivato, Grossmann, Bilck & Yamashita, 2012; Shirai et al., 2013; Tian, Yan, Rajulu, Xiang & Luo, 2017). According to Das et al. (2010), the borax (5 wt%) cross-linked starch/PVOH (50:50 w/w) exhibited higher mechanical properties than the control film without cross-linking, showing improved tensile strength and tensile modulus by 160 and 390%, respectively. The complex formation between three -OH groups of the borate ion and those of starch and PVOH resulted in a highly rigid three-dimensional network structure. Conversely, Ortega-Toro et al. (2015) reported that the lack of interfacial adhesion between PBAT and starch phases promoted film fragility and reduced elongation from 28 to 2.7%, but elastic modulus of the films with low poly ϵ -caprolactone

concentrations (< 40 wt%) increased slightly from 587 to 662 MPa. Thus, the compatibility between starch and synthetic biodegradable polymers is still a challenge and the high cost associated with the use of these polymers (e.g. PLA) make them less competitive compared to petroleum-based polymers.

2.2.4 Incorporation of bioactive compounds in starch-based films

2.2.4.1 Phenolic acid and phenolic compounds from plant extract

Starch-based films can be formulated with bioactive compounds to improve the overall film functional properties to warrant protection to food products. Among bioactives, phenolic compounds were the most studied and have shown great potential to be used in food packaging to preserve against a wide variety of microorganisms (Valdés et al., 2015), other antioxidant additives include tocopherol and some organic acid like ascorbic acid (Fig. 2.4). Antioxidant/antimicrobial effects of phenolic compounds have been attributed to the presence of hydroxyl groups in their chemical structure. Hence, this effect can be strongly affected by the number and position of substitution in the benzene ring, and by the saturated chain length (Albarran, Boggess, Rassolov & Schuler, 2010). Beyond that, these antioxidants can also react with film matrix and modify film structure and properties.

Phenolic compounds can be directly added into films either as a pure chemical component or as an extract from phenolic enriched plants (Fig. 2.4). Such pure compounds are gallic acid (Zhao et al., 2018), ferulic acid (Mathew & Abraham, 2008) and tannic acid (Pyla et al., 2010). On the other hand, widely used plant extracts are rosemary extract (Piñeros-Hernandez, Medina-Jaramillo, López-Córdoba & Goyanes, 2017), thyme extract (Talón, Trifkovic, Vargas, Chiralt & González-Martínez, 2017), *yerba mate* extract (Reis et al., 2015), green tea extract (Perazzo et al., 2014; Talón et al., 2017), pomegranate peel extract (Harini,

Mohan, Ramya, Karthikeyan & Sukumar, 2018a), betel leaves extract (Nouri & Nafchi, 2014) and grapefruit seed extract (Bof, Jiménez, Locaso, Garcia & Chiralt, 2016). Piñeros-Hernandez et al. (2017) reported that increasing the rosemary extract content from 5 to 20 wt% into the cassava starch films led to 3-times higher polyphenol content, with the subsequent increment of the DPPH-radical scavenging activity of the films to more than 65%. Besides, due to the presence of carbonyl groups ($-\text{COO}^-$) in gallic acid of murta leaf extract, it can be suggested that non-dissociated gallic acid can form ester linkages when it reacts with $-\text{CH}_2\text{OH}$ groups of starch, creating cross-linking that enhanced film mechanical properties (Silva-Weiss, Bifani, Ihl, Sobral & Gómez-Guillén, 2013). Similarly, in chitosan-starch-thyme extract blend films, the cross-linking effect due to tannic acid addition inhibited the release of total polyphenols in acid medium, showing less total free polyphenols (4.6 mg gallic acid equivalence/g film), compared to non-cross linked films (11.7 mg gallic acid equivalence/g film) (Talón et al., 2017). Overall, starch-based films incorporated with various phenolic acids and plants extracts exhibited enhanced mechanical strength and water barrier properties through the cross-linking formation, mainly ester linkage. Moreover, the antioxidant activity provided to the film protected food products from oxidation. It is attractive to use a plant extract instead of a pure phenolic compound due to less purification. Also, various phenolic compounds found in the extract may exhibit synergistic effect, resulting in higher antioxidant activity compared to the pure phenolic compound. Table 2.3 summarizes the main studies carried out on phenolic compounds/starch-based film formation.

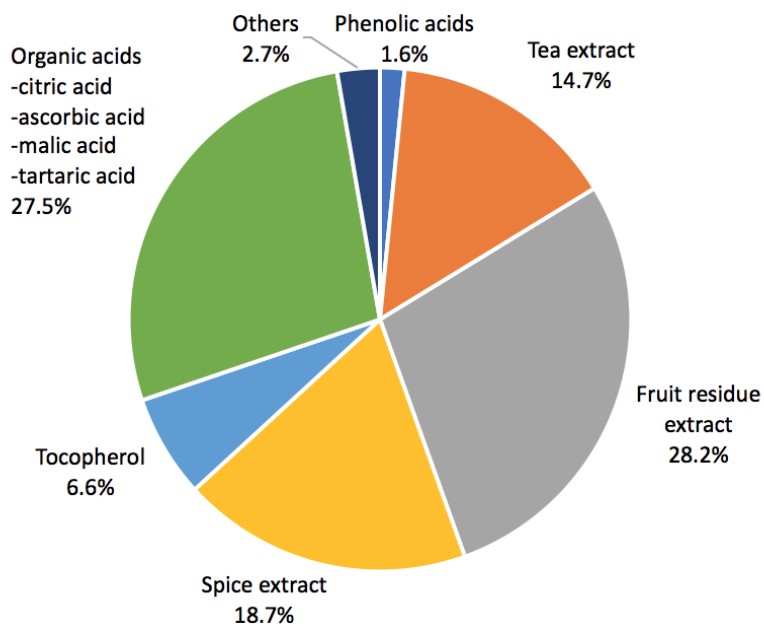


Fig. 2.4 Common antioxidants incorporated in starch-based films. Number of research articles published between 2008 to 2018 obtained from a literature search using the keywords “antioxidants in starch-based films”. Portions of each antioxidant were calculated using the number of publications containing certain antioxidant divided by the total number of publications on antioxidants in starch-based films. (Source: Web of Science database 2008-2018)

Table 2.3 Bioactive starch-based films containing different phenolic acids or plant extracts.

Phenolic acid or plant extract	Method/ film matrix	Film characteristics and improvement	Funtionality/application	Ref
Ferulic acid (0.025-0.2 g/g starch)	Casting, Potato starch: chitosan (1:2 w/w)	-Increased tensile strength from 43 62.7 MPa -Decreased elongation from 30 to 21.6%. -Cross-linking via ester and hydrogen bonds between starch, chitosan and ferulic acid. -Decreased WVP from 1.41 to 1.15 g.mm/m ² .h.kPa.	-Reduced oil peroxide value from 28.5 to 11.5 mg/kg.	Mathew & Abraham (2008)
Gallic acid (0.1 g/g starch)	SCW processing, Chitosan:cassava starch (0.025-0.15:1 w/w)	- Improved tensile strength from 0.51 to 0.83 MPa -Improved elongation from 70.2 to 100.1%. -Increased contact angle from 36.71° to 68.26° for the top surface and from 55.15° to 94.69° for the bottom surface. -Cross-linking via ester and hydrogen bonds and electrostatic interactions between starch, chitosan and gallic acid. -Decreased WVP from 0.67 to 0.36 g.mm/m ² .h.kPa.	ABTS: 548-742 Trolox equivalent mg/g film; FRAP: 395-488 Trolox equivalent mg/g film.	Zhao et al. (2018)
Tannic acid (0.01-0.1 g/g starch)	Casting, Corn starch	-Sustained tannic acid release over 24 h.	-Increased inhibition zone from 12 to 16 mm against <i>L. monocytogenes</i> . -Decreased cell counts of <i>E.coli</i> from an initial 7.1 to 1.86 log CFU/mL. -Complete inactivation of <i>L. monocytogenes</i> with an initial cell count of 6.87 log CFU/mL at 24 h.	Pyla et al. (2010)

Table 2.3 (Continued)

Phenolic acid or plant extract	Method/ film matrix	Film characteristics and improvement	Funtionality/application	Ref
Betel leaves extract (0-0.3 g/g starch)	Casting, Sago starch	-Decreased tensile strength from 6.5 MPa to 4 MPa -Increased elongation at break from 80% to 120%. -Increased WVP from ~4.1 to 7.6 g.mm/m ² .h.kPa. -Increased oxygen permeability from ~0.22 to 0.3 cm ³ .mm/m ² day. -Prevented UV transmission in the wavelengths of 310-350 nm.	Not reported	Nouri & Leila (2014)
Blueberry extract (0.03-0.12 g/g starch)	Casting Pea starch: guar gum (2.5:0.3 w/w)	-Reduced moisture content from 19.33 to 16.49%. -Reduced film solubility from 24.58 to 17.64%. -Reduced swelling degree from 40.83 to 21.16%. -Reduced WVP from 4.62 g.mm/m ² .h.kPa. -Cross-linking between phenolic compounds in extract and starch.	-Increased total phenolic content from 7 to 50 mg gallic acid equivalent/g film. -Increased total flavonoid content from 20 to 75 mg gallic acid equivalent/g of film. -Enhanced antioxidant activity from 1.23 to 19.75 mg trolox equivalent/g film by DPPH and from 0.88 to 16.64 mg trolox equivalent/g film by FRAP.	Saberi et al. (2017)

Table 2.3 (Continued)

Phenolic acid or plant extract	Method/ film matrix	Film characteristics and improvement	Funtionality/application	Ref
Grape pomace extract (0-0.08 g/g starch)	Casting Corn starch	-Improved tensile strength from 143.8 to 158.1 MPa. -Improved elongation from 12.2 to 22.0%. -Increased opacity from 0.23 to 0.49. -Increased water vapor transmission rate from 52.9 to 60.9 g/m ² h. -Increased phenolic releasing from 315 to 675 mg/cm ² .	-Increased released phenolic concentration from 315 to 1206 mg/cm ² film after 30 h.	Xu et al. (2017)
Green tea and basil extracts (5 g starch in 100 mL aqueous extract with 3g green tea or basil leaves, unspecified extract concentration)	Casting, Cassava starch	-Green tea extract added film: Contact angle: 68±3 °C Solubility: 28±1% WVP: 5.2 g.mm/m ² .h.kPa Color: almost white with a very slight Yellow tonality in acidic solution -Basil extract added film: Contact angle: 63±3 °C Solubility: 30±1% WVP: 3.4 g.mm/m ² .h.kPa Color: slight yellow	-Green tea extract added film: Polyphenols content: ~ 2.97 mg/g. -Basil extract added film: Polyphenols content:~ 1.57 mg/g.	Medina-Jaramillo et al. (2017)
Murta leaf extract (0.28 g/g corn starch + chitosan)	Casting, Corn starch:chitosan (3:1 w/w)	-Increased brown color, with b value increased from 2.08 to 63.63. -Decreased tensile strength from 20.56 to 17.13 MPa. -Decreased elongation from 13.52 to 6.57%. -Increased film thickness from 72 to 126 µm. -Cross-linking between phenolic compounds, chitosan and starch.	Not reported	Silva-Weiss et al. (2013)

Table 2.3 (Continued)

Phenolic acid or plant extract	Method/ film matrix	Film characteristics and improvement	Funtionality/application	Ref
<i>Punica granatum</i> peel extracts (minimum inhibitory concentration, value not specified)	Casting Cashew nut shell starch:walnut shell cellulose (7.5:2 w/w)	- Improved tensile strength from 5.21 to 23.58 MPa. -Decreased elongation from 102.60 to 94.14%. -Decreased oxygen transfer rate from 13.81 to 9.47 cm ³ / μmm ² day.kPa. -Decreased moisture uptake from 18.24 to 15.88%.	-DPPH inhibition of 52.12 ± 0.58% -Antimicrobial activity (inhibition zone diameter) 9.14 ± 0.11, 4.25 ± 0.47, 5.26 ± 0.71, 2.38 ± 0.47, 8.57 ± 0.61 and 9.56 ± 0.22 mm against <i>Listeria monocytogenes</i> , <i>Staphylococcus aureus</i> , <i>Escherichia coli</i> , <i>Pseudomonas aeruginosa</i> , <i>Klebsiella pneumonia</i> and <i>Salmonella enteritidis</i> , respectively.	Harini et al. (2018a)
Propolis extract (0-1.0 wt%)	Casting, Cassava starch	-Reduced puncture strength from 22.2 N to 11.3 N at 1.0 wt% propolis extract. -No effect on film tensile strength. -Significant WVP reduction from 7.06 to 2.95 g.mm/m ² .h.kPa at 1.0 wt% propolis extract.	-Increased antioxidant activity from ~380 to 1350 μmol trolox equivalent/100 g film. -Increased total phenolic content from ~ 90 to 700 mg gallic acid equivalent/100 g of film.	de Araújo et al. (2015)
Rosemary extract (unspecified essential oil content, 2.6-10.4 mg/g starch)	Casting, Cassava starch	-Improved tensile strength from 0.5 to 0.8 MPa. -Decreased elongation from 125 to 85%. -Increased contact angle from 39 to 53°.	-Increased total phenolic content from 4.4 to 13.6 mg gallic acid equivalent/g film. -Enhanced DPPH inhibition from 28.6 to 81.9%.	Piñeros-Hernandez et al. (2017)

Table 2.3 (Continued)

Phenolic acid or plant extract	Method/ film matrix	Film characteristics and improvement	Funtionality/application	Ref
Thyme extract (unspecified essential oil) content, 0.15 g/g mixed starch+chitosan) Tannic acid (0.04 g/g chitosan)	Casting, Pea starch:chitosan (1:4 w/w)	-Reduced moisture content from 21.6 to 14.6%. -No significant influence on WVP.	-Improved film antioxidant activity up to 3 times from 0.69 to 2.1 mM TEAC. -The highest polyphenol release (~50%) in acetic acid solution due to chitosan dissolution.	Talón et al. (2017)
<i>Yerba mate extract</i> (0-0.2 g/g starch)	Casting, Cassava starch	-Reduced weight loss from 87 to 80% during thermal degradation. -Reduced film melting temperature from 96 to 86 °C. -Decreased water vapor absorption from 34 to 26%.	Not reported	Jaramillo et al. (2016)
<i>Yerba mate extract</i> (0-0.3 g/g starch) Mango pulp (0-0.2 g/g starch)	Casting, Cassava starch	-Decreased WVP values from 8.6 to 5.74 g.mm/m ² .h.kPa. -Decreased film elongation from 70.28 to 55.15%. -Decreased tensile strength from 5.38 to 1.36 MPa.	-Palm oil packaged with the film containing the highest yerba mate extract and mango pulp content had the lowest decrease in peroxide value (8.70 meq/kg) after 90 days.	Reis et al. (2015)

ABTS: 6-Dydroxy-2,5,7,8-tetramethylchroman-2-carboxylic acid; DPPH: 1, 1-Diphenyl-2- picrylhydrazyl; FRAP: Ferric reducing antioxidant power; TEAC: Trolox equivalent antioxidant capacity; WVP: water vapor permeability.

2.2.4.2 Essential oils

Essential oils, complex liquid mixtures containing volatile aroma compounds from plants, have been intensively studied as bioactive compounds to be added to starch-based films. Various studies have demonstrated that carvacrol and thymol had the highest antibacterial activity among all essential oils tested (Sánchez-González et al., 2011; Soković et al., 2010). However, the use of essential oils has drawback due to its strong odour, so it is important to determine the concentration of essential oil that can be used without influencing organoleptic characteristics of food products (Jiang, Luo, & Ying, 2015; Shen & Kamdem, 2015). Moreover, unlike phenolic compounds, essential oils can create a coarser structure in the film matrix with increased heterogeneity due to its low solubility in the aqueous film-forming solution (Homayouni, Kavooosi & Nassiri, 2017). As such, cracks have been observed when carvacrol essential oil (0.1 w/w%) was incorporated to gelatinized cassava starch films, which further decreased the tensile strength from 0.30 to 0.16 MPa, causing an increase in WVP from 0.69 to 0.99 g.mm/m².h.kPa (Homayouni et al., 2017). Therefore, essential oil is often incorporated at a low concentration (<5 wt% of starch), and the use of an emulsifier is necessary to ensure a stable and homogeneous dispersion of essential oil in the starch film matrix (Souza et al., 2013).

Essential oils that have been studied in starch-based films include thyme essential oil (Mehdizadeh, Tajik, Razavi Rohani & Oromiehie, 2012), cinnamon essential oil (Souza et al., 2013), oregano essential oil (Acosta et al., 2016) and lemon essential oil (Bof et al., 2016), representing 17.3% of all studies on antimicrobial starch packaging (Fig. 2.5).

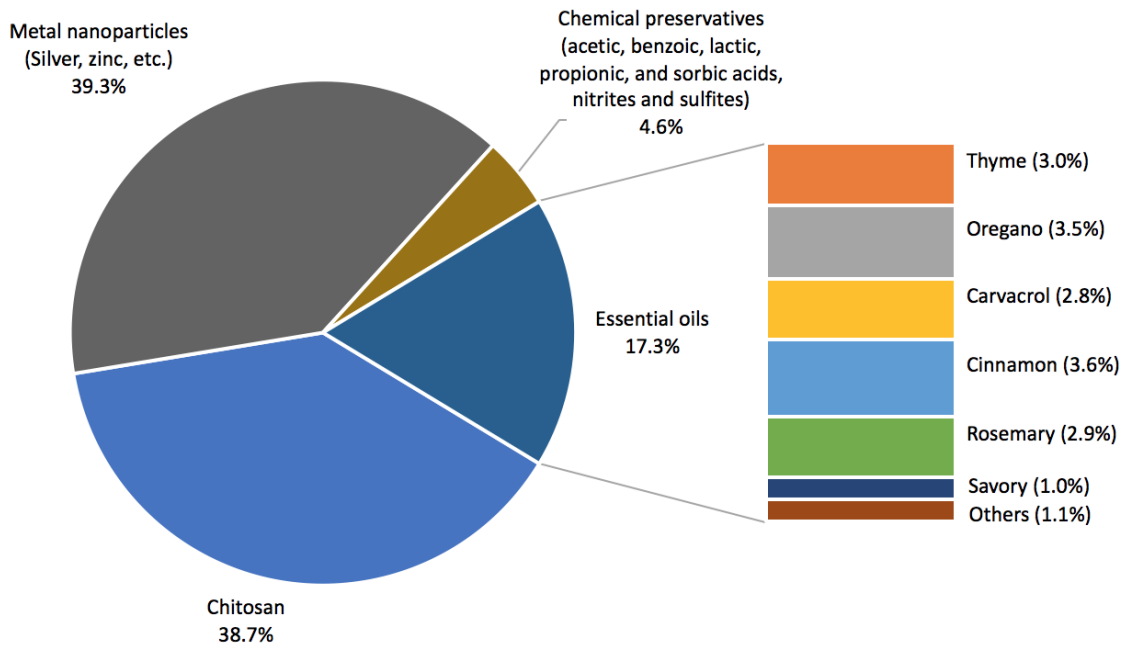


Fig. 2.5 Starch-based films incorporated with antimicrobials.

Number of research articles published between 2008 to 2018 obtained from a literature search using the keywords “antimicrobials in starch-based films”. Portions of each antimicrobial were calculated using the number of publications containing certain antimicrobial divided by the total number of publications on antimicrobial in starch-based films.

(Source: Web of Science database 2008-2018).

The effect of essential oils on mechanical and physico-chemical properties of starch-based films has been studied. Tensile strength and elongation at break of cassava starch films with added cinnamon essential oil (8-16 wt%) were reduced from 2.32 to 1.05 MPa and from 264.03 to 191.27%, respectively, suggesting a loss of starch chain mobility (Souza et al., 2013). Bof et al. (2016) reported that corn starch-chitosan films became slightly yellowish and less transparent with the incorporation of lemon essential oil (1-3 wt%) due to the presence of a dispersed oil phase in the films that promoted light scattering (Jiménez, Fabra, Talens & Chiralt, 2012c). Also, Song et al. (2018) found that compared with the control films, moisture content of the corn/wheat starch films decreased when increasing the lemon essential oil content due to the

hydrophobic nature of essential oil, especially for films that had 2% lemon essential oil, where the water content decreased to half from 23.30 to 10.08%.

In general, starch-based food packaging with the incorporation of essential oils has shown effective antioxidant/antimicrobial results. The preservation of food occurs by diffusion of essential oil from the packaging material to the food, which is influenced by various factors such as the type of essential oil, film matrix composition, food composition, time and temperature of contact. Therefore, the standardization of essential oils in a way that ensures their use without biological variability is a very important issue. Table 2.4 summarizes the main studies carried out on essential oils incorporation to starch-based film and their effect on film properties. The recommended essential oil concentration ranges from 0.1 to 0.5 g/g starch, otherwise, phase separation occurs, deteriorating film structure and lowering mechanical strength. Also, essential oils can negatively affect food sensorial quality.

Table 2.4 Bioactive starch-based films containing different essential oils.

Essential oil	Method/ film matrix	Film characteristics and improvement	Funtionality/application	Ref
Black cumin EO (0.33- 1.33 g/g starch)	Casting, Corn starch	-Reduced swelling degree in water from 231 to 130%. -Decreased tensile strength from 14.43 MPa to 2.3 MPa. -Increased the percentage of elongation at break from 28% to 52%. -Reduced water vapor transfer from 8.58 to 6.2 g/m ² .h. -Increased light absorption between 350-800 nm with the increasing essential oil content.	-Increased total phenolic content from ~2.5 to 4.67 mg gallic acid equivalent/g film. -Increased DPPH scavenging activity from ~5.5 to 12.4%.	Šuput et al. (2016)
Basil or thyme EO (0.1 g/g starch)	Casting, Wheat starch:chitosan (4:1 w/w)	-Exhibited phase separation and the creaming of the oil was evident on the film surface. - Decreased elongation from 4.3 to 3.6 %. -No significant effect on tensile strength. -Decreased oxygen permeability from 6.7 to 3.2 x 10 ² cm ³ /mm ² .atm.day.	-Antioxidant activity of basil essential oil added film (15.9 mg TEAC) > thyme essential oil added film (9.4 mg TEAC).	Bonilla et al. (2013)
Cinnamon EO (0.08-0.16 g/g starch, 0.025 g, Span 70/g EO)	Casting, Cassava starch	-Decreased tensile strength from 3.75 MPa to 1.05 MPa -Increased the percentage of elongation at break from 128.8% to 191.3%. -Increased WVP from 0.15 to 0.62 g.mm/m ² .h.kPa -Increased oxygen permeability from 21.50 to -143.47 cm ³ /m.d.Pa.	-Released amounts of EO varied from 0.88 to 1.19 mg/g film for films incorporated with increasing contents of cinnamon EO.	Souza et al. (2013)

TEAC: Trolox equivalent antioxidant capacity, EO: essential oil.

Table 2.4 (Continued)

Essential oil	Method/ film matrix	Film characteristics and improvement	Funtionality/application	Ref
Cinnamon EO (0.3-0.5 g/g starch)	Casting, Cassava starch	-Reduced WVP from 5.71 to 4.49 g.mm/m ² .h.kPa. -Decreased tensile strength from 1.68 to 0.31 MPa. -Increased elongation from 92.38 to 281.06%. Increased brownish color, with b value increased from 2.08 to 63.63. -Increased film thickness from 290 to 380 μm.	Not reported	Iamareerat et al. (2018)
Lemon EO (0.15-0.46 g/g mixed starch+chitosan)	Casting, Corn starch: chitosan (75:25 w/w)	-Reduced moisture content from 10.5 to 8.67%. -Reduced water solubility from 25.71 to 20% at 25 °C. -Increased film thickness from 80 to 162 μm. -Increased film yellowish with C _{ab} (chroma) increasing from 20.5 to 26.2. -Decreased tensile strength from 14.4 to 6.7 MPa. -No significant effect on elongation. -No significant effect on WVP.	-Best ABTS scavenging activity of 2.2 g TEAC /L for film with 0.46 g EO/g mixed starch+chitosan.	Bof et al. (2016)

TEAC: Trolox equivalent antioxidant capacity, EO: essential oil.

Table 2.4 (Continued)

Essential oil	Method/ film matrix	Film characteristics and improvement	Funtionality/application	Ref
Lemon EO (0.08-0.33 mL/g starch, 0.001 mL Tween 80 or Span 80/mL EO)	Casting, Corn:wheat starch (2.6:3.4 w/w)	-Decreased film whiteness from 60.61 to 54.73. -Decreased tensile strength from 15.50 to 11.18 MPa -Increased elongation from 30.0 to 36.3%. -Reduced moisture content from 23.3 to 10.1%. -Decreased WVP values from 3.68 to 3.08 g/m.s.Pa. - Reduced water solubility from 46.16 to 33.45% at 25 °C.	Not reported	Song et al. (2018)
Oregano, clove and cinnamon bark EO (0.25 g/g mixed cassava starch + gelatin)	Casting, Cassava starch:gelatin (1:1 w/w)	-A porous film structure. -Decreased WVP values (4.2-4.6 g.mm/m ² .h.kPa) compared to the control (5.9 g.mm/m ² .h.kPa). -Decreased oxygen permeability values (0.36-0.43 cm ³ /m.s.Pa) compared to the control (0.52 cm ³ /m.s.Pa). -No significant effect on tensile strength and elongation. -Decreased gloss value from 37 to 12.	Not reported	Acosta et al. (2016)
Oregano EO and pumkin residue extract (0.5 and 0.75 g/g starch, respectively)	Casting, Cassava starch	-Reduced moisture content from 28.1 to 21.3%. -Increased film solubility from 18.4 to 21.9% at 25 °C. -Increased WVP from 0.40 to 0.94 g.mm/m ² .h.kPa.	-Improved DPPH scavenging activity from 13 to 58.4%.	Caetano et al. (2017)

TEAC: Trolox equivalent antioxidant capacity, EO: essential oil.

Table 2.4 (Continued)

Essential oil	Method/ film matrix	Film characteristics and improvement	Funtionality/application	Ref
Oregano or cinnamon leaf EO (0.25 g/g chitosan, 0.001 mL Tween 85/g EO)	Compression molding, Cassava starch:chitosan (3:1 w/w)	-Reduced tensile strength from 20 to 17 MPa. -Reduced elongation from 2.28 to 2%. -Increased WVP from 7.3 to 8.03 g.mm/m ² .h.kPa. -Reduced film thickness from 221 to 207 μm. -No significant effect on film whiteness index and gloss.	Not reported	Valencia-Sullca et al. (2018b)
Thyme EO (0.18-0.73 g/g mixed starch+chitosan, 0.002 mL Tween 20/g EO)	Casting, Corn starch:chitosan (3.5:2 w/w)	- Increased water solubility from 12.54 to 23.39% at 25 °C. -Increased film yellowness index from 13.13 to 21.84. -Decreased film whiteness index from 83.13 to 73.58.	-Increased DPPH scavenging activity from ~9.5 to 42%. -Increased total phenolic content from ~1 to 13 mg gallic acid equivalent/g film.	Mehdizadeh et al. (2012)
<i>Zataria multiflora</i> Boiss EO (0.2-0.6 mL/g starch, 0.001 mL Tween 80/mL EO)	Casting, Corn starch	-Reduced moisture content from 21.95 to 14.04%. -Reduced water solubility from 27.88 to 18.96% at 25 °C. -Increased total color difference from 21.44 to 27.48. -Reduced WVP values from ~ 0.32 to 0.15 g.mm/m ² .h.kPa. -Increased oxygen permeability from ~12 to 15.8 cm ³ μm/m ² .d.kPa. -Decreased tensile strength from ~13.8 to 8 MPa, -Increased elongation from ~ 50 to 162%.	Not reported	Ghasemlou et al. (2013)

TEAC: Trolox equivalent antioxidant capacity, EO: essential oil.

2.2.5 Food systems used to determine film functionality

Generally, most studies showed the *in vitro* efficacy of bioactive films against various microorganisms but limited studies have tested the effect of antimicrobial films on real food products during storage. Often, laboratory methods used culture medium or food simulants, which are far less complex than the actual real food systems (Dutta, Tripathi, Mehrotra, & Dutta 2009; Ramos, Jiménez, Peltzer & Garrigós, 2012). Drawbacks of these laboratory methods indicated the disparity of the laboratory grade results to the real food systems (Sun, Wang, Kadouh & Zhou, 2014b).

2.2.5.1 Food simulants

Migration assay is a common approach to evaluate the release of active compounds from bioactive starch films that are in contact with food products, usually following the European standards (Commission regulation 2015/174 amending and correcting Regulation No 10/2011 on plastic materials and articles intended to come into contact with food) (Requena, Vargas & Chiralt, 2018). Packaging materials have to follow both overall and specific migration limits in order to comply with legislation of food contact materials (Tovar, Salafranca, Sánchez & Nerín, 2005). For example, the overall migration limit of 42.9 mg/kg obtained from the ammonium salt/silver nanoparticles/starch nanocomposite films reached the requirements for food packaging. The maximum overall migration limit is 60 mg (of substances)/kg (of foodstuff or food simulant) for all substances (Abreu et al., 2015).

Ethanol (96%) and 3% acetic acid (v/v) solutions have been used as food simulants for fatty food and aqueous food, respectively (Luchese, Abdalla, Spada & Tessaro, 2018). Results showed that the release of phenolic compounds from blueberry pomace incorporated to cassava starch film was higher when films were immersed into acetic acid than in ethanol during the 10

days of testing. Luchese et al. (2018) used blueberry residue in cassava starch film as a pH indicator in sucrose or sodium chloride solutions of 5 and 10 wt% to mimic sugar and salt contents of food products. It is worth mentioning that the color change of blueberry residue added cassava starch film was independent of the sugar and salt concentration. Requena et al. (2018) investigated the release kinetics of carvacrol essential oil from films composed of cassava starch and polyester (1:1 w/w) in food simulants of aqueous (10% ethanol v/v, 3% acetic acid w/v) and less polar simulants (50% ethanol v/v). They found that the fastest carvacrol release was achieved in 50% ethanol within 30h, due to the high solubility of carvacrol in 50% ethanol.

Even though migration test using food simulants may offer advantages over verification methods with regards to time and cost, the simple composition in simulants cannot reveal the interaction of bioactive compounds with complex food matrix, therefore, comprehensive understanding of migration effect may be more applicable when using a real food product.

2.2.5.2 Disk diffusion for antimicrobial test

Apart from the various food simulants that are used to evaluate migration of bioactive compounds from film matrix, the antimicrobial test on agar medium is a feasible way to determine the antimicrobial activity of starch-based films based on the diameter of inhibition zone. Some commercially available zone reader systems even claim to calculate an approximate minimum inhibitory concentration (MIC) against some microorganisms by comparing clear zone sizes with standard curves (Nijs et al., 2003). Ji et al. (2017) reported the increase of inhibition diameter from 18.22 to 75.45 mm against *Escherichia coli*, from 6.40 to 62.45 mm against *Staphylococcus aureus* and from 5.50 to 59.81 mm against *Bacillus cereus* when chitosan concentration increased from 20 to 50% in corn starch-based films. More recently, the study by

Requena et al. (2018) showed that the nanocomposite films containing different concentrations of cinnamon oil (0.4-0.8 wt%) exhibited large inhibition zone against *E. coli* (21.6-26.1 mm) followed by *S. aureus* (15.3-21.6 mm) and *C. jejuni* (17.1-19.8 mm). The lowest concentration of 0.2% cinnamon oil was effective only against *E. coli*. Also, the antimicrobial effect of nisin added cassava starch (2.31 mg nisin/dm² of film) and natamycin added cassava starch (9.25 mg natamycin/dm² of film) films against *Listeria innocua* and/or *Saccharomyces cerevisiae* was demonstrated by Resa et al. (2014). Results showed that the natamycin from starch films was released into the agar model medium and effectively inhibited the *Saccharomyces cerevisiae* growth, showing a diameter of inhibition zone of 29.7 mm, and similar effect (32.5 mm) was observed for *Listeria innocua* and *Saccharomyces cerevisiae* mixed culture.

However, the results of the disk diffusion test are qualitative, only susceptibility information of one microorganism (e.g. susceptible, intermediate, or resistant) can be acquired from the test. Also, the different incubation conditions (usually 25-37 °C, overnight) during agar diffusion test from the actual food storage (4-10 °C) cannot provide accurate prediction of the antimicrobial efficiency. Hence, the shelf-life test using a food product under the correct practical conditions is more realistic.

2.2.5.3 Application of starch-based films on food products

The benefit of incorporating bioactive compounds into films is that the release of the active compounds can be controlled over an extended period of time to maintain or extend the quality and shelf-life of food products, without the need for direct addition of any additives to the food products (Zhou, Xu & Liu, 2010). Starch based films or coatings have been extensively studied to target delay loss of quality in fresh products, such as fresh-cut apples, tangerines, tomatoes, strawberries, carrots and plums (Basiak, Linke, Debeaufort, Lenart & Geyer, 2019;

Chiumarelli & Hubinger, 2012; Das, Dutta & Mahanta, 2013; Lai, Chen & Lai, 2013; Silva et al., 2012). When applying films or coatings on fruit and vegetable surfaces, their gas permeability property is of great importance. Starch films are known to have a particular low oxygen permeability ($<1 \text{ cm}^3 \mu\text{m}^2 \text{ d kPa}$), but a high WVP ($>1 \text{ g.mm/m}^2.\text{h.kPa}$) (Liu, 2005). For example, grapes without corn starch/gelatin coating (4:1 w/w) reduced their total weight to 82% after 17 days of storage, while the maximum weight loss in the coated fruit was approximately 10% under refrigerated conditions (Fakhouri, Martelli, Caon, Velasco, & Mei, 2015). Another study reported that the use of a cassava starch film formulated with sorbitol as a plasticizer reduced moisture loss of strawberry from 53.44% to 28.17-32.96% after 8-day of storage, resulting in a 5-day extension of strawberry shelf life (Franco et al., 2017). Additionally, the incorporation of chitosan and *Lippia gracilis* Schauer extract (1-3 wt%) into cassava starch film on guavas prevented 2-3 log CFU/g in terms of yeast and mold counts during 10 days of storage at 25 °C. In the same study, a delayed ripening process, reduced browning and inhibited color development in guavas were observed (de Aquino, Blank, & de Aquino Santana, 2015).

On the other hand, meat products provide a rich environment for microorganisms, causing spoilage as well as food originated pathogens due to high contents of nutrients (Addis, 2015). Specially for ready-to-eat meat products, the concern is generated because this product is consumed without further cooking, therefore, it is of great importance to control the microorganism growth on meat surface to ensure food safety and shelf-life. As such, fresh sliced pork covered with a cassava starch-chitosan film (starch:chitosan 70:30 w/w) lowered the total aerobic population by 1 log after 7 days of storage at 10 °C, leading to an extended shelf-life of 3 days compared to pork without any film coating (Valencia-Sullca et al., 2018a). Moreno et al. (2015) conducted both *in vitro* test on agar medium and *in situ* antimicrobial test on minced pork

meat using lactoferrin or lysozyme (0.1 or 0.2 g/g starch) incorporated potato starch film. Results showed no reduction in the growth of *E. coli* and *L. innocua*, probably due to their weak activity and the interactions between lactoferrin or lysozyme with starch chains in the film matrix that hindered their diffusion. In addition, neither lactoferrin nor lysozyme were effective enough when they were applied separately, but a weakly enhanced antimicrobial activity (1 log reduction) against *E. coli* and coliform microbiota on pork meat was observed when they were mixed (lactoferrin:lysozyme 1:1 w/w). These results indicated that the incorporation of bioactive compounds into film matrix may restrict the release of such active agents through cross-link interactions, and further decrease film antimicrobial activity. Table 2.5 provides some examples of selected starch-based films that were applied on food products and their performance in terms of antimicrobial activity.

Table 2.5 Bioactive starch-based films used on various food products.

Film formulation	Applied food product	Effect	Ref
Cassava starch + oregano EO (2 w/v% film-forming solution) and pumpkin residue extract (3 w/v% film-forming solution)	Ground beef	-On day 6, bioactive film reduced <i>Salmonella</i> counts by 0.62 log CFU/g compared with control (film without bioactives). -Cell counts of coliforms and mesophilic microorganisms reduced by 1 log on day 3, but recovered to the same counts on day 6 compared to the control.	Caetano et al. (2017)
Cassava starch + chitosan (0-30 wt%)	Pork meat slices	-The lowest total aerobic counts with 1 log reduction compared to control (6.4 log) after 7 days of storage at 10 °C when using 30 wt% chitosan in film.	Valencia-Sullca et al. (2018a)
Cassava starch + cinnamon EO (0.3-0.5 g/g starch)	Pork meatballs	-Total plate counts remained below the maximum allowable level (10 ⁶ CFU/g) at 0.5 g EO/g starch until 96 h during storage at 25 °C.	Iamareerat et al. (2018)
Cassava starch/chitosan (3:1 w/w) + oregano and cinnamon leaf EO (0.25% w/w, with Tween 85 at 0.1% w/w)	Sliced pork meat	-2-3 log reduction with EO added starch/chitosan bilayer films in both total aerobic and coliform counts compared to uncovered pork meat.	Valencia-Sullca et al. (2018b)
Foxtail millet starch + clove leaf EO (0.3-1.0 v/v% film-forming solution)	Queso blanco cheese	The population of <i>L. monocytogenes</i> on the cheese that was wrapped with the bioactive film containing 1% clove leaf EO increased by 0.45 log CFU/g until 4 days of storage, after which it remained constant; it reached 6.13 log CFU/g after 24 days, thus, resulting in a decrease by 1.19 log CFU/g, compared with that in the control samples.	Yang et al. (2018a)
Corn starch + cinnamon EO (0-4 w/v% film-forming solution)	Raw beef fillets	-Film with cinnamon EO (3 w/v%) reduced lactic acid bacteria counts by 0.55 log CFU/g meat on day 15 of storage. -The <i>Enterobacteriaceae</i> counts were reduced by 0.5 log CFU/g meat.	Radha Krishnan et al. (2015)

EO: essential oil.

Table 2.5 (Continued)

Film formulation	Applied food product	Effect	Ref
Potato starch + lactoferrin or lysozyme (0.1 or 0.2 g/g starch)	Minced pork meat	-No significant differences in the counts of total aerobic meat bacteria after 15 incubation days. -The coliform counts after 14 incubation days showed a reduction of about 1 log, compared to the samples coated with the control film at 10 °C.	Moreno et al. (2015)
Potato starch + <i>Hibiscus sabdariffa</i> extract (concentration not specified)	Pork sausage	-1-1.5 log reduction of <i>L. monocytogenes</i> counts in the first 24 h, but recovered after 2 days. -A decrease of 3 log CFU of <i>L. monocytogenes</i> after 7 days of incubation under refrigeration after sealing in a vacuum package.	Cruz-Gálvez et al. (2018)
Sweet potato starch + thyme EO (0-6 g/g starch)	Shrimp	-Coating treatment with 2 g/100 g of thyme EO reduced aerobic plate counts by 4 log CFU/g. -By increasing thyme EO to 4 g/100 g or 6 g/100 g, the aerobic plate counts was undetectable after 8 days storage at 4 °C.	Alotaibi et al. (2018)
Sweet potato starch + thyme EO (0-6 wt%)	Baby spinach leaves	-A complete inhibition of microbial growth during 8 days of storage with thyme EO concentration >4 wt%. -Film reduced the population of <i>E. coli</i> and <i>Salmonella</i> by more than 4.5 log CFU/g compared to the control.	Issa et al. (2017)

EO: essential oil.

2.2.6 Commercial biodegradable plastics

The arise of bioplastics helps manufacturing companies stay competitive as a result of the increasing demand for sustainability. The composite materials, including biodegradable polymers, such as PLA and PBAT, can be processed by injection molding or extrusion as described in Section 2.2.2. Also, these materials should be comparable to petroleum-based plastics in terms of mechanical and water barrier properties. More importantly, the partial or entire replacement of petroleum-based polymers with biodegradable polymers ensures the high biodegradability of such plastics, minimizing environmental concerns associated with waste disposal.

In 2018, the amount of bioplastics sold was 2.08, it is estimated that the global bioplastics production capacity will increase from around 2.14 million tonnes in 2019 to approximately 2.44 million tonnes in 2022, representing only 1% of total plastic production (European Plastic, 2019). Among them, some starch-based blends with the addition of PLA or polyesters are nowadays marketed at commercial scale, with trademarks such as Mater-Bi® (Novamont, Italy), a starch-based material available in pellets that can be further processed as thermoplastic material to form films or bags. Also, other bioplastic brands are summarized in Table 2.6, such as Bioplast® (Biotech, Germany), Biopar® (BIOP Biopolymer Technologies AG, Germany), Biograde® (FKUR, Germany), Bio-flex® (FKUR, Germany), Biolice® (Limagrain, France), VEGEMAT (VEGEPLAST, France) and Solanyl (Rodenburg Biopolymers, Netherlands), reflecting the diversity of bioplastic applications and their recognition at commercial scale to produce environmentally responsible packaging materials. Full composition of each biodegradable film is not available due to the limited information.

Table 2.6 Commercial bioplastics brands for food-related packaging applications.

Brands	Company name	Main composition	Applications
Biopar®	BIOP Biopolymer Technologies AG, Dresden, Germany	Potato starch, biodegradable synthetic copolyesters and additives suitable for mono layer film blowing	Blown films.
Biograde®	FKUR, Willich, Germany	Cellulose acetate	Injection molding, sheet and extrusion for rigid applications.
Bioplast ®	Biotech, Emmerich, Germany	PLA and potato starch	Blown film, flat film, moldings, profiles and injection moulded products.
Bio-flex ®	FKUR, Willich, Germany	PLA blends	Flexible film applications, such as agricultural, household and hygiene films, thermoformed particles and injection molded products.
Solanyl®	Rodenburg Biopolymers, Oosterhout, Netherlands	Potato starch blends	Bioplastics with common converting processes such as injection moulding, sheet extrusion, profile extrusion, thermoforming and extrusion film blowing.
VEGEMAT®	VEGEPLAST, Bazet, France	Biopolymer blend with cereal flours, and natural fibers	For applications requiring stiffness and good mechanical properties, and temperature resistance.
Biolice ®	Limagrain, Riom, France	Maize flour	Bags, industrial films (single layer or co-extrusion); thermoformed product trays, containers and plant pots.

Moreover, 75% of starch-based polymers are used for packaging applications, including soluble films, bags, tubings, trays as well as filling materials. Other non-food applications are mulch film or slow release fertilizer in the agricultural field and wound healing or oral dissolving for medical treatments (Fig. 2.6).

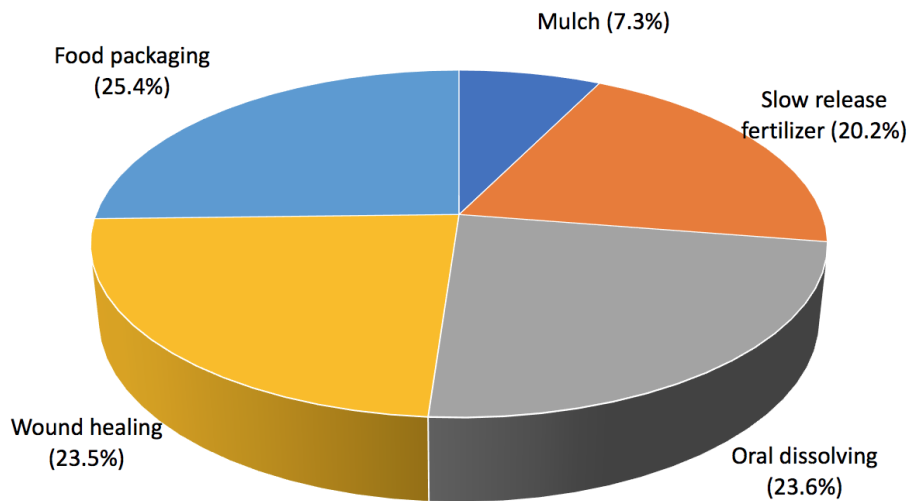


Fig. 2.6 Starch based-films for food and non-food applications. Number of research articles published between 2008 to 2018 obtained from a literature search using the keywords “starch-based film application”. Portions of each application were calculated using the number of publications containing certain application divided by the total number of publications on application in starch-based films. (Source: Web of Science database 2008-2018)

Even though bioplastics are claimed to be biodegradable, biodegradation depends on the soil environment. The most aggressive environment is compost, followed by soil and landfill, due to the different temperatures and the presence of microorganisms in these environments (Rujnić-Sokele & Pilipović, 2017). The PLA for example still needs a thermal trigger to initiate its biodegradation process, where the temperature has to be above its glass transition temperature of 60-65 °C (Rujnić-Sokele & Pilipović, 2017). Another challenge to address is that biodegradable plastics are considered by the recycling industry to affect product quality if they are mixed into the stream of plastics aimed for recycling (European

Commission, 2018). Then, products made of biodegradable plastics should be labeled as such, so that they can be sorted out from recyclables. Furthermore, some concerns started to arise on a possible competition between bioplastics production with food/feed if starch was used to replace the petroleum-based polymers. Therefore, the use of agricultural residue is preferable. Finally, biodegradable materials are also relatively expensive. PLA can be 20-50% more costly than synthetic polymers (e.g. polyethylene). However, prices are coming down as researchers and companies develop more efficient and eco-friendly strategies for producing bioplastics.

2.2.7 Film Biodegradability

Biodegradation is usually defined as a process carried out primarily by bacteria or fungi in which a polymer chain is cleaved or modified by hydrolytic or oxidative enzymatic activity (Kaplan et al., 1994). The assessment of biodegradability of a polymer film using laboratory approaches involve many simulated natural biodegradation processes, but in a controlled way to predict natural environmental susceptibility of materials to biodegradation. Methods that have been developed include enzymatic assays (Tomasi, Scandola, Briesse & Jendrossek, 1996), microbial growth tests (Corti, Muniyasamy, Vitali, Imam & Chiellini, 2010), oxygen demand and CO₂ evolution tests (Otoni et al., 2018) and degradation product quantification (e.g., monomers) (Acioli- Moura & Sun, 2008). The biodegradation process mainly refers to the degradation and assimilation of polymers by living microorganisms into degradation products. For example, starch molecules can be hydrolyzed into glucose by microorganism or enzymes, and then metabolized into carbon dioxide and water (Primarini & Ohta, 2000).

Among all methods described above, the enzymatic degradation and the soil burial method are most commonly used (Nguyen, Do, Grillet, Thuc & Thuc, 2016). Due to the extent of exposure to air, soil microorganisms, and UV radiation, the properties of

biodegradable materials change, causing fracture of the film structure. Pure corn starch film was degraded rapidly in the initial 15 days using soil burial test (soil taken from a culture field), and complete degradation was achieved within 60 days (Guohua et al., 2006). Similarly, Torres et al. (2011) reported total weight losses over 90% after 31 days of pure cassava starch film and pure sweet potato starch film buried in organic compost (unknown composition). Also, Jaramillo et al. (2016) reported >95% decomposition of *yerba mate* extract added cassava starch film after 12 days burial in vegetable soil (unknown composition).

Starch has been added to various synthetic polymers due to its potential advantage to enhance biodegradability. Indeed, the incorporation of starch into PVOH (50:50 w/w) improved the degradation process until 120 days, with a final degradation percentage of 75%. In contrast, the pure PVOH film exhibited a higher resistance against soil burial biodegradation, showing a degradation percentage of less than 20% after 120 days (Guohua et al., 2006). Additionally, Nguyen et al. (2016) found that the biodegradability of linear low density polyethylene films was enhanced by the incorporation of 40 wt% cassava starch. The weight of the blend film in natural soil (unknown compost) decreased about 95 wt% in 5 months. The authors suggested that the cassava starch present in the film was degraded first whereas the polyethylene formed smaller chains with reduced molecular weight compared to the initial polyethylene. It was also noticed that the mechanical properties of starch/synthetic polymer blend films can be modified with an increase of starch content. For example, the incorporation of 50 % (w/w) cassava starch in low density polyethylene film led to a loss of 25% in both the elastic modulus and the tensile strength, and an increase of 70% in elongation compared to the pure polyethylene film (Peres, Pires & Oréfice, 2016).

For enzymatic degradation, the main enzymes responsible for starch degradation are α -amylases, β -amylases, glucoamylases, α -glucosidases, and other debranching enzymes (Azevedo, Gama & Reis, 2003). Synergetic degradation effect (17% weight loss) by

combining α -amylases and glucoamylases on corn starch/poly(ϵ -caprolactone) (30:70 w/w) film was observed compared to the use of only one enzyme with 7-10% weight loss (Azevedo et al., 2003). Glucoamylases showed a better degradation effect on corn starch films than α -, β - amylases because glucoamylases cleaved α -(1-4) bounds and α -(1-6) bounds simultaneously during the different enzymatic reactions. Also, the enzyme activity can be influenced by the media environment and film structure. A slower degradation (25%) by glucoamylase was reported when citric acid was added to the sodium trimetaphosphate cross-linked corn starch film compared to the films without cross-linking (60%), due to the low pH that deactivated the enzymatic reaction (Yun, Wee, Byun, & Yoon, 2008). Even though starch is prone to enzymatic hydrolysis, the methyl substitution in the starch molecule and the dispersion of starch chain into the chains of poly (vinyl alcohol) inhibited the catalytic reaction of amylases by challenging the enzymes to reach the starch molecules, delaying enzymatic degradation by more than 50% (Guohua et al., 2006).

The evaluation of microorganisms effect on film biodegradation is often related to the enzymes produced by microorganisms to biodegrade organic materials. These microorganisms include various bacteria, fungi and yeasts that consume films as a food source so that film original form disappears (Gautam & Kaur, 2013). The more hydrophilic the material, the more susceptible is to the attacked by microorganisms because most microorganisms are active in a high moisture environment. Biodegradability of starch-based films in various microbial environments has been reported (Guohua et al., 2006; Maran, Sivakumar, Thirugnanasambandham & Sridhar, 2014; Prabhat et al., 2013). An earlier study has demonstrated that *B. subtilis* (bacteria), *A. oryzae* and *A. niger* (fungi), three microorganisms that produce amylase, led to a dramatic weight loss of 60% of corn starch/poly (vinyl alcohol) (1:1 w/w) films after 55 days burial in soil obtained from a culture field due to the colonization of microorganisms on film surface. More recently, bacteria

(*Pseudomonas* spp, *Streptococcus* spp, *Staphylococcus* spp, *Micrococcus* spp and *Moraxella* spp), fungi (*Aspergillus niger*, *Aspergillus glaucus* etc), and *Actinomyces* were identified on the surface of polyethylene/starch film (7:3 w/w) (Prabhat et al., 2013). Also, the number of bacteria and fungi counted on cassava/agar (1-3:0.5-1 w/w) films were between 30-43 x 10⁶ and 18-23 x 10³ CFU/g sample, respectively (Maran et al., 2014).

As discussed earlier, some bioactive compounds (e.g. essential oils) are hydrophobic, thus it is hard to form a homogenous network when directly added into the starch matrix. Also, the high volatility and unpleasant aroma may interfere with the effectiveness of essential oil that conveys a strong flavor to food imparting unpleasant sensorial attributes. A strategy to overcome these drawbacks is to use encapsulation that not only improves the film homogeneity but also protects the bioactives from degradation from adverse conditions in food systems. An encapsulated bioactive is known as micro/nanogels that are to be potentially used in films as discussed below.

2.3 Thermosensitive micro/nanogels

The development of innovative smart packaging systems has attracted increasing interest due to their specific structures and properties that can offer interactions between the packaging material and the food, by reacting to external or internal stressors (Biji, Ravishankar, Mohan & Gopal, 2015). Polymers that are considered as stimuli-responsive materials can be classified according to the stimuli they respond to as temperature, pH, ionic strength, light, electric and magnetic field-sensitive (Gao, Ahiabu & Serpe, 2014; Jones & Steed, 2016; Manouras & Vamvakaki, 2017; Petri, 2015; Polo-Corrales, Ramirez-Vick & Hernandez-Ramos, 2018). Specifically, temperature-sensitive polymers exhibit a critical solution temperature (CST) behavior where phase separation is induced by surpassing a certain temperature. By incorporating bioactives into these temperature-sensitive polymers, the controlled release of bioactives can be triggered due to the environmental response of

encapsulating material, thus protecting food products from deterioration through a long-lasting release of bioactives (Fuciños et al., 2014). Temperature-sensitive systems can be classified into various groups, depending on their sources. Some common categories that are widely investigated in the biomedical field include N-isopropylacrylamide copolymers and natural polysaccharides, but very few N-isopropylacrylamide based polymers have been used in food systems, like bioactive releasing (Yildirim et al., 2018), which make these systems attractive for potential application for future research.

2.3.1 N-Isopropylacrylamide copolymers

Most research has been conducted on polymers that display a LCST-type phase transition. Among them, N-substituted polyacrylamides have been extensively studied for chemical and biological applications, such as thermoresponsive nanogels for drug delivery (Bergueiro & Calderón, 2015). The most studied polymer in the family of poly (N-substituted acrylamides) is poly N-isopropylacrylamide (PNIPAM). To better understand the mechanism of phase transition, Otake et al. (1990) introduced the concept of “water cage”, which is surrounding the isopropyl group in PNIPAM. Ebara et al. (2003) explained that the phase transition is the result of dissociation of water molecules around the hydrophobic isopropyl groups of the poly (N-isopropylacrylamide) chain at high temperatures (>32 °C). But, there is still considerable debate on whether “hydrophobic effects” and/or “hydrogen bond effects” dominate the coil-to-globule transition. Other authors, Feil et al. (1993) and Volpert et al. (1998), argued that both “hydrogen bonding” and “hydrophobic interactions” are associated with critical solution temperature changes of the thermoresponsive polymers. They concluded that at the molecular level, the phase transition of temperature-sensitive polymers is a change from hydrated random coil to hydrophobic globule. As the temperature rises and approaches the phase transition temperature, the first step of phase separation is breaking up hydrogen bonds, formed around the polymer coil between water molecules and the NH or C=O groups

of the temperature-sensitive polymers, followed by the collapse of the polymer molecule into a hydrophobic globule. Polymer-polymer interactions are responsible for the aggregation and the subsequent precipitation of the polymer out of the solution as hydrogen bonding becomes weaker and breaks as the temperature increases.

The phase transition around 32 °C and adjustment of this value to a lower temperature range through the incorporation of co-monomers or hydrophilic groups makes poly (N-isopropylacrylamide) (co)polymers a promising polymer in a variety of applications, especially in the controlled release of drugs (e.g. camptothecin, doxorubicin) (Carrero, Posada & Sabino, 2018; Qian & Wu, 2013; Yang, Fu, Yu, Zhou & Cheng, 2018c). However, the narrow and high LCST of PNIPAM limits its application in food packaging. There is scarce research on the potential application of PNIPAM in food active packaging. Only one study reported the synthesis of poly (N-isopropylacrylamide-co-acrylic acid) nanogel on control release of antifungal (pimaricin) through a food model system (agar plate) that simulates the cheese with(out) acidification. Results showed that no growth of *Saccharomyces cerevisiae* was observed at 4 °C during seven days of storage. To modify the LCST of PNIPAM, copolymerization with N-tert-butylacrylamide at 1:1 molar ratio was able to lower the LCST significantly from 32 to ~10 °C (Naha et al., 2009b). Only few studies were conducted on poly (N, N-diethylacrylamide) even though this polymer behaves similarly as poly (N-isopropylacrylamide) with a LCST around 32 °C, but it cannot form hydrogen bonds with the oxygen of water because it lacks the proton of the amide group (Panayiotou, 2004).

Even though cytotoxicity studies performed revealed safe utilization of PNIPAM based nanoparticles as drug delivery carriers (Ahmad et al., 2016; Carrero et al., 2018), the safety concern related to acrylamide-derived materials in food packaging application still

remains unclear and has not been well studied or approved by FDA, therefore, studies using natural polymers are preferred.

2.3.2 Natural polymers

Polymers derived from biomass can be used to produce thermo-reversible gels. The most typical natural polymer solutions that turn into gel phase by lowering the temperature are some cellulose derivatives, which undergo gelation and formation of a network by converting random coil to helix conformation. Methylcellulose and hydroxypropyl methylcellulose are examples attracting interest, because they have high water solubility, which is induced by the chemical substitution of hydroxyl groups to hydrophobic methyl and hydroxypropyl groups. Methylcellulose is prepared from the reaction of alkali-cellulose with dimethyl sulfate or methyl chloride (Mansour, Nagaty & El-Zawawy, 1994). Hydroxypropyl methylcellulose is formed by reacting cellulose with chloromethane and epoxy propane (Wang, Dong, & Xu, 2007). The phase transition temperatures of methylcellulose and hydroxypropyl methylcellulose are between 40-50 and 75-90 °C, respectively (Jain, Sandhu, Malvi & Gupta, 2013). The modification of phase transition temperature needs to be conducted for *in situ* gelling applications such as liquid suppository (Pásztor et al., 2011). For example, hydroxypropyl methylcellulose can be salted out in NaCl and CaCl₂ solutions at a low temperature of 35 °C (Almeida, Rakesh & Zhao, 2014).

Xyloglucan, widely available in cereals, is a major component of plant cell walls (Reiter, 2002). After removing >35% galactose residues by fungal β -galactosidase, the resultant product undergoes thermally reversible gelation (Brun-Graeppi et al., 2010). Interestingly, the increase of galactose removal ratio from 35 to 58% leads to the decrease of sol-gel transition from 40 to 5 °C (Shirakawa, Yamatoya & Nishinari, 1998). This gel was shown to be transformed from the solid to liquid phase upon cooling, making it promising carrier for drug delivery. Mahajan et al. (2012) developed xyloglucan gels and evaluated its

possibility for nasal drug delivery. Xyloglucan with a 45% galactose removal gelled at the optimum concentration of 2.5% (w/v of water) and showed a sustained ondansetron hydrochloride release from 0 to 100% up to 4 h.

Chitosan is not a thermosensitive polymer on its own. But the cationic group (NH_3^+) presented in acidic aqueous media can react with salts that have anionic group through electrostatic attraction between opposite charged chitosan and basic salt, favoring gel formation. As such, glycerol phosphate is selected due to its negatively charged phosphate moiety, resulting in proper control of hydrophobic interactions and hydrogen bonding which are necessary to retain chitosan in solution at neutral pH. A thermosensitive gelling system based on chitosan solutions buffered with glycerol phosphate has been successfully applied to control release of ellagic acid for the treatment of brain cancer (Kim et al., 2010) and injectable hydrogel for bone tissue regeneration because of its good biocompatibility with human body and a tailored phase transition temperature near body temperature (Saravanan, Vimalraj, Thanikaivelan, Banudevi & Manivasagam, 2019). Three major possible reactions were involved for chitosan-based thermogelling systems: 1) electrostatic interaction between the amino groups of chitosan and the phosphate groups; 2) hydrogen bonding between the chitosan chains, resulting from the decrease of electrostatic repulsion after neutralizing chitosan by the addition of glycerol phosphate; and 3) hydrophobic interactions between chitosan molecules (Ruel-Gariepy, Chenite, Chaput, Guirguis & Leroux, 2000).

2.4 Future perspectives

As a result of the increasing demand by customers for safe, high quality, minimally processed and extended shelf-life food products, active packaging is becoming one of the most studied areas. In general, the process of bioactive starch-based film production can be described in Fig. 2.7, where bioactive compounds and reinforcements are added into the film matrix to tailor film mechanical, physico-chemical and morphological properties, providing

the film with unique antioxidant/antimicrobial activities. The use of encapsulation technology can preserve bioactive compounds from degradation and enhance their bioactivity through control release or selective response to the environment (e.g. temperature and pH).

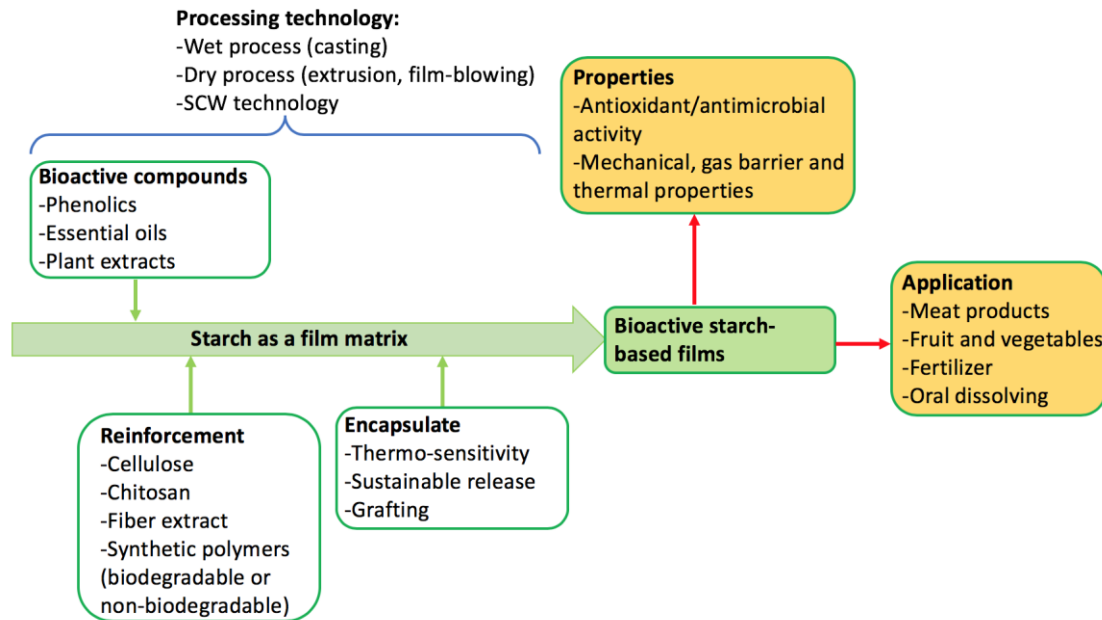
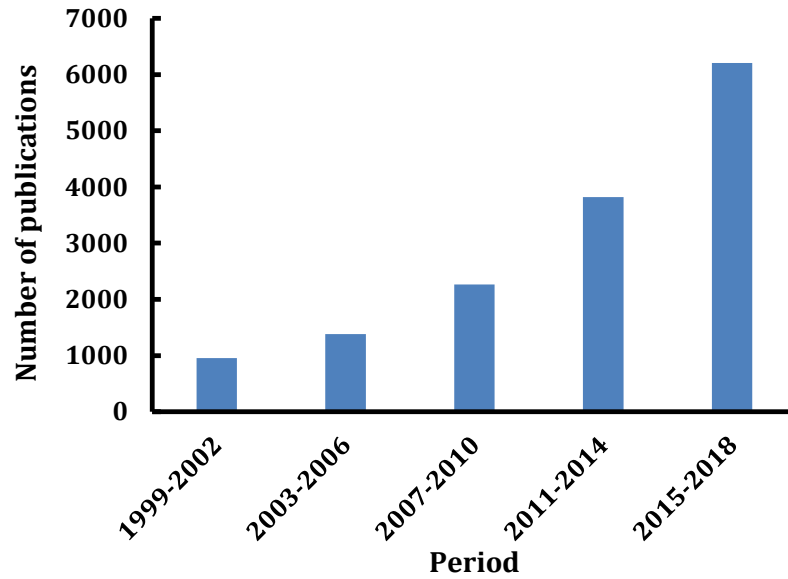
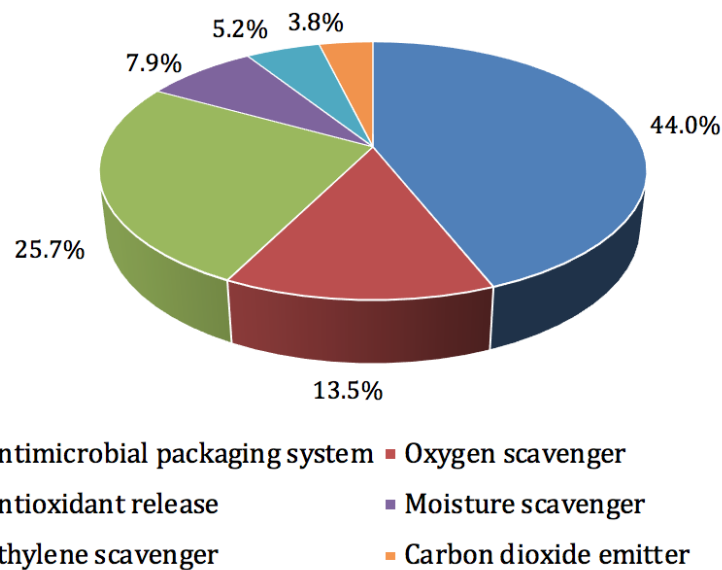


Fig. 2.7 Bioactive starch-based film development and application

As indicated by Web of Sciences, there is a tremendous increase in the number of publications on bioactive packaging and their applications in recent years (Fig. 2.8A). Based on applications, such bioactive packaging can be divided into oxygen, carbon dioxide or ethylene scavengers, and antioxidant releaser or antimicrobial packaging systems (Fig. 2.8B).



(A)



(B)

Fig. 2.8 A) Number of scientific publications on bioactive starch packaging and B) graphical representation of bioactive food packaging by research area. Number of research articles published between 1999 to 2018 obtained from a literature search using the keywords “bioactive starch-based films” and “active food packaing”. Portions of each functionality of food packaing were calculated using the number of publications containing certain food packaing functionality divided by the total number of publications on food packaing functionality. (Source: Web of Science database 1999-2018).

Although throughout this review, we have discussed promising improvement on bioactive starch-based films in terms of mechanical, structural and functional properties, future directions on food packaging research need to be specified on overcoming remained challenges to fulfill environment and market requirement.

The growing environmental awareness make it necessary to look for alternative packaging materials to replace at least partially (30-50%) synthetic plastics. Among bio-based materials, starch-based plastics occupied a relevant position due to its advantages of low cost, biodegradability, sustainable production, and good processing capability various techniques. However, starch films produced by conventional methods using exhibited drawbacks of brittleness, highly hydrophilic nature and poor mechanical properties. Therefore, different strategies aimed to improve the properties of starch-based films have to be investigated, such as blending with other polymers or incorporation of bioactive compounds. The use of these strategies allows us to obtain a wide range of film with diverse properties, enabling a broad scale of applications. The future direction for researchers and the packaging industry in terms of producing starch-based synthetic polymer blends with commercial utility are:

- 1) Overcoming miscibility problems at high starch contents (>50 wt%), 2) avoiding mechanical property deterioration at high starch contents, even in compatibilized blends, and 3) reducing costs, especially for biodegradable starch-polyester blends at low starch contents (<30 wt%).
- On the other hand, development of biodegradable packaging material from agricultural residues properly managed would reduce their environmental impact upon disposal. But, it should be technically and economically practicable.

Then, increase consumer trust and acceptance of new packaging technologies regarding to gas exchange control, smart packaging indicators and antimicrobial packaging:

- Future studies should be directed towards characterizing the dynamics of the interactions between the food, the packaging material and the environment in terms of O₂/CO₂ permeation and production by fresh fruit and vegetables, which could lead to the development of optimal gas exchange packaging material that preserve food with high quality.
- Food safety and shelf-life can be controlled in a smart way, where the use of new indicators in food packing should directly present some information about the freshness, edibility, quality, and safety of food to consumers with cost effectiveness. These devices could be placed inside the primary packaging so that they have direct contact with the atmosphere surrounding the food or with the food itself. Therefore, direct indicators have become a main future direction of research.
- To successfully implement antimicrobial packaging in the market, it is essential to select the right package for the antimicrobial agent and the environmental conditions faced by a particular food product. A multidisciplinary approach involving researchers from all fields, particularly, food technology, engineering, microbiology and materials science, is necessary to create antimicrobial packaging with a promising future in the food packaging industry.
- Future research should amplify the evaluation of film protective effect from the *in vitro* model test in laboratory to real food systems.

Finally, detailed regulations and standardization of the bioactives composition (e.g. essential oils) would be needed for their safe application. In addition, studies are necessary to confirm if bioactives are safe to use in the food industry at doses able to produce efficiency.

Chapter 3: Hydrolysis of Cassava Starch, Chitosan and Their Mixtures in Pressurized Hot Water Media*

3.1 Introduction

Low molecular weight starch, widely used in food, nutraceutical, and pharmaceutical industries, can be produced from the hydrolysis of polysaccharides (Das & Pal, 2015; Miyazaki, Van Hung, Maeda, & Morita, 2006). Starch, one of the most abundant carbohydrates in biomass, is a polysaccharide consisting of glucose monomers connected with α - (1 - 4) and α - (1 - 6) linkages. Starch is composed of amylose with a linear structure, and amylopectin with a branched structure. Starch hydrolysates typically used in the industry (maltodextrin and glucose) are produced by acid hydrolysis, requiring large amounts of solvents such as sulphuric or hydrochloric acids. After hydrolysis with these acids, the solutions need to be neutralized with sodium or potassium hydroxide, increasing environmental concerns. On the other hand, the enzymatic process yields specific products like reducing sugars, but the process is slow with up to 36 h (Konsula & Liakopoulou-Kyriakides, 2004) and involves the high cost of the enzymes.

Another biopolymer available is chitosan (*N*-deacetylated derivative of chitin), which is the second major polymer after cellulose. The high molecular weight of chitosan, which results in a poor solubility at neutral pH and high viscosity in aqueous solutions, limits its potential uses in the food and pharmaceutical areas. Similarly, water soluble low molecular weight chitosan can be produced by acidic or enzymatic hydrolysis of the chitosan polymer. The enzymatic process is generally preferable because the molecular weight distribution of the hydrolyzed chitosan can be readily controlled and alterations in the chemical composition of the reaction product are minimized. Various commercial enzymes, including chitinases, chitosanases, glucanases, lipases

*A version of this chapter has been published. Zhao, Y. and Saldaña, M.D.A. (2018). Hydrolysis of Cassava Starch, Chitosan and Their Mixtures in Pressurized Hot Water Media. *The Journal of Supercritical Fluids*. In press.

and proteases, are available (Andrews, 1993). But, the high cost associated with the use of enzymes reduces the application of enzymatic methods in the industry.

Another promising approach for polysaccharide hydrolysis consists on applying pressurized hot water without the use of additives, as the process requires only water that is environmentally friendly, non-toxic and widely available in nature; consequently, neutralization and desalination processes can be eliminated, avoiding solvent recovery and minimizing waste production. The unique physicochemical properties of pressurized hot water, e.g. reduced dielectric constant and increased ionic product, promotes acid/base hydrolysis (Brunner, 2009). These properties make pressurized hot water a green alternative reaction medium for the depolymerization of natural polymers (Brunner, 2009). Various studies have shown the possibility of starch conversion to produce glucose. Starch from sweet potato was decomposed in a batch reactor at hydrothermal conditions (180-240 °C, 10-30 min, unspecified pressure) in the absence of a catalyst (Nagamori & Funazukuri, 2004). Glucose yields were negligible at temperatures below 180 °C. However, the degradation product (5-hydroxymethylfurfural) from glucose appeared after 10 min at 240 °C (Nagamori & Funazukuri, 2004). In a similar study on hydrolysis of sweet potato starch, Miyazawa & Funazukuri (2005) reported a glucose yield of 4% after 15 min at 200 °C and unspecified pressure. A higher glucose production (53%) was obtained when the medium was acidified with CO₂, and the amount of glucose produced increased linearly with increasing CO₂ content from 0 to 0.32g (Miyazawa & Funazukuri, 2005). All these studies targeted glucose production therefore high temperatures above 180 °C were used. To the best of our knowledge, chitosan hydrolysis in pressurized hot water is not reported. One study used sub- and supercritical water (300-400 °C, unspecified pressure, 0.5-15 min) as a pre-treatment before the enzymatic degradation of chitin. The yield of *N,N'*-diacetylchitobiose at 400 °C for 1 min was up

to 37%, compared to 5% without the pre-treatment (Osada et al., 2012). Another study used sub- and supercritical water (300-400 °C, unspecified pressure, 0.5-40 min) to purify chitosan from crab shell by removing protein (30% decomposition). They also found that the average molecular weight of pure chitin decreased from 760 kDa to 0.9 kDa after 2 min at 400 °C and the distance between chitin chains increased as indicated by XRD the analysis due to the weakening of hydrogen bonds, promoting enzymatic degradation (Osada et al., 2015).

To date, there is no study on pressurized hot water hydrolysis of starch or chitosan at 75-150 °C under 50-155 bar to produce valued-added products, like low molecular weight starch and chitosan. Therefore, the objective of this study was to use a green reaction approach to produce valuable compounds from starch and chitosan, understand the effect of pressure and temperature on reaction mechanisms of pure cassava starch, pure chitosan and their mixtures in pressurized hot water media. Also, characterize the biopolymer hydrolysates with respect to amylose content, reducing end yield, molecular weight, hydrodynamic diameter, charge and crystallinity.

3.2 Materials and methods

3.2.1 Materials

Cassava starch was kindly provided by CbPAK Tecnologia (Rio de Janeiro, RJ, Brazil). Chitosan (75-85% deacetylated) with medium molecular weight of 190-310 kDa was purchased from Sigma Aldrich (Oakville, ON, Canada). Gallic acid (ACS reagent, $\geq 99.5\%$) was acquired from Sigma Aldrich (Oakville, ON, Canada). Purified water from a Milli-Q system (Millipore, Bellerica, MA, USA) was used.

3.2.2 Methods

3.2.2.1 Production of hydrolysates

Hydrolysis was carried out using the subcritical fluid reaction system (Fig. 3.1) (Alvarez, Cahyadi, Xu, & Saldaña, 2014). First, hydrolysis was carried out using pure cassava starch (13 g) or chitosan (1.95 g, with 0.5 wt% gallic acid) or starch/chitosan mixtures (0.5 wt% gallic acid, 0.025-0.15 g chitosan/g starch) in pressurized hot water media. For each experiment, known amounts of compounds were preloaded inside the reactor with a volume of 270 mL. Then, the reactor was filled with Milli-Q water using a HPLC pump. The mixture inside the reactor was homogenized using a double helix stirrer for 5 min prior to applying the desired temperature and pressure. Then, the reaction was performed for 10 min. After cooling, the reacted starch and starch/chitosan mixture solution were unloaded and precipitated with 99% ethanol (1:4 v/v), and the resulting suspensions were passed through a Buchner funnel with Whatman No. 5 filter paper. The precipitates were dried at room temperature for 48h, then ground and passed through a 100-mesh sieve. The supernatants were also collected for reducing sugar analysis by HPLC. The reacted chitosan solutions were freeze dried for further characterization.

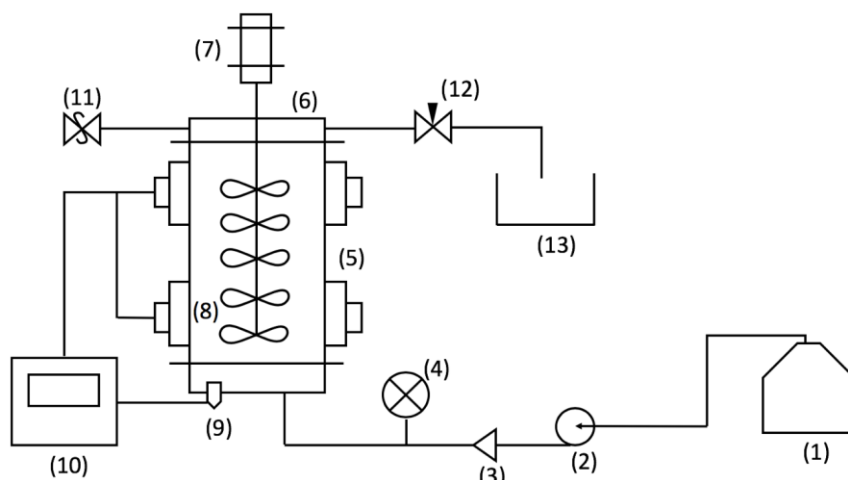


Fig. 3.1 Subcritical fluid reaction system: (1) Solvent reservoir, (2) Pump, (3) One-way valve, (4) Pressure gauge, (5) Band heaters, (6) Pressurised fluid reaction vessel, (7) Motor stirrer controlled by the control panel, (8) Stirrer, (9) Thermocouple, (10) Temperature controller, (11) Safety valve, (12) Back pressure regulator, and (13) Sample collection.

Hydrolysis of pure cassava starch and pure chitosan were first investigated in pressurized hot water media at temperatures of 75, 100, 125 and 150 °C and pressures of 50, 85, 120 and 155 bar. Then, different chitosan/starch ratios (0, 0.025, 0.05, 0.075, 0.1 and 0.15 g chitosan/g starch) were evaluated in pressurized hot water media at 100 °C and 85 bar. These conditions were chosen based on preliminary results.

3.2.2.2 Hydrodynamic diameter, zeta potential and molecular weight

The hydrodynamic diameter, zeta potential values and average molecular weight of the hydrolysates were measured using a Malvern Zetasizer Nano-ZS instrument (Malvern, Worcestershire, UK). For a typical determination, solutions were prepared by dissolving the dried pressurized hot water treated starch and starch-chitosan complex in dimethyl sulfoxide (DMSO) and chitosan in Milli-Q water at the concentration of 0.1 mg/mL. All measurements were performed in triplicate.

3.2.2.3 Reducing end

The reducing end assay was carried out following the method described by Imoto & Yagishita (1971). Briefly, 0.6 mL of a 0.5 M sodium carbonate solution containing 0.5 g/L potassium ferricyanide was mixed with 0.45 mL of the sample solution. The mixture was heated for 15 min at 100 °C and the absorbance was read at 420 nm.

3.2.2.4 Reducing sugar

Reducing sugars ($DP \leq 6$) in the starch and starch/chitosan hydrolysates were determined by HPLC (Agilent, Santa Clara, CA, USA) equipped with a refractive index detector using a SUPELCO Pb column operating at 70 °C, with a water flow rate of 0.6 mL/min.

3.2.2.5 Amylose content

For amylose content determination, starch (0.1 g) was dissolved in heated DMSO (10 mL) at 85 °C for 15 min (Hoover & Ratnayake, 2002). Then, this solution was diluted to 25 mL in a volumetric flask with Milli-Q water. An aliquot (1 mL) of this solution was later diluted with 50 mL of water, and 5 mL of a solution of iodine (0.0025 mol/L) in potassium iodide (0.0065 mol/L) was added with continuous mixing. The absorbance of the solution was read at 600 nm.

3.2.2.6 Color

The color parameters (L, a and b) of the pressurized hot water treated cassava starch and chitosan hydrolysates were determined with a Hunter Lab colorimeter (CR-400/CR-410, Konica Minolta, Ramsey, NJ, USA) that uses a D65 illuminant with an opening of 14 mm and a 10° standard observer according to the ASTM D2244 method (ASTM, 2011). The reacted solution (5 mL) was poured into a transparent plastic cup of 1 cm height x 3.5 cm diameter, which was then placed on the surface of a white standard plate (calibration plate values of $L^* = 93.49$, $a^* = -0.25$

and $b^* = -0.09$). The total color difference (ΔE), yellowness index (YI) and whiteness index (WI) were calculated with equations (3.1-3.3):

$$\Delta E = \sqrt{(L^* - L)^2 + (a^* - a)^2 + (b^* - b)^2} \quad (3.1)$$

$$YI = 142.86 \text{ b/L} \quad (3.2)$$

$$WI = 100 - [(100 - L)^2 + a^2 + b^2]^{0.5} \quad (3.3)$$

3.2.2.7 X-Ray diffraction (XRD) and relative crystallinity

The pressurized hot water treated cassava starch was analyzed at $5-55^\circ$ (2θ) with a scanning speed of $1^\circ/\text{min}$ in a Rigaku Geigerflex Powder Diffractometer (Rigaku, Tokyo, Japan) equipped with a cobalt tube, graphite monochromator and scintillation detector operated at 38 kV and 38 mA. The relative crystallinity (RC) value was measured by the ratio of the relative area of the crystalline peak to the total area of the diffractogram, expressed as percentage (%), and calculated by the JADE 9.1 software.

3.2.2.8 Differential scanning calorimetry (DSC)

Retrogradation properties of the pressurized hot water treated cassava starch were analyzed by a differential scanning calorimeter (DSC, TA instrument Q1000, New Castle, DE, USA). The treated starch samples were stored in a refrigerator at 4°C for 1, 3, 7, 11 and 14 days. Then, the samples were precipitated with 99% ethanol (1:4 v/v), and the resulting suspensions were passed through a Buchner funnel with Whatman No. 5 filter paper. The precipitates were dried at room temperature for 48h, then ground and passed through a 100-mesh sieve. For each DSC analysis, 4 mg of starch sample and Milli-Q water (1:2, w/w) were placed in pre-weighed aluminium sample pans. The pans were sealed hermetically to prevent moisture loss and kept overnight. A sealed empty aluminium pan was used as reference. The sample was held isothermally at 20°C for 1 min before heating from 20 to 140°C at $10^\circ\text{C}/\text{min}$. The onset, peak

and conclusion temperatures and the enthalpy (ΔH_r , J/g) associated with the retrograded starch were calculated. The ΔH_r was used to indicate the enthalpy of amylopectin starch retrogradation (Yu, Ma, & Sun, 2010).

3.2.2.9 Fourier transform infrared (FT-IR) spectroscopy

Transmittance spectra of pure cassava starch, pure chitosan and starch-chitosan complexes after pressurized hot water treatment were characterized using a Fourier transform infrared spectrometer (FT-IR) Nicolet 8700 (Thermo Fisher Scientific Inc, Waltham, MA, USA) equipped with a Smart Specular for grazing angle attenuated total reflectance. The experiments were conducted in the range of 4000 to 800 cm^{-1} with a resolution of 4 cm^{-1} and a total of 64 scans per sample. Data collection was done using the Nicolet Omnic 8.3 software.

3.2.2.10 Statistical analysis

The experiments were done at least in duplicates. The R studio software was used to conduct analysis of variance (ANOVA). Tukey's test was used to identify significant difference at $p < 0.05$ between means of each sample.

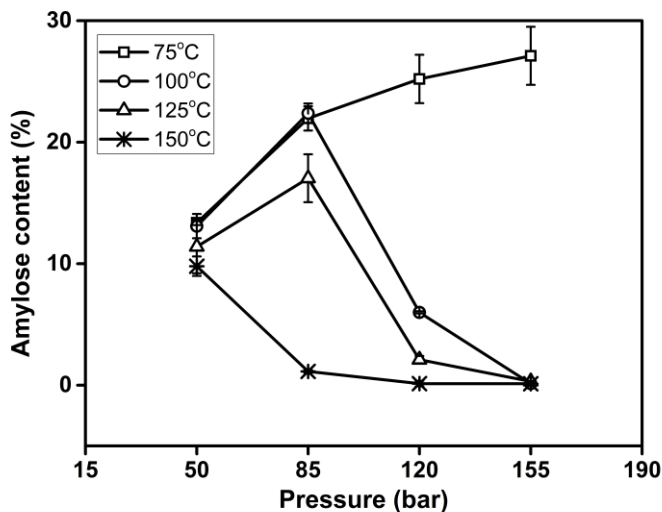
3.3 Results and discussion

3.3.1 Amylose production of cassava starch hydrolysates and its effect on starch retrogradation and crystallinity

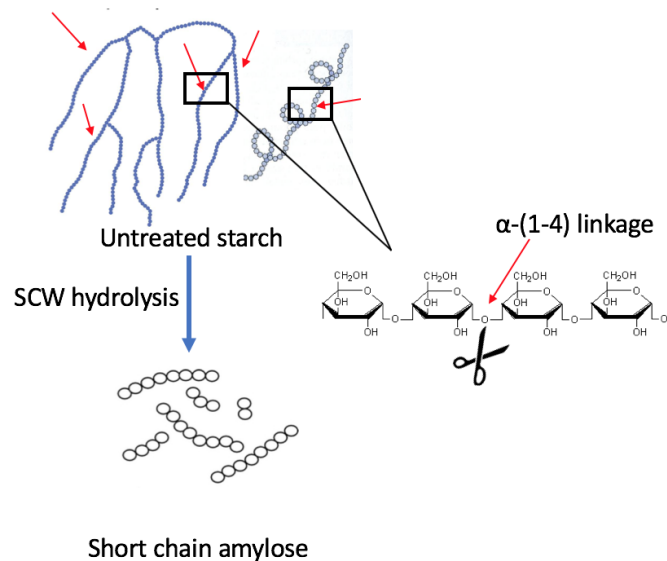
Fig. 3.2A shows the amylose content of cassava starch treated with pressurized hot water at 75 to 150 °C and 50 to 155 bar (Table A.1, appendix A). The amylose content provided information on the extent of starch hydrolysis. In general, cassava starch has amylose values ranging from 16% to 20% (Hoover, 2001). The amylose content of native cassava starch used in this study was 16.9%. At 75 °C, the amylose content increased continuously from 13.4% to 27.1% with increasing pressure from 50 to 155 bar as long amylose chains and branched

amylopectin chains were broken into short chains of amylose, increasing the amylose yield. Cassava starch was reported to have long amylopectin branch chain length ($DP > 28$) compared to maize, rice, wheat and barley ($18 < DP < 23$, Jane et al., 1999), therefore, cassava starch was a better choice for film formation in terms of the ability to form networks. At 100 and 125 °C, the yield of amylose peaked at 85 bar, reaching 22.4% and 17.3%, respectively. At these temperatures, when high pressures (≥ 120 bar) were used, the amylose content significantly reduced to less than 1%. This reduction can be attributed to a possible two-stage depolymerisation at 100 and 125 °C: first, short chain amylose is formed as a result of depolymerization from long amylose chains and branched amylopectin chains, similarly to the behavior observed at 75 °C, followed by a subsequent depolymerization to dextrans. Also, severe decrease on amylose content was observed at 150 °C and all pressures investigated. Under pressurized hot water conditions, starch molecules undergo depolymerization through debranching at the α - (1 \rightarrow 6) glycosidic bonds or decomposing within the chain between α - (1 \rightarrow 4) glycosidic bonds (Fig. 3.2B). Earlier studies mainly focused on glucose production under hydrothermal conditions operated at temperatures above 180 °C (Moreschi, Petenate & Meireles, 2004; Nagamori & Funazukuri, 2004). Nagamori & Funazukuri (2004) reported that more than 900 g/kg of the carbon in the initial sweet potato starch sample was converted to soluble products, such as maltodextrins, glucose or even 5-hydroxymethylfurfural at temperatures above 180 °C. A noticeable increase of glucose content from 0 (180 °C, 10 min) to 632 g/kg was observed at 200 °C within 30 min treatment. In another study by Moreschi et al. (2004), subcritical water in the presence of CO₂ (CO₂ flow rate and amount not reported) was used to hydrolyze ginger bagasse starch to oligosaccharides. The production of dextrose equivalence was 17-29% at 200 °C and 150 bar within a reaction time up to 15 min. The authors proposed a first-

order hydrolysis with respect to the starch concentration at 200 °C. In the first step (<1 min), intermediate size compounds (not specified) were formed, followed by a further hydrolysis to low molecular weight compounds (DP < 20) in the second step. At temperatures of 210-270 °C, Rogalinski et al. (2008) observed higher hydrolysis rate of corn starch than the hydrolysis rate of cellulose in subcritical water at 250 bar based on glucose production, with an increase from 0.0006 to 0.0317 s⁻¹, however, cellulose degradation was detected from 240 to 310 °C, with a reaction rate constant of 0.0214 s⁻¹ at 270 °C.



(A)



(B)

Fig. 3.2 A) Amylose content of pure cassava starch after pressurized hot water treatment at 75-150 °C and 50-155 bar for 10 min, and B) hydrolysis scheme of cassava starch

Fig. 3.3 shows the XRD patterns of native cassava starch (Fig. 3.3a), cassava starch gelatinized at 90 °C (Fig. 3.3b) and cassava starch after pressurized hot water treatment at 75-150 °C and 50-155 bar (Fig. 3.3c-j). The XRD results were used to determine starch crystalline structure and recrystallization of pressurized hot water treated samples. Native cassava starch exhibited characteristic diffraction peaks at 15°, 17°, 17.6° and 22°, representing the B-type crystalline structure. However, these main diffraction peaks disappeared after pressurized hot water treatment, suggesting that crystalline arrangements in B-type starches were disrupted by pressurized hot water (Fig. 3.3c-j). Also, a large reduction in relative crystallinity value from 11.28% to 6.97% was observed in starches treated at temperatures of 75-150 °C (Fig. 3.3c-f). One study reported decreased intensities of XRD (21.7-12.3%) for hydrothermally (120 °C, 60 min, unspecified pressure) treated cassava starch with moisture contents of 10-30% compared

with untreated sample (24.3%) (Andrade, de Oliveira, Colman, da Costa & Schnitzler, 2014). Lower relative crystallinity values (6.97-11.28%) were obtained in our study due to the large amount of water used (5% starch solution), as water disrupts starch crystalline structure during the heating process. Similarly, the peak intensities and crystallinity in the hydrothermally treated potato starches (40% moisture content) decreased, with a noticeable reduction from 40% to 14% after heating at 100 °C for 30 min, and annealing at 70 °C for 12 h (Lee, Shin, Kim, Choi & Moon, 2011), due to the double-helical movement during heat-moisture treatment that disrupted starch crystallites and changed crystallite orientation (Gunaratne & Hoover, 2002). New peaks found at around 13° and 20° (Fig. 3.3c-f) can be characterised for crystallographic parameters of V_H-type crystals for gelatinized starch prepared from solution. Similarly, Teixeira et al. (2014) reported that high pressure (760 bar) treated wheat starch showed small peaks around 12° and 19.5°, indicating V_H-type crystallinity that results from starch deformation.

Crystalline pattern and relative crystallinity range (8.57-9.00%) of all starches (Fig. 3.3g-j) did not markedly change upon treatment with pressures ranging from 50 to 155 bar at 100 °C, which was in agreement with a previous study, where the XRD patterns and relative crystallinity of cassava starch were hardly affected by pressure (200-1000 bar) (Che et al., 2007). However, a decrease of the diffraction peak intensity (unspecified value) with increase of high hydrostatic pressure from 1500 to 6000 bar could be clearly observed in red adzuki bean starch (Li et al., 2015). Starch crystallinity depends on amylose content, which influences network formation in gels and composites to provide desired mechanical properties. For example, amylose retrogradation determines the initial hardness of a starch gel due to fast amylose recrystallization, while amylopectin retrogradation determines the final hardness of a starch gel due to slow recrystallization of amylopectin (Delcour et al., 2010).

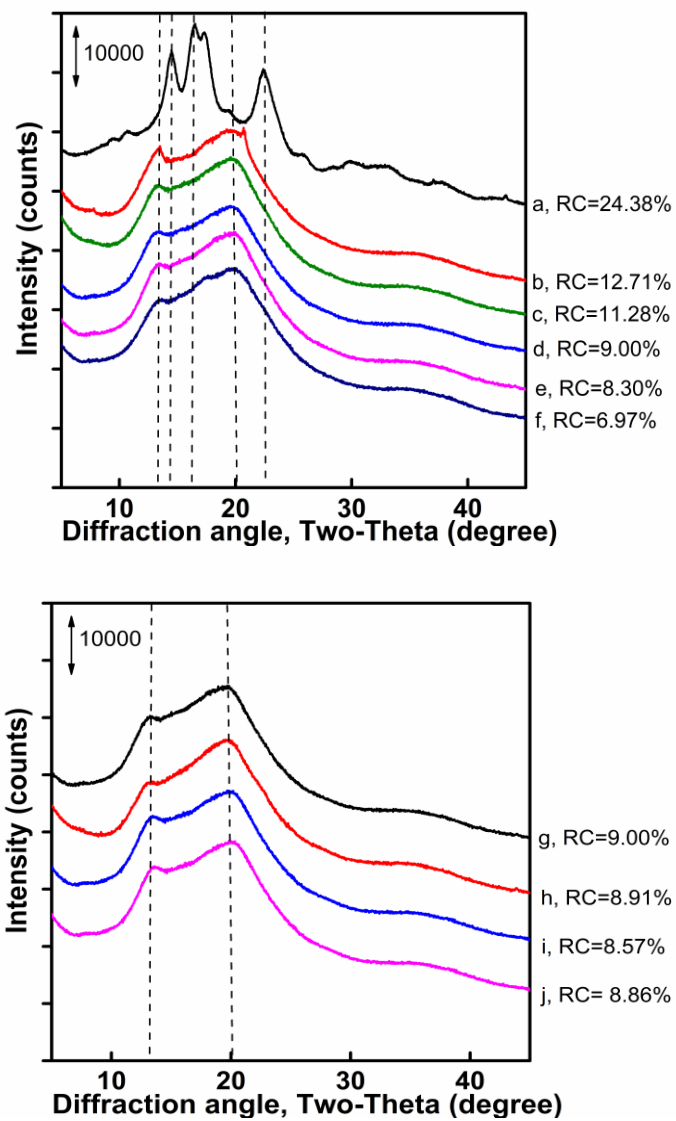


Fig. 3.3 XRD patterns and relative crystallinity (RC, %) of: a) native cassava starch, b) pure cassava starch gelatinized at 90 °C, c-f) pure cassava starch after pressurized hot water treatment at 75-150 °C and 85 bar, and g-j) pure cassava starch after pressurized hot water treatment at 50-155 bar and 100 °C for 10 min.

Table 3.1 shows the starch retrogradation properties of onset, peak and conclusion temperatures and enthalpy (ΔH_r). Starch retrogradation is a process in which disaggregated amylose and amylopectin chains in a gelatinized starch paste reassociate to form more ordered structures (Biliarderis, 1992). The variations in the DSC transition temperatures (T_o , T_p , and T_c) together with the XRD data provided information on how amylose and amylopectic molecules rearrange during storage up to two weeks at 4°C.

Native cassava starch had the lowest onset, peak and conclusion temperatures of 52.86 °C, 62.8 °C and 71.97 °C, respectively. The onset, peak and conclusion temperatures of pressurized hot water treated starch increased with the increasing temperatures from 75 to 150 °C at 85 bar. The shift of the peak temperature to a higher temperature indicated the growth of more organized crystallites that resulted from the dextrin content increase after pressurized hot water treatment, where more dextrin content indicated that a more stable crystalline structure was formed. This observation was contradictory to the reported by Rodríguez-Sandoval et al. (2008), where the retrograded cassava flour (84% starch, 1.1% protein) produced by boiling water developed a lower-temperature shoulder, indicating that the increase of the endotherm of retrograded starch during storage at 4 °C largely results from the growth of less perfect crystallites. In our study, the onset, peak and conclusion temperatures of pressurized hot water treated starch were little influenced by storage time up to two weeks. This behaviour agrees with the study of Yu et al. (2009), who reported no changes in the onset, peak and conclusion temperatures of cooked rice (79.74%-81.33% total carbohydrates content) retrogradation with storage time up to two weeks.

Increasing storage time from 0 to 14 days increased the starch retrogradation enthalpy of all samples. Comparing the retrogradation enthalpy (ΔH_r) of pressurized hot water treated cassava starch at storage of 14 day; starch treated at 75 °C had the highest ΔH_r value (18.68 J/g),

followed by 100 °C (18.31 J/g) and 125 °C (12.21 J/g), while at 150 °C starch showed the lowest ΔHr of 5.39 J/g, suggesting faster retrogradation of starch with high amylose content. Most recrystallizations of pressurized hot water treated starch occurred during the first 3 days of storage, followed by a slower retrogradation process until 14 days. Starch retrogradation usually consists of crystallization of amylose developed in the early stages and slow crystallization of amylopectin occurring during storage. Biliarderis (1992) reported that amylose retrogradation occurred within one day and crystal nuclei growth was initiated and promoted by retrograded amylose, therefore, high amylose content induced fast starch retrogradation with high ΔHr value. Similarly, Yu et al. (2009) observed an increase of ΔHr value from 1.79 to 3.41 J/g with the increasing amylose content from 23.94 to 35.73%. They also found that ΔHr values were positively correlated with amylose content ($0.603 \leq r \leq 0.822$, $P < 0.01$) during storage (0-14 day). Interestingly, the amylose content reported in Fig. 3.2 was positively correlated with the ΔHr values reported in Table 3.1 ($r^2 = 0.938$). Starch amylose content and amylose-amylopectin associations during retrogradation play a significant role in determining various properties of starch gels and composites. As ΔHr represents the amount of energy required to break down the double helices and the complex network formed during retrogradation, the high ΔHr value means a more stable network, which is favorable to produce solid structures (films and aerogels).

Table 3.1 Retrogradation characteristics of pure cassava starch after pressurized hot water treatment during storage for 0, 1, 3, 7, 11 and 14 days.

Sample	Storage time (days)	T _o (°C)	T _p (°C)	T _c (°C)	ΔH _r (J/g)
Native cassava starch	0	52.86	62.8	71.97	13.87
Control	0	95.37	105.35	115.8	10.45
	1	94.87	105.39	116.39	11.41
	3	95.23	106.42	115.92	13.39
	7	95.12	106.49	115.38	14.17
	14	95.74	105.83	115.79	14.48
75 °C, 85 bar	0	96.56	106.23	116.34	7.98
	1	96.32	106.52	116.39	9.93
	3	96.75	106.78	116.20	13.81
	7	97.01	107.01	116.64	16.99
	14	96.85	106.39	116.29	18.68
100 °C, 85 bar	0	98.63	107.59	117.39	7.43
	1	99.21	108.32	116.74	9.12
	3	98.41	107.34	117.39	13.98
	7	98.52	107.48	116.44	16.32
	14	98.56	108.36	117.86	18.31
125 °C, 85 bar	0	99.31	109.68	121.42	5.12
	1	99.39	110.34	122.53	7.32
	3	99.61	109.34	121.40	8.98
	7	98.90	110.83	122.46	10.58
	14	98.83	110.94	122.69	12.21
150 °C, 85 bar	0	100.25	114.37	130.10	2.31
	1	100.32	115.53	131.45	3.20
	3	101.32	114.63	131.59	3.43
	7	100.43	115.89	130.78	4.98
	14	101.17	116.32	131.49	5.39

T_o: onset temperature; T_p: peak temperature; T_c: conclusion temperature; and ΔH_r: retrogradation enthalpy.

3.3.2 Reducing end yield of cassava starch and chitosan hydrolysates

The starch hydrolysate was further characterized by the reducing end yield as shown in Fig. 3.4A (Table A.2, appendix A). Reducing end yield was used to estimate the extent of depolymerization as starch and chitosan are biopolymers composed of sugars. The breaking of these polymers produces smaller compounds that expose reducing ends, as indicated by the increase of reducing end yield. The decreased amylose content and increased reducing end yield indicated the formation of low molecular weight compounds due to hydrolysis at temperatures (100-150 °C) and pressures (85-155 bar) investigated. The depolymerization was less significant at 75 °C. At 155 bar and all temperatures investigated, the reducing end yields were twice compared with the reducing end yield obtained at 50 bar. Moreover, the effect of temperature was more pronounced, where the reducing end yield increased around five times at 150 °C compared with the yield obtained at 75 °C. The role of pressure was mainly to retain water in the liquid phase, while temperature accelerated the reaction kinetics through dissociating water molecules into acidic hydronium ions (H_3O^+) and basic hydroxide ions (OH^-), accelerating acid- or base-catalyzed reactions. The highest yield (38.6 mg glucose equivalent/g starch) was obtained at 150 °C and 155 bar. However, no reducing sugar ($\text{DP} \leq 6$) in the starch hydrolysate was detected by HPLC at all conditions investigated (data not shown), indicating the production of low molecular weight starch instead of reducing sugars. This result is in agreement with the previous study reported by Nagamori & Funazukuri (2004), where glucose yield was negligible at temperatures below 180 °C.

For chitosan hydrolysate (Fig. 3.4B, Table A.2, appendix A), a more effective depolymerization than for starch was obtained as reflected by the increasing reducing end yield at the range of 23.0-81.2 mg N-acetyl-D-glucosamine equivalent/g chitosan at temperatures (75-

150 °C) and pressures (50-155 bar) investigated. The amount of reducing end at 150 °C was favoured by pressure especially above 120 bar. Quitain et al. (2001) studied the amino acid and glucosamine production from shrimp shells by high-temperature (250-300 °C) and high-pressure (300 bar) water. Based on their results, the highest amino acids yield (70 mg/g of dry shrimp shell) from protein hydrolysis was obtained at a reaction temperature of 250 °C in 60 min, meanwhile, deamination of chitosan to glucose occurred due to hydrolysis. Recently, Savitri & Rosyadi (2015) investigated the combination of sonication (500 W and 20 kHz for 120 min at 60 °C) and hydrothermal degradation of chitosan under supercritical CO₂ assisted conditions at temperatures up to 200 °C and pressures up to 230 bar. The hydrolysis product consisted of glucose and 5-hydroxy methyl furfural with yields of 0.2-0.6% and 1.9-14.4%, respectively. Also, glucose was unstable at 200 °C and degraded to 5-hydroxy methyl furfural. As known, furfural is a toxic compound that should be avoided in the product. In this study, there is no furfural formation as no reducing sugar ($DP \leq 6$) was detected by HPLC, and furfural formation requires higher temperatures (>220 °C) (Nagamori & Funazukuri, 2004) than those investigated in this study (75-150 °C and 50-155 bar). Furthermore, if the application of the hydrolyzed polymer is a biodegradable film, an appropriate starch and chitosan chain length is needed to form cross-linked network of the film matrix. Short polymer chain fragments cannot associate to form a film, while polymer chains with long length restrict the movement of polymer when binding together, resulting in less flexible films (Zhao et al., 2018).

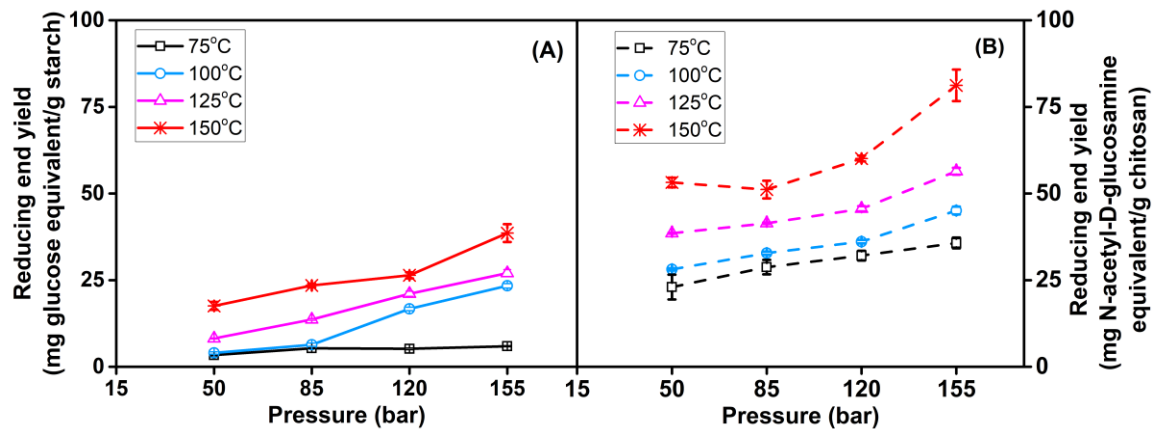


Fig. 3.4 Reducing end yield of: A) pure cassava starch, and B) chitosan after pressurized hot water treatment at 75-150 °C and 50-155 bar for 10 min.

3.3.3 Molecular weight and particle size of cassava starch and chitosan hydrolysates

The average molecular weight of pure cassava starch and chitosan, and the hydrodynamic diameter of chitosan after pressurized hot water treatment are shown in Fig. 3.5 (Table A.3, appendix A). Different polymer molecular weight and particle size distributions revealed the effect of temperature and pressure in pressurized hot water hydrolysis. The molecular weight distributions of the starch hydrolysates shifted to lower molecular weights by increasing temperature and pressure (Fig. 3.5A). Starch average molecular weight decreased to almost half at all temperatures investigated with the increasing pressure from 50 to 155 bar. The most effective reduction of molecular weight from 513.5 to 172.5 kDa occurred from 75 to 150 °C at 50 bar. Within 10 min of reaction, the average molecular weight was reduced from 1243.5 kDa (native cassava starch) to 435.5 kDa (100 °C, 50 bar), which is lower than that reported by Van der Veen et al. (2006), who produced hydrolysed corn starch with molecular weight of 684 kDa at 110 °C for 12 min from the native corn starch with a molecular weight of 2286 kDa, due to the low water content used (starch with 70% moisture content), which limited the amount of water to

hydrolyse the starch. Also, their experiments were not performed under pressurized hot water conditions, preventing water to behave as a catalyst. The particle size of the pressurized hot water treated cassava starch was not determined due to the large diameter of particles ($> 6 \mu\text{m}$), which exceeded the equipment detection limit.

Molecular weight and particle size of pure chitosan after pressurized hot water treatment are shown in Fig. 3.5B and 3.5C. Pressurized hot water showed a more pronounced effect on chitosan hydrolysis than starch hydrolysis. The average molecular weight of untreated chitosan was around 205 kDa. At the lowest temperature (75 °C) used, a reduction from 180.5 to 77 kDa was observed with the increasing pressure from 50 to 155 bar. More than half reduction compared to the untreated chitosan was observed at temperatures over 100 °C at all pressures evaluated. There was no significant difference on the particle size between untreated chitosan (2428.5 nm) and chitosan treated at 75 °C and all pressures investigated (2510.5-2448.5 nm, Fig. 3.5C). At the highest temperature of 150 °C, chitosan particle size was reduced to one tenth of the untreated chitosan particle size. Vårum et al. (2001) reported that the activation energy for chitosan hydrolysis of the two deacetylated (D-D) glycosidic linkages ($158.1 \pm 9.8 \text{ kJ/mol}$) was higher than the activation energy for hydrolysis of the two acetylated glycosidic linkages (A-A, $130.4 \pm 2.5 \text{ kJ/mol}$) and the acetylated and deacetylated (A-D, $134.3 \pm 3.1 \text{ kJ/mol}$) glycosidic linkages. As starch has similar non-acetylated glycosidic linkages to deacetylated glycosidic linkages in chitosan, it required more energy to be hydrolysed (Fig. 3.5D). The untreated chitosan used in this study had a relative crystallinity value of 19.22%, while the native cassava starch had a higher relative crystallinity value of 24.38% (Fig. 3.3a), indicating that chitosan was easier to depolymerize due to the relative high level of amorphous regions. Linear chains of starch molecules are constrained by hydrogen bonds in crystalline structures, then, the

amorphous part was preferentially depolymerized because of the easiness of pressurized hot water access. Tian et al. (2004) reported that in the crystalline region, chitosan was depolymerized by debranching the layers, while the amorphous portion was depolymerized by penetrating through the loose matrix requiring less energy as confirmed by the XRD analysis. The effect of pressure on particle size and molecular weight was less significant, especially above 100 °C. The role of pressure was mainly to retain water in the liquid phase, while temperature accelerated the reaction kinetics. Also, Moreschi et al. (2004) reported that only temperature (176-200 °C) had a statistically significant effect on reducing sugar yield at pressures of 80-220 bar for ginger bagasse starch depolymerization.

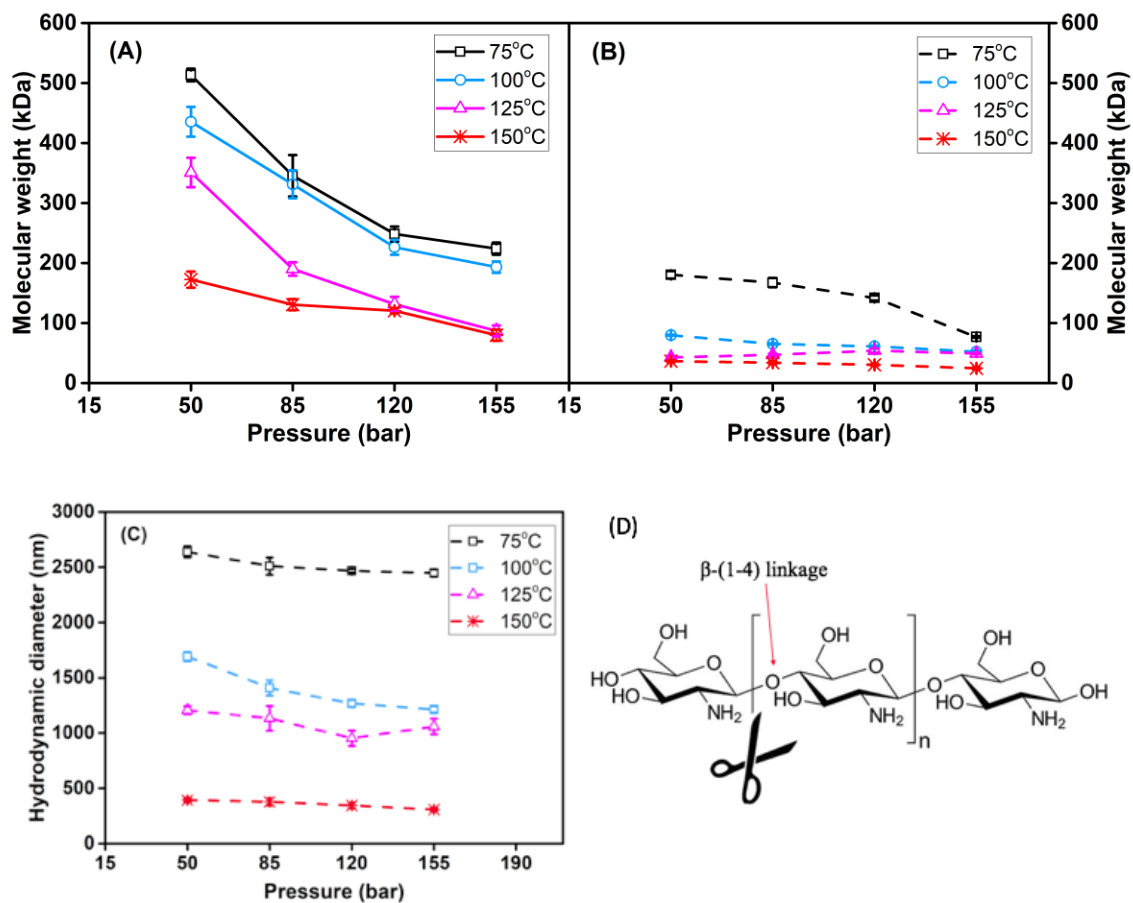


Fig. 3.5 Molecular weight of: A) pure cassava starch, and B) chitosan, and hydrodynamic diameter of: C) chitosan after pressurized hot water treatment at 75-150 °C and 50-155 bar for 10 min, and D) chitosan hydrolysis scheme.

3.3.4 Color performance of pressurized hot water treated cassava starch, chitosan and starch-chitosan complexes

Table 3.2 shows the color change of cassava starch and chitosan hydrolysates and their complex hydrolysates after pressurized hot water treatment. Starch and chitosan may undergo color change after pressurized hot water treatment, affecting the appearance of hydrolysates and final products. Generally, cassava starch was less affected by pressurized hot water treatment compared to chitosan, with little change in color performance with regards to total color

difference, yellowness index and whiteness index. The color of chitosan hydrolysates changed to a more intense yellow with increasing temperature and pressure. Regarding the yellowness index and whiteness index, only chitosan treated at 150 °C increased yellowness significantly compared to the control and other treatment conditions (75-125 °C), with yellowness index of 12.82-15.10 and whiteness index of 89.42-91.40. Previous studies reported that the colored product might be a consequence of Maillard reaction between the amino group and carbonyl group present in chitosan. The experiments conducted by Lim et al. (1999) and Yang et al. (2007) showed that both dry heat (160 °C for 2 h) and autoclave sterilization (under a pressure of 1.15 bar, at 121 °C for 20-45 min) caused darkening of chitosan powder. Coloration of chitosan was accelerated at temperature above 120 °C and long exposure time (>30 min). In our study, after combining cassava starch with increased amount of chitosan up to 15 wt%, no significant color change was observed for the starch-chitosan complexes due to the low reaction temperature of 100 °C and low chitosan/starch ratios used.

Table 3.2 Color performance of cassava starch and chitosan hydrolysates and their complex hydrolysates after pressurized hot water treatment

Temperature (°C)	Pressure (bar)	Cassava starch			Chitosan				
		ΔE	YI	WI	ΔE	YI	WI		
Control		5.25±0.04 ^{ab}	4.77±0.49 ^{ab}	95.66±0.19 ^{cd}	3.64±0.27 ^d	6.09±0.46 ^b	95.68±0.33 ^a		
	50	3.41±0.25 ^{bcdef}	2.02±0.03 ^b	98.23±0.22 ^a	3.46±0.56 ^d	6.02±1.37 ^b	95.74±0.96 ^a		
	85	4.59±0.33 ^{abcd}	2.85±0.15 ^b	96.98±0.32 ^{abcd}	4.53±0.17 ^{cd}	5.55±0.40 ^b	95.66±0.29 ^a		
	120	4.88±0.19 ^{abcd}	4.37±1.44 ^{ab}	96.06±0.54 ^{abcd}	4.59±0.18 ^{cd}	5.10±0.53 ^b	95.85±0.36 ^a		
75	155	5.21±0.33 ^{abc}	4.43±1.67 ^{ab}	95.80±0.49 ^{bcd}	5.02±0.37 ^{bcd}	5.48±0.55 ^b	95.43±0.47 ^a		
	50	3.81±0.25 ^{abcde}	1.89±0.04 ^b	98.06±0.20 ^{ab}	4.48±0.54 ^{cd}	5.71±0.48 ^b	95.59±0.49 ^a		
	85	3.50±0.25 ^{bcdef}	3.29±0.43 ^b	97.41±0.14 ^{abc}	4.17±0.01 ^d	5.24±0.18 ^b	95.98±0.10 ^a		
	120	5.58±0.16 ^a	3.22±0.66 ^b	96.04±0.12 ^{abcd}	4.36±0.31 ^d	5.22±0.09 ^b	95.90±0.10 ^a		
100	155	4.93±0.01 ^{abcd}	5.18±1.41 ^{ab}	95.67±0.66 ^{cd}	4.68±0.14 ^{bcd}	5.34±0.11 ^b	95.69±0.13 ^a		
	50	1.65±0.15 ^{fg}	3.61±0.33 ^b	97.36±0.20 ^{abc}	5.20±0.55 ^{bcd}	7.15±1.32 ^b	94.57±0.88 ^a		
	85	3.09±0.30 ^{defg}	4.37±0.32 ^{ab}	96.88±0.14 ^{abcd}	4.40±0.97 ^d	6.34±1.34 ^b	95.31±1.08 ^a		
	120	2.10±0.19 ^{efg}	4.54±0.44 ^{ab}	96.75±0.39 ^{abcd}	3.82±0.67 ^d	5.43±0.08 ^b	95.98±0.27 ^a		
125	155	4.02±0.42 ^{abcde}	4.17±0.02 ^{ab}	96.66±0.22 ^{abcd}	4.51±0.47 ^{cd}	6.02±0.38 ^b	95.43±0.39 ^a		
	50	1.21±0.31 ^g	4.43±0.26 ^{ab}	95.89±0.43 ^{abcd}	7.19±0.88 ^{ab}	12.82±2.25 ^a	91.01±1.56 ^b		
	85	4.45±1.76 ^{abcd}	4.53±1.16 ^{ab}	92.69±1.79 ^{de}	6.50±0.38 ^{abc}	12.13±0.54 ^a	91.40±0.35 ^b		
	120	3.20±0.03 ^{cdefg}	5.00±0.98 ^{ab}	96.46±0.64 ^{abcd}	7.77±0.46 ^a	13.77±0.84 ^a	90.35±0.58 ^b		
150	155	2.92±0.51 ^{defg}	6.92±0.95 ^a	94.86±0.82 ^c	8.56±0.77 ^a	15.10±1.35 ^a	89.42±0.95 ^b		
	Chitosan/starch ratio (g/g)		0	0.025	0.05	0.075	0.1	0.15	
	100	85	ΔE	3.50±0.25 ^A	4.38±0.18 ^{AB}	5.28±0.10 ^{AB}	4.94±0.28 ^{AB}	5.02±0.94 ^{AB}	5.90±0.50 ^A
			YI	3.29±0.43 ^B	9.10±0.28 ^A	10.52±0.20 ^A	10.01±0.48 ^A	10.06±1.25 ^A	11.41±0.73 ^A
WI			97.41±0.14 ^A	93.5±0.20 ^B	92.43±0.22 ^B	92.80±0.41 ^B	92.46±1.19 ^B	91.55±0.48 ^B	

ΔE: total color difference, YI: yellowness index, and WI: whiteness index.

Data shown as mean ± standard deviation (n = 3). Control: cassava starch gelatinized at 90 °C under 1 atm condition.

^{a-g} Different lowercase letters in the same column indicate significant differences (p < 0.05).

^{A-B} Different uppercase letters in the same row indicate significant differences (p < 0.05).

3.3.5 Cross-linking of chitosan-starch complexes after pressurized hot water treatment

Fig. 3.6A shows the FT-IR spectra of pure cassava starch, pure chitosan and starch/chitosan mixtures after pressurized hot water treatment at 100 °C and 85 bar for 10 min. New peaks at 1717 and 1720 cm^{-1} were found in chitosan hydrolysates (with gallic acid) and starch-chitosan complexes, indicating the formation of ester linkages between the carbonyl groups (-COOH) of gallic acid and the hydroxyl groups (-OH) of chitosan or starch (Fig. 3.6B). The cross-link of cassava starch with chitosan provided core knowledge for network formation that can be further used to produce film, hydrogel or other composites to be applied in food or pharmaceutical areas. Other observations of ester linkages have been reported for chitosan films loaded with gallic acid at 1715 cm^{-1} (Sun, Huang, Hu, Xiong, & Zhao, 2014a). Moreover, the amide-I and NH_2 characteristic peaks at 1554 and 1640 cm^{-1} of chitosan hydrolysate shifted to 1540 and 1627 cm^{-1} in the starch-chitosan complexes, further suggesting that reactions between the starch, chitosan and carbonyl groups of gallic acid occurred via ester linkages. Similar results were reported when murta leaf extract (rich in phenolic acids) was incorporated into corn starch/chitosan blend at 70 °C, as phenolic acids formed electrostatic interactions with chitosan. Ester linkages and hydrogen bonds were also formed between phenolic acids of murta leaf extract and chitosan/starch blends (Silva-Weiss et al., 2013).

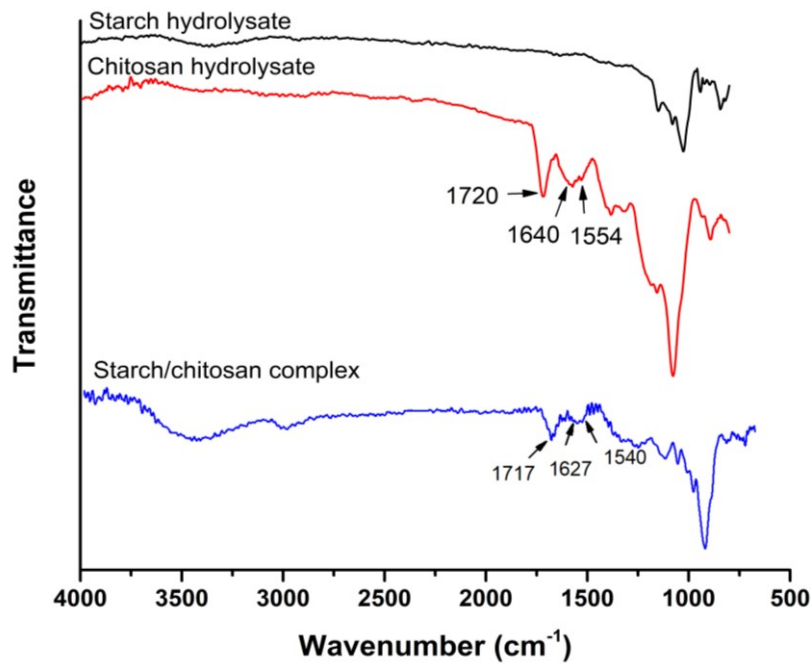


Fig. 3.6 FT-IR spectra of pure cassava starch, pure chitosan and starch-chitosan complexes after pressurized hot water treatment at 100 °C and 85 bar for 10 min.

In addition, molecular weight and charge data confirmed the cross-linking within starch-chitosan complexes (Table 3.3). The molecular weight of starch-chitosan complexes increased 5 folds from 331.4 to 1656 kDa with the increasing ratio of chitosan in the complex. Starch showed a negative zeta potential of -3 or -4 mV, so the increase of zeta potential value to 2.11 mV after mixing with chitosan demonstrated the interactions between starch and chitosan.

Specifically, the high ionic products of H^+ and OH^- in pressurized hot water media facilitated acid- or base-catalyzed reactions. The relatively high density combined with the high water dissociation constant favored ionic reactions. In this study, OH^- produced in pressurized hot water media deprotonated the $-OH$ groups of starch to $-O^-$, making them slightly negative. Also, $-COOH$ groups of gallic acid that were partially dissociated to COO^- and H^+ , while H_3O^+ produced in pressurized hot water media protonated the amino group to $-NH_3^+$, promoting the reactions between starch, chitosan and gallic acid through electrostatic interactions. In addition, part of the non-dissociated gallic acid forms ester linkages after

reacting with $\text{-CH}_2\text{OH}$ groups of starch and chitosan polymers, contributing to the formation of starch/chitosan complexes (Fig. 3.6B).

Table 3.3 Molecular weight and zeta potential values of chitosan-starch complexes after pressurized hot water treatment at 100 °C and 85 bar for 10 min.

Chitosan/starch ratio (g/g)	0	0.025	0.05	0.075	0.1	0.15
Molecular weight (kDa)	331.4±23.4 ^d	950.0±5.6 ^c	955.0±17.7 ^{bc}	1216.0±36.7 ^{abc}	1511.0±78.5 ^{ab}	1656.0±31.1 ^a
Zeta potential (mV)	-3.85±0.30 ^d	0.08±0.01 ^c	0.15±0.01 ^c	0.29±0.02 ^{bc}	0.63±0.08 ^b	2.11±0.00 ^a

Data shown as mean ± standard deviation ($n = 3$).

^{a-d} Different lowercase letters in the same row indicate significant differences ($p < 0.05$).

3.4. Conclusions

The use of pressurized hot water offers an innovative green reaction process to control hydrolysis of pure starch, pure chitosan and their mixtures. Cassava starch was hydrolysed to short chain amylose at 75-100 °C, followed by further depolymerization to compounds with less than 100 kDa. High amylose contents were obtained at 85 bar for 75 °C (21.9%), 100 °C (22.4%) and 125 °C (17.3%). Reducing end yield increased five times at 150 °C compared with the yield at 75 °C. However, no reducing sugar ($DP \leq 6$) was detected by HPLC at all conditions investigated. The increase of storage time and amylose content led to the increase of starch retrogradation enthalpy. For chitosan treated with pressurized hot water, a significant molecular weight decrease from 180.5 to 77 kDa was found with the increasing pressure from 50 to 155 bar at 75 °C. But, the effect of pressure on molecular weight was less significant, especially above 75 °C, where maximum 30% drop in molecular weight was observed at 100, 125 and 150 °C from 50 to 155 bar. Chitosan color change was accelerated at 150 °C and all pressures investigated as shown by the increase of yellowness values. Furthermore, pressurized hot water favored reactions between starch and chitosan through hydrogen bonds, ester linkages and electrostatic interactions, forming starch-chitosan complexes. Therefore, pressurized hot water technology provides a promising green reaction alternative to obtain low molecular weight starch and chitosan, and starch-chitosan complexes with tailored charges for various applications in the food and nutraceutical industry.

Chapter 4: Use of Potato By-products and Gallic Acid for Development of Bioactive Film Packaging by Pressurized Hot Water Technology*

4.1. Introduction

Recently, there have been considerable environmental concerns due to the excessive use of petroleum-based packaging materials. Today, most plastics bags are made of petroleum-based sources, which requires up to 50 years to decompose. But, the plastic debris generated cannot be decomposed entirely, instead microplastics of <5 mm are formed. They are known to harm marine life, which mistake them for food, and therefore can be consumed later by humans via seafood consumption. There are also concerns that microplastics can accumulate toxic chemicals and pollute the soil (Arthur, Baker, & Bamford, 2009). In addition, it is challenging to dispose plastics in landfills in a sustainable way. Therefore, there is a need to develop alternative biodegradable plastics. In recent years, bioactive films have attracted considerable attention as they provide antioxidant, antimicrobial, antibrowning, barrier to oxygen, carbon dioxide, and UV-vis light by incorporation of natural active compounds in packaging systems or biopolymer-based films that modify the film structure and functionality for food applications.

Starch, a natural biopolymer, is abundant, renewable, inexpensive, environmentally friendly, and easy to be chemically modified. These advantages make starch an attractive and promising bio-resource for packaging applications. Root and tuber crops are the second major source of starch after cereals, including potato, cassava, yam and taro. Potato is the largest vegetable crop in Canada, accounting for 30% of all vegetables. According to Statistics Canada, a production of 4.8 million tons of potato was achieved in 2017 in Canada (Statistics Canada, 2007). As a result of growing production of processed potato products (mashed

* A version of this chapter has been published as “Zhao, Y. and Saldaña, M.D.A. (2019). Use of Potato By-products and Gallic Acid for Development of Bioactive Film Packaging by Subcritical Water Technology. *The Journal of Supercritical Fluids*. 143, 97-106.

potatoes, chips and fries), considerable amounts of waste are generated. In addition, approximately 40-50% of potatoes are not suitable for human consumption (Charmley, Nelson & Zvomuya, 2006), including the by-products of potato peel and potato cull. However, potato peel is a good source of phenolic compounds (25–125 mg/100 g). Phenolic acids such as chlorogenic acid, caffeic acid, ferulic acid and gallic acid are found in potato peel (Singh & Saldaña, 2011), while potato cull is a rich source of starch. Amylopectin and amylose are two major components of starch. Amylose makes starch films more rigid, whereas the branched structure of amylopectin leads to different mechanical properties, influencing the tensile stress (Tharanathan, 2003). However, bioactive films made of starch has some disadvantages, such as high water solubility, poor water barrier properties and poor mechanical properties (Davoodi, Kavooosi & Shakeri, 2017) and poor mechanical properties (Mathew, Brahmakumar & Abraham, 2006), limiting their applications in the food industry. Various chemical approaches have been employed to overcome these disadvantages. Chemical modification is one of the approaches usually undertaken to improve film properties. Earlier, potato starch film cross-linked with 5 wt% citric acid showed improved tensile strength from 9 to 23 MPa (Reddy & Yang, 2010). In another study, oxidized potato starch film with 1.5 wt% active chlorine added had less water vapor permeability ($< 5.8 \text{ g}\cdot\text{mm}/\text{m}^2\cdot\text{day}\cdot\text{kPa}$), but resulted in a lower tensile strength of $< 2.3 \text{ MPa}$ (Fonseca et al., 2015). In addition, incorporation of synthetic or bio-based composites is another effective strategy to reinforce film properties. For example, the water absorption of potato-poly lactic acid-nanoclay blend film was decreased by 12% compared to the pure potato starch film (54.4%), and a significant increase in tensile strength from 1.8 to 8.0 MPa was also reported (Ayana, Suin & Khatua, 2014). Recently, Noshirvani et al. (2017) reported that potato starch film solubility in water decreased significantly from 20.8% to 11.9% due to the hydrogen bonding generated between hydroxyl groups of starch, polyvinyl and cellulose nanocrystals.

Therefore, modification of bioactive starch films is of great importance to explore their applications in the food packaging field.

Traditional methods used to produce starch films are casting, extrusion blowing, injection, and thermo-compression. However, the poor miscibility of functional additives with starch and the break down of molecules by intense shear are still challenges for these techniques (Liu et al., 2009). Only two studies reported the use of pressurized hot water technology, where the pressurized hot water can be a catalyst or reaction medium to promote interactions between phenolics and starches (Zhang, 2015; Zhao et al., 2018). Recently, gallic acid-chitosan-cassava starch film showed prolonged ham shelf-life up to 25 days (Zhao et al., 2018). But, more studies are needed to understand the reaction process and the effect of using potato by-products and gallic acid on film properties. Therefore, the aim of this study was to develop bioactive films of potato by-products with(out) gallic acid using pressurized hot water technology to improve film cross-linking and antioxidant activity.

4.2. Materials and methods

4.2.1 Materials

Red potato was purchased from a local supermarket (Edmonton, AB, Canada). Glycerol (> 95% purity, certified ACS grade) was purchased from Fisher Scientific (Ottawa, ON, Canada). Chemicals, including sodium acetate trihydrate (99%), glacial acetic acid (99.7%), hydrochloric acid (ACS reagent, 37%), ferric chloride hexahydrate (ACS reagent, 97%), 2,2'-azino-bis(3-ethylbenzothiazoline-6-sulphonic acid) diammonium salt (HPLC, ≥ 98%), ethanol (> 95%), 2,2'-azinobis (3-ethyl-benzothiazoline-6-sulfonic acid) (ABTS), 6-hydroxy-2, 5, 7, 8-tetramethylchroman-2-carboxylic acid, Folin-Ciocalteau's phenol reagent, calcium chloride (96%, anhydrous), sodium carbonate (anhydrous, ACS reagent, ≥ 99.5%), gallic acid (97.5-102.5% titration), potassium persulfate (ACS reagent, ≥ 99%), and 2,4,6-

tris(2-pyridyl)-s-triazine ($\geq 98\%$) were acquired from Sigma Aldrich (Oakville, ON, Canada). Purified water from a Milli-Q system (Millipore, Bellerica, MA) was used.

4.2.2 Bioactive film development

Bioactive films were produced using subcritical fluid technology described in Chapter 3 (Section 3.2.2). The subcritical fluid reaction system is described in Fig. 3.1. Potato cull was first blended (Magic Bullet Blender MBR-1101, Homeland Housewares, NY, USA) for 3 min, then known amounts of potato cull, potato peel or gallic acid, glycerol and water were preloaded inside the reactor (volume of 270 mL). Then, the reactor was filled with Milli-Q water using a HPLC pump and the mixture inside the reactor was homogenized by a double helix stirrer for 5 min. After the desired temperature and pressure were reached, the reactor was held at these conditions for 10 min for starch gelatinization and reaction. The cooling process was performed right after and the reacted solution was unloaded for degassing. For each film, 80 g of the degassed solution was cast into a plastic petri dish of 15 cm diameter. After drying the films at 40 °C for 48 h in an oven (Model 655G, Fisher Scientific IsoTemp[®] oven, Toronto, ON, Canada), films were removed and conditioned at 30% RH and 25 °C for at least 48 h prior to further characterizations. These condition parameters were recommended to maintain good film stability (Zhang, 2015).

The different formulations tested in the present study for bioactive films based on potato by-products are summarized in Table 4.1. First, potato peel was added as the only resource of phenolics at different ratios of potato cull (0, 0.5, 1 and 1.3 g peel/g cull). A maximum loading of 1.3 g potato peel was used due to limitations of the volume. Attempts using 1.4 g peel/g cull failed as the stirrer did not work properly, leading to inadequate reaction that resulted in big chunks of potato peel in the film. The reaction was conducted at 50-190 bar and 100-150 °C. Then, at the best temperature (125°C) and pressure (120 bar), the influence of the glycerol/cull starch ratio (0, 0.5, 1, 1.5 and 2 g glycerol/g cull starch) on the

mechanical properties was investigated at the highest potato peel loading (1.3 g peel/g cull) to find the optimized condition. To further improve antioxidant activity of the film, gallic acid was used instead of the peel as previous studies in our laboratory demonstrated the stability of gallic acid under subcritical water conditions (Zhang, 2015). Gallic acid/cull starch ratios of 0, 0.1, 0.2 and 0.3 g gallic acid/g starch were evaluated. Cull starch means that results were based on the starch content of the potato cull.

Table 4.1 Formulations of bioactive films based on potato by-products.

Weight of potato cull (g)	Potato peel/potato cull ratio (g/g)	Glycerol/starch ratio (g/g)	Gallic acid/starch ratio (g/g)	
36	0:1	0.5:1	0:1	
	0.5:1			
	1:1			
	1.3:1			
	1.3:1	0.5:1	0:1	
		1:1		
		1.5:1		
		2:1		
		0:1	1:1	0:1
				0.1:1
			0.2:1	
			0.3:1	

4.2.3 Film characterization

4.2.3.1 Structural properties

A Fourier transform infrared (FT-IR) spectrometer Nicolet 8700 (Thermo Fisher Scientific Inc, Waltham, MA, USA) supplied with a Smart Specular GATR (Grazing Angle Attenuated Total Reflectance) was used to collect FTIR spectra of bioactive films. The spectra were recorded between 4000-700 cm^{-1} with a 4 cm^{-1} spectral resolution and a total of 128 scans per sample. Nicolet Omnic 8.3 software was used to collect the data.

X-ray diffraction patterns of bioactive films were performed using a Rigaku Geigerflex powder diffractometer (Rigaku, Tokyo, Japan) with a cobalt tube, graphite

monochromator and scintillation detector operated at 38 kV and 38 mA. The diffraction patterns were obtained from 5 to 50° (2θ) at a scanning rate of 1° min⁻¹. The relative crystallinity (RC) value was calculated by the JADE 9.1 software and expressed as the ratio of the relative area of the crystalline peak to the total area of the diffractogram in percentage (%).

4.2.3.2 Mechanical properties

Six thickness measurements were taken at random positions on the film using a digital micrometer (Model 543-522A, Mitutoyo, Tokyo, Japan) with a precision of 0.001 mm, the average value was used to calculate the film tensile strength. Six film samples (5 cm x 1cm) of each formulation were measured for tensile strength (TS) and percent elongation at break (E%) using a texture analyzer (5960 Dual Column Tabletop Testing system with Instron® Bluehill® Software, Instron, Norwood, MA, USA) following the ASTM standard method D882 (ASTM, 1999). Equilibrated film specimens were clamped between grips, force (N) and deformation (mm) were recorded during extension at 4 mm min⁻¹, with an initial distance between the grips of 30 mm.

4.2.3.3 Physico-chemical properties

Preconditioned (30% RH, 23 °C) film samples (4 cm²) were used to determine the water activity with a water activity meter (Aqualab 4TE, Pullman, WA, USA). The moisture content of the films was measured by drying the samples at 105°C to a constant weight (Horwitz, 2000) and calculated using the following equation:

$$\text{Moisture content (\%)} = \frac{(m_A - m_B)}{m_B} \times 100 \quad (4.1)$$

where, m_A = weight (g) of the film sample before drying, and m_B = weight (g) of the film sample after drying. All measurements were done in triplicate.

Film solubility in water (WS) is defined as the percentage of the dry matter of film which is solubilized after 24 h immersion in water. Film specimens (4 cm²) were immersed and agitated in 50 mL of Milli-Q water at 4, 25 and 50 °C for 24 h. Then, films not solubilized in water were filtered and dried to a final constant weight. Experiments were performed in triplicate and the solubility was calculated as follows:

$$WS (\%) = \frac{(m_0 - m_F)}{m_0} \times 100 \quad (4.2)$$

where, m_0 is the weight (g) of the dried film calculated based on the moisture content of the initial film, and m_F is the weight (g) of the dried undissolved film.

The methodology described in the ASTM E96-00 method (ASTM, 2000) was used to determine the film water vapor permeability (WVP). Films were sealed on Payne-permeation cups (1003, Sheen instruments, Cypress, CA, USA), containing 3.5 g anhydrous calcium chloride (0% RH) and placed inside a desiccator at 75% RH and 23 °C. After steady state conditions were reached, samples were weighed seven times over a 7-day period. Slopes were calculated by linear regression ($R^2 \geq 0.99$). The film WVP was determined as follows:

$$WVP = (WVTR \times H) / \Delta P \quad (4.3)$$

where, WVTR is the water vapor transmission rate (g m⁻² h⁻¹) through the film, calculated from the slope of the straight line divided by the exposed film area (m²), H is the film thickness (mm), and ΔP is the vapor pressure differential across the film (Pa). Each film sample was evaluated at least in triplicate.

4.2.3.4 Optical and morphological properties

Film transparency was measured at 600 nm using a spectrophotometer (Genova, Barloworld Scientific, Essex, UK) according to the standard method ASTM D1746-92 (ASTM, 1992). The film transparency value was calculated by the equation of Nawapat and Thawien (2013):

$$\text{Transparency value} = -\frac{\log T_{600}}{H} \quad (4.4)$$

where, T_{600} and H are the transmittance at 600 nm and film thickness (mm), respectively. The greater value represents the lower transparency of the film.

The color values (L , a and b) of the bioactive films were measured with a Hunter Lab colorimeter (CR-400/CR-410, Konica Minolta, Ramsey, NJ, USA) that uses a D65 illuminant with an opening of 14 mm and a 10° standard observer according to the ASTM D2244 method (ASTM, 2011). Film samples were placed on a white standard plate ($L^* = 93.49$, $a^* = -0.25$, $b^* = -0.09$), the total color difference (ΔE), yellowness index (YI) and whiteness index (WI) were calculated as:

$$\Delta E = \sqrt{(L^* - L)^2 + (a^* - a)^2 + (b^* - b)^2} \quad (4.5)$$

$$YI = 142.86 b/L \quad (4.6)$$

$$WI = 100 - [(100 - L)^2 + a^2 + b^2]^{0.5} \quad (4.7)$$

where L^* , a^* and b^* are the color values of the standard white board, L , a and b are the color values of the film.

A gloss meter (GM 268, M&I instrument, Mississauga, ON, Canada) was used to measure the gloss of both film sides at 60° , following the ASTM standard D523 method (ASTM, 1999). Experiments were performed in triplicate and all results were expressed as gloss units (GU).

Film contact angle was determined using a Dynamic Angle and Tension Analysis instrument (FTA200, First Ten Angstroms, Inc. Portsmouth, VA, USA). Each contact angle value reported was the mean value of five measurements taken at random locations on the film. The value was obtained 5s after the droplet contacted the surface and was measured on both sides of the film.

Scanning electron microscope (SEM) (Zeiss Sigma 300 VP-FESEM, Oberkochen, Germany) was used to investigate the surface morphology of pure gallic acid and bioactive film surfaces and fractures. Film samples were cut into strips, frozen in liquid nitrogen and then fractured. Film samples were mounted on SEM specimen stubs with double-size conductive carbon tape and sputter-coated with gold using a Nanotek SEMprep 2 sputter coater (Nanotech, Manchester, UK).

4.2.3.5 Functional properties

Phenolic content from films (0.2 g) that were cut into small pieces were extracted with 50% ethanol (10 mL) at 23 °C under constant shaking for 24 h, and centrifuged at 5000 \times g for 10 min. The supernatant collected was used to analyze total phenolic content and antioxidant activity.

4.2.3.5.1 Determination of total phenolic compound content

Total phenolic content in the film extract was determined with the Folin-Ciocalteu reagent according to a modified method of Sarkar et al. (2014), using gallic acid as the standard. Supernatant (0.04 mL) was thoroughly mixed with 3.16 mL of distilled water and 0.2 mL of Folin–Ciocalteu reagent. After 6 min, 0.6 mL of sodium carbonate solution was added. Then, the mixture was incubated in a dark place for 2h at room temperature, and the absorbance was read at 765 nm using a spectrophotometer. All measurements were performed in duplicate. The results were expressed as mg gallic acid equivalent/g film sample.

4.2.3.5.2 Ferric Reducing Antioxidant Power (FRAP) Assay

The antioxidant activity of the film extract was measured according to the FRAP assay described by Benzie and Strain (1996). Briefly, 3 mL of freshly prepared FRAP reagent, consisting of 300 mM acetate buffer (pH 3.6), 10 mM TPTZ (2,4,6-tris(2-pyridyl)-s-triazine) in 40 mM hydrochloric acid and 20 mM ferric chloride at 10:1:1 v/v/v ratio, was mixed with

100 μL of sample and 300 μL Milli-Q water. After 30 min of incubation at 37 $^{\circ}\text{C}$, the sample absorbance was recorded at 593 nm. All measurements were performed in triplicate.

4.2.3.5.3 Inhibition of the 2,2'-azinobis (3-ethyl-benzothiazoline-6-sulfonic acid) (ABTS)

Assay

The ABTS free radical scavenging activity of the film extract was determined following methodology reported by Re et al. (1999). The ABTS radical cation solution was prepared by reacting the stock solution of 7 mM ABTS with 2.45 mM potassium persulfate at 1:1 v/v ratio. Then, the mixture was left to stand in a dark place for 16h before use. For each analysis, 3 mL of diluted ABTS radical cation solution ($A_{734\text{nm}} = 0.7 \pm 0.02$) was mixed with 100 μL of the sample solution, the absorbance was measured after 15 min of incubation at 30 $^{\circ}\text{C}$. All measurements were performed in triplicate. The radical scavenging activity was expressed as the percentage disappearance of the ABTS⁺:

$$\text{ABTS Inhibition (\%)} = 100 (A_0 - A_1)/A_0 \quad (4.8)$$

where, A_0 is the absorbance of the blank, and A_1 is the absorbance of the sample solution.

4.3 Results and discussion

Results obtained at pressures of 50–190 bar showed less total phenolic content of potato peel at 100 $^{\circ}\text{C}$ (4.88 ± 0.29 – 5.17 ± 0.31 mg gallic acid equivalent/g film) compared to the phenolic content obtained at 125 $^{\circ}\text{C}$ (6.25 ± 0.06 – 7.67 ± 0.12 mg gallic acid equivalent/g film). At 150 $^{\circ}\text{C}$ and same pressure range of 50–190 bar, hydrolysis of starch occurred, reducing the starch chain length that is essential for the formation of strong interactions, leading to less cross-linking, and less elongation (Zhao et al., 2018). Also, Zhang (2015) reported high degree of starch depolymerization at 150 $^{\circ}\text{C}$, resulting in non-homogenous films with increased film solubility in water, and poor mechanical properties. Therefore, to maximize the phenolic content from potato peel while avoiding starch depolymerization, a temperature of 125 $^{\circ}\text{C}$ was selected. Pressures of 50–190 bar can facilitate to form a

homogeneous film solution. But, a pressure of 190 bar induced strong association between amylopectin and amylose, preventing the plasticizer glycerol to interact with both amylopectin and amylose, that resulted in less flexible films. Therefore, to produce homogeneous and flexible potato by-product films, 120 bar and 125 °C was selected for further film property evaluation.

4.3.1 Structural properties

Fig. 4.1 shows the FT-IR spectra of pure gallic acid and bioactive films based on potato by-products produced with different gallic acid/potato cull starch ratios. In the spectrum of pure gallic acid, the bands observed at 3600-3200 cm^{-1} represented stretchings of the different -OH groups (Sun et al., 2014b). The bands at 1701 and 1620 cm^{-1} corresponded to the C=O stretch of conjugated acids, while the bands at 1425 and 1263 cm^{-1} corresponded to -COOH groups (da Rosa et al., 2013). The bands at 1308-1174 cm^{-1} corresponded to vibrations of C-H in the aromatic ring and O-H of the phenol alcohol (Neo et al., 2013).

For bioactive films based on potato by-products, peaks observed at 1200-990 cm^{-1} suggested the C-O stretching vibrations of starch, similar findings were reported by Jamróz et al. (2018) for potato starch-furcellaran-gelatin film. Peak at 1658 cm^{-1} revealed the existence of O-H stretching from water in the films, becoming more evident with the increasing of gallic acid content in the film. This behaviour suggests an increasing film water absorption due to the hydrophilicity of gallic acid, in agreement with results shown in Table 4.2, where the higher moisture content of bioactive films was observed with more gallic acid added. In addition, a broad band for O-H stretching at 3680-3100 cm^{-1} and the peak for C-H stretching at 2929 cm^{-1} were observed. Similar observations were reported when ferulic acid was incorporated in potato starch-chitosan blend films (Mathew & Abraham, 2008). In our study, new peaks at 1710 and 1425 cm^{-1} became more evident with the increasing amount of gallic acid, indicating the formation of ester linkages between the carbonyl groups (-COOH) of

gallic acid and the hydroxyl groups (-OH) of starch in potato cull. Also, ions produced (H_3O^+ and OH^-) at subcritical conditions activated the -OH groups of potato cull starch and -COOH groups from gallic acid, promoting the reactions among them. The C=O group from carboxylic acids was also reported in cassava starch film loaded with rosemary extracts at 1714 and 1750 cm^{-1} (Piñeros-Hernandez et al., 2017). Other observations of ester linkages have been reported for chitosan films loaded with gallic acid at 1715 cm^{-1} (Sun et al., 2014b). No significant difference was observed in the spectra of potato peel incorporated films and films with no gallic acid added (0 g GA/g cull starch), because of the small amount of potato peel loaded to the reactor, influencing the amount of phenolics (data not shown).

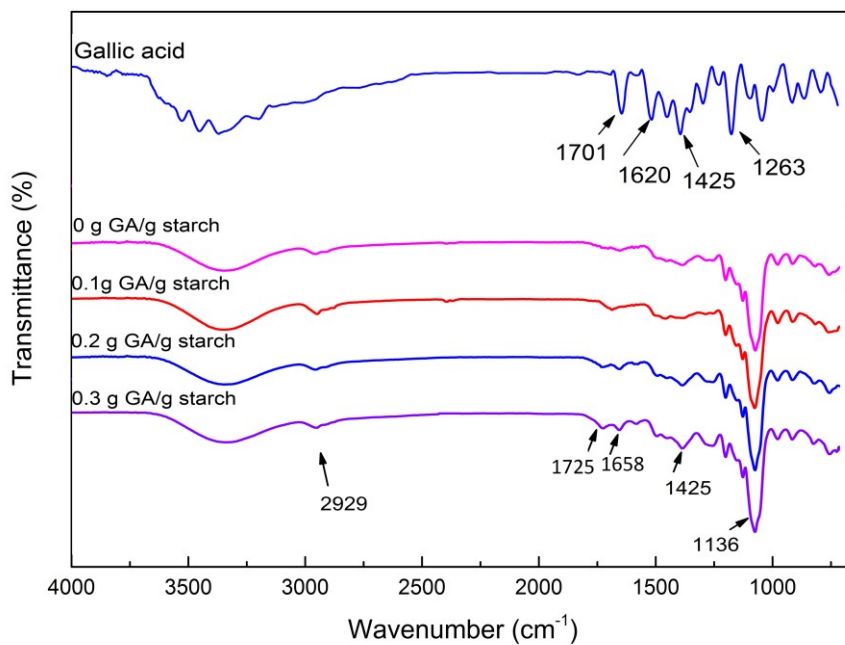


Fig. 4.1 FT-IR spectra of pure gallic acid (GA) and bioactive films based on potato by-products at different GA/potato cull starch ratios of 0-0.3 g/g and constant glycerol/starch ratio of 1 g/g at 120 bar and 125 °C.

Fig. 4.2 shows the X-ray diffraction patterns of the untreated potato cull and bioactive films based on potato by-products produced with different concentrations of gallic acid. All systems showed typical behavior of tuber starches with type B crystalline structure, with

characteristic diffraction peaks at 17° and 22°. Bioactive films after pressurized hot water treatment (4.2b-e) had different XRD patterns compared to the untreated potato cull (4.2a). After pressurized hot water treatment, films showed an enhanced diffraction peak at 19.7 ° with(out) the addition of gallic acid due to starch retrogradation during drying and storage. Amylose recrystallization occurred in the early stage of drying at 40 °C followed by the slow recrystallization of amylopectin during storage at 23 °C and 30 %RH. Similarly, Bangyekan et al. (2006) reported the difference in recrystallization of amylose and amylopectin in cassava starch films coated with 1-4 wt% chitosan solution using an automatic film coater. The characteristic peak at 17° also became less evident in the bioactive films produced due to the formation of intermolecular hydrogen bonds between -OH groups of starch and gallic acid, preventing the crystallization of starch. The untreated potato cull had a higher RC (12.91%) compared with potato by-product films (6.77-10.69%), as native crystalline form of starch was modified during reaction and a slow re-crystallisation of amylose and amylopectin occurred afterwards. A significant decrease in RC of potato by-products films was observed at a high concentration of gallic acid (0.3 g/g cull starch), probably because the additional gallic acid acted as a plasticizer, decreasing the activation energy and forming most stable crystalline structure, facilitating polymeric chain mobility. Similarly, the appearance of a more amorphous pattern was observed in ferulic acid incorporated starch-chitosan blend films (Mathew & Abraham, 2008), suggesting good miscibility of all components, which delayed the retrogradation phenomenon. Potato peel had no significant effect on the RC of bioactive films, showing similar XRD patterns with the film that had no gallic acid added (4.2b), due to the limited amount of potato peel loaded to the reactor, influencing phenolic concentration (data not shown).

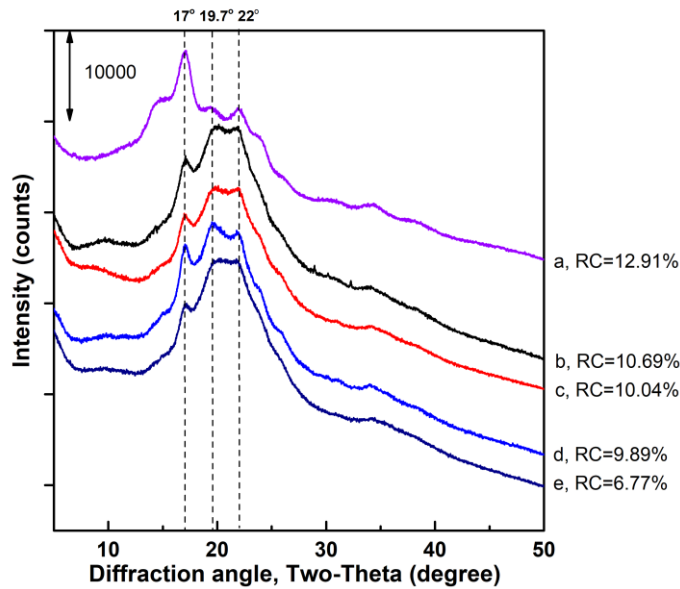


Fig. 4.2 XRD patterns and relative crystallinity (RC, %) of: a) freeze dried potato cull and bioactive films based on potato by-products: b) 0 g GA/g potato cull starch, c) 0.1 g GA/g potato cull starch, d) 0.2 g GA/g potato cull starch, and e) 0.3g GA/g potato cull starch produced with constant glycerol/starch ratio of 1 g/g at 120 bar and 125 °C.

4.3.2 Mechanical properties

Fig. 4.3 shows data on the mechanical properties of bioactive films based on potato by-products with different potato peel/cull ratios, glycerol/cull starch ratios and gallic acid/cull starch ratios (Table B.1, appendix B). The tensile strength of films increased significantly from 2.5 to 9.0 MPa with increasing potato peel content up to 1.3 times the potato cull, whereas the elongation at break decreased from 28.5 to 10.2% (Fig. 4.3A). The tensile strength of films shown in Fig. 4.3 are comparable to some of the commercial packaging films used on cheese and ham products that were acquired from the local supermarket (11-13 MPa), but depending on the application, stronger films might be preferred to protect foods from mechanical damage. An increase of 3.6 times in tensile strength was observed with the highest potato peel loaded in the reaction, because the potato peel had high content of fiber. Potato peel has around 27-55% cellulose, 11% hemicelluloses and 7-14% lignin (Lenihan et al., 2010; Rommi et al., 2016), while potato cull has less than 3%

fiber and 80% starch (Lisińska & Leszczyński, 1989). Also, cellulose nanofibers (1% and 2%) from potato peel waste enhanced the tensile strength of polyvinyl alcohol-potato starch film by 19% and 38%, respectively (Chen, Lawton, Thompson & Liu, 2012). Elongation showed an opposite trend compared to the tensile strength trend. Cross-linking of starch molecules with gallic acid limits the mobility of the starch molecules, leading to lower elongation.

The tensile strength and elongation of potato by-products films were also affected by glycerol content (Fig. 4.3B). Compared to the control film, the elongation values of the films increased from 12.7 to 30.8% with the incorporation of glycerol at a concentration of 1 g/g cull starch. However, there was a significant reduction in strength at a glycerol concentration above 1 g/g cull starch. A higher concentration of plasticizer resulted in lower tensile strength of the investigated films. Plasticizers interfere with the arrangement of the starch chains and the hydrogen bonding, decreasing starch interactions and cohesiveness and affecting the crystallinity, flexibility and other physical properties of the films. The amount of glycerol to be added should be decided based on the tensile strength and elongation required for a particular application. In this study, to obtain the best elongation, the glycerol/cull starch ratio of 1 g/g was selected.

The addition of gallic acid to potato cull at different concentrations caused significant effect on film mechanical properties (Fig. 4.3C). The increase of gallic acid/cull starch ratio from 0 to 0.3 g/g resulted in the decrease of tensile strength from 3.0 to 1.6 MPa. However, film elongation increased to the highest value of 28.2% when 0.2 g gallic acid/g cull starch was added, followed by a slowly decrease with 0.3 g gallic acid/g cull starch. This phenomenon is often described as the anti-plasticizing effect, where rigidity increases and film flexibility reduces (Chang, Karim, & Seow, 2006). A similar trend was reported by Rachtanapun & Tongdeesoontorn (2009), when 40 mg gallic acid/g starch was added into the rice flour/cassava starch blend film. A lower elongation (14%) was obtained compared with

the control (20%). A possible explanation is that gallic acid has a small size and molecular weight (170 g/mol) that could fit between starch chains, just like glycerol, increasing evenly chain mobility and enhancing the initial plastic effect. The hydrophilic part of the gallic acid could interact with glycerol or water, facilitating its presence between starch chains.

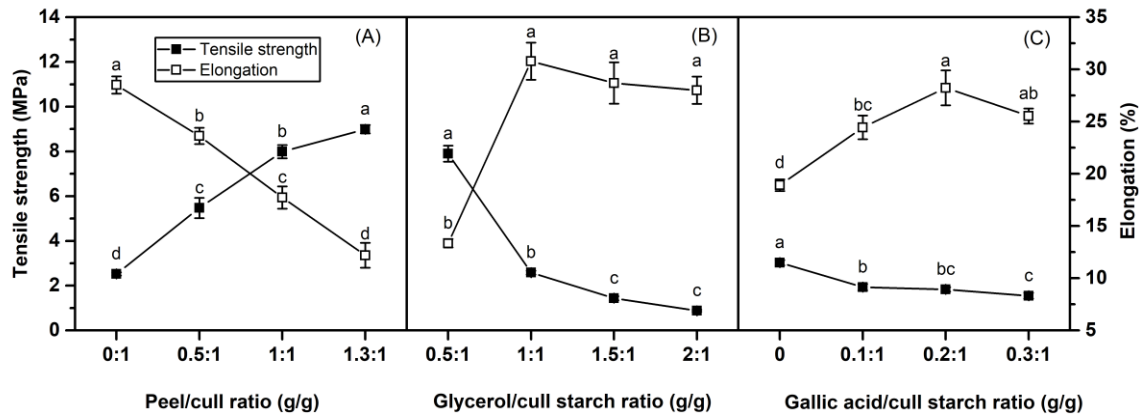


Fig. 4.3 Tensile strength and elongation at break for bioactive films based on potato by-products of: A) potato peel/cull ratios (0-1.3 g/g) and glycerol/potato cull starch ratio (0.5 g/g), B) glycerol/potato cull starch ratios (0.5-2 g/g) and potato peel/cull ratios (1.3 g/g), and C) GA/potato cull starch ratios (0-0.3 g/g) and glycerol/potato cull starch ratio (1 g/g) produced at 120 bar and 125 °C.

4.3.3 Physico-chemical properties

Table 4.3 shows the moisture content, water activity and WVP of bioactive films based on potato by-products. Water activity indicates the free or available water in the film matrix that allows microbial growth and chemical and enzymatic reactions. Thus, a low film water activity restricts the amount of free water for bio-chemical reactions and further ensures food stability. The water activity can be related to the Flory-Huggins theory that describes the thermodynamic interaction mainly between the blends of synthetic polymers or synthetic polymer solutions (Flory, 1942). But, because the biopolymers react with water through hydrogen bonds, Flory-Huggins theory does not apply (Van der Sman, 2017).

The reaction process occurred in pressurized hot water, using temperatures above 100 °C and reaction time of 10 min, being also considered as a sterilization process. Both

water activity and moisture content decreased with the increase of potato peel content. However, the moisture content increased when gallic acid was incorporated into the films. As gallic acid has hydroxyl groups in their structures, it increases water affinity to the film. The non cross-linked gallic acid increased the hydrophilicity characteristics of bioactive films. Values of water activity for different starch based films have been reported as 0.473 for native cassava starch films and 0.492 for sodium trimetaphosphate modified cassava starch films (Gutiérrez, Tapia, Pérez & Famá, 2015), and 0.11-0.56 for tapioca starch films with different glycerol contents (Chang et al., 2006). All bioactive films based on potato by-products produced in this study had water activity lower than 0.09, preventing water to act as a solvent to favor chemical/biochemical reactions and growth of microorganisms. Thus, films produced with pressurized hot water technology have the possibility to minimize bacterial growth on their own.

The initial WVP reduction in the gallic acid added film is the result of cross-linking and formation of ester linkages between -OH groups of starch and -COOH groups of gallic acid. When 0.3 g GA/g cull starch was added, more active sites for water binding were available. Therefore, the affinity for water molecules increased in these films, resulting in higher water diffusion, providing films with higher WVP. In an earlier study, the WVP of the ferulic acid incorporated potato starch-chitosan film was the lowest (1.15×10^{-2} g.mm/kPa.h m^2) at a concentration of 75 mg ferulic acid/100g blend solution, however, it increased to 1.31×10^{-2} g mm/kPa.h. m^2 at a higher concentration of 100 mg ferulic acid/100g blend solution in the film (Mathew & Abraham, 2008). The bioactive films produced in this study (Table 4.2) showed better water vapor barrier properties than the films prepared using potato peel and soy lecithin (3.0-5.3 g mm/kPa h m^2) (Kang & Min, 2010) and the thymol loaded potato starch films (1.22 g mm/kPa h m^2) (Davoodi et al., 2017). The decrease of water activity and moisture content in potato peel added films led to a decrease of WVP due to the

dense film structure, limiting the space between starch molecules for water absorption. This effect is more evident at high potato peel loading of > 1g peel/g cull. However, the 100 to 1000 times higher WVP values of starch-based films compared to traditional petroleum-based films still is a challenge. But, starch-based films were reported to exhibit excellent oxygen barrier properties, which is comparable to typical packaging plastics, such as low-density polyethylene and ethylvinyl alcohol (<1 cm³ μm/m² d kPa , Ahmed et al., 2012).

Table 4.2 Moisture content, water activity and water vapour permeability of bioactive films based on potato by-products.

Potato peel/cull ratio (g/g)	Moisture content (%)	Water activity	WVP (g.mm/kPa.m ² .h)
0:1	24.00±0.61 ^a	0.0891±0.0012 ^a	1.39±0.10 ^a
0.5:1	18.69±0.46 ^b	0.0822±0.0012 ^b	1.03±0.04 ^{ab}
1:1	17.73±0.20 ^b	0.0727±0.0002 ^c	0.93±0.08 ^b
1.3:1	14.88±0.29 ^c	0.0671±0.0027 ^d	0.54±0.02 ^c
GA/potato cull starch ratio (g/g)	Moisture content (%)	Water activity	WVP (g.mm/kPa.m ² .h)
0:1	18.07±0.56 ^c	0.0893±0.0027 ^a	1.45±0.11 ^b
0.1:1	19.72±0.36 ^b	0.0868±0.0017 ^a	0.66±0.02 ^d
0.2:1	22.78±0.30 ^a	0.0870±0.0018 ^a	1.08±0.04 ^c
0.3:1	23.11±0.50 ^a	0.0851±0.0036 ^{ab}	1.98±0.06 ^a

WVP: water vapour permeability. Bioactive films produced at potato peel/cull ratios (0-1.3 g/g) and glycerol/potato cull starch ratio (0.5 g/g), or GA/potato cull starch ratios (0-0.3 g/g) and glycerol/potato cull starch ratio (1 g/g) at 120 bar and 125 °C.

Data shown as mean±standard deviation (*n* = 3).

^{a-d}Different lowercase letters in the same column indicate significant differences (*p* < 0.05).

Fig. 4.4 shows the film solubility in water and contact angle of bioactive films based on potato by-products with different potato peel/cull ratios and gallic acid/cull starch ratios (Table B.2, appendix B). The use of potato peel reduced film solubility in water, whereas the

addition of gallic acid increased the film solubility in water. Moreover, film solubility in water was favored at 50 °C. The effect of additives on the solubility of films in water depends on the inherent hydrophobicity or hydrophilicity of the additives. The use of sodium ascorbate increased solubility of oxidized potato starch films in water (Kowalczyk et al., 2018), while the incorporation of zein increased surface hydrophobicity of the carboxymethyl potato starch film (Takahashi, Ogata, Yang & Hattori, 2002). Potato peel was also found to significantly lower the film solubility from 96 to 39% of ultrasound treated potato peel and sweet lime pomace based biopolymer films due to the compacted matrix (Borah, Das & Badwaik, 2017), making the blend film less accessible to water. A similar trend was reported by Kang and Min (2010), where the film solubility in water was higher with the film formed by 3 g peel/100 g solution (41-43%) than the film formed by 5 g peel/100 g solution (31-41%). Current packaging for food products made of petroleum polymers are not soluble. Different applications require different film solubility. As the films produced in our study are relatively hydrophilic, some soluble film applications are possible, such as seasoning sachets in instant noodles or the wrap covering the detergent tablets. The focus of thesis was to develop food packaging films with unique antioxidant/antimicrobial activities. By extending food shelf-life and ensuring food safety, less food waste is generated. More research is still needed to improve the hydrophobicity and mechanical strength of starch-based films, in order to replace petroleum-based films.

In Figure 4.4B, the addition of potato peel had little influence on both surface contact angle of the films. Films with potato peel added in our study had higher top surface contact angle ($> 75^\circ$) compared to the films prepared from pure potato peel (53-81°) by Rommi et al. (2016) also because of the lack of starch in their films, very little elongation of 2-11% was obtained (Rommi et al., 2016). However, an increase of gallic acid content caused a significant decreased in contact angle values for both top and bottom surfaces due to the

hydrophilicity of gallic acid. Potato peels are composed of 30% starch, 27-55% cellulose, 11% hemicelluloses and 7-14% lignin (Lenihan et al., 2010; Rommi et al., 2016). During hot pressurized water treatment, starch granules in potato peel swelled and collapsed, resulting in amylose and amylopectin gelatinization. Also, phenolic acids (e.g. gallic acid, chlorogenic acid, caffeic acid) were extracted from potato peel. These amylose and amylopectin have the free hydroxyl groups to react with the carboxyl groups of phenolic acids, forming ester linkages. However, due to the small amount of potato peel loaded into the reactor, the characteristic peak of ester linkages on FTIR was not visible (Fig. 4.1?). The surface of potato peel will form porous structure due to the rupture of starch. In addition, hydroxyl groups of starch and cellulose formed hydrogen bonds that restricted the free hydroxyl groups to bind with water, improving hydrophobicity of film surfaces.

To improve film hydrophobicity and mechanical strength, there are two options to consider. First, by coating another layer of biodegradable/hydrophobic polymer (i.e. PLA) on top of the starch-based films. The advantage of this process is that the starch-based film produced in our study is ready to use, and the coating procedure is relatively easy to perform. The second method is to mix PLA with the starch solution. The starch component can be shielded from contact with water if the dispersed starch phase is embedded within the hydrophobic PLA matrix. Moreover, it would be spontaneous for the hydrophobic PLA to form the outer layer in order to lower the surface tension of the material, hence, improving the water resistance aspect of the blend. However, new studies should be designed on the antimicrobial activity due to the change of film formulation that will influence the cross-linking and effectiveness of bioactives in the film.

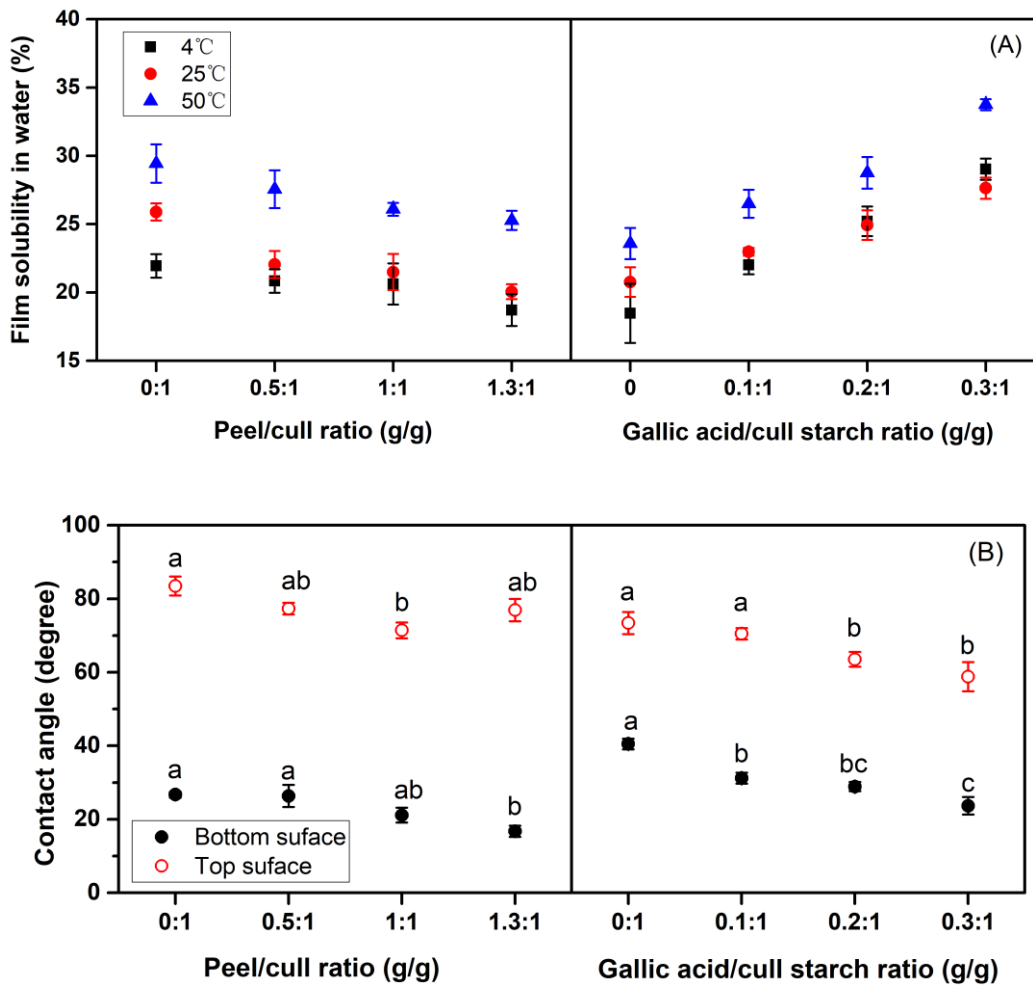


Fig. 4.4 A) Film solubility in water at 4, 25 and 50 °C, and B) top and bottom surfaces contact angle of bioactive films based on potato by-products with different potato peel/cull ratios (0-1.3 g/g) and constant glycerol/potato cull starch ratio (0.5 g/g) or GA/potato cull starch ratios (0-0.3 g/g) and constant glycerol/potato cull starch ratio (1 g/g) at 120 bar and 125 °C.

4.3.4 Optical and morphological properties

Table 4.3 shows WI, YI and ΔE of bioactive films based on potato by-products. Color and transparency of packaging films are important indexes with regards to the general product appearance, consumer acceptance and application. In general, films with potato peel added appeared slightly yellow and less white, which was visualized by the increment of the YI and reduction of the WI, respectively. This color change is attributed to the increased

phenolics content from potato peel in the film. As previously reported by Singh and Saldaña (2011), high recovery of phenolic compounds from potato peels resulted in dark color of extract solutions. The transparency values increased with increasing potato peel loading, suggesting that higher peel contents provided the films with more opacity as the high value represents low transparency of the film. This indicates a poor film homogeneity due to the presence of phenolics and fiber of potato peel. However, opposite trend was observed in film with gallic acid added. It had higher brightness, expressed by relative high WI and low YI values. Also, films with gallic acid added had a decreased transparency values, indicating less opacity.

The surface roughness of the films was reflected in the gloss values where films with smoother surfaces provided a higher gloss value. As observed in Table 4.3, the top surface had low gloss values. For the potato peel added films, the increase of peel content had little effect on the gloss. On the contrary, a smoother top surface was obtained for gallic acid added films, due to well dissolution of gallic acid and starch debranching during pressurized hot water treatment, avoiding dispersed particles on the film surface.

Table 4.3 Color performance, transparency, and gloss of top and bottom surfaces of bioactive films based on potato by-products

Potato peel/cull ratio (g/g)	Color performance			Transparency	Gloss (GU)	
	ΔE	YI	WI		Top	Bottom
0:1	6.28±0.01 ^d	6.84±0.04 ^c	92.31±0.02 ^a	1.54±0.15 ^c	10.78±1.06 ^a	76.20±6.18 ^a
0.5:1	7.39±0.07 ^c	8.74±0.19 ^b	89.94±0.26 ^b	1.88±0.13 ^b	8.80±0.84 ^{ab}	77.10±4.36 ^a
1:1	8.14±0.32 ^b	9.42±0.16 ^b	89.51±0.61 ^b	2.07±0.06 ^{ab}	8.15±0.55 ^{ab}	83.93±6.44 ^a
1.3:1	9.28±0.27 ^a	11.30±0.22 ^c	87.80±0.28 ^c	2.20±0.12 ^a	7.70±0.44 ^b	81.73±2.22 ^a

GA/potato cull starch ratio (g/g)	Color performance			Transparency	Gloss (GU)	
	ΔE	YI	WI		Top	Bottom
0:1	6.29±0.00 ^a	6.86±0.10 ^a	92.33±0.07 ^b	1.62±0.03 ^a	10.41±0.75 ^c	76.62±7.26 ^{ab}
0.1:1	4.08±0.15 ^d	5.29±0.13 ^b	93.83±0.56 ^a	1.50±0.04 ^b	14.50±0.92 ^b	83.70±1.58 ^a
0.2:1	5.10±0.17 ^{bc}	5.15±0.18 ^b	92.43±0.33 ^b	1.05±0.01 ^c	15.60±0.89 ^b	71.70±6.90 ^b
0.3:1	4.93±0.19 ^b	5.01±0.24 ^b	92.55±0.23 ^b	0.74±0.02 ^d	18.00±1.36 ^b	81.85±3.89 ^{ab}

ΔE : total color difference, YI: yellowness index, WI: whiteness index, GA: gallic acid, GU: gloss unit.

Bioactive films produced at potato peel/cull ratios (0-1.3 g/g) and glycerol/potato cull starch ratio (0.5 g/g), or GA/potato cull starch ratios (0-0.3 g/g) and glycerol/potato cull starch ratio (1 g/g) at 120 bar and 125 °C.

Data shown as mean±standard deviation ($n = 3$).

^{a-d}Different lowercase letters in the same column indicate significant differences ($p < 0.05$).

Fig. 4.5 shows SEM images of surface morphology of bioactive films based on potato by-products. Untreated potato cull was ground into powder, showing an irregular shape with different particle size of 63.6-133.3 μm (Fig. 4.5a). Bumps on the surfaces of potato peel incorporated films were caused by potato peel fibre, becoming more prominent with the increasing content of potato peel used. This bump may be attributed to the insufficient reaction time and less water available, where extra potato peel also limited the space inside the reactor for a good gelatinization to occur. To overcome this disadvantage, ultrasound treatment can be used to depolymerize the potato peel fiber.

In Fig. 4.6a, gallic acid showed a stick like shape. With the addition of gallic acid into bioactive films from 0 to 0.3 g gallic acid/g cull starch, the surface became more homogeneous and smoother, with less bumps (Fig. 4.6b-e), indicating good reaction of the starch and the gallic acid. Therefore, the release of the amylose from the starch granules favored the cross linking between molecules of starch molecules and gallic acid, resulting in a homogeneous film. The smooth surface when ferulic acid was added into the potato starch-chitosan blend film was reported by Mathew & Abraham (2008). However, both recrystallization and slight phase separation were observed in the SEM images of gallic acid incorporated films at a high concentration of 0.4 g/g cull starch (Fig. 4.6f-g), being responsible for the reduction in tensile strength observed at that high concentration.

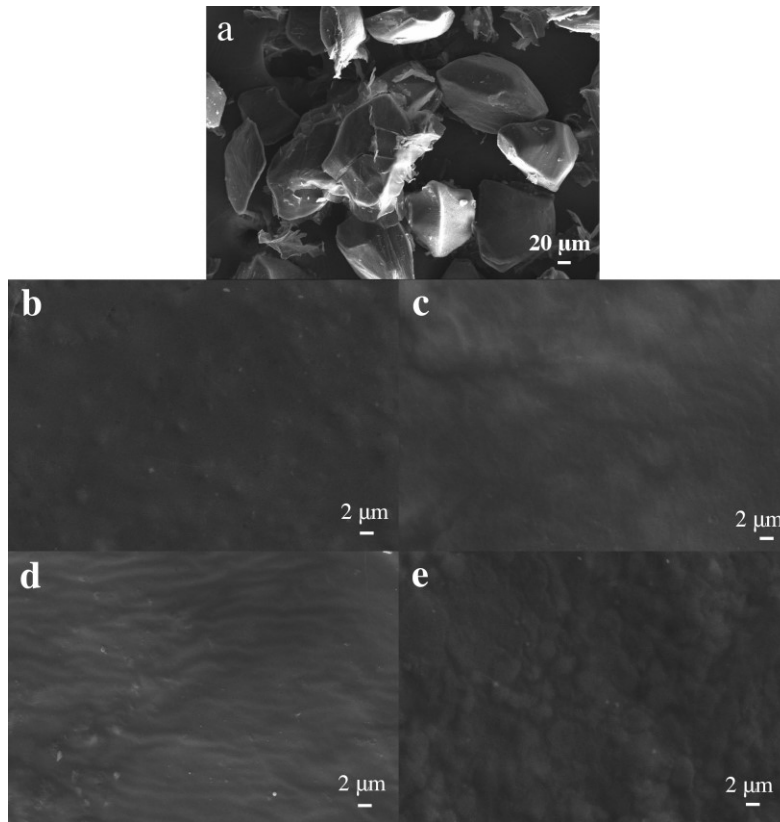


Fig. 4.5 SEM images of: a) ground potato cull, and bioactive films based on potato by-products: b) 0 g peel/g cull, c) 0.5 g peel/g cull, d) 1.0 g peel/g cull, and e) 1.3 g peel/g cull with constant glycerol/potato cull starch ratio of 0.5 g/g produced at 120 bar and 125 °C.

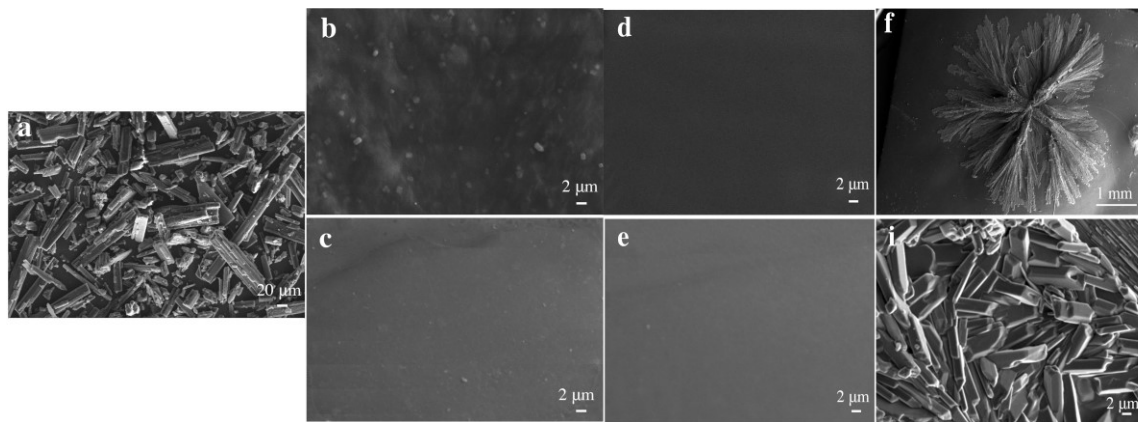


Fig. 4.6 SEM images of: a) pure gallic acid, and bioactive films based on potato by-products: b) 0 g GA/g potato cull starch, c) 0.1 g GA/g potato cull starch, d) 0.2 g GA/g potato cull starch, e) 0.3g GA/g potato cull starch, and f-g) 0.4 GA/g potato cull starch with constant glycerol/potato cull starch ratio of 1 g/g produced at 120 bar and 125 °C.

4.3.5 Antioxidant activity and total phenolic content of potato by-product films

Fig. 4.7 shows the total phenolic content and antioxidant activity of bioactive films based on potato by-products (Table B.3, appendix B). Increasing the amount of potato peel in the film increased the total phenolic content (0.3-6.1 mg gallic acid equivalent/g film) and antioxidant activity (1.1-73.1 mg Trolox equivalent/g film using the FRAP method and 1.5-93.2 mg Trolox equivalent/g film using the ABTS method). High antioxidant activity of packaging films delays oxidative spoilage of food products. As expected, the more gallic acid used for film formation, the higher antioxidant activity of the film (1.1-1899.1 mg Trolox equivalent/g film for the FRAP and 1.5-1974.0 mg Trolox equivalent/g film for the ABTS). Both FRAP and ABTS methods provided comparable trends of antioxidant activity of bioactive films (Fig. 4.7). However, due to the potato peel loading limitation, bioactive films with potato peel added (Fig. 4.7A) had lower antioxidant activity than those films with gallic acid added (Fig. 4.7B). As the bioactive film dissolving process was performed in 24h, free or weakly bounded gallic acid in the film was released to the solution. Therefore, the remaining gallic acid (around 50%) was bounded through chemical cross-linking as confirmed by FT-IR (Fig. 4.1). When twice or three folds amount of gallic acid were added into the film, the total phenolic content released increased to 111.9 and 172.3 mg gallic acid equivalent/g film respectively, therefore, resulting in bioactive films with higher antioxidant activity.

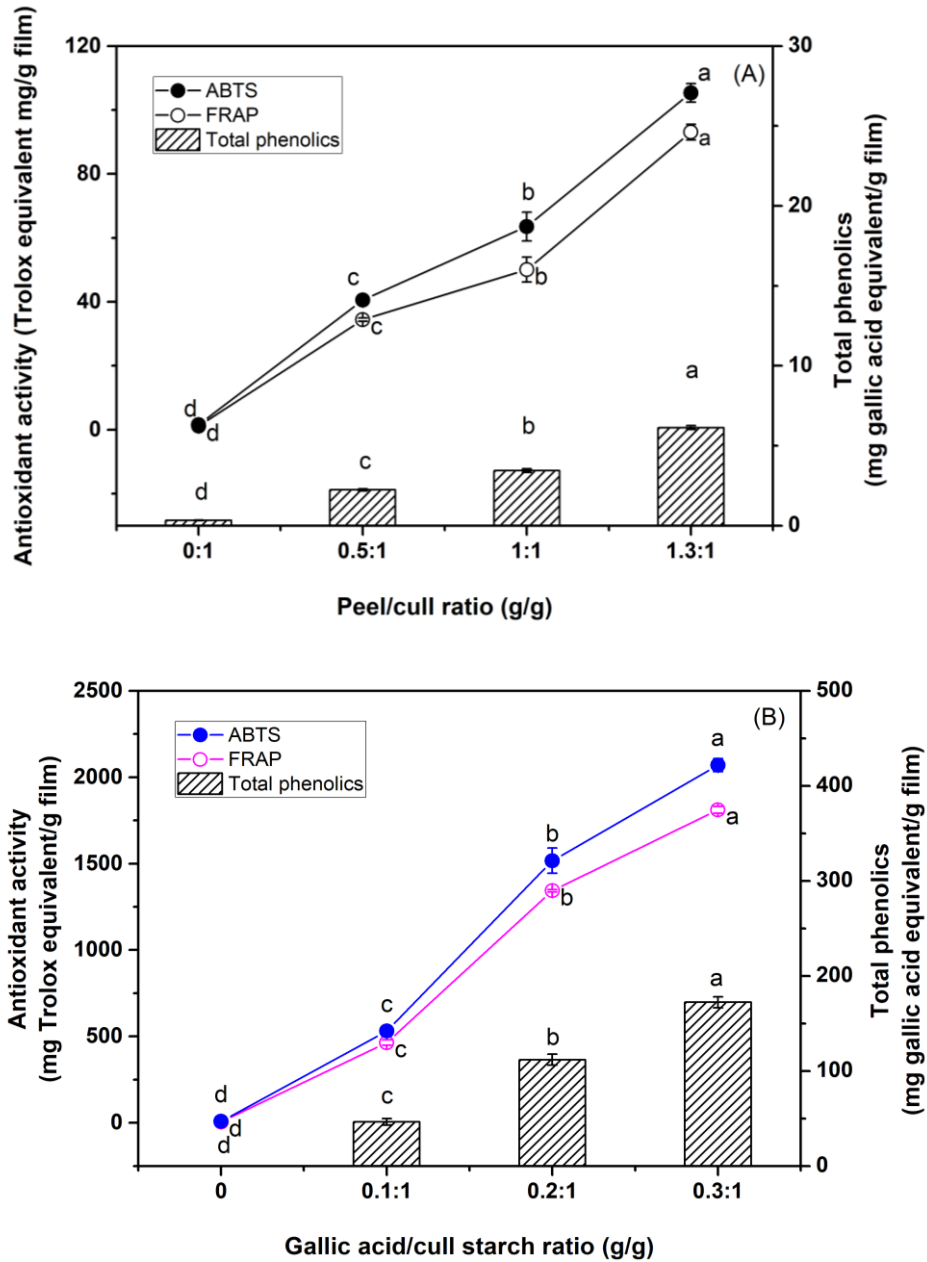


Fig. 4.7 Total phenolic content, and antioxidant activity by ABTS and FRAP methods of bioactive films based on potato by-products with different: A) potato peel/cull ratios (0-1.3 g/g) and constant glycerol/potato cull starch ratio of 0.5 g/g, and B) GA/potato cull starch ratios (0-0.3 g/g) and constant glycerol/potato cull starch ratio of 1 g/g produced at 120 bar and 125 °C.

4.4 Conclusions

Potato by-products, peel and cull, were successfully used to form bioactive films with unique antioxidant properties using pressurized hot fluid technology. New data on physico-chemical, mechanical and functional properties was obtained using a green pressurized hot water technology and potato by-products. The optimized conditions to produce films from potato peel and cull with improved elongation and antioxidant properties were achieved at 125 °C, 120 bar, 1.3 g peel/g cull and 1 g glycerol/g cull, while films with potato cull and gallic acid had best elongation at 125 °C, 120 bar, 1 g glycerol/g cull and 0.2 g gallic acid/g cull. Gallic acid incorporated in the films promoted the formation of cross-linking through ester bonds, creating a smooth surface and homogenous bioactive film. This is the first study that loaded more gallic acid (0.3 g/g starch) into the bioactive film. Gallic acid acted as an anti-plasticizer at high concentrations of 0.2 g gallic acid/g cull starch. With the increasing amount of gallic acid incorporated in the film, higher antioxidant activity was achieved. But, potato peel had less effect on the antioxidant activity due to loading limitation, resulting in increased yellowness and roughness. The bioactive films made of potato by-products can have a number of applications in the food industry due to their low water activities and might prevent potential microbial growth.

Chapter 5: Development of Antimicrobial Films Based on Cassava Starch, Chitosan and Gallic Acid Using Pressurized Hot Water Technology*

5.1 Introduction

The use of renewable, sustainable and environmentally friendly biopolymers for food packaging materials may reduce waste caused by petroleum-based packaging materials. Alternative biodegradable plastics were developed with natural polymers, including starch, cellulose, protein, polylactide family and polyhydroxyalkanoates family (Peelman et al., 2013). Among them, cassava starch is an abundant, renewable and inexpensive biopolymer that can be chemically modified for use as biopolymer in packaging applications. Starch is composed of two major components, amylose and amylopectin, where amylose provides starch film rigidity, and the branched structure of amylopectin decreases tensile stress (Tharanathan, 2003). But, starch-based films have drawbacks, including high water solubility, brittle nature and poor mechanical properties (Mathew et al., 2006), limiting their application in food products. Therefore, the use of plasticizers and its blending with other polymers are required to improve those properties (Sanyang, Sapuan, Jawaid, Ishak & Sahari, 2015).

The addition of active compounds in packaging systems provides additional functionality but also modifies the film structure and mechanical properties. Food packaging is termed as active when it performs certain desirable roles in addition to providing barrier properties. These systems can include antioxidants, antimicrobial agents or oxygen scavengers (Božič, Gorgieva & Kokol, 2012; Sun et al., 2014b). Although these compounds can be naturally or synthetically derived, bioactive compounds from natural resources are preferred by consumers. Chitosan, a

*A version of this chapter has been published as “Zhao, Y., Teixeira, J. S., Gänzle, M. G., & Saldaña, M. D. A. (2018). Development of antimicrobial films based on cassava starch, chitosan and gallic acid using subcritical water technology. *The Journal of Supercritical Fluids*, 137, 101-110.

cationic polysaccharide derived from deacetylation of chitin, has been used for antimicrobial packaging films (Dutta et al., 2009). Its use has improved the tensile strength of rice starch films (Bourtoom & Chinnan, 2008). Chitosan also lowered the water vapor permeability and provides greater hydrophobicity to the starch film (Dang & Yoksan, 2016). Chitosan has antibacterial activity against Gram-positive bacteria, e.g. *Staphylococcus aureus*, Gram-negative bacteria, e.g. *Escherichia coli* as well as yeasts and molds (Kong et al., 2010; Lopez et al., 2014). Thermoplastic corn starch formulations with 10% chitosan inhibited growth of *S. aureus* and *E. coli* (Lopez et al., 2014). The antibacterial activity of chitosan relates to interaction of the positively charged polysaccharides with biological membranes, leading to membrane disruption and permeabilization, and cell death (Kong et al., 2010; Mellegård, Strand, Christensen, Granum & Hardy, 2011).

Conventional methods used to produce starch films are casting, extrusion blowing, injection, and thermo-compression (Liu et al., 2009). Among them, the most commonly used is the cast film-forming dispersion. Using this method, after the gelatinization and homogenization steps, film-forming dispersions are poured or cast on dishes to allow drying at controlled conditions. Poor miscibility of functional additives (anti-oxidant or antimicrobial compounds), however, may lead to phase separation and formation of heterogeneous films. For extrusion, once the starch is in an amorphous state, it can be extruded using a film-blowing die. In this case, gelatinization is achieved at low moisture content due to the high-shear and high-pressure conditions used, which breaks down the starch granules, allowing fast water transfer into the starch molecules. However, the intense shear can break down the molecule chain and cause poor film mechanical properties (Liu et al., 2009). Pressurized hot water technology has been used for formation of bioactive starch films (Zhang, 2015). Pressurized hot water acts as a

catalyst and reaction medium to improve loading of phenolic acids in starch (Zhang, 2015). At pressurized hot water conditions, the water dissociates into acidic hydronium ions (H_3O^+) and basic hydroxide ions (OH^-), accelerating acid- or base-catalyzed reactions. Also, the relatively high density ($961\text{--}925\text{ kg/m}^3$) combined with the high dissociation constant of pressurized hot water favor ionic reactions. The effect of antimicrobial compounds on film properties, however, is poorly understood. Therefore, the aim of this study was to develop bioactive cassava starch films using pressurized hot water technology to improve mechanical and antimicrobial properties. The antimicrobial activity of the bioactive films against spoilage organisms on ham was also investigated.

5.2 Materials and methods

5.2.1 Materials

Cassava starch was provided by CbPAK Tecnologia S/A (Rio de Janeiro, Brazil). Chitosan (75–85% deacetylated) with medium molecular weight of 190-310 kDa and gallic acid (97.5–102.5% titration) were purchased from Sigma Aldrich (Oakville, ON, Canada). Glycerol (>95% purity, certified ACS grade) was purchased from Fisher Scientific (Ottawa, ON, Canada).

5.2.2 Preparation of bioactive films

Bioactive films were prepared with a film-forming solution of cassava starch, chitosan, glycerol, gallic acid and water using pressurized hot water technology, following the procedure described in Chapter 4 (Section 4.2.2). A fractional factorial design with five parameters, including temperature, pressure, gallic acid/starch ratio, glycerol/starch ratio and chitosan/starch ratio, was investigated to find optimal mechanical properties (Table 5.1). At optimal conditions for best elongation, 0, 0.025, 0.05, 0.075, 0.1 and 0.15 g chitosan/g starch ratios were investigated.

Table 5.1 Parameters evaluated for bioactive starch film formation.

Parameter				
Temperature (°C)	75	100	125	150
Pressure (bar)	50	85	120	155
Gallic acid/starch ratio (g/g)	0	0.1	0.2	0.3
Glycerol/starch ratio (g/g)	0	0.5	1	1.5
Chitosan/starch ratio (g/g)	0	0.025	0.05	0.1

5.2.3 Film characterization

Film structural properties of FT-IR spectra and X-ray diffraction patterns, mechanical properties of tensile strength and percent elongation at break, physico-chemical properties of water activity, moisture content, film solubility in water and water vapor permeability, optical properties of transparency, color, gloss and contact angle, and functional properties of total phenolic content and antioxidant activity by FRAP and ABTS methods were performed following the methods described in Chapter 4 (Section 4.2.3)

5.2.4 Statistical analysis

The R Studio software (Version 0.99.903, R studio, Inc., Boston, MA, USA) was used to conduct analysis of variance (ANOVA). Significant differences were identified with Tukey's test as post-hoc analysis at an error probability of 5% ($p < 0.05$).

5.3 Results and discussion

The use of pressurized hot water technology offers an innovative green alternative to produce bioactive cassava starch films for the food packaging industry. Films produced with cassava starch can act as carriers of antioxidants or antimicrobials, resulting in final products with extended shelf-life.

5.3.1 Chemical properties of bioactive starch films

Pressurized hot water not only gelatinizes and hydrates the starch but the combination of high temperature and low pH also catalyzes chemical reactions, facilitating cross-linking between starch, chitosan, and gallic acid. Chemical properties of starch films were evaluated with FTIR. The typical region of polysaccharide bands at 1180-957 cm^{-1} (Fig. 5.1) is attributed to C=C and C=O stretchings and the bending mode of C-H bonds. The bands observed at 3600-3200 cm^{-1} in pure gallic acid correspond to stretching modes of the different -OH groups (Sun et al., 2014b). A broad peak from 3680 to 3100 cm^{-1} represents hydrogen bonds within the pure cassava starch and chitosan (Fig 5.1A), and starch, gallic acid-starch films and gallic acid+chitosan starch films (Fig. 5.1B). For chitosan, specifically, this broad peak can be also attributed to the N-H and OH-O stretching vibrations (Liu, Adhikari, Guo & Adhikari, 2013). In addition, peaks observed for chitosan at 1640 cm^{-1} and 1550 cm^{-1} (Fig. 5.1A) indicated the amide-I absorption band and the amide-NH₂ absorption band, respectively (Wan, Wu, Yu, & Wen 2006). In the case of gallic acid, the bands at 1701 and 1620 cm^{-1} corresponded to the C=O stretch of conjugated acids, and the bands at 1425 cm^{-1} and 1263 cm^{-1} corresponded to the -COOH bend (da Rosa et al., 2013). The bands in the 1308-1174 cm^{-1} regions corresponded to the bending vibrations of C-H in the aromatic ring and O-H of the phenol (Neo et al., 2013).

Compared with the spectra of pure chitosan (Fig. 5.1A), the amide-I and NH₂ characteristic peaks in the spectra of gallic acid+chitosan loaded starch film shifted from 1550 cm^{-1} to 1541 cm^{-1} and from 1640 cm^{-1} to 1627 cm^{-1} (Fig. 5.1B), respectively. This shift suggests reactions between the hydroxyl groups of starch and the amino groups of chitosan (Liu et al., 2013). Also, the peak at 1627 cm^{-1} became evident, over-lapping with that of amide I in the gallic acid + chitosan starch film, further suggesting that reactions between the starch,

chitosan and carbonyl groups of gallic acid occurred via ester linkages (Fig. 5.1B). Moreover, characteristic carboxyl groups (-COOH) of phenolic acids were found at about 1700-1720 cm^{-1} (Mayachiew & Devahastin, 2010). A new peak (1715 cm^{-1}) was found in the gallic acid-starch film and gallic acid+chitosan starch film, which was also reported in the chitosan-corn starch film with murta leaves extract (Silva-Weiss et al., 2013). Ester linkages were also reported for chitosan film loaded with tannic acid at 1730 cm^{-1} (Rivero, García & Pinotti, 2010) and gallic acid at around 1715 cm^{-1} (Božič et al., 2012). Ferulic acid enhanced the cross-linking between starch and chitosan (Mathew & Abraham, 2008). Other concentrations (0.025-0.1 g chitosan/g starch) were also analyzed (data not shown), and same peaks were found as the spectrum of gallic acid + chitosan starch film shown in Fig. 5.1B.

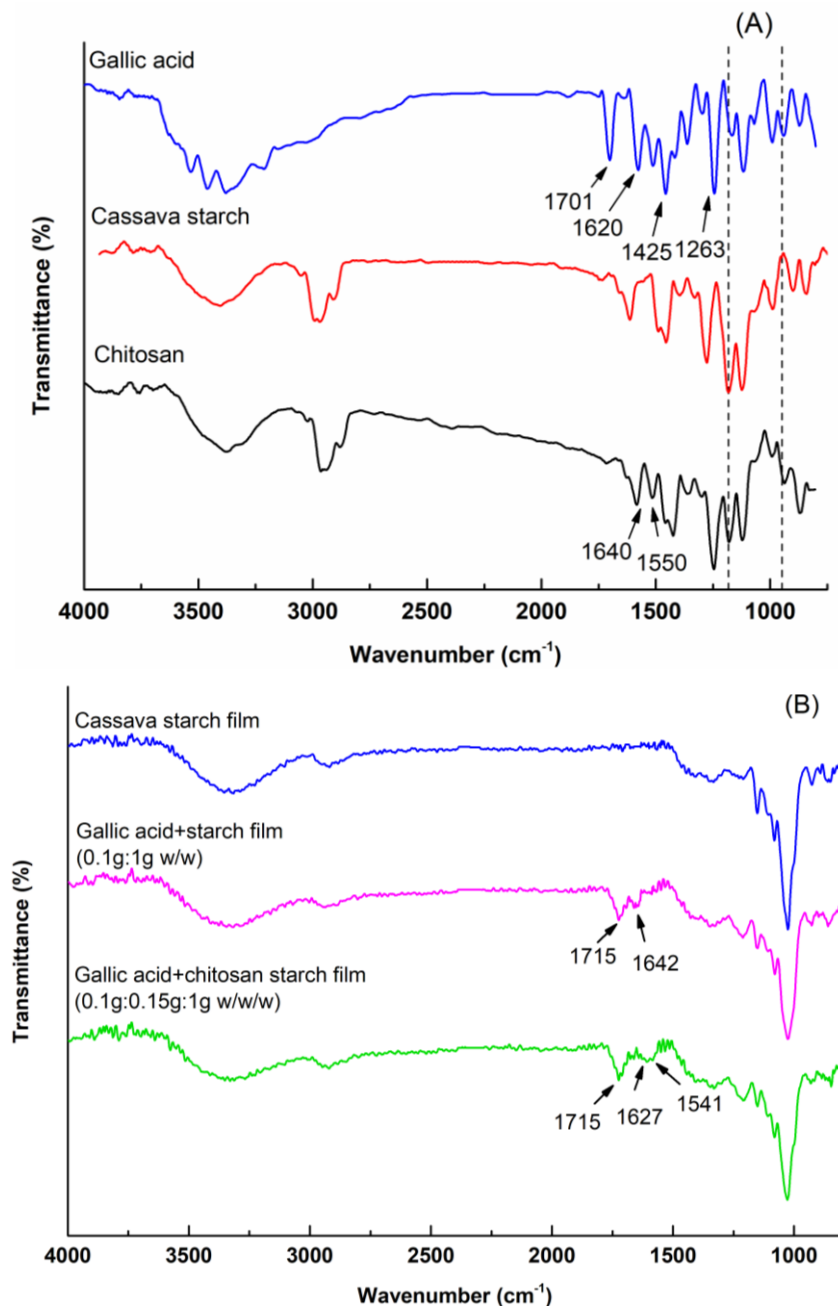


Fig. 5.1 FTIR spectra of: A) pure gallic acid, cassava starch and chitosan, B) cassava starch film, gallic acid+starch film (0.1 g gallic acid/g starch, 0.5 g glycerol/g starch) and gallic acid+chitosan starch film produced at a chitosan/starch ratio of 0.15 g/g starch, gallic acid/starch ratio of 0.1 g/g and glycerol/starch ratio of 0.5 g/g at 85 bar and 100 °C.

Starch crystallinity was determined by X-ray diffraction (Fig. 5.2). The two main diffraction peaks in the chitosan were observed at $2\theta = 9.4^\circ$ and 20.25° , in agreement with the findings of Bangyekan et al. (2006) and Liu et al. (2013), where the small peak at approximately 9.4° (2θ) indicated the small crystalline fraction embedded in the amorphous matrix of chitosan and the second peak at $21-22^\circ$ (2θ) was observed in chitosan film prepared by dissolving chitosan in acid solution (Ritthidej, Phaechamud & Koizumi, 2002). For the pure cassava starch and gallic acid+chitosan starch films, the characteristic peak of B-type crystalline structure was found at $2\theta = 17^\circ$. In addition, a diffraction peak at 19.7° was attributed to amylopectin recrystallization in the film during storage. The crystallinity of starch films should be determined by the crystallization of amylose developed in the early stage of film formation, and the slow crystallization of amylopectin occurring during storage (Bangyekan et al., 2006). Moreover, a small peak found around 20° indicated V-type crystallinity that results from interactions of glycerol with single amylose helices. This crystalline structure is formed by the crystallization of amylose in single helices, involving glycerol or lipids, and can be further divided into three types (V_h , V_a and E_h) based on the folding structure (Ahmed, Tiwari, Imam & Rao, 2012).

Addition of chitosan to starch decreased the crystallinity of starch films. The characteristic peak of chitosan (9.4°) also became less evident in the chitosan-cassava starch films due to the formation of intermolecular hydrogen bonds between chitosan and starch that prevents the crystallization of starch and alters the chitosan structure. A small decrease in crystallinity from 15.83 to 13.65% of high amylose corn starch film after the addition of chitosan was also observed by Liu et al. (2013). The crystalline peaks of native cassava starch (5.90° , 14.95° , 17.60° , 19.65° , and 22.21°) shifted slightly to lower degrees (5.25° , 14.90° , 16.75° ,

19.20°, and 21.35°) when chitosan was added, indicating the formation of hydrogen bonds between cassava starch and chitosan (Fig. 5.2).

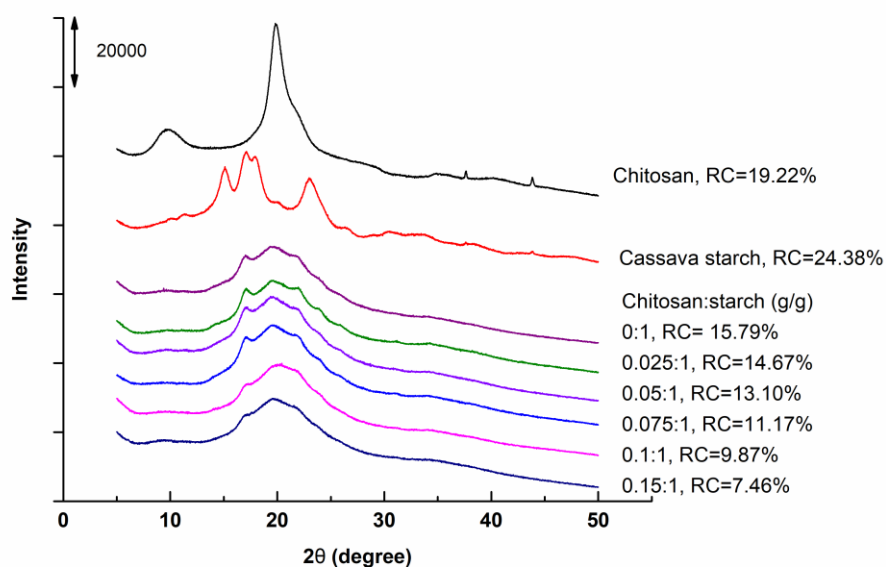


Fig. 5.2 XRD patterns and relative crystallinity (RC) of pure chitosan, native cassava starch and bioactive cassava starch films with different chitosan/starch ratios of 0-0.15 g/g, constant gallic acid/starch ratio of 0.1 g/g and glycerol/starch ratio of 0.5 g/g at 85 bar and 100 °C.

5.3.2 Mechanical properties of bioactive starch films

Determination of tensile strength and elongation provided insight into mechanical properties of starch films. Among all formulations from the fractional design to produce films, 100 °C, 85 bar, 0.5 g glycerol/g starch, 0.1 g gallic acid/g starch and 0.025 g chitosan/g starch had the best elongation (94.7%, Table 5.2). To further evaluate the effect of chitosan addition at optimized conditions of temperature, pressure, gallic acid/starch ratio and glycerol/starch ratio on mechanical and antimicrobial properties, 0, 0.25, 0.05, 0.075, 0.1 and 0.15 g chitosan/g starch ratios were investigated. The tensile strength of the cassava starch films increased from 0.51 to 0.83 MPa with increasing chitosan content, whereas the elongation at break increased from 70.2

to 100.1%, followed by a decrease to 65.7% at 0.15 g chitosan/g starch ratio (Fig. 5.3, Table C.1, appendix C). It is hypothesized that, the amino group (NH_2) of chitosan was protonated to NH_3^+ at hot pressurized conditions, while the ordered crystalline structures of starch molecules were modified during the gelatinization process, resulting in the OH^- groups being exposed to readily form hydrogen bonds with NH_3^+ of the chitosan, facilitating the reaction between chitosan and cassava starch.

Also, the addition of gallic acid and chitosan to cassava starch films facilitated ester linkages after reaction with $-\text{CH}_2\text{OH}$ groups of the starch and chitosan, producing a stronger film structure with less chain mobility. Other interactions, such as electrostatic interactions between COO^- of gallic acid and protonated amino groups (NH_3^+) of chitosan increased film tensile strength. Three reaction mechanisms were proposed to account for incorporation of gallic acid into cassava starch/chitosan films: (1) through free radical-mediated cross-linking, (2) by esterification with the hydroxyl groups of chitosan and starch, and (3) by the quinone-mediated reaction. However, limited chain mobility led to the reduction of elongation of the bioactive cassava starch films, where the highest elongation (100.1%) was achieved at 0.05g chitosan/g starch in our study (Fig. 5.3) but less elongation (20-30%) was obtained in the study of Mathew and Abraham (2008). Therefore, mechanical properties of bioactive films should be customized according to the film application of the bioactive film.

Mechanical properties of packaging films are important in determining the physical strength they can withstand under specific conditions of temperature and RH (Ahmed et al., 2012). Low strength of starch-based films remains a challenge. To increase film strength, nano-clay (Cyras, Manfredi, Ton-That & Vázquez, 2008) or fiber can be added or blended with either

biodegradable or non-biodegradable polymers that have low water permeability (Peelman et al., 2013). But, this addition can compromise film elongation and homogeneity.

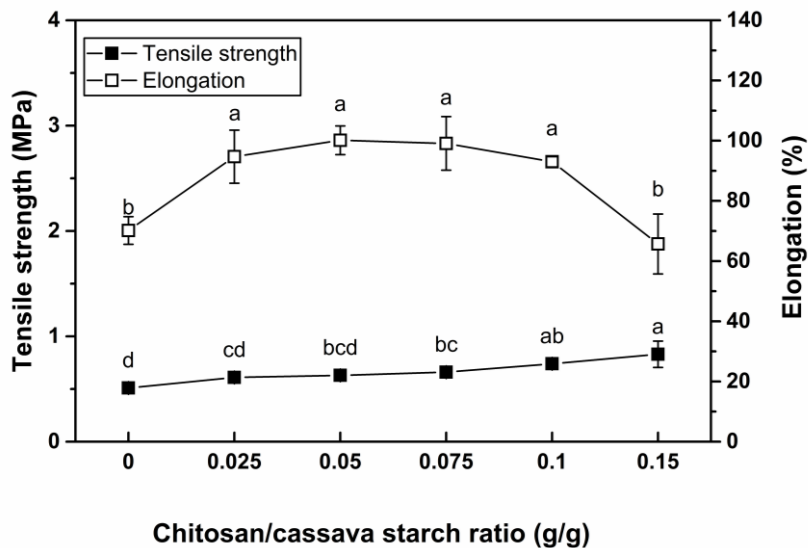


Fig. 5.3 Mechanical properties of bioactive cassava starch films with different chitosan/starch ratios of 0-0.15g/g, constant gallic acid/starch ratio of 0.1 g/g and glycerol/starch ratio of 0.5 g/g at 85 bar and 100 °C.

5.3.3 Water activity, solubility and water vapor permeability of bioactive starch films

The water activity of the film influences the film solubility and water vapor permeability. Films with low water activity ($a_w < 0.3$) contain less transferable free water, resulting in low water permeability. At high water activity ($a_w > 0.6$), water is available to act as a solvent, favoring chemical/biochemical reactions and growth of microorganisms (Veiga-Santos, Oliveira, Cereda, Alves & Scamparini, 2005). The decrease of water activity and moisture content (Table 5.2) indicated that the number of active sites for water binding decreases due to the formation of strong bonds between cassava starch, chitosan, and gallic acid, as discussed previously. This effect is more evident at high chitosan loading cassava starch films (0.15 g chitosan/g starch) due to strong interactions. Wang et al. (2015) reported a significant decrease in moisture content

when chitosan films were incorporated with *Lycium barbarum* fruit extract, suggesting possible interactions between chitosan and the fruit extract, reducing the availability of hydroxyl groups and amino groups of chitosan to interact with water. As a result, the WVP of the films can be improved by limiting moisture transfer within the film structure.

The solubility of films in water is an important factor when selecting a film for specific applications. Bioactive film solubility in water decreased at all temperatures investigated with the addition of chitosan (Fig. 5.4A, Table C.2, appendix C). These values are similar to reported chitosan/starch-based films, with 20% to 40% solubility (Vásconez et al., 2009; Nouri & Nafchi, 2014). Prior studies reported that chitosan addition to starch reduced film solubility from 35% to 25% (Vásconez et al., 2009), depending on the amount of cross-linking compounds present during the film forming process. However, the sago starch film solubility increased from 24% to 28.5% after incorporating with betel leaves extract with an unknown composition of phenolic compounds (Nouri & Nafchi, 2014), indicating the lack of cross-linking. As observed in Fig 5.4B (Table C.2, appendix C), the contact angle results showed the same tendency observed for film solubility in water, where the increase of contact angle from 36.71° to 68.26° for the top surface and from 55.15° to 94.69° for the bottom surface revealed the transition from hydrophilicity to hydrophobicity. A lower increase of the contact angle was observed in the study of Cyras et al. (2008), where an increase in chitosan content up to 20 wt% significantly increased the contact angle values of the cassava starch/ montmorillonite composite film.

In addition, the intermolecular hydrogen bond formation between cassava starch and chitosan molecules reduced the number of free hydroxyl groups that could interact with water molecules, resulting in the decreased of WVP in films (Table 5.2). High degree of cross-linking resulted in the formation of ester linkages and electrostatic bonds between cassava starch, gallic

acid, and chitosan as observed in the FT-IR spectra (Fig. 5.1), contributing to the reduction of WVP. Similarly, WVP of the potato starch film decreased with the addition of ferulic acid due to the formation of quinones (Mathew & Abraham, 2008). Although chitosan is a hydrophilic polymer because of its hydroxyl and amino groups, the arising hydrophobicity, low moisture absorption and low permeability are possibly due to the following reasons: (1) the increasing cross-linking interactions between starch, chitosan and gallic acid lower solubility of the films in water, increasing hydrophobicity, (2) β -(1 \rightarrow 4) glucopyranosyl linkages in chitosan had better packing structure or higher crystallinity than the α -(1 \rightarrow 4) glucopyranosyl linkages of starch, resulting in less moisture/water absorption values, difficulting chitosan depolymerization, and (3) acetyl groups in chitosan avoid the transportation of water vapor through the films.

Barrier properties such as water vapor permeability and oxygen permeability of packaging films greatly influence the quality of food products. Starch based films exhibit excellent oxygen barrier properties comparable with typical packaging plastics, such as low-density polyethylene and ethylvinyl alcohol (Ahmed et al., 2012). This is particularly beneficial to ham products with a high fat content as the film can prevent fat rancidity and inhibit the growth of aerobic bacteria.

Table 5.2 Physical properties of bioactive cassava starch films.

Chitosan/starch ratio (g/g)	Moisture content (%)	Water activity	WVP (g.mm/m².h.kPa)
0	20.80±0.31 ^a	0.35±0.01 ^a	0.67±0.06 ^a
0.025	15.47±0.62 ^b	0.32±0.01 ^{ab}	0.57±0.01 ^{ab}
0.050	12.31±0.54 ^b	0.30±0.01 ^b	0.52±0.05 ^{bc}
0.075	12.79±0.42 ^b	0.30±0.01 ^b	0.49±0.03 ^c
0.100	12.87±0.28 ^c	0.28±0.01 ^{bc}	0.46±0.03 ^{cd}
0.150	9.29±0.64 ^d	0.24±0.02 ^c	0.36±0.02 ^d

Bioactive cassava starch films produced with different chitosan/starch ratios of 0-0.15g/g, constant gallic acid/starch ratio of 0.1 g/g and glycerol/starch ratio of 0.5 g/g at 85 bar and 100 °C. ^{a-d}Different lowercase letters in the same column indicate significant differences ($p < 0.05$). Data show as mean±standard deviation ($n = 3$).

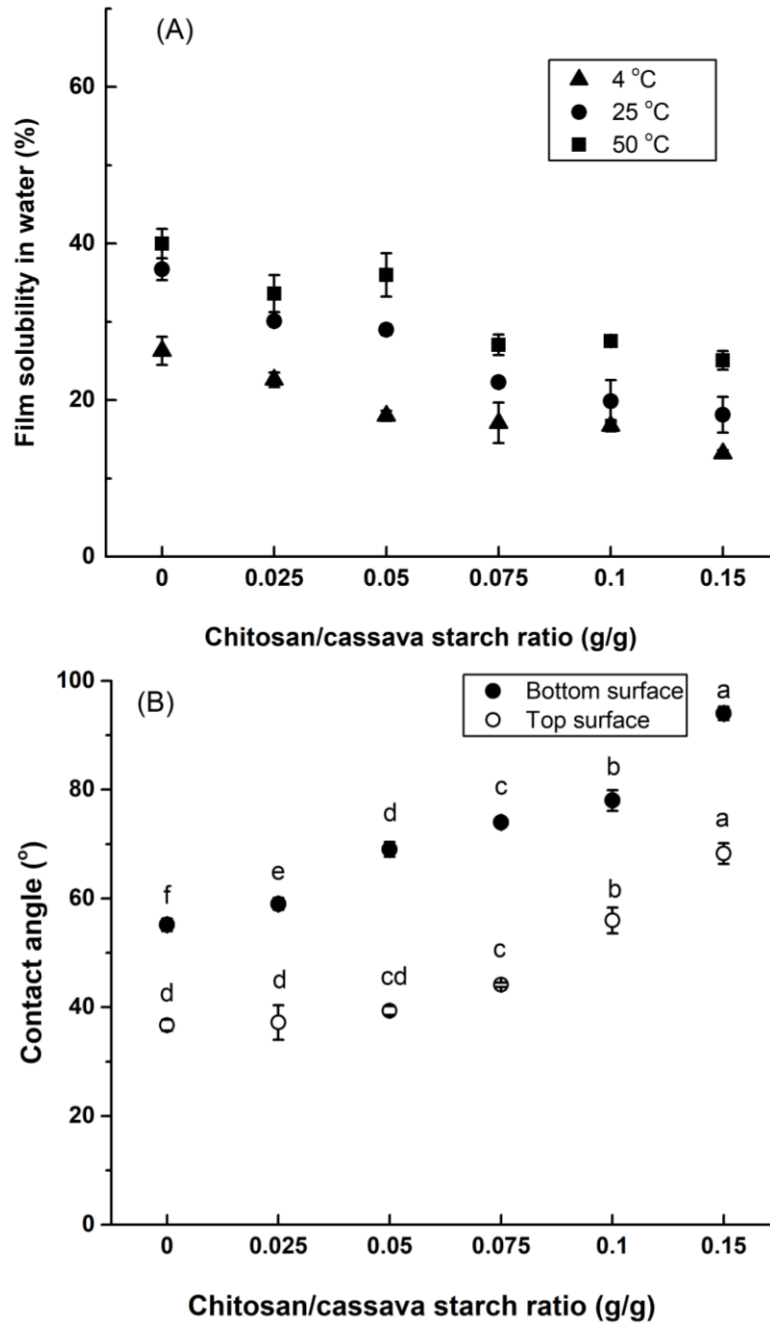


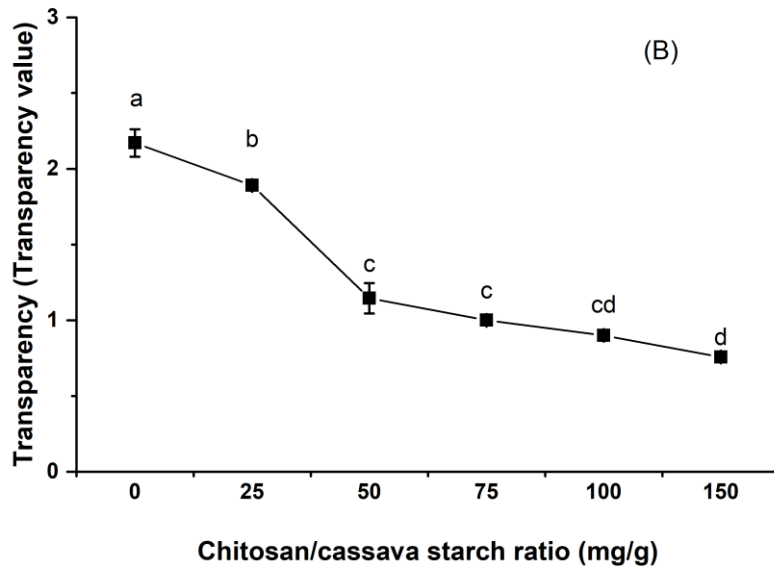
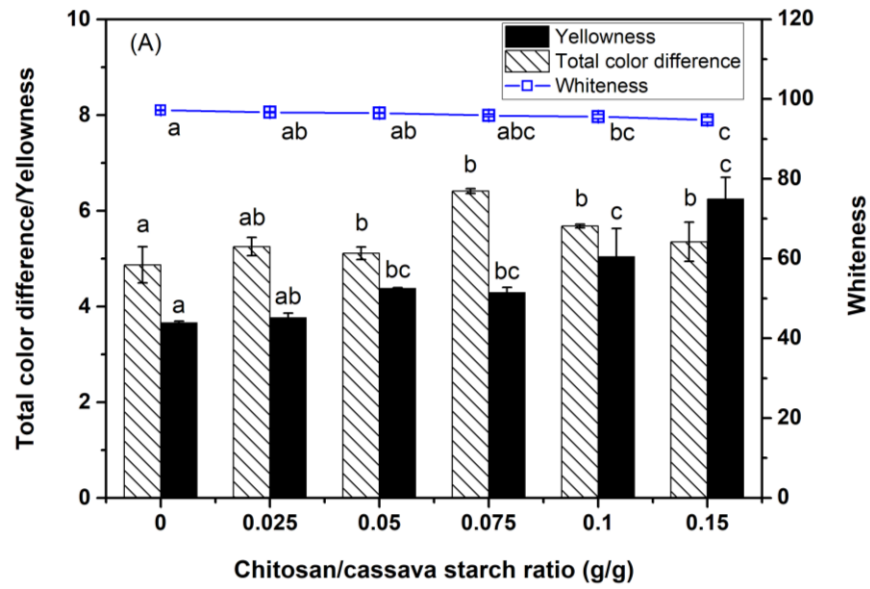
Fig. 5.4 A) Film solubility in water at 4, 25 and 50°C, B) top and bottom surfaces contact angle of bioactive cassava starch films with different chitosan/starch ratios of 0-0.15g/g, constant gallic acid/starch ratio of 0.1 g/g and glycerol/starch ratio of 0.5 g/g at 85 bar and 100 °C.

5.3.4 Optical and morphological properties

Color and transparency of packaging films are important indexes with regards to the general product appearance, consumer acceptance, and application. In general, cassava starch films with chitosan added appeared slightly yellow and less white, as visualized by the increment of the YI values and reduction of the WI values (Fig. 5.5A, Table C.3, appendix C). This color might also indicate the chemical reactions, in particular Maillard reaction between the carbonyl group of the carbohydrate ends with the amine group of the chitosan molecule (Leceta, Guerrero, Ibarburu, Dueñas & De la Caba, 2013). However, in terms of the total color difference, no significant difference was observed, where the incorporation of chitosan had no influence on the color appearance of the cassava starch films. The transparency values of all films decreased with increasing chitosan loading (Fig. 5.5B, Table C.3, appendix C), suggesting that higher chitosan contents provided the films with less opacity as the lower value represents higher transparency of the film. This also indicates a good film homogeneity, as an inhomogeneous phase in the films promotes light scattering, being responsible for opacity.

The roughness of the surface of the films was reflected in the gloss values measured. Films with smoother surfaces provided a higher gloss value. As observed in Fig. 5.5C, the top surface had low gloss values (Table C.3, appendix C). The gloss values of chitosan-cassava starch films were in the range of 8.15-54.55 and 14.45-88.90 units for the top and bottom surfaces, respectively, whereas the control film had values of 6.75 and 8.05 on the top and bottom surfaces, respectively, reflecting more roughness and less even film surfaces. For the chitosan-cassava starch films, the gloss values increased with an increase in the chitosan concentration. This is coherent with the miscible nature of starch and chitosan, avoiding the subsequent effect of dispersed particles on the film surface. On the contrary, a less smooth

surface was obtained in wheat starch-chitosan films after incorporating resveratrol, due to the immiscibility of resveratrol and starch, which resulted in phase separation (Bonilla et al., 2013).



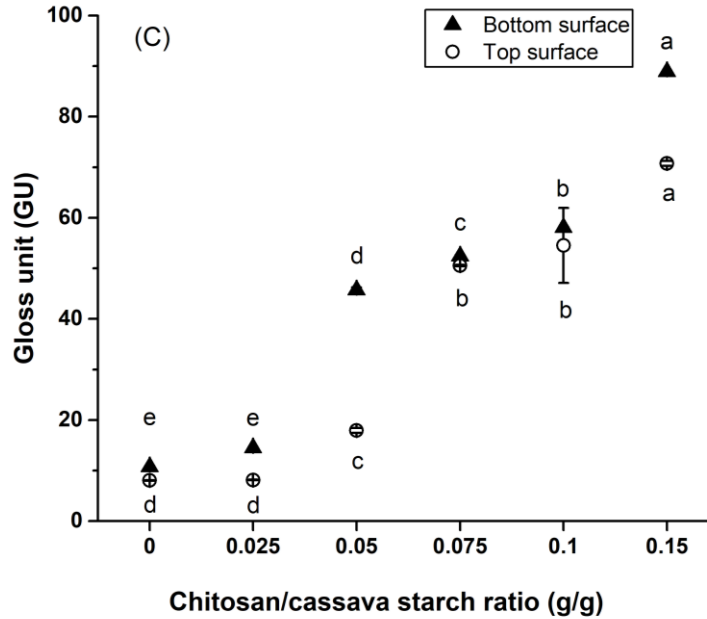


Fig. 5.5 A) Color performance (total color difference, whiteness index and yellowness index), B) transparency, and C) top and bottom surfaces gloss of bioactive starch films with different chitosan/starch ratios of 0-0.15 g/g, constant gallic acid/starch ratio of 0.1 g/g and glycerol/starch ratio of 0.5 g/g at 85 bar and 100 °C.

5.3.5 Antioxidant activity of bioactive films

Antioxidant activity of packaging films may delay oxidative spoilage of food products. The Trolox equivalent antioxidant capacity values and total phenolic contents released from the films decreased significantly as a function of the increasing chitosan concentration added to the film (Fig. 5.6, Table C.4, appendix C). In 24 h, free or weekly bounded gallic acid was released to the solution. Gallic acid that was strongly bound to the film matrix through chemical cross-linking as observed by FT-IR did not contribute to antioxidant activity. As a result of the formation of stronger cross-links for high chitosan-cassava starch film, less gallic acid (35 gallic acid equivalent mg/g film) was released at 150 mg chitosan/g starch ratio. Although the ABTS method provided higher values (548-742 Trolox equivalent mg/g film) compared to the FRAP

method (395-488 Trolox equivalent mg/g film), both techniques provided comparable trends and antioxidant activity values.

Increasing chitosan concentration decreased the anti-oxidant activity of aqueous extracts obtained from starch films. Chitosan had little contribution to the antioxidant activity, which may be attributed to the following factors: (1) The decreased solubility of film in water due to inter-/intra-molecular bond network, (2) the lack of a H⁺ atom donor to serve as a good antioxidant (Pasanphan & Chirachanchai, 2008), and (3) its strong metal ion chelating ability because of its nitrogen atom, preventing antioxidant activity in presence of some cations (Taghizadeh & Bahadori, 2014). As a result, some strategies must be implemented to improve the chitosan antioxidant activity. Improving its solubility in neutral aqueous solutions by introducing the H⁺ atom donor group via functionalizing with other groups, such as sulfate, carboxymethyl, and hydroxypropyl groups (Xie, Xu, & Liu, 2001), or compounds like gallic acid (Pasanphan & Chirachanchai, 2008).

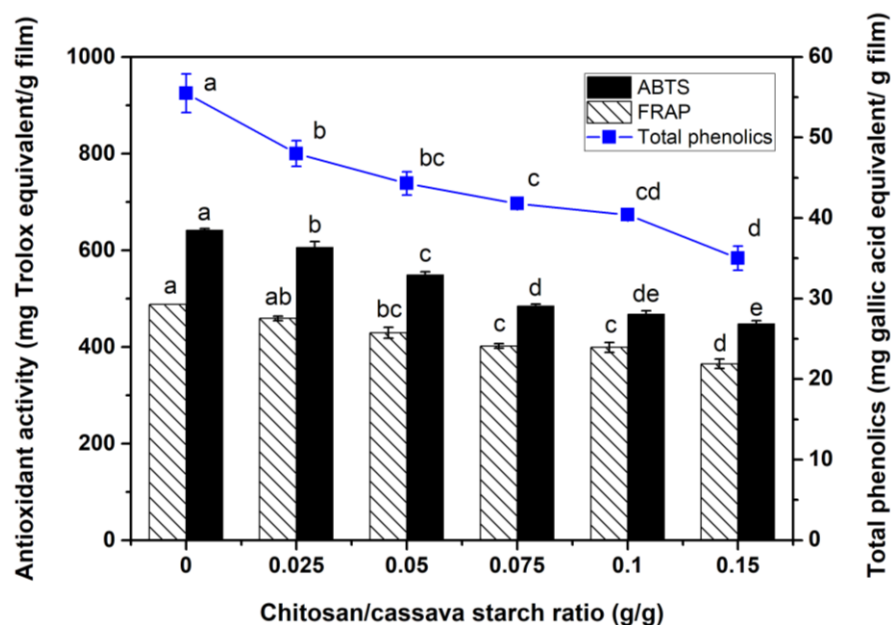


Fig. 5.6 Total phenolic content, antioxidant activity (ABTS and FRAP methods) of bioactive starch films with different chitosan/starch ratios of 0-0.15 g/g, constant gallic acid/starch ratio of 0.1 g/g and glycerol/starch ratio of 0.5 g/g at 85 bar and 100 °C.

5.3.6 Antimicrobial activity of bioactive films

The antimicrobial activity of chitosan-starch films was evaluated with cooked ham that was inoculated with a 5 strain cocktail of meat spoilage microbiota. Meat spoilage is observed after obtaining bacterial cell counts of approximately 10^7 - 10^8 CFU/cm² (Fig. 5.7, Table C.5, appendix C). Cell counts of un-inoculated ham remained below the detection limit throughout 4 weeks of storage (data not shown). On ham covered with starch film without chitosan, organisms of the spoilage cocktail reached high cell counts after two weeks of refrigerated storage. Addition of 25 and 150 mg chitosan/g starch to the packaging film delayed growth of spoilage microbiota by one and two weeks, respectively (Fig. 5.7), representing an extension of the shelf

life by 50 and 100%, respectively. The antimicrobial packaging film, however, did not completely eliminate or inhibit spoilage microbiota during refrigerated storage of 28 days.

Few studies have assessed the antimicrobial activity of bioactive packaging films in food applications (Dutta et al., 2009). Ready-to-eat meats are perishable and easily contaminated with spoilage microorganisms that are capable of growth in a refrigerated processing environment (Miller et al., 2014). The challenge study with cooked ham and a cocktail of spoilage organisms provides unprecedented information on the actual inhibition of growth of spoilage microorganisms by antimicrobial packaging films. The most commonly used disk inhibition zone assay provides a general indication on the antimicrobial activity of films, but only for less complex matrix compared to food products, with improper storage conditions that can not reflect the real performance of films. Chitosan-cassava starch film had no effect on inhibiting the growth of *Salmonella enteritidis*, *E. coli*, *S. aureus* and *B. cereus* in an inhibition zone assay (Pelissari et al., 2009). But, other studies indicated inhibition zones of up to 29 mm and 28 mm for *E. coli* and *S. aureus*, respectively, when chitosan addition increased to 15% (Shen et al., 2010). Therefore, bioactive cassava starch films obtained in this study are effective to delay the growth of spoilage organisms and extend the shelf life of ham.

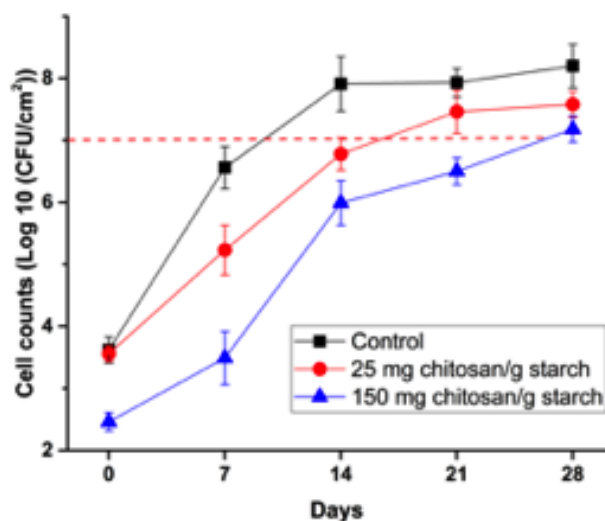


Fig. 5.7 Growth of a 5 strain cocktail of meat spoilage microbiota containing *Brochothrix thermosphacta* FUA3558, *Carnobacterium maltaromaticum* FUA3559, *Leuconostoc gelidum* FUA3560 and FUA3561, and *Lactobacillus sakei* FUA3562 on the surface of cooked ham during storage at 4°C. The ham was covered with a starch film (control, squares), or with starch films containing 25 mg (circles) or 150 mg chitosan (triangles)/g starch and bacterial cell counts were enumerated over 28 d of storage. Cell counts of un-inoculated ham remained below the detection limit throughout the 4 weeks of storage.

5.4 Conclusions

The use of pressurized hot water technology offers an innovative green alternative to produce bioactive cassava starch films for the food packaging industry. Pressurized hot water is advantageous because it not only hydrates and gelatinizes starch, but also acts as a catalyst to support formation of cross-links, especially the ester linkages between the carboxyl groups (-COOH) of gallic acid and the hydroxyl groups (-OH) of chitosan and cassava starch. Addition of chitosan to cassava starch also prevented the crystallization of starch in the films. The different cross-linking improved tensile strength but reduced elongation, and contributed to the reduction of film solubility in water and water vapor permeability. The addition of chitosan had no influence on the color performance of films, and the homogenous film structure was even more

transparent. Also, films produced with cassava starch can act as carriers of antioxidants/antimicrobials. As a result of the cross-linking, less gallic acid was released from the film matrix and chitosan had little contribution to the antioxidant activity but its antimicrobial activity extended the shelf life of refrigerated, cooked ham up to 25 days.

Chapter 6: Bioactive Cassava Starch Films Incorporated with Chitosan and Carvacrol Essential Oil for Packaging Produced by Pressurized Hot Water Technology*

6.1 Introduction

The increasing concern on food safety and the use of petroleum based plastic packaging contribute to the accumulation and inappropriate disposal of these plastics with high durability. Bioactive starch films are an alternative to extend food shelf-life and minimize the use of non-renewable plastics (Zhao et al., 2018; Zhao & Saldaña, 2019). The use of different starch sources such as corn, cassava, wheat, rice, potato and pea to obtain biodegradable plastics has been extensively studied as starch is abundant, biodegradable, accessible at a relatively low cost, and has good thermoplastic properties (Basiak, Lenart & Debeaufort, 2017a). Starch is composed of linear amylose and highly branched amylopectin. Physical cross-linkages in the macromolecular starch network are formed mainly by inter/intra-molecular hydrogen bonds between amylose and amylopectin (Miles, Morris & Ring, 1985), where amylose contributes to the high film tensile strength, while amylopectin resulted in more amorphous regions, limiting both film mechanical strength and elongation (Li et al., 2011). A wider application of starch film is limited by its water solubility and brittleness. In addition to starch, chitosan, the second most widespread polysaccharide after cellulose, shows unique biodegradability and antimicrobial activity. Furthermore, chitosan possesses advantages to be used as an edible packaging material owing to its good film-forming properties of stabilizing emulsions, and improving mechanical and water barrier properties (Siripatrawan & Harte, 2010). By combining the advantages of starch and chitosan, it is possible to overcome the poor mechanical properties of these films and improve film stability.

* A version of this chapter has been submitted to the journal of Food Packaging and Shelf life as “Zhao, Y. and Saldaña, M.D.A. (2019). Bioactive Cassava Starch Films Incorporated with Chitosan and Carvacrol Essential Oil for Packaging Produced by Subcritical Water Technology. 150

To develop bioactive packaging films with antioxidant/antimicrobial activities, starch has been combined with various natural bioactive compounds, such as phenolic compounds (Pyla et al., 2010), essential oils (Valencia-Sullca et al., 2018b) or even natural extracts (Piñeros-Hernandez, Medina-Jaramillo, López-Córdoba & Goyanes, 2017) containing these compounds to satisfy consumers demand for the use of natural preservatives. Various studies on the antimicrobial activity of essential oils have shown that carvacrol is one of the most effective antibacterial agents (Guarda, Rubilar, Miltz & Galotto, 2011; Nair, Kiess, Nannapaneni, Schilling & Sharma, 2015). Carvacrol, an isoprenyl phenol, is the main compound of oregano essential oil. Carvacrol (75-375 mg/L) effectively inhibited the growth and survival of various microorganisms, including *Listeria monocytogenes*, lactic acid bacteria (Nair et al., 2015), *Escherichia coli*, *Staphylococcus aureus*, *Listeria innocua*, *Saccharomyces cerevisiae* and *Aspergillus niger* (Guarda et al., 2011). The presence of a free hydroxyl group attached to the aromatic ring in the carvacrol structure provides antimicrobial activity (Ben Arfa, Combes, Preziosi-Belloy, Gontard & Chalier, 2006).

The volatile active substances of essential oils can be easily lost if essential oils are applied directly on a food surface by dipping, powdering or spraying. To avoid this problem, an alternative is the incorporation of essential oil within the films. Emiroğlu, Yemiş, Coşkun & Candoğan (2010) reported that soy protein edible films incorporated with oregano or thyme essential oils (5%) resulted in 1.13 and 1.27 log reductions of *Pseudomonas* spp. count on ground beef patties, respectively. The incorporation of 100 mg carvacrol/g starch significantly increased the antioxidant activity of tapioca starch dispersions from 0 to 167 µg/mL ABTS radical scavenging capacity (IC₅₀) (Homayouni et al., 2017). However, in another study, the addition of oregano essential oil (0.25 w/w%) did not promote any antimicrobial action in

chitosan monolayer films and cassava starch-chitosan bilayer films applied to the cold-stored sliced pork, due to carvacrol loss during film production (Valencia-Sullca et al., 2018b). Unlike phenolic compounds, carvacrol could create a coarser structure to the film matrix with increased heterogeneity due to its low solubility in the film-forming solution (Homayouni et al., 2017). Cracks have been observed in the carvacrol (0.1 w/w%) incorporated gelatinized tapioca starch films, which further decreased the tensile strength from 0.30 to 0.16 MPa, causing an increase in water vapor transmission from 0.69 to 0.99 g mm/kPa m² h (Homayouni et al., 2017).

The low miscibility of essential oils with starch limits its application in the starch films. Traditional thermal treatment usually heats the starch film forming solution at ambient pressure, therefore the native starch is hardly modified and shows limited reactivity with essential oil. Compared to other traditional film forming methods, like extrusion blowing, casting and thermo-compression, pressurized hot water technology has shown promising ability to promote chemical reactions by improving cross-linking (Zhang, 2015; Zhao et al., 2018; Zhao & Saldaña, 2019). The addition of chitosan using pressurized hot water technology improved the film mechanical properties and water vapor permeability. Development of bioactive starch films have been studied extensively using traditional technologies, whereas no study has been conducted on developing starch-based films with essential oil using pressurized hot water technology. Therefore, the objective of this study was to produce carvacrol essential oil incorporated chitosan-cassava starch films by pressurized hot water technology and evaluate the effect of carvacrol addition on the film mechanical, optical, structural, water barrier properties and antioxidant activity.

6.2 Materials and methods

6.2.1 Materials

Cassava starch was provided by CbPAK Tecnologia (Rio de Janeiro, Brazil). Chitosan (75-85% deacetylated, with medium molecular weight of 190-310 kDa) and carvacrol (99%, FG) were purchased from Sigma Aldrich (St. Louis, MO, USA). Glycerol (>95% purity, certified ACS grade) and lecithin (soybean) were acquired from Fisher Scientific (Hampton, NH, USA).

6.2.2 Bioactive film preparation

Bioactive films were prepared with a film-forming solution of cassava starch, chitosan, glycerol, carvacrol and water using pressurized hot water technology, following the procedure described in Chapter 4 (Section 4.2.2). For each experiment, known amounts of cassava starch (13 g), chitosan (0.025 g/g starch), carvacrol (0-0.195 g/g starch) emulsified with 20 w/v% lecithin and glycerol (0.5 g/g starch) were mixed with water and preloaded into the reactor. A fractional factorial design composed of temperature (75-125 °C), pressure (50-120 bar), chitosan/starch ratio (0-0.05 g/g starch), and carvacrol/starch ratio (0-0.098 g/g starch) were first investigated to find optimal mechanical properties (Table 6.1). At optimal conditions for best elongation, different ratios of 0, 0.049, 0.098, 0.147, and 0.195 g carvacrol/g starch were investigated.

Table 6.1 Process parameters evaluated for carvacrol incorporated chitosan-cassava starch film formation.

Process parameter			
Temperature (°C)	75	100	125
Pressure (bar)	50	85	120
Chitosan/starch ratio (g/g)	0	0.025	0.05
Carvacrol/starch ratio (g/g)	0	0.049	0.098

6.2.3 Film characterization

Film structural properties of FT-IR spectra and X-ray diffraction patterns, mechanical properties of tensile strength and percent elongation at break, physico-chemical properties of water activity, moisture content, film solubility in water and water vapor permeability, optical properties of transparency, color, gloss and contact angle, and functional properties of total phenolic content and antioxidant activity by FRAP and ABTS methods were performed following the methods described in Chapter 4 (Section 4.2.3).

6.2.5 Biodegradability test

Biodegradation of potato by-product films and cassava starch-based film incorporated with chitosan or carvacrol was determined using the compost burial method reported by Nguyen et al. (2016) with slight modifications. The organic compost (Miracle-Gro Clay) was purchased from a local market, Canadian tire (Edmonton, AB, Canada). Briefly, 4 trays with approximate capacity of 5 L were filled with compost. The film samples were cut into 2 cm x 2 cm squares and buried in the compost at the depth of 5 cm. Then, trays were placed in an oven at 30 °C. The compost was kept moist by sprinkling water (~15 mL) every 24 h to maintain 40-45% humidity. The degradation of film samples was studied at regular time intervals of 5 days by removing the samples carefully from the compost and brushing them gently to remove the compost adhering on the surface. The film specimen was dried at 105 °C for 24 h and weighed to obtain the final weight. Weight loss of the film sample over time was used to indicate degradation rate in the compost burial test (Nguyen et al., 2016). The percentage weight loss is calculated using the following equation:

$$\text{Weight loss (\%)} = \frac{(m_0 - m_1)}{m_0} \times 100 \quad (6.1)$$

where, m_0 is the initial film weight, and m_1 is the remaining weight after film degradation in the compost. Experiments were performed in triplicate.

6.2.4 Statistical analysis

The R Studio software (Version 0.99.903, R studio, Inc., Boston, MA, USA) was used to conduct analysis of variance (ANOVA). Significant differences were identified with Tukey's test as post-hoc analysis at an error probability of 5% ($p < 0.05$).

6.3 Results and discussion

Among all formulations from the fractional design to produce films, 75 °C, 120 bar and 25 mg chitosan/g starch had the best elongation ($231.8 \pm 16.0\%$, Table 6.2). ANOVA analysis showed that temperature (p -value < 0.001), pressure (p -value < 0.001), chitosan/starch ratio (p -value < 0.001) and carvacrol/starch ratio (p -value < 0.001) significantly influenced film elongation (Table D.1, appendix D). To further evaluate the effect of carvacrol addition at optimized conditions of temperature, pressure and chitosan/starch ratio on physico-chemical, mechanical, and functional properties, 0, 0.049, 0.098, 0.147, 0.198 g carvacrol/g starch ratios were investigated.

Table 6.2 Elongation of carvacrol incorporated chitosan-cassava starch films using a fractional factorial design.

Temperature (°C)	Pressure (bar)	Chitosan/starch ratio (g/g)	Carvacrol/starch ratio (g/g)	Elongation (%)
100	50	0	0	55.1±4.9
100	85	0.025	0.049	160.5±3.4
100	120	0.05	0.098	120.2±0.6
125	50	0.025	0.098	N/A
125	85	0.05	0	211.5±5.4
125	120	0	0.049	197.2±9.1
75	50	0.05	0.049	175.5±7.5
75	85	0	0.098	90.2±5.4
75	120	0.025	0	231.8±16.0

N/A: film was not formed under this condition.

6.3.1 Structural properties

Fig. 6.1 shows the FT-IR spectra of pure cassava starch film (Fig. 6.1a), chitosan-cassava starch film (Fig. 6.1b) and carvacrol incorporated to chitosan-cassava starch films (Fig. 6.1c-f). For all bioactive films, the broad band at 3600-3100 cm^{-1} can be attributed to O-H stretching. The bands at 2922 cm^{-1} and 1073 cm^{-1} corresponded to the C-H and C-O stretching vibrations, respectively (Pelissari et al., 2009). Compared with pure cassava starch film (Fig. 6.1a), the -OH band of starch (3290 cm^{-1}) shifted to a higher wavenumber (3324 cm^{-1}) when chitosan was added, indicating the formation of intermolecular hydrogen bonds of starch with chitosan (Dang & Yoksan, 2015). Other characteristic peaks of chitosan were difficult to identify due to the relatively small amount of chitosan used (0.025 g/g starch) and the overlap of N-H stretching in the same region of O-H stretching at 3600-3100 cm^{-1} (Liu et al., 2013).

The addition of carvacrol essential oil resulted in the appearance of new bands. The band observed at 1600 cm^{-1} can be attributed to the aromatic ring insaturations in the carvacrol molecule (Arrieta, Peltzer, del Carmen Garrigós & Jiménez, 2013), which became more evident

with the increasing of carvacrol content in the bioactive film. Moreover, the band at 1223 cm^{-1} with an increased intensity compared to the control (Fig. 6.1a-b) indicated the aromatic hydroxyl groups of carvacrol (Fig. 6.1c-f). Similarly, the benzene ring insaturations at bands between 1600 and 1400 cm^{-1} and carvacrol hydroxy group at 1223 cm^{-1} were observed in oregano essential oil (0.1-1.0%) incorporated cassava starch-chitosan films (0.065 g chitosan/g starch) (Pelissari et al., 2009). Furthermore, a new peak (1730 cm^{-1}) was found with the addition of carvacrol essential oil into chitosan-cassava starch films (Fig. 6.1c-f), which was attributed to the formation of the ester linkages. Pelissari et al. (2009) stated that oregano essential oil may act as a catalyst to oxidise hydroxyl radicals of the starch, chitosan, or glycerol, promoting the formation of carbonyl groups during the extrusion process when producing cassava starch-chitosan films incorporated with oregano essential oil. Similar finding was reported in chitosan films with carvacrol (9.6-90.0 ppm), where carbonyl groups were found at 1740 cm^{-1} (Rubilar et al., 2013), facilitating ester linkages formation with hydroxyl groups of carvacrol (Fig. 6.1c-f). Therefore, FT-IR spectra provided an indication of the effective incorporation of carvacrol to the starch/chitosan matrix.

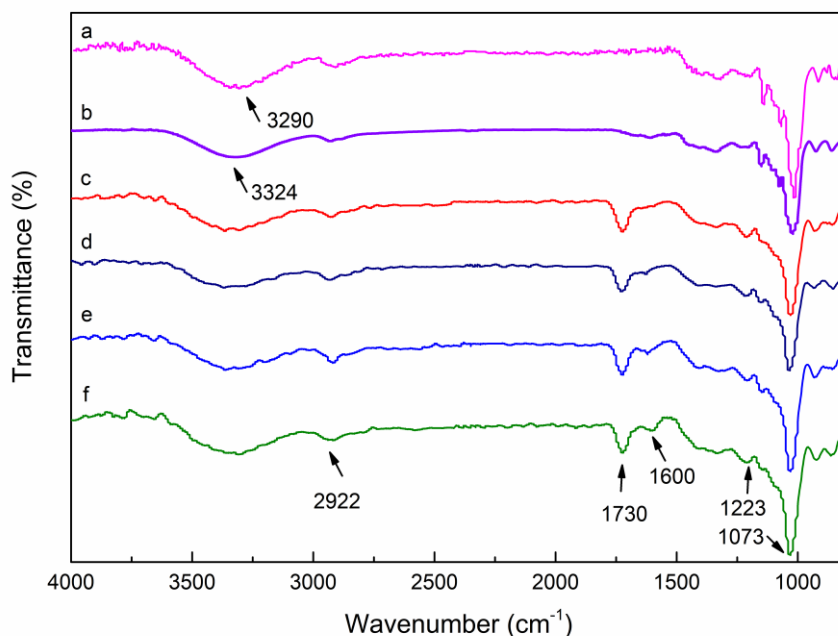


Fig. 6.1 FT-IR spectra of: a) pure cassava starch film, and bioactive films produced at a constant chitosan/starch ratio of 0.025g/g, glycerol/starch ratio of 0.5 g/g, and different carvacrol/starch ratios: b) 0 g/g, c) 0.049 g/g, d) 0.098 g/g, e) 0.147 g/g, and f) 0.195 g/g produced at 75 °C and 120 bar.

Fig. 6.2 shows the XRD patterns of native cassava starch (Fig. 6.2a), chitosan-cassava starch film and carvacrol essential oil incorporated at different concentrations to chitosan-cassava starch films (Fig. 6.2b-f). The native cassava starch (Fig. 6.2a) showed typical behavior of tuber starch with B type crystal structure at diffraction peaks of $2\theta=17^\circ$ and 22° . For bioactive films (Fig. 6.2c-f), the crystalline structure of starch changed compared to chitosan-cassava starch film (Fig. 6.2b). The peaks at 13° and 20.1° can be attributed to the single helical crystal structure of V-type formed by amylose-glycerol complexes (Tiwari, Imam, Rao & Ahmed, 2012). The cassava starch retrogradation phenomenon during storage was also observed by Jaramillo et al. (2016) in yerba mate extract added to cassava starch edible films with a diffraction peak around at 20° . The addition of carvacrol to films may increase the macromolecular mobility,

allowing formation of microcrystalline junction of starch and essential oil, leading to recrystallization. The film without carvacrol (Fig. 6.2b) had a decreased crystallinity of 6.20% compared to native cassava starch (24.38%) as the pressurized hot water treatment promoted starch gelatinization, causing disruption of the double helix conformations of cassava starch. However, XRD patterns of the films containing different amounts of carvacrol essential oil (Fig. 6.2c-f) are different to the film without essential oil (Fig. 6.2b), with increased intensity and film crystallinity from 10.16% to 19.78% due to the essential oil addition into the film matrix. Similarly, Hosseini, Rezaei, Zandi & Farahmandghavi (2016) reported that oregano essential oil increased gelatin/chitosan nanoparticles composite film crystallinity as indicated by the increased peak intensity at 2θ around 26° .

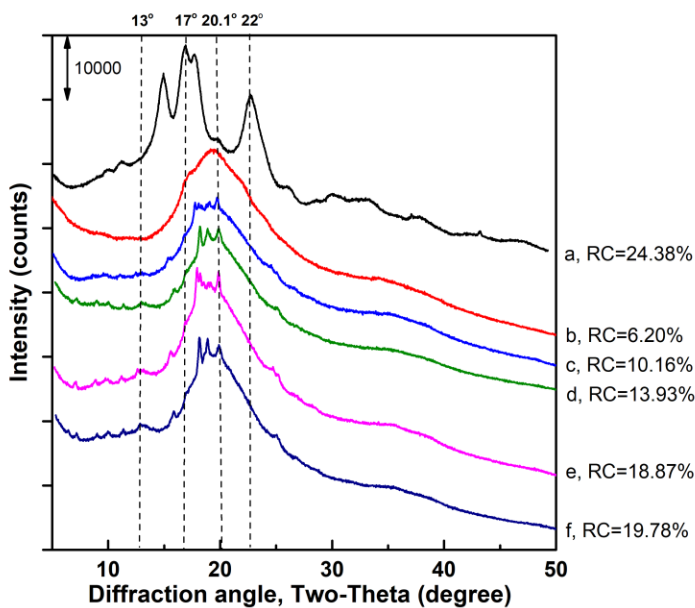


Fig. 6.2 XRD patterns and relative crystallinity (RC) of: a) native cassava starch, and bioactive films produced at a constant chitosan/starch ratio of 0.025g/g , glycerol/starch ratio of 0.5 g/g and different carvacrol/starch ratios: b) 0 g/g, c) 0.049 g/g, d) 0.098 g/g, e) 0.147 g/g, and f) 0.195 g/g produced at 75°C and 120 bar.

6.3.2 Mechanical properties

Fig. 6.3 shows mechanical properties of chitosan-cassava starch films with(out) carvacrol essential oil. In general, the addition of carvacrol essential oil to bioactive films reduced the film stretchability and stiffness. A significant reduction in tensile strength from 0.46 to 0.19 MPa was observed when increasing essential oil concentration from 0.098 to 0.195 g/g starch, while the elongation decreased from 231.8% to 56.5% at carvacrol essential oil concentrations of 0.098 g/g starch. The discontinuities introduced in the film matrix by oil droplets can contribute to the loss of film cohesion and mechanical resistance. Previous studies described different effects when essential oils were added into films (Moradi et al., 2012; Souza et al., 2013). Souza et al. (2013) reported that the addition of cinnamon essential oil (0.08-0.16 g/g starch) into cassava starch film lowered the tensile strength from 2.32 to 1.05 MPa and the elongation from 256.1% to 191.3%, respectively. In another study by Moradi et al. (2012), significant reduction in tensile strength from 24 to 3 MPa and elongation from 29% to 10% of chitosan films were also reported with the addition of *Zataria multiflora* Boiss essential oil at 0.5 g/g chitosan. The authors attributed this result to an increase in pore size of the films, which created possible rupture points. In a recent study, cassava starch-chitosan bilayer films (starch:chitosan=3:1 w/w) containing oregano essential oil (0.25 g/g chitosan) exhibited lower tensile strength of 17 MPa than films without essential oil (20 MPa) (Valencia-Sullca et al., 2018b). And, a much lower elongation of 1.9% was obtain compared with films produced in our study (Fig. 6.3). Carvacrol essential oil could act as a plasticizer, increasing chain mobility by weakening intermolecular interactions. Similarly, Li, Ye, Lei & Zhao (2018a) reported the decrease of film mechanical strength from 5.2 to 2.6 MPa due to the discontinuity caused by oregano essential oil addition (0.18-0.55 mL/g

starch) in the sweet potato film structure, resulting in weaker molecular interactions in the film matrix due to the plasticizing effect of essential oil.

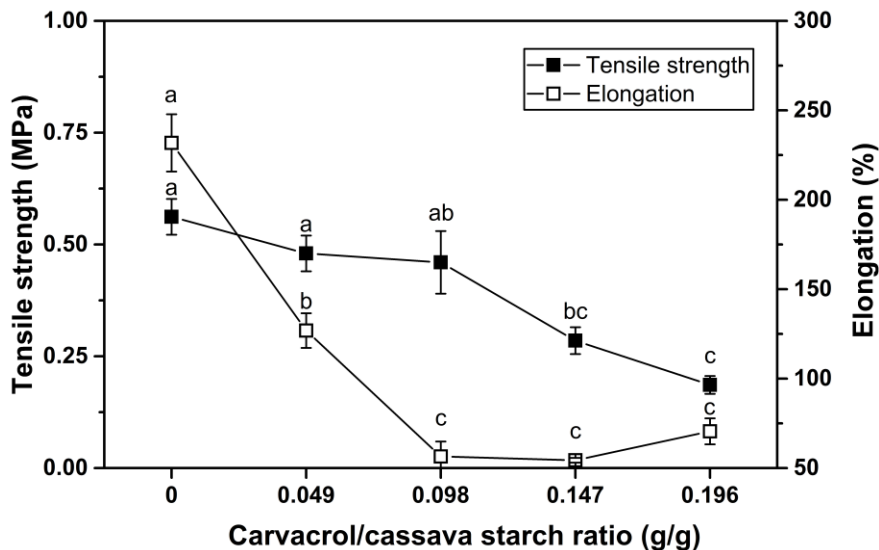


Fig. 6.3 Mechanical properties of bioactive starch films produced at different carvacrol/starch ratios of 0-0.195 g/g, constant chitosan/starch ratio of 0.025 g/g and glycerol/starch ratio of 0.5 g/g produced at 75 °C and 120 bar.

6.3.3 Physico-chemical properties

Table 6.3 shows the effects of incorporating carvacrol essential oil on the physico-chemical properties of chitosan-cassava starch films (Table D.2, appendix D). The film prepared with 0.098 g carvacrol/g starch showed the lowest moisture content, water activity and water vapor permeability. Several studies have shown reduced water vapor permeability values in film after incorporating essential oils. Acosta et al. (2016) reported a significant water vapor permeability decrease to 4.2 g.mm/kPa m² h for cinnamon essential oil (0.25 g/g mixed starch+gelatin) added cassava starch-gelatin film compared with the film without essential oil. Oregano essential oil addition (0.18-0.55 mL/g starch) to sweet potato film lowered the water vapor permeability values from 0.76 to 0.24 g.mm/kPa.m².h (Li et al., 2018a). This reduction of

water vapor permeability may be due to: 1) the hydrophobic nature of essential oil that provided hydrophobicity to the film matrix and hence impeded the water adsorption; 2) formation of ester-linkages between carvacrol essential oil and starch that resulted in lower starch-water interactions, leading to the lower water retention and uptake of the films; 3) the scattered essential oil droplets blocked the continuous water diffusion tunnels in the film matrix, thereby decreasing water vapor permeability (Acosta et al., 2016); and 4) the presence of essential oil on the film surface delayed the wetting process of the film as demonstrated by the increased contact angle (Table 6.3). However, increasing carvacrol essential oil content above 0.098 g/g starch into chitosan-cassava starch films significantly increased moisture content from 8.48 to 13.75% and water activity from 0.2185 to 0.2793 (Table 6.3). As reported by Jouki, Mortazavi, Yazdi & Koocheki (2014a), essential oil addition can improve film solubility or water adsorption capacity on quince seed mucilage film with 2% thyme essential oil. The film showed a loose sponge-like structure with micro-pores distributed throughout the film matrix, leading to the reduced interactions of polymer chain in the network, making the water adsorption and film solubilization easier. The process of water vapor transfer in films depends on the hydrophilic-hydrophobic balance of the film matrix and the final film microstructure. In the study of Maizura, Fazilah, Norziah & Karim (2007), the addition of lemongrass oil (0.1-0.4 v/w %) into saga starch-alginate film caused an increase of water vapor permeability due to the greater flexibility in the polymeric structure that contributed to the increased water absorption in the film. In addition, Souza et al. (2013) observed that water vapor permeability values increased in films of cassava starch added with cinnamon essential oil (0.4-0.8 g/g starch), which values are similar to the water vapor permeability values (0.41-0.62 g.mm/kPa.m².h) obtained in our study (Table 6.3). This increase in water vapor permeability could be attributed to the porous microstructure caused by the

exudation of excess carvacrol essential oil. Moreover, the increased crystallinity in the film matrix (Fig. 6.2c-f) could promote ruptures in the amorphous zones, leading to the formation of channels where water molecules can diffuse easily (Jiménez et al., 2012c).

With regard to the film surface contact angle, increasing carvacrol essential oil concentration caused a significant increase of contact angle values from 67.14° (no carvacrol) to 98.12° (0.195 g carvacrol/g starch), due to the hydrophobic nature of the added essential oil as well as the loss of hydroxyl groups for cross-linking. Also, there was no significant difference in the measurements of contact angle for the bottom surface, however, the top surface showed an improved hydrophobicity, possibly due to the migration of essential oil from the bottom to the top interface, which was favored by the density difference of the two phases. Similar results were reported when olive oil (15%) was added to the chitosan film, where lower (<10%) concentrations had little effect on the film top surface contact angle (Pereda, Amica & Marcovich, 2012). Thus, adding hydrophobic agents like essential oil can increase the surface hydrophobicity, leading to an increase of contact angle of films. Moradi et al. (2012) reported an increase of contact angle from 53° to 64° and 69° for chitosan films with 0.25 and 0.5 g *Zataria multiflora* Boiss essential oil /g chitosan, respectively. Lower contact angle values of 49-53° were obtained in the cassava starch film added with rosemary extracts (0.026-0.104 mg/g starch) compared to our study (Table 6.3) (Piñeros-Hernandez et al., 2017).

Table 6.3 also shows that chitosan-cassava starch films incorporated with the least carvacrol content had the lowest film solubility in water at all temperatures studied. This result could be ascribed to a decrease in the film hydrophilicity with the addition of hydrophobic essential oil. Moreover, the interactions between essential oil and the hydroxyl groups of starch reduced availability of hydroxyl groups for interaction with water molecules, consequently

resulting in a more water-resistant film. However, higher carvacrol concentrations (>0.047 g/g starch) led to an increase of film solubility in water. This behavior has also been reported in other starch-based films. Carvacrol at concentrations of 100 mg/g starch significantly increased tapioca starch film solubility from 35 to 45% at 25 °C (Homayouni et al., 2017). The authors attributed this behavior to the coarseness of the films caused by carvacrol that weaken the interactions, stabilizing the starch network. With respect to the influence of temperature, the increase in film solubility with increasing temperature from 4 to 50 °C was due to the enhanced starch and chitosan movements and increased energy levels of the water to permeate film.

Table 6.3 Physico-chemical properties of carvacrol incorporated chitosan-cassava starch films produced at 75 °C and 120 bar.

Carvacrol/starch ratio (g/g)	Moisture content (%)	Water activity	WVP (g.mm/kPa.m ² .h)	Contact angle (°)		Film solubility in water (%)		
				Top	Bottom	4 °C	25 °C	50 °C
0	14.24±0.15 ^a	0.2929±0.0122 ^{ab}	0.62±0.03 ^b	67.14±2.43 ^d	95.13±2.42 ^{ab}	29.34±2.54 ^{bc}	36.37±2.63 ^c	32.88±2.73 ^b
0.049	14.07±0.36 ^a	0.3049±0.0028 ^a	0.62±0.10 ^b	75.16±1.60 ^c	84.49±2.87 ^b	22.61±2.66 ^c	31.51±2.52 ^c	42.28±2.02 ^b
0.098	8.48±0.58 ^b	0.2185±0.0018 ^c	0.40±0.04 ^c	74.36±3.17 ^c	96.32±1.13 ^a	35.43±3.42 ^{bc}	40.43±3.65 ^{bc}	46.05±2.60 ^b
0.147	12.98±0.61 ^a	0.2907±0.0052 ^{ab}	0.75±0.03 ^b	86.54±0.91 ^b	91.14±1.39 ^{ab}	37.89±4.41 ^b	52.89±2.66 ^{ab}	61.76±5.51 ^a
0.195	13.75±0.04 ^a	0.2793±0.0021 ^b	0.95±0.09 ^a	98.12±2.61 ^a	97.64±0.90 ^a	53.57±3.25 ^a	61.07±3.96 ^a	68.00±4.86 ^a

Bioactive starch films produced at different carvacrol/starch ratios of 0-0.195 g/g, constant chitosan/starch ratio of 0.025 g/g and glycerol/starch ratio of 0.5 g/g at 75 °C and 120 bar.

WVP: water vapor permeability. Data shown as mean±standard deviation (n = 3).

^{a-d}Different lowercase letters in the same column indicate significant differences (p < 0.05).

6.3.4 Optical properties

Table 6.4 shows the color performance, transparency and gloss values of carvacrol incorporated to chitosan-cassava starch films. No significant differences were observed among YI values of films studied. The only difference between films with or without carvacrol essential oil was observed based on ΔE values. For film whiteness, films with the highest essential oil content showed significant less white compared to the control. This result is consistent with findings of Mehdizadeh, Tajik, Razavi Rohani & Oromiehie (2012), where emulsified starch-chitosan composite films became less white with the incorporation of essential oils. In another study, when savory essential oil at 0.50% or higher concentration was incorporated, the color tended to yellowish as indicated by the increase of b value. Also, L values decreased and color of the film tended to darken (Atef, Rezaei & Behrooz, 2015). The transparency of the bioactive films significantly decreased with the increase of carvacrol content, as indicated by the increased transparency value from 1.58 to 5.06 (Table 6.4). This effect is probably due to the increase in diffuse reflectance provoked by light scattering in the oil droplets, which lowers both the light scattering intensity and the film whiteness index (Jiménez et al., 2012c). Earlier, an increase in lemon essential oil concentration from 0.5 to 2 v/v% also significantly reduced the transparency of corn and wheat starch films, providing more opaque films (Song et al., 2018). Chen & Liu (2016) reported that the transparency of the cellulose sulfate films significantly decreased from 66.9% to 50.2% with the increase of mustard essential oil content from 0.4 to 1.2 v/v%.

The incorporation of carvacrol essential oil greatly reduced the gloss of both film top and bottom surfaces due to the rearrangement of the chains near the surface, where essential oils produced structural irregularities at the surface level of the films, which directly reduced film gloss. Acosta et al. (2016) attributed this gloss reduction to oil creaming during the drying period,

where the oil exuded to the surface of the dried film. This can further explain why the bottom surface showed higher gloss values (7.20-80.55) than the top surface (6.20-16.70). As known, the essential oil has low density, so it exuded to the top film surface. Similarly, the less smooth film surfaces were also observed by Bof, Jiménez, Locaso, Garcia & Chiralt (2016) in lemon essential oil (1-3 wt%) incorporated corn starch-chitosan (75:25 w/w) blend films.

Table 6.4 Optical properties of carvacrol incorporated chitosan-cassava starch films produced at 75 °C and 120 bar.

Carvacrol/starch ratio (g/g)	Color performance			Transparency	Gloss (GU)	
	ΔE	YI	WI		Top	Bottom
0	3.11±0.15 ^b	3.96±0.64 ^a	97.18±0.40 ^a	1.58±0.21 ^c	16.70±0.14 ^a	80.55±0.35 ^a
0.049	4.94±0.14 ^a	4.21±0.07 ^a	96.66±0.14 ^{ab}	3.93±0.15 ^b	9.70±0.14 ^b	53.30±0.14 ^b
0.098	4.58±0.24 ^a	4.23±0.04 ^a	95.82±0.22 ^{bc}	3.97±0.07 ^b	9.30±0.14 ^b	21.45±0.07 ^c
0.147	5.08±0.19 ^a	3.97±0.12 ^a	96.38±0.22 ^{abc}	4.54±0.18 ^{ab}	5.95±0.21 ^c	7.45±0.07 ^d
0.195	4.52±0.04 ^a	4.50±0.26 ^a	95.62±0.21 ^c	5.06±0.12 ^a	6.20±0.14 ^c	7.20±0.14 ^d

Bioactive starch films produced at different carvacrol/starch ratios of 0-0.195 g/g, constant chitosan/starch ratio of 0.025 g/g and glycerol/starch ratio of 0.5 g/g at 75 °C and 120 bar.

ΔE : total color difference, YI: yellowness index, WI: whiteness index, GU: gloss unit.

Data shown as mean±standard deviation ($n = 3$).

^{a-d}Different lowercase letters in the same column indicate significant differences ($p < 0.05$).

6.3.5 Functional properties

Fig. 6.4 shows the total phenolic content and total antioxidant activity of carvacrol incorporated chitosan-cassava starch films (Table D.3, appendix D). As expected, total phenolic content of films increased significantly by incorporating carvacrol essential oil. The highest total antioxidant activity value (84.9 mg Trolox equivalent/g film for ABTS and 61.0 mg Trolox equivalent/g film for FRAP) was obtained for the film formulated with 0.195 g carvacrol/g starch, which increased 25 folds more than the control. The chitosan-cassava starch films with no essential oil showed low antioxidant activity by ABTS (3.49 mg Trolox equivalent/g film) and FRAP (1.33 mg Trolox equivalent/g film) methods. This low total antioxidant activity is probably due to the reaction of the free radicals with the free residual amino groups from chitosan that formed ammonium groups (Moradi et al., 2010).

Antioxidant properties have been reported for essential oil incorporated films. In the study by Mehdizadeh et al. (2012), corn starch-chitosan film incorporated with 0.5 and 1% thyme essential oil exhibited around ~17 and ~35% DPPH scavenging activity, respectively, with corresponding ~7 and ~10.5 mg gallic acid/g film. In another study, the DPPH scavenging activity of 45% was observed in quince seed mucilage films with 1% of oregano essential oil (Jouki, Yazdi, Mortazavi & Koocheki, 2014b). Moreover, the addition of 0.1 g thyme essential oil/g starch to wheat starch-chitosan films provided 9.4 mg TEAC value (amount of sample that produced the same absorbance reduction as 1 mM Trolox solution) of antioxidant activity (Bonilla et al., 2013). Jouki et al. (2014b) also reported that at all thyme essential oil concentrations added to the quince seed mucilage films, there was a linear correlation between total phenolic content and antioxidant activity.

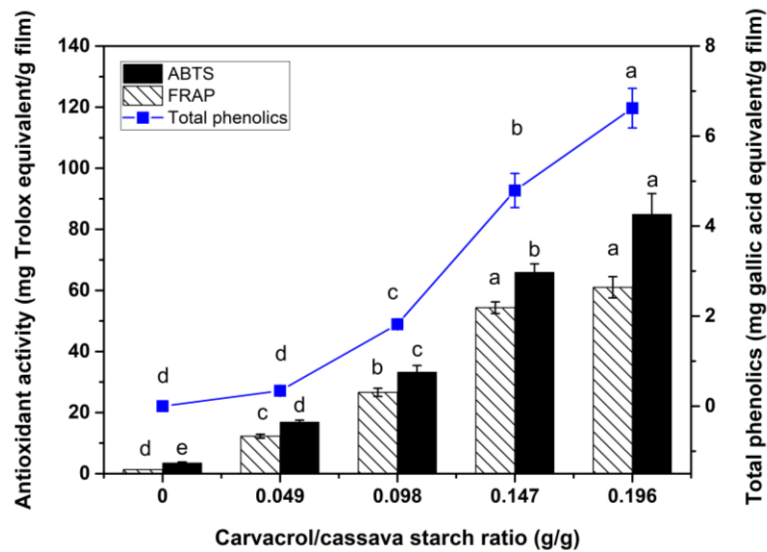


Fig. 6.4 Total phenolic content, total antioxidant activity (ABTS and FRAP methods) of bioactive starch films with different carvacrol/starch ratios of 0-0.195 g/g, constant chitosan/starch ratio of 0.025 g/g and glycerol/starch ratio of 0.5 g/g produced at 75 °C and 120 bar.

6.3.6 Biodegradability test

The weight loss during degradation of bioactive starch-based films in compost is shown in Fig 6.5 (Table D.4, appendix D). In general, the use of potato peel and cull led to the longest degradation times (>85 days, Fig. 6.5a) in compost compared to films produced with potato cull/gallic acid (Fig. 6.5b), cassava starch/gallic acid/chitosan (Fig. 6.5c) and cassava starch/chitosan/essential oil (Fig. 6.5d), with a total weight loss of more than 90% after 45 days. The highest percentage of weight loss (99.1%) was observed for potato cull film with no potato peel added, followed by 95.6%, 93.3% and 93.1% for films loaded with 0.5, 1 and 1.3g peel/g cull, respectively. The high content of fiber in potato peel not only improves the film tensile strength, but also enhances film resistance to degradation (Fig. 6.5a). As reported, potato peel

has around 30-61% cellulose, 13% hemicelluloses, 8-16% lignin and 10% ash on a dry basis (Lenihan et al., 2010; Rommi et al., 2016), while potato cull has less than 3% fibre and 82% starch with other components such as 8% protein, 6.5% ash and 0.5% lipids on a dry basis (Lisinska & Leszczynski, 1989). Palma-Rodríguez et al. (2016) reported less degradation (70%) of corn starch/wood fiber (45.4:8.8 w/w) foams in 42 days than native corn starch (100%) due to the presence of wood fiber.

All films investigated in our study displayed a similar degradation behavior that can be represented in three stages. In the first stage, samples achieved a weight loss of 9.4-12.2% in the first 5 days, possibly due to the leaching of glycerol. This behavior was only observed in films with 0 or 0.5g potato peel/g cull added. The glycerol leaching behavior was also reported by Torres et al. (2011), who observed 30% weight loss of pure cassava starch film and pure sweet potato starch film in a first degradation stage of 24 h. In the second stage, the weight loss of bioactive films increased steadily, until the majority (65.9-84.5%) of film decomposed at 35 days. During this stage, film degradation was mainly attributed to microbial attack to highly disordered and accessible starch chains at the film surface. In previous studies (Urbanek et al., 2017; Maran et al., 2014; Gattin et al., 2002), several microorganisms have been identified to degrade starch films. For example, *Clonostachys rosea* showed 100% degradation of corn and potato starch films and 52.91% degradation of poly(ϵ -caprolactone) films in 30 days (Urbanek et al., 2017). Other predominant microorganisms identified in the degraded cassava starch films were *Pseudomonas* sp., *Streptococcus* sp., *Bacillus* sp. and *Moraxella* sp. (Maran et al., 2014). Other two fungal strains that degraded starch were *Aspergillus fumigatus* and *Agrobacterium radiobacter*, which were isolated from a 2-month-old mature compost made of municipal waste (Gattin et al., 2002). But, Du et al. (2008) found that it is difficult for bacteria to degrade corn

starch in the initial stage, so fungi and actinomycete were mainly evaluated. The actinomycete isolated in their study were identified as micromonospora, nocardia and treptomycete. Moreover, the actinomycete degrading ability was found to closely relate with the degree of modification and hydrophobic property of starch. The higher the degree of oxidation and cross-linking in starch, the less its susceptibility to microorganisms attack. In the third stage (>35 days until the end of the degradation test), the rate of degradation is slow, until the last remaining films was consumed (Gattin et al., 2002).

Compared with the potato peel/cull film, potato cull/gallic acid films had a shorter degradation time up to 65 days with more than 93% weight loss (Fig. 6.5b). Gallic acid behaved as a cross-linker at concentrations < 0.2 g/g starch, whereas an excess of gallic acid caused the anti-plasticizer effect, leading to the deterioration of film properties (e.g. decrease of tensile strength, increase of moisture absorption and water vapor permeability). This behavior explains the reason why films with 0.3 g gallic acid/g cull starch showed the fastest degradation as free gallic acid dissolved due to water absorption, creating porous film structure that is less resistant to microorganisms attack. Four degradation stages were observed: 1) leaching of glycerol or gallic acid within the first 5 days; 2) a lag phase between 5-15 days for microorganisms to adapt to the environment as a result of possible decreasing pH caused by gallic acid dissolution; 3) films were degraded steadily from 15 to 35 days, and 4) the declined degradation up to 65 days (Fig. 6.5b). The lag phase between the time that microorganisms were introduced and the detectable microbial degradation began was reported by Foulk and Bunn (2007) on acclimated microorganisms collected from a local lake and soil environment, showing a growth lag ranging from 9.3h (30 °C) to 90h (16 °C) of acetylated soy protein film.

Fig. 6.5c and d shows the weight loss of cassava starch/gallic acid/chitosan films and cassava starch/chitosan/carvacrol essential oil films in compost burial during 45 days. All cassava starch-based films showed a complete biodegradation within a shorter time (45 days) compared to potato cull films (Fig. 6.5a and b >65 days). These findings might be attributed to the hydrophilicity of cassava starch compared to potato fiber, which increased the hygroscopic characteristics of the films and promoted the growth of microorganisms during degradation, increasing the film weight loss (Maran et al., 2014). A lag phase within the initial 5 days of the cassava starch/gallic acid/chitosan films and cassava starch/chitosan/carvacrol essential oil films can be observed due to the presence of antimicrobials (gallic acid, chitosan or carvacrol essential oil), inhibiting the microorganisms action. In addition, microorganisms must have the appropriate conditions of temperature, moisture, pH, and oxygen availability to grow and produce enzymes that are mainly responsible for the biodegradation (Fouk and Bunn, 2007). The rapid degradation occurred earlier (5-20 days) in both cassava starch-based films than potato by-product films (15-35 days). Degradation of cassava starch films in the soil (unspecified composition) indicated that starch acted as an energy source for microorganism growth, and its higher water sorption promoted the activity of the soil microorganism (Maran et al., 2014). Danjiaji et al. (2002) observed holes on the sago starch/linear low density polyethylene (15:100, w/w) blend film surface after 3 months and a significant degradation after 12 months due to microbial activity. Xiong et al. (2008) reported that 70% weight loss of corn starch/polyvinyl alcohol (5:1, w/w) films occurred in 100 days. Torres et al. (2011) reported a total weight loss of 99.35% for cassava starch films after 30 days. Moreover, starch modification can influence the film biodegradability due to different interactions like acetylation. The films made with acetylated rice starch showed a higher rate of CO₂ release, consequently a higher percentage of

degradation compared to native rice starch films. The fast biodegradability of acetylated rice starch films with a degree of substitution of 0.24-0.81 can be attributed to the insertion of acetyl groups that reduced inter- and intramolecular hydrogen bonds, allowing the absorption of water and facilitating the action of soil microorganisms (Colussi et al., 2017).

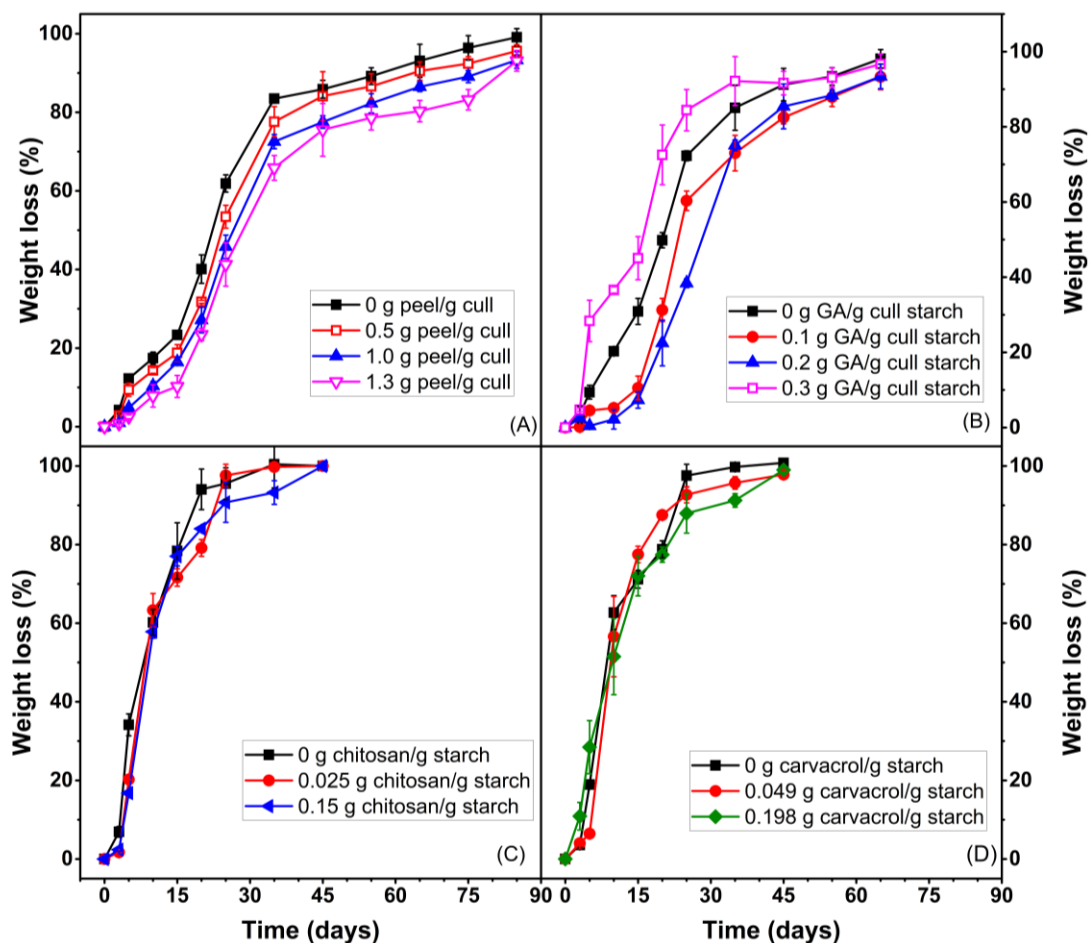


Fig. 6.5 Weight loss curves of: a) potato peel/cull films, b) potato cull/gallic acid films, c) cassava starch/gallic acid/chitosan films, and d) cassava starch/chitosan/carvacrol films during biodegradation in compost as a function of time.

6.4. Conclusions

This study suggests that carvacrol essential oil incorporated to chitosan-cassava starch films produced by pressurized hot water technology showed potential to be used as active films.

Mechanical, structural, optical, physico-chemical and antioxidant activity of chitosan-cassava starch films were influenced by the addition of carvacrol essential oil. The pressurized hot water media acted as a catalyst, promoting chemical reactions by enhancing cross-linkings through ester linkages of carvacrol essential oil and starch. An increase in essential oil content resulted in significantly lower tensile strength and elongation at break. Incorporation of carvacrol at a low concentration improved the moisture barrier properties of the film and film solubility in water, while high concentrations produced coarser structure of the film matrix, resulting in higher water vapor permeability values, moisture content, water activity and film solubility in water. Although films became opaquer with the addition of carvacrol essential oil, the total color difference was not significant, indicating little influence on the film color performance. The total phenolic content and total antioxidant activity of films improved dramatically. Also, the antioxidant activity data can serve as a guide for selection of film applications. Incorporating essential oils into starch films provides a novel way to enhance the safety and shelf-life in food systems. Carvacrol, a strong antimicrobial agent, can be an important barrier against microbial contamination in the food industry.

The biodegradation times for the potato peel/cull films, potato cull/gallic acid films, cassava starch/gallic acid/chitosan films and cassava starch/chitosan/carvacrol films were 85, 65, 45 and 45 days, respectively. Potato cull-based films showed less weight loss (93.1-99.1%) compared to the 100% degradation of cassava starch-based films, due to the fibre content of potato peel (~90%) and cull (~3%). The potato cull/gallic acid film with 0.3 g gallic acid/g cull starch showed higher weight loss (45.0-92.2%) than those of films with 0.1 or 0.2 gallic acid/g cull starch (7.3-75.1%) at fast degradation stage of 15-35 days, due to the dissolution of excess gallic acid that created a porous film structure which is less resistant to microorganism attack.

For cassava starch-based films, the high starch hydrophilicity facilitated water uptake after burial in compost that promoted the entrance of microorganisms, exhibiting high weight loss (~100%) in short times (45 days). However, no significant influence of chitosan or carvacrol contents on cassava starch-based film biodegradability was observed due to the low antimicrobial loading (≤ 15 wt% of starch). Overall, all bioactive starch-based films prepared are considered biodegradable and can be used in biodegradable food packaging applications.

Chapter 7: Use of Pressurized Hot Water Technology to Develop Cassava Starch/Chitosan Bioactive Films Reinforced with Cellulose Nanofibers From Canola Straw*

7.1 Introduction

There has been considerable attention on the development of biodegradable films using starch due to its biodegradability, abundance, and low cost. Several studies reported the use of starches from different sources to prepare films and coatings with different properties (Davoodi et al., 2017; Luchese et al., 2018). Nevertheless, starch films exhibit various challenges, such as strong hydrophilic character and poor mechanical properties, limiting their applications in food packaging (Adnan & Arshad, 2017). To overcome these challenges, starch has been blended with synthetic polymers, such as polyethylene (45-75 wt%) (Nguyen et al., 2016), poly(ϵ -caprolactone) (20-80 wt%) (Ortega-Toro et al., 2015) and polypropylene (5-20 wt%) (Roy, Ramaraj, Shit & Nayak, 2011). However, starch is immiscible with most of these synthetic polymers at the molecular level, requiring the use of cross-linkers, e.g. maleic anhydride. Also, the biodegradability of the starch film is compromised due to the addition of synthetic polymers.

In this respect, chitosan biopolymer was used as a filler for starch-based films. Chitosan had a good miscibility with starch (starch:chitosan, 2:1-0.5:1 w/w) as reported by a shift of the amino group of chitosan to 1621.96 cm^{-1} in rice starch/chitosan blend films (2008). Recently, Zhao et al. (2018) reported a reduction of water vapor permeability from 0.67 to $0.36\text{ g mm/m}^2\text{ h KPa}$ when 15 wt% of chitosan was incorporated into cassava starch films. In addition, film solubility in water decreased at all temperatures investigated (4-50 °C) with the addition of chitosan (Zhao et al., 2018). However, the poor mechanical strength of starch-based films filled with chitosan still remain a challenge. To improve mechanical strength of starch-based films, researchers used

* A version of this chapter has been submitted to the Journal of Supercritical Fluids as “Zhao, Y., Huerta R. R., Saldaña, M.D.A. (2019). Use of Subcritical Water Technology to Develop Cassava Starch/Chitosan Bioactive Films Reinforced with Cellulose Nanofibers From Canola Straw. 177

natural fibers like cellulose, as a reinforcement for thermoplastic starch (Hietala, Mathew & Oksman, 2013; Li et al., 2018b). Cellulose is often found in the form of long straight fibrils with nano-sized diameter, and a length of more than a few micrometers aligned as amorphous or crystalline regions (Morán, Alvarez, Cyras & Vázquez, 2008). In nature, cellulose fibrils are enclosed with hemicellulose and lignin. Hemicellulose with a highly branched random structure consists of saccharides, such as xylose, mannose, arabinose and glucose, while lignins are cross-linked phenolic polymers composed of phenyl-propane units (Morán et al., 2008). Various methods have been used to obtain cellulose fibers from wood and other plant sources, which involve treatments with alkali or acid to remove lignin and hemicellulose (Alemdar & Sain, 2008; Saïd Azizi Samir, Alloin, Paillet & Dufresne, 2004). To minimize the impact of alkali or acid pollution in the environment, pressurized aqueous ethanol was recently used to obtain cellulose from canola and barley straw, with 45% and 54% lignin removal at 180 °C/50 bar using 20% ethanol, respectively (Huerta & Saldaña, 2018b). However, cellulose is insoluble in water, compromising its applications as fillers to biocomposites. Therefore, to expand cellulose use the production of nanosized cellulose is required, which means that at least one dimension is in nanoscale (1–100 nm). Cellulose nanofibers (CNFs) have gained attraction due to their unique characteristics such as high surface to volume ratio, high surface area and high tensile strength (Takagi & Asano, 2007). Several mechanical approaches such as high pressure homogenization, grinding, cryocrushing and high intensity ultrasonication have been used to disintegrate cellulose fibers into CNFs. Chen et al. (2011) used a combination of ultrasonication and chemical pre-treatment (alkali and acid hydrolysis) to obtain CNFs (5-20 nm in width and several micrometers in length) from poplar wood using >1000 W for 30 min. In another study, CNFs (73-89 nm in diameter) from banana peel after eliminating non-cellulosic compounds were obtained using

ultrasound at 200 W for 1 h (Harini, Ramya & Sukumar, 2018b). The ultrasonic impact can gradually disintegrate the micron-sized cellulose fibers into nanofibers by cavitation (Tischer, Sierakowski, Westfahl Jr, & Tischer, 2010). The addition of CNFs to starch-based films has been proved to improve film mechanical strength (Hietala et al., 2013; Li et al., 2018b). An increment of tensile strength from 8.8 to 17.5 MPa was observed when 20 wt% CNFs was added to the potato starch film. Also, the moisture diffusion coefficient slightly decreased from 1.66×10^{-9} to 1.27×10^{-9} cm²/s (Hietala et al., 2013). Similarly, Li et al. (2018b) reported that CNFs improved the tensile strength of corn starch film from 21.09 to 28.87 MPa at 15 wt% CNFs. However, the incorporation of 20 wt% CNFs in the composite film produced selective aggregation and non-homogeneous films. Despite these promising and attractive properties of nano-sized cellulose fillers, the use of pressurized hot water technology to produce bioactive starch films with CNFs has yet to be explored. Therefore, the main goal of this study was to produce cassava starch/chitosan films reinforced with CNFs obtained from canola straw via pressurized fluid technology combined with ultrasonication. The films produced using pressurized hot water technology were evaluated for structural, optical, mechanical, physico-chemical and functional properties.

7.2 Materials and methods

7.2.1 Materials

Cassava starch was provided by CbPAK Tecnologia (Rio de Janeiro, Brazil). Canola straw was provided by Dr. Barry Irving (University of Alberta, Edmonton, AB, Canada). Chitosan (75-85% deacetylated, with molecular weight of 190-310 kDa) was purchased from Sigma Aldrich (St. Louis, MO, USA).

Chemicals, including glycerol (>95% purity, certified ACS grade), sodium acetate trihydrate (99%), glacial acetic acid (99.7%), hydrochloric acid (37%, ACS reagent), gallic acid (97.5-102.5% titration), sulfuric acid (72%, ACS reagent), ferric chloride hexahydrate (97%, ACS reagent), 2,2'-azino-bis(3-ethylbenzothiazoline-6-sulphonic acid) diammonium salt (HPLC, $\geq 98\%$), ethanol (>95%), 2,2'-azinobis (3-ethyl-benzothiazoline-6-sulfonic acid) (ABTS), 6-hydroxy-2,5,7,8-tetramethylchroman-2-carboxylic acid, Folin–Ciocalteu's phenol reagent, calcium chloride (96%, anhydrous), sodium carbonate (anhydrous, $\geq 99.5\%$, ACS reagent), potassium persulfate ($\geq 99\%$, ACS reagent), and 2,4,6-tris(2-pyridyl)-s-triazine ($\geq 98\%$) were purchased from Sigma Aldrich (St. Louis, MO, USA). Purified water from a Milli-Q system (Millipore, Burlington, MA, USA) was used.

7.2.2 Preparation of cellulose nanofibers (CNFs) from canola straw

Canola straw was ground and sieved to <1 mm particle size in a centrifugal mill (Retsch, Haan, Germany). Subcritical fluid treatment of canola straw was performed in a semi-continuous flow type system as described by Huerta & Saldaña (2018b). Briefly, the reaction vessel was loaded with 3 g of canola straw and 27 g of glass beads (2.3 mm diameter) and placed inside the oven. Aqueous ethanol was delivered at 5 mL/min for 40 min under constant pressure. The experiments were conducted at optimized conditions of 180 °C, 50 bar and ethanol concentration of 20% (v/v) based on the highest hemicellulosic sugars removal reported by Huerta & Saldaña (2018b). Then, the pressurized aqueous ethanol (PAE) solid residue was oven-dried at 30 °C, ground and sieved to a particle size of <106 μm . The obtained cellulose nanofibers had 63.1% cellulose, 7.7% hemicellulose and 20.0% of lignin. Then, the aqueous dispersion (0.025, 0.05, 0.075 and 0.1 g cellulose/g starch) was treated with a high intensity ultrasonicator (Model FS-1200N, Shanghai Sonxi Ultrasonic Instrument Co., Shanghai, ZJ, China) equipped with a

cylindrical titanium alloy probe tip of 2 cm in diameter. The ultrasonication treatment was carried out at output power of 1200 W for 30 min, under an ice water bath to prevent heat generation (Huerta & Saldaña, 2018a).

7.2.3 Preparation of bioactive films

Cassava starch (13 g) was mixed with chitosan (0.15 g/g starch), glycerol (0.5 g/g starch), gallic acid (0.1 g/g starch) and CNFs aqueous dispersion (0g, 0.325g, 0.65g, 0.975g or 1.3g in 200 mL, corresponding to 0, 0.025, 0.05, 0.075 and 0.1 g cellulose nanofiber/g starch) in the reactor (270 mL) of the subcritical fluid system (Zhao & Saldaña, 2019) as described earlier in Chapter 4 (Section 4.2.2). Cassava starch added with only glycerol (0.5 g/g starch) and CNFs (0.1 g/g starch) was used as the control. Then, the reactor was filled with Milli-Q water using a HPLC pump. The mixture was homogenized by a double helix stirrer for 5 min followed by the reaction conducted at the desired temperature and pressure for 10 min under stirring. The reacted solution was then cooled to 50 °C and degassed. For each film, 50 g of solution was cast into a plastic petri dish with a diameter of 15 cm, and dried at 40 °C for 48 h in an oven (Model 655G, Fisher Scientific IsoTemp ® oven, Toronto, ON, Canada). Finally, the obtained films were removed and conditioned at 30% RH and 25 °C for at least 48 h until further characterizations. Process parameters evaluated for cellulose nanofibers reinforced cassava starch/chitosan/gallic acid film are shown in Table 7.1.

Table 7.1 Process parameters evaluated for CNFs reinforced cassava starch/chitosan/gallic acid film formation.

	Pressure (bar)	Chitosan/starch ratio (g/g)	Gallic acid/starch ratio (g/g)	Temperature (°C)	CNFs/starch ratio (g/g)
CNFs reinforced film	85	0.15	0.1	75	0
				100	0.025
				125	0.05
					0.075
					0.1
Control	85	0	0	100	0.1

CNFs: cellulose nanofibers, and control: cassava starch film with only 0.5 g glycerol/g starch and 0.1 g CNFs/g starch.

7.2.4 Film characterization

Film structural properties of FT-IR spectra, mechanical properties of tensile strength and percent elongation at break, physico-chemical properties of water activity, moisture content, film solubility in water and water vapor permeability, optical properties of transparency, color, gloss and contact angle, morphology properties by SEM and TEM, functional properties of total phenolic content and antioxidant activity by FRAP and ABTS methods were performed following the methods described in Chapter 4 (Section 4.2.3).

Film samples (~13 mg) were submitted to thermogravimetric analysis on a Thermogravimetric Analyzer (TA instrument Q50, New Castle, DE, USA) under nitrogen atmosphere. Samples were heated at a rate of 10 °C/min from ambient temperature to 600 °C (Hebeish, Farag, Sharaf, & Shaheen, 2014).

7.3. Results and discussion

7.3.1 Mechanical properties

The tensile strength and elongation at break of CNFs reinforced cassava starch films are reported in Table 7.2. There is a considerable increase in the tensile strength of CNFs reinforced

films compared to cassava starch/chitosan/gallic acid film without CNFs at all temperatures investigated. The CNFs reinforced films produced at 100 °C showed higher tensile strength (0.83-10.51 MPa) than films produced at 75 °C (0.51-9.01 MPa) and 125 °C (0.37-5.27 MPa), due to the inadequate starch/chitosan/gallic acid/cellulose interactions at low temperature of 75 °C and starch/chitosan depolymerization at high temperature of 125 °C, which limited the formation of starch-chitosan network in film matrix. A recent study (Zhao & Saldaña, 2018) on cassava starch/chitosan hydrolysis indicated that the highest amylose production (22.4%) was obtained at 100 °C/85 bar. The amylose produced under this condition maintained appropriate chain length that can react with chitosan to form a strong network, which was also confirmed by the increase of molecular weight of starch-chitosan complexes from 331.4 to 1656.0 kDa with the increasing chitosan content from 0 to 0.15 g/g starch (Zhao & Saldaña, 2018). The control cassava starch film with only 0.1 g CNFs/g starch but no gallic acid or chitosan added exhibited lower tensile strength and higher elongation compared to cassava starch/chitosan/gallic acid film with the same CNFs loading, due to the lack of cross-linking (ester and electrostatic interactions). The highest cassava starch/chitosan/gallic acid film tensile strength (10.51 MPa) was achieved at 100 °C and 85 bar using 0.1 g CNFs/g starch due to the uniform distribution of the CNFs in the starch/chitosan matrix, resulting in excellent compatibility between starch, chitosan, gallic acid and CNFs. In addition, cellulose has a more linear three-dimensional structure than starch, thus improving its interactions with starch and chitosan molecules through hydrogen bonds (Teacă, Bodîrlău & Spiridon, 2013). In contrast, the elongation at break decreased from 65.72% to 34.03% due to the addition of CNFs that hindered the plasticizing efficacy of glycerol and decreased the mobility of starch and chitosan chains (Muscat, Adhikari, McKnight, Guo & Adhikari, 2013). A similar behavior was reported with the increase of potato film tensile strength from 8.8 to 16.4

MPa with the addition of 10 wt% softwood CNFs, with a much lower film elongation of 8.8% (2013). Moreover, due to the aggregation that occurred in films with 15 and 20 wt% of CNFs, the tensile strength did not increase above 17.5 MPa. Due to the better mechanical strength of films produced at 100 °C and 85 bar (0.83-10.51 MPa) compared with films produced at 75 °C (0.51-9.01 MPa) and 125 °C (0.37-5.27 MPa), further characterizations were conducted only for films produced at 100 °C and 85 bar.

Table 7.2. Mechanical properties of CNFs reinforced cassava starch/chitosan/gallic acid films.

Temperature (°C)	CNFs/starch ratio (g/g)	Tensile strength (MPa)	Elongation (%)
75	0	0.51±0.06	85.23±5.74
	0.025	5.27±0.00	67.64±4.62
	0.05	7.38±0.11	58.79±2.21
	0.075	8.19±0.09	47.55±4.08
	0.1	9.01±0.16	30.88±2.01
100	0	0.83±0.13	65.72±9.95
	0.025	6.74±0.31	55.18±3.42
	0.05	8.04±0.15	45.88±1.88
	0.075	9.93±1.02	36.24±4.22
	0.1	10.51±0.13	34.03±3.62
	0.1 (Control)	7.35±0.28	40.59±3.03
125	0	0.37±0.03	56.11±2.95
	0.025	3.96±0.29	48.37±3.97
	0.05	3.41±0.34	40.05±1.00
	0.075	4.53±0.41	44.48±1.54
	0.1	5.27±0.40	32.86±2.98

CNFs: cellulose nanofibers, control: cassava starch film with only 0.5 g glycerol/g starch and 0.1 g CNFs/g starch. Bioactive films produced at different temperatures and constant 0.5 g glycerol/g starch, 0.15 g chitosan/g starch, 0.1 g gallic acid/g starch at 85 bar.

7.3.2 Structural properties

Fig. 7.1 shows the FT-IR spectra of canola straw after PAE (20%) treatment (Fig. 7.1a), cassava starch/chitosan/gallic acid film (Fig. 7.1b) and cassava starch/chitosan/gallic acid films reinforced with CNFs (Fig. 7.1c-d). The reaction for film formation was conducted between 75-

125 °C, which was a low temperature range to disintegrate CNFs. Also, the peak at around

896 cm^{-1} in SCW and PAE treated canola straw corresponded to the β -glycosidic linkages of cellulose, indicating that cellulose was preserved after the pressurized treatment (Huerta & Saldaña, 2018). Delignification of biomass using SCW was reported to occur at temperatures > 200 °C (Bruner, 2009). However, due to the partial removal of lignin and hemicellulose by PAE (20%) treatments, hydroxyl groups on CNFs surface are released and exposed from the compressed cellulose–hemicellulose–lignin structure, favoring hydrogen bonding formation between cellulose and starch during film formation. From the SEM images of the study by Huerta & Saldaña (2018). The straw residues obtained after the PAE (20%) treatments at 180 °C and 50 bar showed clear cracks and large pores on the surface, indicating partially removal of lignin and hemicellulose.

For canola straw after PAE (20%) treatment (Fig. 7.1a), the broad peak between 3200-3600 cm^{-1} corresponded to O-H stretch band due to vibrations of hydroxyl groups linked by hydrogen bonds in cellulose (Yang et al., 2007). The peak at 2920 cm^{-1} can be attributed to the aliphatic saturated C-H stretching vibration in cellulose and hemicellulose (Kaushik, Singh & Verma, 2010). The cassava starch/chitosan/gallic acid films containing CNFs (Fig. 7.1c-d) exhibited similar FT-IR spectra as the cassava starch/chitosan/gallic acid film (Fig. 7.1b) due to the chemical similarities between starch and cellulose, where the broad band at 3200-3600 cm^{-1} (assigned to O-H stretching) and near 2910 cm^{-1} (assigned to C-H stretching) were observed in all films. The unique fingerprint region for polysaccharides of 800-1500 cm^{-1} was assigned to C-C and C-O stretching and C-H bending vibrations (Mendes et al., 2016). The new peak at 1720 cm^{-1} in bioactive films (Fig. 2b-d) was assigned to C=O stretching vibration of ester bonds due to the addition of gallic acid, indicating the ester bonds between the hydroxyl groups of starch/chitosan/cellulose and the carboxyl group of gallic acid (Zhao & Saldaña, 2018).

Furthermore, the wavenumber of the peak for O-H stretching vibrations shifted from 3330 to 3340 cm^{-1} as CNFs content changed from 0 to 0.1 g/g starch, suggesting hydrogen bonds between cellulose and starch molecules as a result of the addition of CNFs into cassava starch/chitosan/gallic acid films.

The wave number band at 1658 cm^{-1} was strongly influenced by the amount of water molecules bound to the films. This peak shifted to 1610 cm^{-1} as the CNFs concentration increased, indicating a different amount of water associated with the film, which is consistent with the water activity determined in this study (Table 7.3).

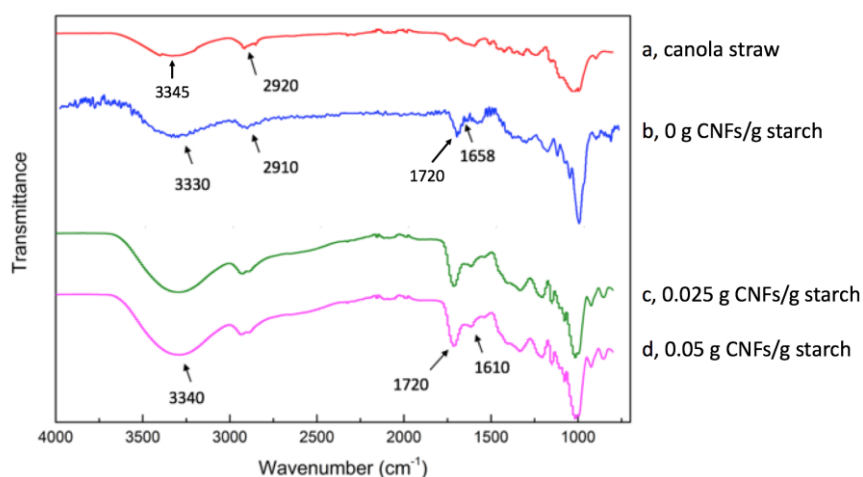


Fig. 7.1 FT-IR spectra of: a) pressurized aqueous ethanol (20%) treated canola straw, and b-d) CNFs reinforced cassava starch/chitosan/gallic acid films with different CNFs/starch ratios, constant chitosan/starch ratio (0.15 g/g) and gallic acid/starch ratio (0.1 g/g) produced at 100 °C and 85 bar.

7.3.3 Physico-chemical properties

Table 7.3 shows the moisture content, water activity, water vapor permeability and film solubility in water of cassava starch/chitosan/gallic acid reinforced with CNFs. Starch naturally has poor moisture resistance, so the addition of CNFs is an effective way to reduce its moisture sensitivity and thereby improve mechanical strength (Table 7.2) and stability (Fig. 7.2). The

control cassava starch film with only 0.1 g CNFs/g starch but no gallic acid or chitosan added was less resistant to moisture compared to CNFs reinforced cassava starch/chitosan/gallic acid film at the same CNFs loading, indicating high availability of hydroxyl groups in starch and cellulose that promotes water absorption. The incorporation of CNFs in composite films reduced the moisture content from $9.29 \pm 0.64\%$ to $7.54 \pm 0.13\%$, due to the lower water affinity of CNFs compared with starch. There was no significant difference among the films reinforced with 0.05 to 0.1 g CNFs/g starch, which moisture contents varied from $8.81 \pm 0.01\%$ to $7.54 \pm 0.13\%$. Film water activity also experienced a reduction from 0.24 ± 0.02 to 0.16 ± 0.01 when increasing CNFs concentrations from 0 to 0.1 g/g starch. The number of active -OH groups for water binding decreased due to the formation of hydrogen bonds between starch, chitosan and CNFs, reducing the film water activity. Babaei et al. (2015) reported the reduction of water uptake up to 14% in CNFs (10 wt%) incorporated corn starch films. However, in our study, pores were observed in the films with 0.075 and 0.1 g CNFs/g starch (Fig. 7.3j and k), decreasing the effectiveness of CNFs binding with starch and chitosan molecules, thus the improvement of water resistance was not significant.

Owing to the highly ordered chain distribution, CNFs are less hydrophilic than starch, making them effective to improve the barrier properties (Kaushik et al., 2010). The water vapor permeability was 0.36 ± 0.02 g.mm/kPa.m².h for the film without CNFs, which reduced significantly to 0.31 ± 0.01 and 0.26 ± 0.01 g.mm/kPa.m².h for the films containing 0.025 and 0.05 g CNFs/g starch, respectively. The films containing 0.075 g CNFs/g starch showed significant low water vapor permeability of 0.20 ± 0.02 g.mm/kPa.m².h that can be attributed to the highly crystalline and hydrophobic character of cellulose in comparison to the starch molecule. The addition of CNFs also introduced a tortuous path for water molecules to pass

through as reported by Kristo and Biliadeis (2007). However, additional amount of CNFs might conglomerate to form a heterogeneity film, which in turn facilitates the water vapor permeation, and holes in the film matrix as observed in the SEM images (Fig. 7.3 j and k). Similar trend was reported by Shankar & Rhim (2016), where the water vapor permeability decreased linearly from 4.75 to 3.49 g.mm/kPa.m².h when nanocellulose (average diameter = 649.6 nm) was added up to 3 wt% in agar film, then it increased slightly to 4.39 g.mm/kPa.m².h at 5 wt% nanocellulose.

The film without CNFs had a low initial contact angle of about 68.23°. With the incorporation of 0.025 g CNFs/g starch into the film matrix, the contact angle increased significantly to 84.46°, this increment was not significant when CNFs content was higher than 0.05 g/g starch, from 91.53 to 94.94° with 0.1 g CNFs/g starch added. This behavior corresponded to the hydrophobic characteristics of the cellulose in comparison with starch hydrophilic properties. The formation of hydrogen bonds between starch, chitosan and CNFs reduced the interaction between water and the hydroxyl groups of the starch-based films. Similarly, a considerable increase of contact angle from 38.2 to 96.3° was observed by Slavutsky & Bertuzzi (2014) when cellulose nanocrystals (3 wt%, average length of 247.5 nm and average diameter of 10.1 nm) was incorporated to corn-starch films.

The addition of CNFs reduced the film solubility in water significantly from 13.20% to 9.34% at 4 °C, from 18.10% to 11.25% at 25 °C and from 25.10% to 16.15% at 50 °C (Table 7.3). This reduction is an indicative of strong interactions between starch and chitosan chains with cellulose through hydrogen bonds in the film matrix. Slavutsky & Bertuzzi (2014) reported that the reduction observed in solubility from 26.6% to 18.5% of corn starch films reinforced with cellulose nanocrystals (3 wt%) obtained from sugarcane bagasse is mainly related to the strong hydrogen bond formation between hydroxyl groups of the starch and cellulose. According to EI

Halal et al. (2015), the cellulose in sodium hypochlorite oxidized barley starch films reduced the film solubility from 23.5% to 17.4% at the cellulose concentration of 20 wt%, due to lower hygroscopicity of the cellulose fibers in relation to starch.

Table 7.3 Physico-chemical properties of CNFs reinforced cassava starch/chitosan/gallic acid films produced at 100 °C and 85 bar.

CNFs/starch ratio (g/g)	Moisture content (%)	Water activity	WVP (g.mm/kPa.m ² .h)	Contact angle (°)		Film solubility in water (%)		
				Top	Bottom	4 °C	25 °C	50 °C
0	9.29±0.64 ^a	0.24±0.02 ^a	0.36±0.02 ^a	68.23±1.89 ^c	94.70±1.25 ^a	13.20±0.36 ^{ab}	18.10±2.26 ^a	25.10±1.27 ^a
0.025	9.50±0.28 ^a	0.21±0.01 ^a	0.31±0.01 ^b	84.46±3.91 ^b	93.07±1.91 ^a	13.90±0.73 ^a	19.20±0.47 ^a	24.61±1.59 ^a
0.05	8.81±0.01 ^{ab}	0.22±0.02 ^a	0.26±0.01 ^c	91.53±1.23 ^a	93.74±2.26 ^a	11.93±0.16 ^{ab}	16.62±1.30 ^{ab}	21.66±1.57 ^{ab}
0.075	7.77±0.24 ^b	0.19±0.01 ^{ab}	0.20±0.02 ^d	92.90±2.34 ^a	92.24±2.64 ^a	11.28±0.65 ^{bc}	14.07±0.68 ^{ab}	18.45±1.42 ^{bc}
0.1	7.54±0.13 ^b	0.16±0.01 ^b	0.23±0.01 ^{cd}	94.94±1.60 ^a	95.01±1.44 ^a	9.34±0.91 ^c	11.25±1.34 ^b	16.15±0.64 ^c
0.1 (Control)	7.79±0.21 ^b	0.17±0.01 ^b	0.27±0.01 ^c	95.34±1.25 ^a	94.91±1.95 ^a	10.93±0.91 ^{bc}	14.55±1.04 ^{ab}	20.67±1.23 ^{ab}

CNFs: cellulose nanofibers, control: cassava starch film with only 0.5 g glycerol/g starch and 0.1 g CNFs/g starch, WVP: water vapor permeability.

Bioactive films produced at different CNFs/starch ratios and constant glycerol/g starch ratio of 0.5 g/g, chitosan/starch ratio of 0.15 g/g and gallic acid/starch ratio of 0.1 g/g at 85 bar and 100 °C.

Data shown as mean±standard deviation ($n = 3$).

^{a-c}Different lowercase letters in the same column indicate significant differences ($p < 0.05$).

7.3.4 Thermal properties

Fig. 7.2 shows the thermal behavior of canola straw after PAE (20%) treatment, cassava starch/chitosan/gallic acid film and cassava starch/chitosan/gallic acid films reinforced with 0.025 and 0.1 g CNFs/g starch produced at 100 °C and 85 bar. In the case of PAE (20%) treated canola straw, thermal degradation occurred with most significant loss in weight (58.2%) between 315°C and 400°C. The peak decomposition temperature of canola straw occurred at 378.1 °C, while the DTG curves of bioactive films showed lower decomposition temperatures of 329.3-330.6 °C (Fig. 7.2B). But, these temperatures are still higher than the peak degradation temperatures of pure cassava starch and pure chitosan reported earlier at 321 and 302 °C, respectively (Valencia-Sullca et al., 2018a), and the peak degradation temperature of thermoplastic starch foamed composites reinforced with CNFs (0.5-1.5 wt%) at 315 °C (Ghanbari, Tabarsa, Ashori, Shakeri & Mashkour, 2018), indicating a more stable film structure in our study.

The TG curves (Fig. 7.2A) of cassava starch/chitosan/gallic acid reinforced with 0 and 0.025 g CNFs/g starch showed an initial weight loss between 90 and 225 °C, which corresponded to a weight loss of absorbed moisture. Similarly, Syafri et al. (2018) reported the weight loss between 100-225 °C, which was associated with water evaporation in CNFs reinforced cassava starch hybrid composites (cassava starch:CNFs ratio of 1:0.2-0.8 w/w). However, the moisture loss of cassava starch/chitosan/gallic acid films reinforced with 0.1 g CNFs/g starch was not significant due to the low moisture content in films, which is consistent with the results of film moisture (Table 7.3). The second stage was the major decomposition of starch, chitosan and cellulose, which occurred between 225-400 °C. All film samples displayed a similar thermal behavior at the temperature range of 225-400 °C and the influence of CNFs on

the peak degradation temperature was found to be negligible. However, the residual weights of bioactive films (18.2-21.7%) were higher than that of the canola straw (11.3%) due to the ester linkages and hydrogen bonds formed in the films (Fig. 7.1). The high residual weights of bioactive films also indicated a good adhesion effect between CNFs and the film matrix composed of starch and chitosan. Similarly, Prachayawarakorn et al. (2013) reported that the thermal stability of cassava starch-fiber composites increased with the increasing fiber filler content (5-15 wt% fiber), as indicated by the reduced weight loss from 53.7 to 52.1% for Jute fiber and 58.8 to 47.6% for Kapok fiber.

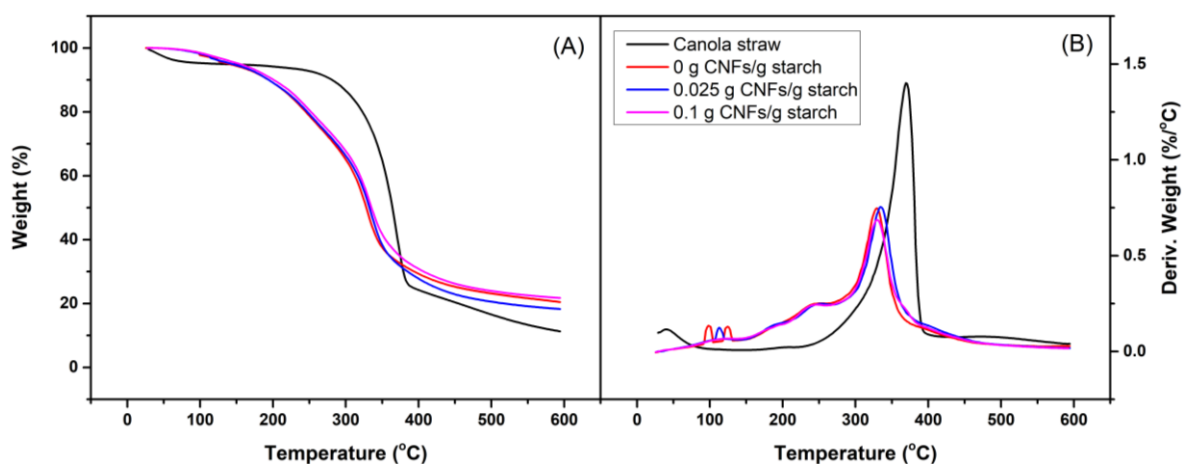


Fig. 7.2 (A) TG, and (B) DTG curves of pressurized aqueous ethanol (20%) treated canola straw and CNFs reinforced cassava starch/chitosan/gallic acid films with different CNFs/starch ratios and constant glycerol/g starch ratio of 0.5 g/g, chitosan/starch ratio of 0.15 g/g and gallic acid/starch ratio of 0.1 g/g produced at 85 bar and 100 °C.

7.3.5 Morphological properties

Fig. 7.3 shows the top (Fig. 7.3b-f) and fractured (Fig. 7.3g-k) surfaces of the cassava starch/chitosan/gallic acid films reinforced with different CNFs contents (0-0.1 g CNFs/g starch) by SEM. The CNFs incorporated into the starch films had an average diameter of 22 nm as observed by transmission electron microscope image (Fig. 7.3a). The film with no CNFs filler

displayed a smooth top and fractured surface as shown in Fig. 4b and g, while the films with CNFs (Fig. 7.3c-f) showed rougher top surfaces with increasing CNFs contents. The well dispersed bundles of CNFs can be observed embedded in the films (Fig. 7.3c-h). The fiber surfaces appeared to be covered by starch, attesting the strong adhesion between the composite components. It can also be observed, from the fractured surfaces of films, that CNFs were distributed homogeneously and randomly within the film samples, without pores or cracks formation at CNFs concentrations ≤ 0.05 g/g starch. All CNFs were incrustated in the continuous starchy film matrix. This affinity or compatibility between CNFs and starch matrix can be attributed to the chemical similarities of starch and cellulose, the nanoscale of the fibers and hydrogen bondings between CNFs and starch (Lu et al., 2005). Similar results were recently reported for corn starch films containing sugar beet CNFs (<10 wt%) (Li et al., 2018b). This extent of homogeneous distribution of CNFs in the starch film greatly improved their mechanical properties (Table 7.2). However, pores were noticed in films with > 0.05 g CNFs /g starch, exhibiting a heterogenous appearance (Fig. 7.3f and k), probably due to the selective agglomeration of CNFs, which leads to the inhomogeneity (Fig. 7.3f and k).

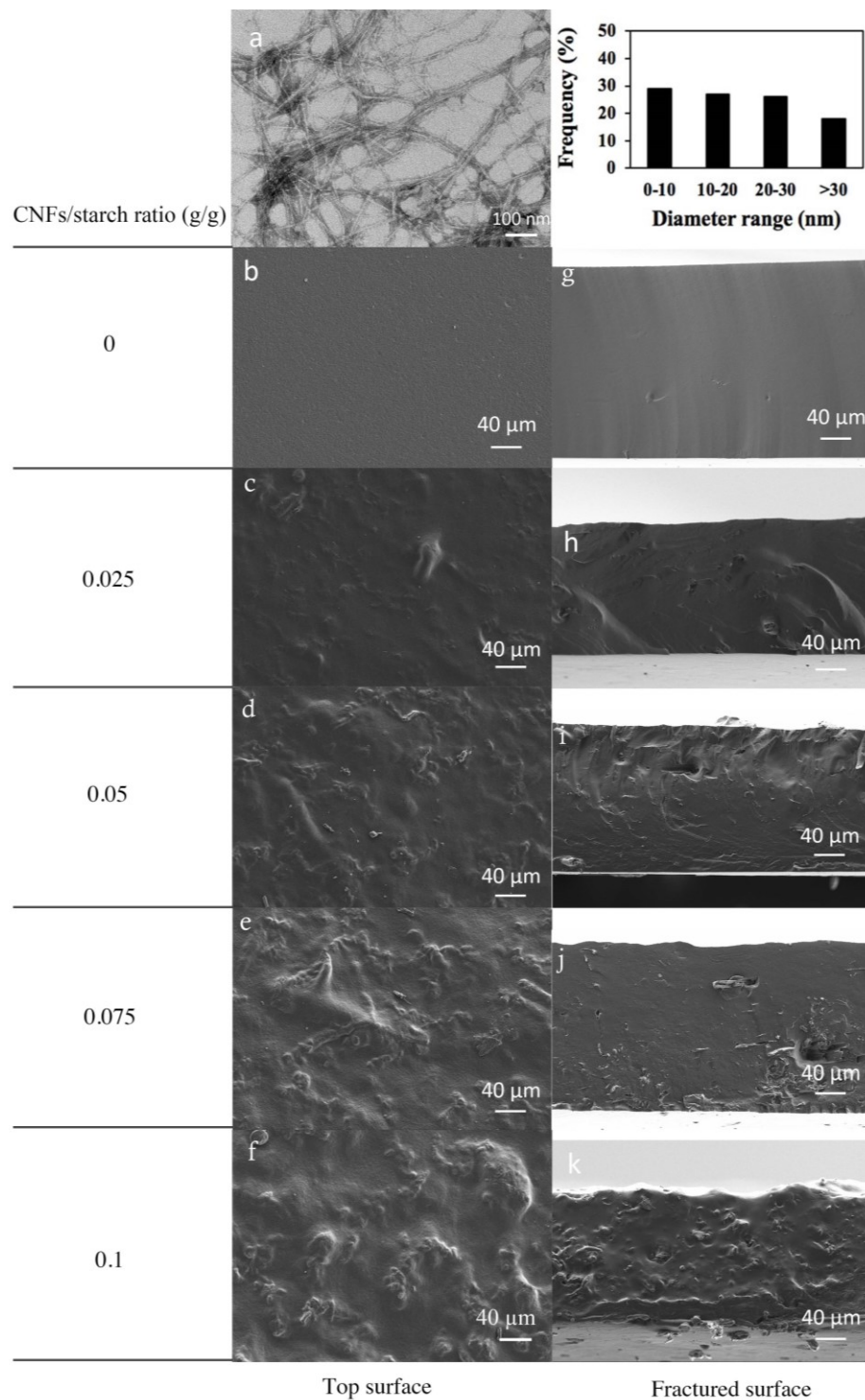


Fig. 7.3 TEM image of: a) CNFs from canola straw after ultrasonication, and SEM images of: b-f) top surfaces and g-k) fractured surfaces of CNFs reinforced cassava starch/chitosan/gallic acid films with 0-0.1 g CNFs/g starch, constant chitosan/starch ratio (0.15 g/g) and gallic acid/starch ratio (0.1 g/g) produced at 100 °C and 85 bar.

7.3.6 Optical properties

Table 7.4 summarizes the color performance, transparency and gloss values of CNFs reinforced cassava starch/chitosan/gallic acid films. The amount of CNFs had significant effect on the color of bioactive films. In general, films became darker as evidenced by the significant increase of yellowness values from 6.25 ± 0.50 to 14.49 ± 0.06 as the content of CNFs increased from 0 to 0.1 g/g starch. Also, a decreased in whiteness values was observed, which are less significant at various CNFs concentrations, due to the presence of residual lignin (20 wt%) in CNFs prepared from canola straw. In terms of the total color difference, only films with CNFs loading >0.05 g/g starch showed difference with the rest of the films. To prepare whiter and more transparent films, bleached CNFs can be used, but the bleaching process involves the use of non-environmentally friendly alkaline solution like NaOH and is a time-consuming process that requires several hours of operation (El Miri et al., 2015). Films in this study were prepared using pressurized hot water technology that is a green process without the use of chemicals.

The transparency values of CNFs reinforced films were significantly higher than that of the film without CNFs filler, indicating that the filling with CNFs decreased the transparency of the films. The presence of a disperse phase promotes opacity due to the differences in the concentration and particle size of the filler and the refractive index of both phases (Villalobos, Chanona, Hernández, Gutiérrez & Chiralt, 2005). These observations are consistent with the findings of as potato starch films reinforced by softwood CNFs (Hietala et al., 2013) and potato starch films added with CNFs from cotton fiber (Savadekar & Mhaske, 2012).

The gloss values of films without CNFs were the highest, with 70.75 ± 0.50 GU for the top surface and 88.90 ± 0.14 GU for the bottom surface, whereas composite films showed very

low values for the top surfaces coinciding with the roughness of the composite film surface, as observed with SEM images (Fig. 7.3). The CNFs concentration showed little influence on the bottom surface gloss, showing gloss values from 86.15 ± 1.49 GU to 82.35 ± 1.49 GU with no significant difference. This is probably because starch, chitosan and CNFs form a dense structure when contacted with the smooth surface of the petri dish. The control cassava starch film with only 0.1 g CNFs/g starch but no gallic acid or chitosan added had slightly rougher top surface than that of the CNFs reinforced cassava starch/chitosan/gallic acid film, revealing less ordered arrangement of starch and cellulose in the film. Jiménez et al. (2012b) reported the loss of gloss during storage of corn starch film added with hydroxypropyl methylcellulose, probably due to a molecular rearrangement, which modifies film surface topography.

Table 7.4 Optical properties of CNFs reinforced cassava starch/chitosan/gallic acid films produced at 100 °C and 85 bar.

CNFs/starch ratio (g/g)	Color performance			Transparency	Gloss (GU)	
	ΔE	YI	WI		Top	Bottom
0	5.32±0.40 ^b	6.25±0.50 ^d	94.86±0.62 ^a	0.76±0.01 ^c	70.75±0.50 ^a	88.90±0.14 ^a
0.025	4.69±0.34 ^b	8.76±0.07 ^c	89.96±3.02 ^{ab}	1.81±0.10 ^b	15.55±0.64 ^b	86.15±1.49 ^{ab}
0.05	5.35±0.30 ^b	11.73±0.26 ^b	88.98±0.32 ^b	2.00±0.03 ^b	10.05±0.35 ^b	84.55±0.64 ^b
0.075	10.75±0.10 ^a	12.10±0.14 ^b	84.72±0.04 ^b	3.64±0.05 ^a	4.35±0.14 ^c	83.90±0.14 ^b
0.1	9.94±0.22 ^a	14.49±0.06 ^a	84.61±0.19 ^b	3.71±0.04 ^a	4.10±0.21 ^c	82.35±1.49 ^b
0.1 (Control)	9.70±0.45 ^a	13.93±0.18 ^a	85.34±0.84 ^b	3.44±0.24 ^a	3.26±0.39 ^d	80.55±2.36 ^b

CNFs: cellulose nanofibers, control: cassava starch film with only 0.5 g glycerol/g starch and 0.1 g CNFs/g starch, ΔE : total color difference, YI: yellowness index, WI: whiteness index, GU: gloss unit.

Bioactive films produced at different CNFs/starch ratios and constant glycerol/g starch ratio of 0.5 g/g, chitosan/starch ratio of 0.15 g/g and gallic acid/starch ratio of 0.1 g/g at 85 bar and 100 °C.

Data shown as mean±standard deviation ($n = 3$).

^{a-d}Different lowercase letters in the same column indicate significant differences ($p < 0.05$).

7.3.7 Antioxidant activity

Fig. 7.4 shows the total phenolic content and antioxidant activity of CNFs reinforced cassava starch/chitosan/gallic acid films evaluated by FRAP and ABTS methods (Table E.1, appendix E). Although the initial loading of gallic acid (0.1g/g starch) was constant in all films, the free gallic acid released from different films were different. The film with no CNFs showed the lowest total phenolic content (35.07 ± 1.36 mg gallic acid equivalent/g film) and antioxidant activity (365.40 ± 9.44 mg Trolox equivalent/g film for FRAP and 448.19 ± 6.17 mg Trolox equivalent/g film for ABTS), due to the cross-linking of gallic acid with starch and chitosan that prevented gallic acid releasing. However, when 0.025 g/g starch of CNFs was incorporated, an increase of gallic acid release was observed, probably because the CNFs introduced heterogeneity between starch molecules that influenced the reaction between starch and gallic acid, increasing the amount of free gallic acid. While with the increasing amount of CNFs, new cross-links including ester linkages and hydrogen bondings between gallic acid and cellulose formed, resulting in the trap of gallic acid in the film matrix, therefore, less free gallic acid was available. Films with 0.1 g CNFs/g starch showed a total phenolic content of (40.97 ± 0.66 mg gallic acid equivalent/g film) and antioxidant activity of (428.14 ± 35.37 mg Trolox equivalent/g film) for FRAP and (480.50 ± 2.99 mg Trolox equivalent/g film) for ABTS, which was not significantly different from the film without CNFs. Similar reduced antioxidant release was also reported by Priya et al. (2014), where the formation of hydrogen bonds between citric acid and *G. optiva* fibers in starch/poly(vinyl alcohol)/citric acid film limited the release of citric acid from the film matrix, resulting reduced inhibitory zone diameter (1.2-1.5 cm) against *S. aureus* and *E. coli* compared to films with no cellulosic fiber added (1.5-1.7 cm).

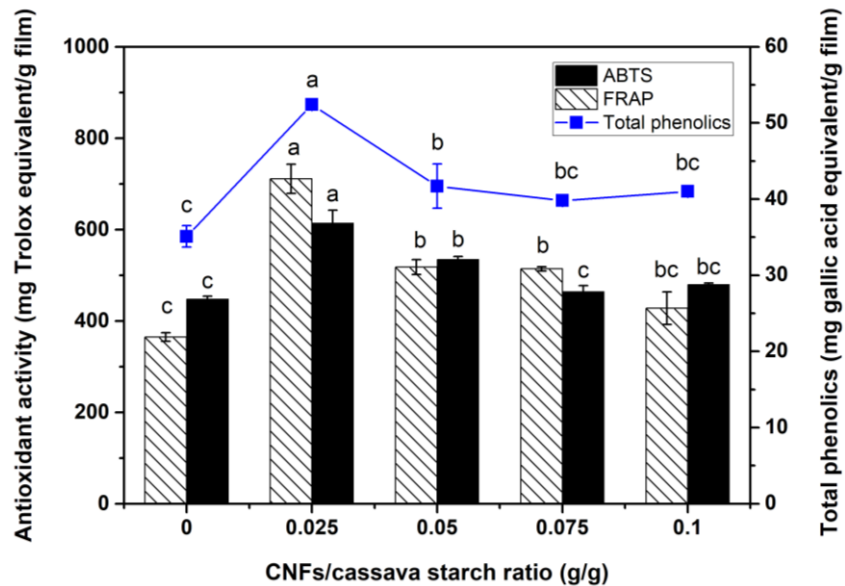


Fig. 7.4 Total phenolic content, and total antioxidant activity of CNFs reinforced cassava starch/chitosan/gallic acid films with different CNFs/starch ratios, constant chitosan/starch ratio (0.15 g/g) and gallic acid/starch ratio (0.1 g/g) produced at 100 °C and 85 bar. ABTS: 6-Dydroxy-2,5,7,8-tetramethylchroman-2-carboxylic acid, and FRAP: Ferric reducing antioxidant power. ^{a-d}Different lowercase letters in the same pattern indicate significant differences ($p < 0.05$).

7.4 Conclusions

The incorporation of cellulose nanofibers (CNFs) from canola straw significantly enhanced cassava starch/chitosan/gallic acid film properties. The CNFs reinforced cassava starch/chitosan/gallic acid films produced at 100 °C and 85 bar, with increasing tensile strength from 0.83 to 10.51 MPa. Furthermore, CNFs with an average diameter of 22 nm were uniformly distributed in the starch film matrix at CNFs concentrations ≤ 0.05 g/g starch, resulting in cross-linking with chitosan, starch and gallic acid that improved film moisture resistance. Using 0.075 g CNFs/g starch, films showed the lowest water vapor permeability value (0.20 ± 0.02 g.mm/kPa.m².h). Also, less free gallic acid was available due to the cross-linking of gallic acid with starch/chitosan/CNFs in the starch-based films. However, the incorporation of CNFs

(>0.05 g/g starch) led to bumpy surfaces and less transparent films with yellowish color. In general, bioactive starch-based films reinforced with CNFs prepared by pressurized hot water technology provided an environmentally-friendly alternative for food packaging, e.g. hot dog (by replacing the casings) and non-food packaings. The addition of CNFs as reinforcing agent successfully improved the tensile strength of starch-based films.

Chapter 8: Antimicrobial Activity of Bioactive Starch Films Against *L. monocytogenes* and Reconstituted Meat Microbiota on Ham*

8.1. Introduction

Ready to eat (RTE) foods including RTE meats represent a growing segment of the overall food market owing to their convenient use by consumers (Alberta Agriculture and Forestry, 2017). The main food safety concern related to RTE meat products is contamination with *Listeria monocytogenes*. *L. monocytogenes* may grow to high cell counts during refrigerated storage of RTE meats (Yousef & Lou, 1999) and cause life-threatening infections in at-risk individuals (Farber & Peterkin, 1991; WHO, 2004). Because RTE meats are typically consumed without further cooking, the risk of *Listeria* infection depends on the cell counts of *L. monocytogenes* that is consumed. A contamination ranging from 0.04 to 100 cfu *Listeria* / g is considered an acceptable risk in most jurisdictions (WHO, 2004; FSIS, 1989). The contamination of RTE meats is primarily attributed to post-cooking contamination (ICMSF, 2018). In addition to process hygiene, the addition of preservatives to RTE meats to prevent growth of *Listeria* is a key measure to reduce the risk of foodborne listeriosis (Mejlholm et al., 2010).

Microbiota of RTE meats predominantly consist of *Brochothrix thermosphacta* (Miller, Liu & McMullen, 2014), *Carnobacterium* spp. (Horita et al., 2018), psychrotrophic lactobacilli (Giello, La Storia, De Filippis, Ercolini & Villani, 2018) and *Leuconostoc* spp. (Maksimovic et al., 2018). These psychrotrophic and micro-aerophilic bacteria can cause discoloration, gas and slime production, or produce off-odors and off-flavors (Borch, Kant-Muermans & Blixt 1996; Pothakos, Snauwaert, De Vos, Huys & Devlieghere, 2014). However, many strains of *Lactobacillus* spp. and *Carnobacterium* grow

*A version of this chapter will be submitted to International Journal of Food Microbiology as “Zhao, Y., Teixeira, J. S., Gänzle, M. G., and Saldaña, M. D. A. (2019). Antimicrobial Activity of Bioactive Starch Films Against *L. monocytogenes* and Reconstituted Meat Microbiota on Ham.

to high cell counts without negatively affecting product quality; some of these strains are used as (bacteriocin--producing) biopreservatives to inhibit growth of *Listeria* during refrigerated storage (Drider, Fimland, Hechard, McMullen & Prevost, 2006; Nilsson et al., 2005; Schillinger, Kaya & Lücke, 1991)

Common methods used to control microbial contamination of RTE meats include in-package thermal pasteurization, high pressure processing, and product-reformulation with preservatives (Murphy et al., 2003; Seman, Borger, Meyer, Hall & Milkowski, 2002; Teixeira, Maier, Miller, Gänzle & McMullen, 2016). In-package thermal pasteurization eliminates *L. monocytogenes* but also compromises product quality by inducing shrinkage and drip loss in the products (Murphy et al., 2003). Current commercial high pressure processes reduce cell counts of *L. monocytogenes* by 4 log(cfu / g) only (Teixeira et al., 2016) and thus require combination with high hygienic processing standards, or with other antimicrobial agents, such as nisin or essential oils (Hereu, Bover-Cid, Garriga & Aymerich, 2012; Saraiva et al., 2016). Antimicrobials such as sodium lactate, sodium diacetate, and potassium benzoate are extensively used to extend the shelf-life and ensure the safety of meat products (Seman et al., 2002), new natural derived antimicrobial agents for use in meat products include phenolic compounds (Starčević et al., 2015), essential oils (Sirocchi et al., 2017) and chitosan (Arslan & Soyer, 2018). Chemical preservatives, however, also affect the sensory quality of the products.

Microbial contamination of RTE meats occurs at the surface, therefore, the use of natural antimicrobials in packaging films can control spoilage and pathogenic microorganisms on the product. Chitosan is a film-forming cationic polysaccharide with antimicrobial activity which is suitable for production of packaging films with antimicrobial activity. The use of chitosan-based active packaging films reduced cell counts of *Listeria*, or to inhibited growth of spoilage

microbiota on RTE meats (Guo, Jin, Wang, Scullen & Sommers, 2014; Zhao et al., 2018). In addition, the addition of rosemary and licorice extract to packaging films growth of delayed *L. monocytogenes* on cooked ham (Zhang, Kong, Xiong, & Sun, 2009). Preliminary studies that assessed the antimicrobial activity of chitosan-gelatine films on microbiota of cod demonstrated differential activity of the film against different groups of bacteria (Gómez-Estaca, De Lacey, López-Caballero, Gómez-Guillén & Montero, 2010), however, studies that document the differential activity of chitosan based films on *Listeria monocytogenes* and spoilage or protective RTE microbiota are currently unavailable. It was therefore the aim of this study to investigate the effect of bioactive starch films containing gallic acid, or chitosan and gallic acid or carvacrol for RTE ham on growth of *L. monocytogenes* and reconstituted meat microbiota. RTE ham was produced according to current commercial practice in Canada (Teixeira et al., 2016), cut aseptically, and inoculated with a 5 strains cocktail of *L. monocytogenes* and / or a 5 strain cocktail representing microbiota of RTE meats (Teixeira et al., 2016).

8.2. Material and Methods

8.2.1. Bacterial strains and growth conditions

A cocktail of strains containing *L. monocytogenes* FSL J1-177, FSL C1-056, FSL N3-013, FSL R2-499, and FSL N1-227 (Fugett, Fortes, Nnoka & Wiedmann, 2006) and a “reconstituted meat microbiota” cocktail containing *Brochothrix thermosphacta* FUA3558, *Carnobacterium maltaromaticum* FUA3559, *Leuconostoc gelidum* FUA3560, *Leuconostoc gasicomitatum* FUA3561 and *Lactobacillus sakei* FUA3562 (Teixeira, Repková, Gänzle & McMullen, 2018) were used in this study.

Strains of *L. monocytogenes* were aseptically streaked from -80 °C stock cultures onto Tryptic Soy (TS) agar (Difco, Becton–Dickinson, Sparks, MD, USA), followed by inoculation

into TS broth (TSB) and incubation overnight at 37 °C. Fresh broth was inoculated with 1% (v/v) of the overnight culture and incubated at 37 °C to the stationary growth phase. Strains of reconstituted meat microbiota were prepared in the same manner but grown on All Purpose Tween (APT) agar and broth at 25 °C. For preparation of cocktails, an equal volume of each individual culture was mixed to form a 5-strain cocktail of *L. monocytogenes* or reconstituted meat microbiota. These cocktails were harvested by centrifugation ($7000 \times g$ for 10 min), re-suspended in saline solution (0.85% NaCl) and diluted. Growth conditions are summarized in Table 8.1.

Table 8.1. Bacterial strains and growth conditions used in this study.

Strains	Growth conditions	Reference
<i>L. monocytogenes</i> FSL J1-177	TSB, 37 °C	Fugett et al. (2006)
<i>L. monocytogenes</i> FSL R2-499	TSB, 37 °C	Fugett et al. (2006)
<i>L. monocytogenes</i> FSL C1-056	TSB, 37 °C	Fugett et al. (2006)
<i>L. monocytogenes</i> FSL N1-227	TSB, 37 °C	Fugett et al. (2006)
<i>L. monocytogenes</i> FSL N3-013	TSB, 37 °C	Fugett et al. (2006)
<i>Brochothrix thermosphacta</i> FUA3558	APT, 25 °C	Miller et al. (2014)
<i>Carnobacterium maltaromaticum</i> FUA3559	APT, 25 °C	Miller et al. (2014)
<i>Leuconostoc gelidum</i> FUA3560	APT, 25 °C	Miller et al. (2014)
<i>Leuconostoc gelidum</i> FUA3561	APT, 25 °C	Miller et al. (2014)
<i>Lactobacillus sakei</i> FUA3562	APT, 25 °C	Miller et al. (2014)

8.2.2 Antimicrobial preparation

Gallic acid (GA) (97.5-102.5% titration), chitosan (75-85% deacetylated) with medium molecular weight of 190-310 kDa and carvacrol (Food grade, >99%) were obtained from Sigma Aldrich (Oakville, ON, Canada). Gallic acid stock solution (22.5 g/L) was prepared in sterilized distilled water. Chitosan stock solution (11.25 g/L) was prepared in 2% (w/w) citric acid solution and carvacrol stock solution (56.56 g/L) was prepared in 0.8% (w/w) lecithin solution.

8.2.3 Determination of the combined activity of gallic acid or carvacrol and chitosan with the checkerboard method

The checkerboard procedure was carried out to determine the combination of inhibitory and bactericidal activity of GA or carvacrol and chitosan against *L. monocytogenes* and reconstituted meat microbiota. Briefly, 100 µL of TS or APT broth was added to each well of a 96-well microplate. Combinations of GA + chitosan or carvacrol + chitosan stock solutions (100 µL) were added to separate wells and serially 2-fold diluted across the plate in a two-dimensional

way. Stationary phase cultures of *L. monocytogenes* or reconstituted meat microbiota were 10-fold diluted in TS or APT broth, respectively, to a final concentration of about 10^8 cfu/mL, and microplates were inoculated with 50 μ L of the diluted culture. Plates were incubated for 24 h at 37 °C for *Listeria* or 25 °C for reconstituted meat microbiota.

8.2.4 Sample preparation and inoculation

Previously manufactured experimental cooked ham, with a known formulation and sodium chloride concentration of 3% (w/w), was used in this study (Teixeira et al., 2016). The ham was sliced aseptically and uninoculated slices of ham had a total aerobic plate count of less than 100 cfu / cm² after slicing. Individual slices of ham (50 cm² surface area with 3 mm thickness) were surface inoculated with the cocktail of *L. monocytogenes* and/or the cocktail of reconstituted meat microbiota to achieve cell counts of about 10^3 cfu *Listeria*/cm² and/or 10^4 cfu reconstituted meat microbiota /cm². Experimental groups were categorized as follows: (i) *L. monocytogenes*, (ii) reconstituted meat microbiota, and (iii) *L. monocytogenes* combined with reconstituted meat microbiota. Each of the three experimental groups were covered with the antimicrobial films (2 cm² surface area). Samples were aseptically packed, sealed and stored at 4 °C for up to 28 days. Uninoculated ham served as control; the cell counts of control samples remained below the detection limit of 100 cfu / cm² throughout 28 days of storage. Detection of surviving cells was determined by surface plating as described below. Experiments were performed in triplicate.

8.2.5 Detection of surviving cells

The presence or absence of *L. monocytogenes* and/or reconstituted meat microbiota was monitored after 0, 7, 14, 21 and 28 days of storage at 4 °C following the method described earlier (Zhao et al., 2018). Un-inoculated ham samples were prepared and stored for 28 days at 4 °C to

ensure the absence of contaminating microbiota from the meat prior to the experiment and after storage. Samples were opened aseptically, and the film and ham, collected using a laboratory cork borer (2 cm² surface area), were transferred to a sterile 50 mL centrifuge tube and dilute with sterile saline (0.85% NaCl). Ham and film samples were homogenized for 60 s prior to serial dilutions.

Surviving cells were determined by surface plating on selective PALCAM (Becton-Dickinson) agar (*L. monocytogenes* combined with reconstituted meat microbiota) and on non-selective TS (*L. monocytogenes*) or APT agar (reconstituted meat microbiota and *L. monocytogenes* combined with reconstituted meat microbiota). Appropriate dilutions were plated and incubated at 37 °C (PALCAM and TS agar) or 25 °C (APT agar) for 48 h.

8.2.6 Extraction of total DNA and PCR

For microbial analysis, 1 mL aliquot of the homogenate wash from samples stored for 28 days at 4 °C was centrifuged (5000 × g for 10 min) to collect bacterial cells, and total DNA was extracted from the pellet using DNeasy Blood and Tissue Kit (Qiagen, Ontario, Canada) following the Gram-positive bacteria protocol provided by the manufacturer. DNA was amplified by PCR with Taq DNA polymerase and dNTPs from Invitrogen (Burlington, Canada). Species-specific primers LMG4-F and LMG4-R were designed targeting to the corresponding unique sequences using PrimerQuest Tool (IDT, California). The specificity of the candidate primers was confirmed by Nucleotide BLAST (<https://blast.ncbi.nlm.nih.gov/Blast.cgi>) and 1% agarose gel after PCR. Species-specific primers were purchased from Integrated DNA technologies (Coralville, USA) and are listed in Table 8.2. PCR products were visualized after electrophoretic separation on agarose gels.

Table 8.2. Primers and conditions.

Species	Sequence (5'-3')	Amplicon size / Tm	Reference or target
<i>Brochothrix thermosphacta</i>	Bcr3r – GTTGTCCGGAATTATTGGG Bcr3f – CTCCTCTTCTGTCCTCAAG	121 bp / 58 °C	Pennacchia et al. (2009)
<i>Carnobacterium maltaromaticum</i>	Cpis – TTTATTTTTAATTAATAACCC 23S-7 – GGTACTIONTAGATGTTTCAGTTC	>500 bp / 48 °C	Cailliez-Grimal et al. (2007)
<i>Leuconostoc gelidum</i>	LMG4-F – GTCTACCTTCTTTGCCCTTACA LMG4-R – TTCCAAACGAACCTGGAGATAG	431 bp / 60 °C	23S rRNA (This study)
<i>Lactobacillus sakei</i>	16S – GCTGGATCACCTCCTTTC Ls – ATGAAACTATTAAATTGGTAC	220 bp / 52 °C	Bertheir & Ehrlich (1999)

8.3 Results

8.3.1 Inhibitory activity of gallic acid or carvacrol as a function of chitosan concentration against *L. monocytogenes* and reconstituted meat microbiota

To determine the relative activity of gallic acid and carvacrol against the 10 strains of *Listeria* and RTE microbiota, their inhibitory effect was determined alone and in combination with chitosan. At 1.875 g/L, chitosan alone inhibited all strains of *L. monocytogenes*. Gallic acid showed higher MIC values (15 g/L) than carvacrol (0.61 g/L). Carvacrol and chitosan acted synergistically in *Listeria* inhibition as shown by the pronounced convex shape of the curve (Fig. 8.1B, Table F.1, appendix F) while synergistic activity of gallic acid and chitosan was much less pronounced (Fig. 8.1A, Table F.1, appendix F).

Reconstituted meat microbiota was less sensitive to all antimicrobial combinations (Fig. 8.2, Table F.2, appendix F). Chitosan alone inhibited meat microbiota at 7.5 g/L, which is four times higher than the MIC against *L. monocytogenes*. At least two-fold increase of MIC of carvacrol (1.22 g/L) was observed and gallic acid at 15 g/L was not inhibitory to the strains used. Even in combination with 3.75 g / L chitosan, gallic acid at the highest concentration did not inhibit all strains representing meat microbiota (Fig. 8.2A). Carvacrol exhibited additive activity with chitosan (Fig. 8.2B).

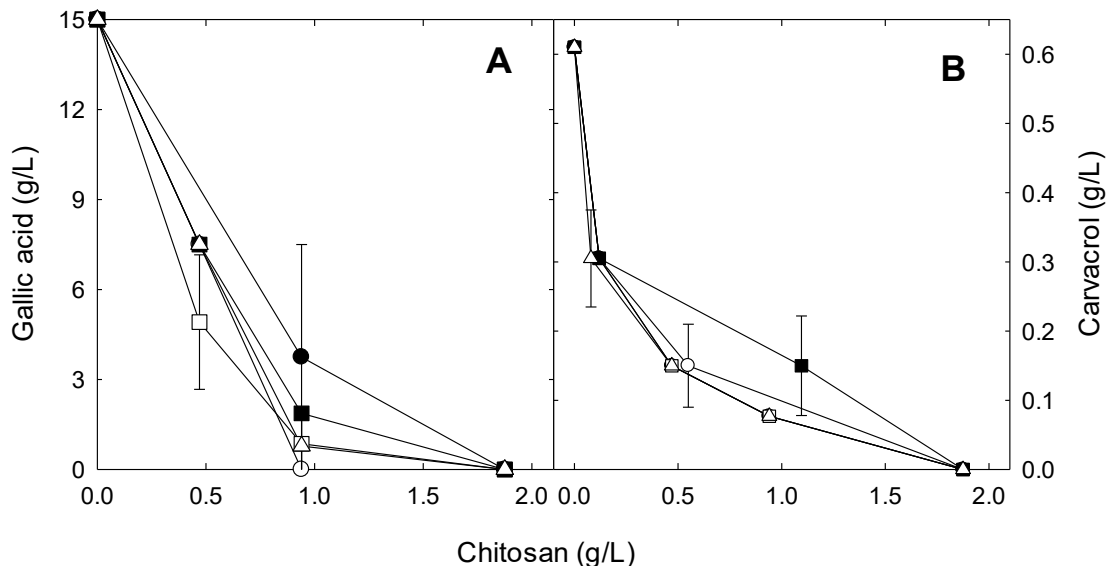


Fig. 8.1 Minimal inhibitory concentration (g/L) of gallic acid (**Panel A**), and carvacrol (**Panel B**) as a function of chitosan concentration (g/L) for *L. monocytogenes* strains FSL J1-177 (○), FSL C1-056 (●), FSL N3-013 (□), FSL R2-499 (■), and FSL N1-227 (Δ). Data are means ± standard deviations of triplicate independent experiments.

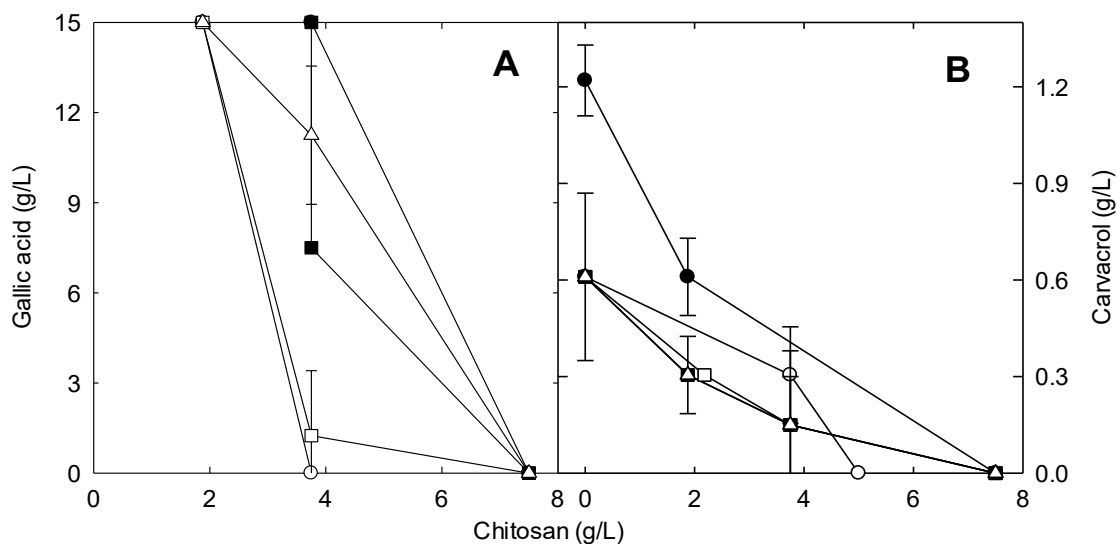


Fig. 8.2 Minimal inhibitory concentration (g/L) of gallic acid (**Panel A**), and carvacrol (**Panel B**) as a function of chitosan concentration (g/L) for *Brochothrix thermosphacta* FUA3558 (○), *Carnobacterium maltaromaticum* FUA3559 (●), *Leuconostoc gelidum* FUA3560 (□) and FUA3561 (■), and *Lactobacillus sakei* FUA3562 (Δ). Data are means ± standard deviations of triplicate independent experiments.

8.3.2 Bioactive starch films on inhibition of individual *L. monocytogenes* or reconstituted meat microbiota on ham

Chitosan was incorporated at a level of 0.025 or 0.150 g / g starch as antimicrobial agent in cassava starch films to provide antimicrobial activity (Zhao et al., 2018). Based on the *in vitro* activity of gallic acid and carvacrol, films additionally containing 0.1 g gallic acid / g starch or up to 0.195 g carvacrol / g starch. Packaging films were also produced from cull potatoes, a starch-rich by-product of potato processing, alone or with addition of gallic acid (Zhao & Saldaña, 2019). The inhibition of *L. monocytogenes* on ham is shown in Fig. 8.3. Cell counts on TS (Figure 8.3A, Table F.3, appendix F) and PALCAM (Figure 8.3B, Table F.3, appendix F) agar were not different, indicating that *L. monocytogenes* on ham were not sublethally injured. Cell counts of un-inoculated ham remained below the detection limit (< 100 cfu/cm²) throughout 4 weeks of storage. On ham packaged with starch films or films from cull potatoes, *L. monocytogenes* grow to high cell counts after 21 d of storage at 4°C. Addition of up to 0.3 g gallic acid / g starch delayed growth of *L. monocytogenes* by one week (Figure 8.3A and B). Starch films containing chitosan and gallic acid inhibited growth over 4 weeks of refrigerated storage (Fig. 8.3A and B), however, *L. monocytogenes* was detected on at least one of the three replicates throughout four weeks of storage. Starch films with chitosan and carvacrol also inhibited growth of *L. monocytogenes* throughout 4 weeks of storage. Incorporation of carvacrol at 0.195 g/g starch reduced initial cell counts by 0.5 log cfu / cm² but *L. monocytogenes* remained detectable in one of the three replicates throughout 4 weeks of storage.

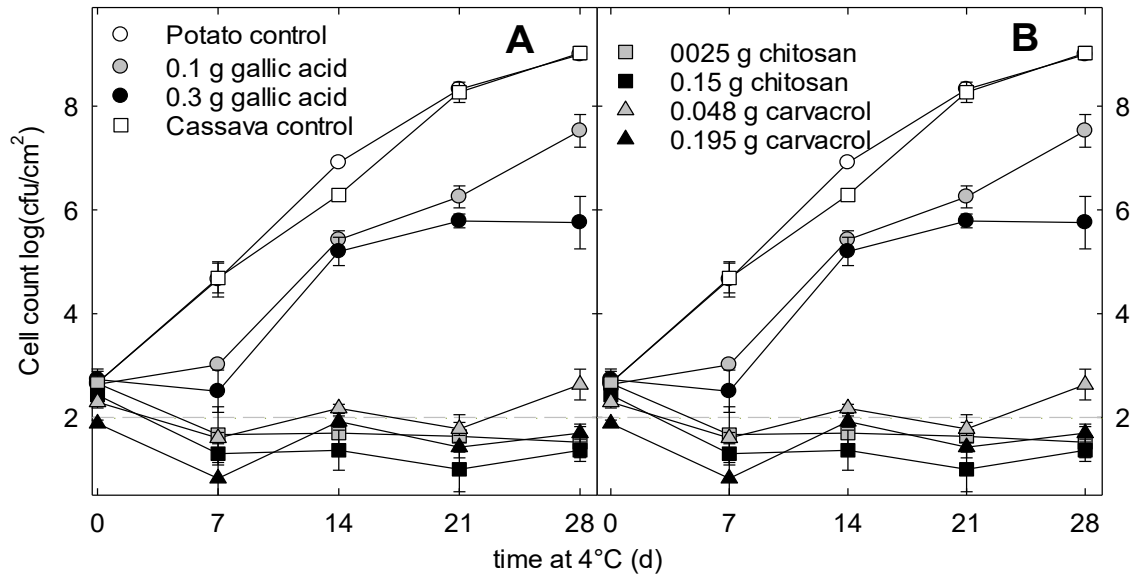


Fig. 8.3 Growth of a 5 strain cocktail of *L. monocytogenes* strains: FSL J1-177, FSL C1-056, FSL N3-013, FSL R2-499, and FSL N1-227 on the surface of cooked ham during storage at 4 °C, bacteria were counted on A) TSB and B) PALCAM agar. The ham was covered with a potato starch film (Potato control), or with a cassava starch film (Cassava control), or potato films containing 0.1 g or 0.3 g gallic acid/g starch, or with cassava starch films containing 0.1 g gallic acid/g starch and 0.025 g or 0.15 g chitosan /g starch, or with cassava starch films containing 0.025 g chitosan /g starch and 0.048 g or 0.195 g carvacrol /g starch. Bacterial cell counts were enumerated over 28 d of storage. Cell counts of un-inoculated ham remained below the detection limit throughout the 4 weeks of storage. Data are means \pm standard deviations of triplicate independent experiments. Symbols crossing the dot line indicate cell counts below the detection limit of 2 log CFU/cm².

Consistent with the *in vitro* MIC data, reconstituted meat microbiota were more resistant to starch films containing gallic acid, or chitosan with gallic acid or carvacrol (Fig. 8.4, Table F.4, appendix F). On ham covered with starch films without antimicrobials, reconstituted meat microbiota grow to high cell counts after two weeks of refrigerated storage. The growth of reconstituted meat microbiota on ham covered with 0.1 g gallic acid/g starch packaging film was comparable to the cull potato control but addition of 0.3 g gallic acid/g starch to the packaging film delayed growth of meat microbiota. Adding 0.1 g gallic acid / g starch in combination with 0.025 or 0.15 g chitosan/g to the packaging film delayed growth of reconstituted meat microbiota

by one or two weeks. On ham covered with films containing both carvacrol and chitosan, the initial cell counts of reconstituted meat microbiota were reduced by 1 – 2 log (cfu/cm²) and re-growth of the organisms was inhibited. Cell counts on ham covered with film containing chitosan and 0.195 g carvacrol/g starch remained below 7 log (cfu/cm²). Depending on the type of organism growing on RTE ham, a cell count of 10⁶ to 10⁷ cfu / cm² may lead to spoilage (Fung, 2009). The antimicrobial packaging film, however, did not completely eliminate or inhibit reconstituted meat microbiota during refrigerated storage of 28 days (cell counts > 6 log (cfu/cm²)).

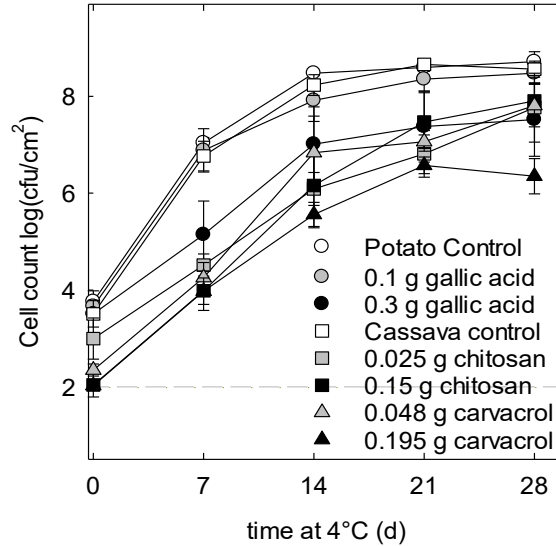


Fig. 8.4 Growth of a 5 strain cocktail of reconstituted meat microbiota containing *Brochothrix thermosphacta* FUA3558, *Carnobacterium maltaromaticum* FUA3559, *Leuconostoc gelidum* FUA3560 and FUA3561, and *Lactobacillus sakei* FUA3562 on the surface of cooked ham during storage at 4 °C, bacteria were counted on APT agar. The ham was covered with a potato starch film (Potato control), or with a cassava starch film (Cassava control), or potato starch films containing 0.1 g or 0.3 g gallic acid/g starch, or with cassava starch films containing 0.1 g gallic acid/g starch and 0.025 g or 0.15 g chitosan /g starch, or with cassava starch films containing 0.025 g chitosan /g starch and 0.048 g or 0.195 g carvacrol /g starch. Bacterial cell counts were enumerated over 28 d of storage. Cell counts of un-inoculated ham remained below the detection limit throughout the 4 weeks of storage. Data are means ± standard deviations of triplicate independent experiments. Symbols crossing the dot line indicate cell counts below the detection limit of 2 log CFU/cm².

8.3.3 Bioactive starch films on inhibition of combined *L. monocytogenes* and reconstituted meat microbiota on ham

Furthermore, to understand complex microorganism behaviour of survival of *L. monocytogenes* and reconstituted meat microbiota on RTE ham packaged with antimicrobial starch films, ham was inoculated with the mixture of a cocktail of 5 *L. monocytogenes* strains and a cocktail of 5 reconstituted meat microbiota strains (Fig. 8.5, Table F.5, appendix F). The total cell counts of combined microorganisms on ham were predominantly determined by the reconstituted meat microbiota. An initial cell count reduction of 1.5 log (cfu/cm²) was observed on ham with films containing carvacrol or chitosan (Fig. 8.5A). Total cell counts on ham covered with starch film containing 0.1 g gallic acid / g starch showed no difference to cull potato control after 14 days of storage, while the addition of 0.3 g gallic acid / g starch delayed bacterial growth (Fig. 8.5A). The use of 0.1 g gallic acid / g starch combined with 0.025 or 0.15 g chitosan/g in cassava starch films and films with 0.025 g chitosan / g starch and 0.048 g carvacrol / g starch reduced total viable plate counts by 1-1.5 log (cfu/cm²) (Fig. 8.5A). The most pronounced inhibitory effect was observed on ham covered with film containing 0.025 g chitosan / g starch and 0.195 g carvacrol / g starch. In these products, the cell counts of *L. monocytogenes* were more than 7 log (cfu/cm²) (Fig. 8.5B) when compared to cell counts of *L. monocytogenes* in the absence of antimicrobials and competing microbiota (Fig. 8.5B).

Reconstituted meat microbiota reduced growth of *L. monocytogenes* even in the absence of antimicrobials in the packaging films (Fig. 8.5B). Growth of *L. monocytogenes* was also delayed on ham covered with cull potato starch film containing 0.1 g gallic acid / g starch. More importantly, in combination with the reconstituted meat microbiota, high concentration of gallic acid (0.3 g / g starch), chitosan or carvacrol completely inhibited growth of *L. monocytogenes*,

with *L. monocytogenes* remained detectable in one of the three replicates throughout 4 weeks of storage.

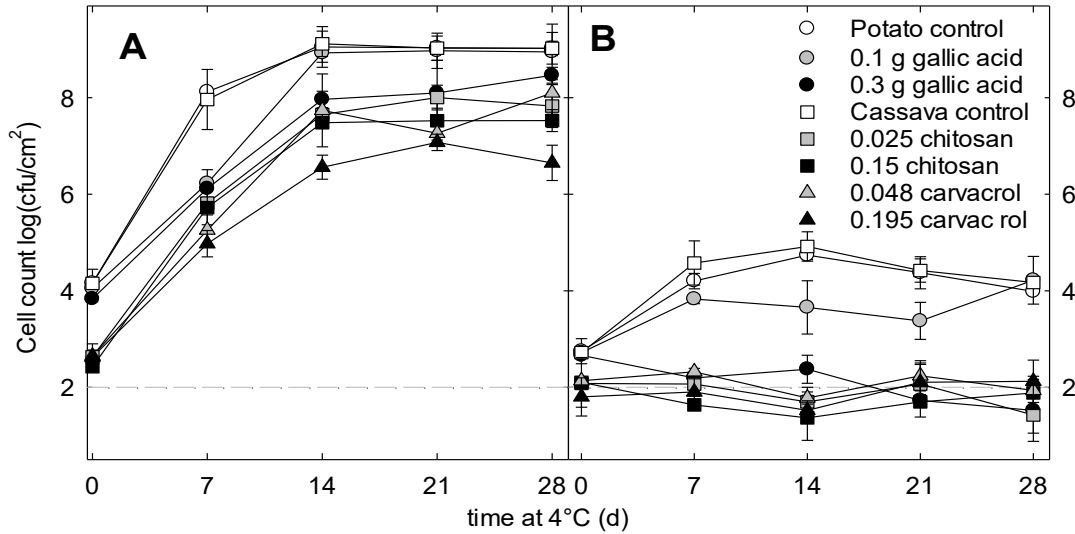


Fig. 8.5 Growth of the mixture of a 5 strain cocktail of reconstituted meat microbiota containing *Brochothrix thermosphacta* FUA3558, *Carnobacterium maltaromaticum* FUA3559, *Leuconostoc gelidum* FUA3560 and FUA3561, and *Lactobacillus sakei* FUA3562 and a 5 strain cocktail of *L. monocytogenes* strains: FSL J1-177, FSL C1-056, FSL N3-013, FSL R2-499, and FSL N1-227 on the surface of cooked ham during storage at 4 °C, bacteria were counted on A) APT and B) PALCAM agar. The ham was covered with a potato starch film (Potato control), or with a cassava starch film (Cassava control), or potato films containing 0.1 g or 0.3 g gallic acid/g starch, or with cassava starch films containing 0.1 g gallic acid/g starch and 0.025 g or 0.15 g chitosan /g starch, or with cassava starch films containing 0.025 g chitosan /g starch and 0.048 g or 0.195 g carvacrol /g starch. Cell counts of un-inoculated ham remained below the detection limit throughout the 4 weeks of storage. Data are means \pm standard deviations of triplicate independent experiments. Symbols crossing the dot line indicate cell counts below the detection limit of 2 log CFU/cm².

8.3.4 Individual strains of reconstituted meat microbiota detection on ham using PCR

Because different bacterial species differ with respect to their impact on product quality, dominant *meat* microbiota on ham at different storage times were identified after isolation of community DNA from the surface of the ham, followed by species-specific or genus-specific PCR (Table 8.3). The primers readily differentiated *B. thermosphacta*, *C. maltaromaticum*, *Lc.*

gelidum and *Lb. sakei*, however, the two strains of *Lc. gelidum* were not differentiated. *Lc. gelidum* was predominant in all populations collected from different antimicrobial packaging films that covered ham. Consistent with the MIC and cell counts data, packaging films with gallic acid had little impact on the composition of meat microbiota. All 4 species that were included in the strain cocktail for reconstitution of meat microbiota were present on the ham covered with gallic acid loaded film after 28 d of storage, however, *C. maltaromaticum* was not detected in all replicates (Table 8.3). In contrast, inclusion of chitosan into starch films inhibited all meat microbiota with exception of *Lc. gelidum*. After 28 d of storage of ham that was covered with any of the films containing chitosan in combination with gallic acid or carvacrol, *Lc. gelidum* was the only organisms that was detected.

Table 8.3. Detection of individual strains in reconstituted meat microbiota stored for 28 days.

Species / Films [antimicrobial]	Potato by- product Control	Cassava Starch Control	Gallic acid (g/g)		Chitosan (g/g) ¹		Carvacrol (g/g) ²	
			0.1	0.3	0.025	0.15	0.048	0.195
<i>Brochothrix thermosphacta</i> FUA3558	+	+	+	+	-	-	-	-/+
<i>Carnobacterium maltaromaticum</i> FUA3559	+	+	+	-/+	-	-	-	-
<i>Leuconostoc gelidum</i> FUA3560	+	+	+	+	+	+	+	+
<i>Leuconostoc gelidum</i> FUA3561	+	+	+	+	+	+	+	+
<i>Lactobacillus sakei</i> FUA3562	+	+	+	+	-	-	-	-/+

Abbreviations: (+) present; (-) absent; (-/+) positive in one of the triplicates.

¹: Cassava starch-based films containing constant gallic acid concentration at 0.1 g /g starch and 0.025 g or 0.15 g chitosan/g starch.

²: Cassava starch-based films containing constant chitosan concentration at 0.025 g /g starch and 0.048 g or 0.195 g carvacrol/g starch.

8.4. Discussion

RTE ham is processed prior to final packaging, and is consumed without further cooking; therefore, contamination with spoilage organisms and pathogens prior to packaging determines the storage life and the safety of the products. Antimicrobial packaging provides an additional hurdle for inhibition of contaminants. Laboratory tests of packaging films with culture media or model foods that are far less complex than actual food systems may not accurately predict the *in situ* inhibitory effect (Dutta et al., 2009; Ramos et al., 2012; Sun et al., 2014b). This study therefore evaluated the MICs of combined antimicrobials and antimicrobial efficiency of bioactive starch films on a meat product. Several natural bioactive agents were effective in laboratory applications but did not show antibacterial activity in food because they were rendered inactive by the specific characteristics of the food and storage conditions (Malhotra, Keshwani & Kharkwal, 2015). Especially for essential oils, whose antimicrobial activity is related to the lipophilicity of themselves that enable essential oils to pass through the cell membrane to react with proteins in cell (Dorman & Deans, 2000) the fat content in food matrix strongly influence their activities by increasing the diffusion path length or sequestering (Weiss, Loeffler & Terjung, 2015). Other components in food, e.g. proteins, may bind phenolic compounds, lowering the amount available for controlling microbial growth (Tassou, Koutsoumanis & Nychas, 2000).

Because different strains of the same species can differ substantially with respect to their sensitivity to antimicrobial interventions, novel food preservation technologies are generally validated with strain cocktails (Hoque, Bari, Juneja & Kawamoto, 2008; Solomakos, Govaris, Koidis & Botsoglou, 2008). Moreover, antimicrobial interventions differentially affect the competitiveness of non-pathogenic meat microbiota (Teixeira et al., 2018), which may influence

spoilage of RTE meats. The strain cocktail used in the present study to reconstitute meat microbiota represents the diversity of spoilage microorganisms that are normally found in RTE meat products. Among 150 bacterial isolates from commercially available RTE meats, *Lc. gelidum*, *C. maltaromaticum*, *Lb. sakei* and *B. thermosphacta* accounted for more of the isolates (Miller et al., 2014). To our knowledge, this is the first study using the combination of *L. monocytogenes* and reconstructed meat microbiota consisting of lactic acid bacteria for antimicrobial film demonstrating.

The cell counts data is in agreement with MICs observations that the reconstituted meat microbiota were less sensitive to all antimicrobials used. Among the three antimicrobials tested, gallic acids showed the poorest antimicrobial activity against both *L. monocytogenes* and reconstituted meat microbiota due to the presence of 3 hydroxyl groups in gallic acid that are bonded to the aromatic ring, increasing the polarity of molecules and reducing their capacity to cross the cell membrane (Sánchez-Maldonado, Schieber & Gänzle, 2011). Poor MIC results (>5 mM) of gallic acid were reported at different pH values of 5 to 7 (Miyague, Macedo, Meca, Holley & Luciano, 2015).

Adding chitosan to starch films showed noticeable complete inhibition of *L. monocytogenes* to less than 100 cfu/cm² (Fig. 8.3). This satisfied the requirements of the regulation in order to guarantee food safety and extend storage life (WHO, 2004). Only few studies applied chitosan into packaging films to control pathogen growth on food products, and the lethality of chitosan is limited at 2 log reduction of cell counts. Earlier, cell counts of *L. monocytogenes* exposed to 0.3% chitosan impregnated LDPE films recovered to 7 log cfu / mL after 12 h exposure (Park, Marsh & Dawson, 2010), and only 0.8 or 1 log cfu / cm² decrease of cell counts of *Listeria innocua* or *L. monocytogenes* were obtained on RTE deli turkey meat or

black radish, respectively, using chitosan films (Guo et al., 2014; Jovanović, Klaus & Niksić, 2016). Even though, *L. monocytogenes* elimination is not necessary and growth inhibition is sufficient when combined with process hygiene, e.g. potassium lactate / sodium diacetate in current RTE meats, which are aiming to extend the lag phase or dormant phase of pathogens and thereby prolonging the shelf life of food products (Stekelenburg & Kant-Muermans, 2001). Therefore, the use of chitosan in starch films in our study demonstrated the potential application on RTE meat to replace chemical preservatives.

In general, gram-positive bacteria were more sensitive to essential oils than gram-negative bacteria, and *L. monocytogenes* strains were among the most sensitive (Gutiérrez, Rodriguez, Barry-Ryan & Bourke, 2008). Even at minimum carvacrol concentration (0.048 g/g starch) applied into the film formulation, carvacrol essential oil showed complete inhibition against *L. monocytogenes*, which was important as higher concentrations could imply a sensorial impact, altering the natural taste of the ham by exceeding the acceptable flavor thresholds. Experiments on the antimicrobial activity of essential oils incorporated packaging film against *L. monocytogenes* in food products have been well documented and interest continues to the present (Sánchez-González et al., 2011). Rosemary and thyme released from the sachet restricted the growth of *L. monocytogenes* on mozzarella cheese, resulting in a 2.5 log cfu / g reduction on day 9 at 10 °C (Han, Patel, Kim & Min, 2014). Chitosan films with 1% and 2% oregano essential decreased the cell count of *L. monocytogenes* on bologna slices by 3.6 to 4 logs (Zivanovic, Chi & Draughon, 2005). But none of them showed complete inhibition of *L. monocytogenes*.

In our study, high reconstituted meat microbiota competed with *L. monocytogenes* and inhibited its growth. Inhibition of *L. monocytogenes* by microbial antagonism of lactic acid bacteria in meat was previously reported (Balay, Dangeti, Kaur & McMullen, 2017; Chaillou et

al., 2014; Woraprayote et al., 2016). Lactic acid bacteria are characterized by their fast growth rates at refrigeration temperatures; nutrient depletion, acid production and the strain-specific production of bacteriocins contributes to inhibition of *L. monocytogenes* (Cornu, Billoir, Bergis, Beaufort & Zuliani, 2011; Woraprayote et al., 2016). These factors make lactic acid bacteria promising biopreservatives for replacement of chemical preservatives, however, some of the lactic acid bacteria also contribute to spoilage by formation of off-odours or slime. Rot or acid odours produced by relatively low cell counts of *B. thermosphacta* decrease consumer acceptance (Vermeiren, Devlieghere, De Graef & Debevere, 2005). *Leucnostoc* species spoil RTE meats by slime production when sucrose is present (Pothakos et al., 2014). In contrast, *Lb. sakei* and *C. maltaromaticum* did not impair sensory attributes or consumer acceptance of RTE meat products (Bredholt, Nesbakken & Holck, 2001; Vermeiren et al., 2005) The present study demonstrates that reconstituted meat microbiota in combination with antimicrobial packaging films inhibited *L. monocytogenes* during 28 d of refrigerated storage. In these products, cell counts of *L. monocytogenes* remains below 100 cfu / cm² and thus satisfied the criteria for safe consumption based on WHO regulations (WHO, 2004). Moreover, it is important in antimicrobial films that the spectrum of inhibited microorganisms be determined. In our study, chitosan-starch films with gallic acid or carvacrol selected *Lc. gelidum* as dominant microorganisms on ham. Increasing use of antimicrobial films may create a situation leading to an ecological imbalance of resistant spoilage microorganisms. *Lc. gelidum* was found to prevail on *Lactobacillus* spp. and *C. maltaromaticum* under refrigeration temperatures, representing up to 81% of the spoilage-related microbial consortium in all spoiled end (Pothakos, Stellato, Ercolini & Devlieghere, 2015), favouring slime production if sucrose presence.

8.5 Conclusions

This challenging antimicrobial test on ham demonstrated the successful use of antimicrobial starch packaging as an important strategy to control reconstituted meat microbiota and foodborne pathogens, particularly for RTE meat products. The cell count test data were coherent with the MIC assay data, where antimicrobial starch films with gallic acid was the least effective antimicrobial. Among all formulations, starch films with chitosan and carvacrol successfully inhibited *L. monocytogenes* growth during the storage period of 4 weeks, with cell counts below 100 cfu / cm² that satisfied the criteria for safe consumption, indicating potential replacement of chemical preservatives. However, the film antimicrobial effect was less significant on reconstituted meat microbiota, resulting in shelf-life extension up to 2 weeks. The dominance of *Lc. gelidum* among other lactic acid bacterial was highlighted.

Chapter 9: Nanogels of Poly-N-isopropylacrylamide, Poly-N,N-diethylacrylamide and Acrylic Acid for Controlled Release of Thymol*

9.1. Introduction

In recent years, active food packaging has attracted considerable attention as they provide antioxidant, antimicrobial and other functional properties (antibrowning, barrier to oxygen, carbon dioxide, and UV–vis light). The incorporation of natural active compounds in packaging systems that can modify the film structure and functionality is required for a number of food applications. The term active packaging and intelligent packaging was first introduced by Regulation 2004/1935/EC of the European Parliament and Council (Parliament, 2004). The difference between the two is that active packaging acts directly with the packaged product to release bioactive compounds to improve the quality of packaged food and extend shelf-life, while intelligent packaging monitors the condition of packaged food or the surrounding environment, for instance providing information on the freshness of the food (Parliament, 2004). Among bioactive compounds, essential oils from plant materials are widely used as antimicrobial agents. Their antimicrobial properties are mainly due to the presence of terpenoids and phenolic compounds (e.g. thymol, carvacrol, eugenol, etc.) (Oussalah, Caillet, Saucier & Lacroix, 2007). Several studies have demonstrated that thymol had high antibacterial activity (Al-Mariri, Swied, Oda & Al Hallab, 2013; Sokolik, Ben-Shabat-Binyamini, Gedanken & Lellouche, 2018). Al-Mariri et al. (2013) reported that thymol had the strongest ability to inhibit the growth of some Gram-negative bacteria, such as *E. coli* O157, *S. typhimurium*, *Klebsiella pneumoniae*, *Yersinia enterocolitica* O9, *Brucella melitensis*, *P. aeruginosa* and *Proteus spp.* (0.375 < minimum inhibitory concentration <1.5 $\mu\text{L}/\text{mL}$). Recently, Sokolik et al. (2018) reported that 0.2-0.4

*A version of this chapter has been published as” Zhao, Y., Sun, W., & Saldaña, M. D. A. (2018). 223 Nanogels of poly-N-isopropylacrylamide, poly-N, N-diethylacrylamide and acrylic acid for controlled release of thymol. Journal of Polymer Research, 25(12), 25

mg/mL thymol encapsulated in bovine serum albumin microsphere completely inhibited *E. coli* within 3 h. However, essential oils are volatile, easily oxidize and have a strong smell that is sometimes unpleasant. Also, the release kinetics of essential oils from the packaging matrix has a significant effect on the antimicrobial activity and potential applications of films in food packaging.

Encapsulation is an efficient approach to increase the physical stability of bioactive compounds and enhance their bioactivity during food processing and storage (Donsì, Annunziata, Sessa & Ferrari, 2011). Moreover, encapsulated antimicrobials can be released in food at a controlled rate to deliver effective inhibitory concentrations over extended time periods and thereby extending shelf-life, often a small amount is needed (< 1-10%), depending on the effectiveness of antimicrobials (Min & Krochta, 2005). After coating cucumber with cinnamon essential oil loaded into chitosan nanoparticles (1.5 g/L), the shelf life of cucumber was estimated as 21 days at 10 °C (Mohammadi, Hashemi & Hosseini, 2015). Also, Fernandes et al. (2017) reported a mesophilic bacteria reduction of 1.36 and 0.73 log cycles after 3 and 15 days of storage, respectively, in Minas Frescal cheese compared to the control, with the application of whey protein isolate and inulin encapsulated rosemary essential oil.

Ready-to-eat foods can be contaminated post processing through contamination from food-contact surfaces. The ideal model of controlled release is to maintain the active agent concentration above the critical effectiveness concentration with respect to the contaminating microorganisms that are likely to be present. According to Ulloa et al. (2017), thymol amounts released from 10 and 20% thymol loaded maltodextrin microcapsules after 2 days were 161 to 172 ppm, respectively, which were sufficient to inhibit *S. cerevisiae*. The release behavior of these antimicrobial agents depended on water diffusion, macromolecular matrix relaxation

kinetics, and active compound diffusion through the swollen polymeric network. Chen et al. (2015) reported twice releasing amount of eugenol than thymol in the first hour due to weaker hydrophobic attraction between eugenol and zein than that of thymol and zein. In addition, a higher releasing amount of *Carum copticum* essential oil was observed in acidic pH (90%) compared to basic or neutral pH (65-75%), which could be attributed to the partial dissolution and swelling property of chitosan nanoparticles due to ionic repulsion of protonated free amino groups (NH_3^+) on chitosan chains (Esmaeili & Asgari, 2015).

The properties of encapsulation material are important factors influencing antimicrobial release. Poly (N-isopropyl acrylamide) (PNIPAM) is a temperature-responsive polymer, which undergoes a phase transition at around 32 °C by changing from hydrated random coil to hydrophobic globule. The temperature in which this phase transition occurs is called the lower critical solution temperature (LCST). The swelling percentage of PNIPAM can be high, over 1000% below 32 °C, but decrease dramatically to less than 30% when the temperature exceeds 40 °C (Carrero, Posada & Sabino, 2018). Polyacrylamides are non-toxic chemicals, but its monomer acrylamide is toxic and can cause peripheral neuropathy (Howland, 1981). One study showed that polyacrylamides were stable at room temperature in the presence of fluorescent lights with no acrylamide or hydrolysis products detected after 15 days (Caulfield et al., 2003). Also, no acrylamide was detected in polyacrylamides subjected to thermal degradation conditions (95 °C). However, hydrolysis of the side chain amides to acid groups occurred. Substantial chain scission by thermal degradation of polyacrylamide occurs at temperatures above 300 °C (Xiong et al., 2018).

PNIPAM nanogels have been largely studied especially in controlled release of drugs and tissue engineering. The copolymer, Poly (*N*-isopropylacrylamide-*co*-*N*-vinyl-2-pyrrolidone), had

a LCST that increased from 30 to 60°C with increasing *N*-vinyl-2-pyrrolidone content (Dincer, Rzaev & Piskin, 2006). Similarly, PNIPAM can have a lower LCST by copolymerization with a hydrophobic monomer of *N*-tert-butylacrylamide (Naha et al., 2009a). When the mole ratio of 50:50 was used, the LCST significantly shifted from 32 °C to ~10 °C. Only a few studies were conducted on poly (*N*, *N*-diethylacrylamide) (PNDEA) even though this polymer behaves similarly as PNIPAM but without the ability to form hydrogen bondings with the oxygen of water because it lacks the proton of the amide group (Shen & Zhang, 2009). However, the narrow and high LCST of PNIPAM limits its application in food packaging. Therefore, the main objective of this study was to develop thermosensitive nanogels using *N*-isopropylacrylamide, with the copolymerization of *N*, *N*-diethylacrylamide and acrylic acid. Then, evaluate control thymol release of the nanogels to prevent microbial contamination.

9.2 Materials and methods

9.2.1 Materials

N-isopropylacrylamide (NIPAM, ≥99% purity), *N,N'*-methylenebisacrylamide (BIS, ≥99.5% purity), sodium dodecyl sulfate (SDS, ≥99% purity), potassium persulfate (KPS, ≥99% purity) aluminum oxide (activated, acidic) and thymol (≥99% purity) were purchased from Sigma-Aldrich (St. Louis, MO, USA) and used without any further purification. *N,N*-diethylacrylamide (NDEA, >98%) purchased from TCI (Tokyo, Japan) and acrylic acid (AA, 99%) purchased from Sigma-Aldrich were purified to eliminate the inhibitor by passing through a column packed with aluminum oxide.

9.2.2 Synthesis of homopolymers and copolymers

Homopolymers of poly *N*-isopropylacrylamide (PNIPAM), poly *N,N*-Diethylacrylamide (PNDEA) and poly acrylic acid (PAA), and copolymers of *N*-isopropylacrylamide-co-acrylic

acid-co-*N,N*-Diethylacrylamide (NIPAM:AA mole ratio of 10:1) at five different molar ratios of co-monomers (100:0, 85:15, 75:25, 65:35 and 50:50 of NIPAM/NDEA) were synthesized by employing the free radical polymerization method. First, certain amounts of monomers reported in Table 9.1 and 26.10 mg of crosslinker (*N,N*-methylenebisacrylamide) were dissolved in 90 mL Milli-Q (MQ) water with 43.94 mg sodium dodecyl sulfate and degassed by bubbling with nitrogen gas for 30 min. Polymerization was induced by adding 64.63 mg potassium persulfate as an initiator in 10 mL MQ water and heating at 70 °C for 4 h. The synthesized nanogel solution was dialyzed with molecular weight cutoff of 12,000 Da against distilled water for 5 days to remove free surfactants and unreacted monomers. The solution was then freeze-dried and nanogels obtained were stored at 4 °C for further use.

Table 9.1 Polymers used for synthesis of nanogels

Name	PNIPAM/PNDEA			
	(molar ratio)	NIPAM (g)	NDEA (μL)	AA (μL)
PNDEA	-	0	1860	0
PNIPAM	-	1.54	0	0
PAA	-	0	0	932
PID100/0	100/0	1.54	0	93.2
PID85/15	85/15	1.309	279	93.2
PID75/25	75/25	1.155	465	93.2
PID65/35	65/35	1.001	651	93.2
PID50/50	50/50	0.77	930	93.2

PID: Polymer of Isopropylacrylamide and Diethylacrylamide

9.2.3 Preparation of thymol-loaded nanogels and self-assembly on chitosan film

Thymol-loaded nanogels were prepared using a self-assembly method previously reported (Duan et al., 2011) with slight modifications. Briefly, polymers (200 mg) and thymol (120 mg) were dispersed in 50 mL ethanol. The mixed solution was stirred at room temperature

for 24 h and then centrifuged at 6580 \times g for 20 min to collect the nanogels. Then, any free thymol was removed from the surface of the nanogels using ethanol by successive centrifugations (6580 \times g, and 5 min, three times) where all washing solutions collected were analyzed for thymol quantification. The resultant thymol-loaded nanogels after three ethanol washings were collected, freeze dried and stored for further use. The amount of thymol encapsulated was calculated from the difference in the concentration of the initial thymol solution loaded and that of the supernatant combined with the three washings. The amount of thymol was determined using the UV spectrophotometer (SpectraMax M3, USA), measuring the absorbance at a wavelength of 275 nm with reference to a freshly prepared calibration curve. Encapsulation efficiency and thymol loading were calculated using the following equations:

$$\text{Encapsulation efficiency (\%)} = \frac{\text{weight of total thymol feed} - \text{weight of free thymol}}{\text{weight of total thymol feed}} \times 100\% \quad (9.1)$$

$$\text{Loading capacity (\%)} = \frac{\text{weight of total thymol feed} - \text{weight of free thymol}}{\text{weight of thymol loaded nanogels}} \times 100\% \quad (9.2)$$

Chitosan film was prepared by casting 50 g of 2 wt% chitosan solution in 2% citric acid with glycerol at 1 g/g chitosan on to 15-cm diameter petri dish and dried at 40 °C for 48 h. Then, the dried film was dipped into the aqueous polymer suspension with or without thymol-loaded (5 mg/mL thymol equivalent). After drying for 30 min, films were washed with water for three times to remove non-grafted polymers.

9.2.4 Thymol release from nanogels

The *in vitro* thymol release behavior from the thymol-loaded nanogels was studied in phosphate buffer solutions at different pH (0.02M, pH = 2, 6 and 8). The selected pH range is common for most food products (e.g. juice, meat products, egg). The freeze-dried nanogels containing 10 mg of thymol were dispersed in 2 mL of different buffer solutions, which was

transferred to a dialysis membrane bag with molecular cutoff of 12,000 Da. Then, the sample-containing bag was immersed in 10 mL buffer solution and kept at 4, 15 and 25 °C with continuously stirring at 150 rpm. At selected time intervals, 1mL of the release medium outside the dialysis bag was withdrawn and an equal volume of fresh buffer solution was added. The amount of thymol in the withdrawn solution was determined using the UV spectrophotometer, measuring the absorbance at 275 nm. Each experiment was performed in triplicate.

9.2.5 Nanogel characterization

9.2.5.1 Particle size measurement

The hydrodynamic diameters (defined by the size of a hypothetical hard sphere that diffuses in the same fashion as that of the particle being measured) of all polymer nanogels in solution were measured using a Malvern Zetasizer Nano-ZS instrument (Malvern, Worcestershire, UK). For a typical determination, solutions were prepared by dissolving the polymer nanogels in MQ water at 4 °C overnight. Approximately 0.7 mL of a 0.1 mg/mL of polymer nanogel in MQ water were analyzed as a function of temperature from 15 to 35°C with a temperature interval of 5 °C. At least 10 min was allowed for each sample temperature to reach equilibrium before any measurement.

When determining the effect of different pH values on particle size, freeze dried nanogels were dissolved in phosphate buffers (0.02 M, pH = 2, 6 and 8) at the concentration of 0.1mg/mL. All measurements were conducted in triplicate.

9.2.5.2 Zeta potential measurement

The zeta potential of particles in MQ water was measured using a Malvern Zetasizer Nano-ZS instrument (Malvern, Worcestershire, UK). The sample preparation for zeta potential measurement was the same as particle size measurement. Although zeta potential values are

affected by temperature, measurements were only conducted at room temperature due to equipment limitation, using a concentration of 0.1 mg/mL, which is within the recommended range so that the particle size is not influenced by concentration. All measurements were performed in triplicate.

9.2.5.3 Fourier transform infrared spectroscopy analysis

Infrared spectra of nanogels were characterized by the Fourier transform infrared spectrometer (FTIR) on a Nicolet 8700 Spectrometer (Thermo Fisher Scientific Inc., Waltham, MA, USA), equipped with a Smart Specular for GATR (Grazing Angle Attenuated Total Reflectance). The freeze-dried nanogels were pressed onto the diamond internal reflection element of the GATR accessory. The experiments were conducted in the range of 4000 to 700 cm^{-1} with a resolution of 2 cm^{-1} and a total of 128 scans per sample. Data collection was done using the Nicolet Omnic 8.3 software.

9.2.5.4. Thermogravimetric analysis (TGA)

The thermal properties of nanogels were measured using a Thermogravimetric Analyzer (TA instrument Q50, New Castle, DE, USA) following a previous method (Hebeish et al., 2014). Decomposition profiles of TGA were recorded at a heating rate of 10 $^{\circ}\text{C}/\text{min}$ between room temperature and 600 $^{\circ}\text{C}$ under nitrogen atmosphere

9.2.5.5 Nuclear magnetic resonance (NMR) measurement

The ^1H NMR spectra were performed on an Agilent/Varian Inova s400 Spectrometer (Santa Clara, CA, USA), operating at a proton frequency of 400 MHz in D_2O at 25 $^{\circ}\text{C}$ (referenced to external acetone at 2.225 ppm).

9.2.5.6 Turbidity or transmittance measurement

Turbidity or transmittance of nanogel polymer solutions (10 mg/mL) was monitored in the temperature range of 8 to 35 °C at 355 nm using a UV-vis spectrophotometer. At least 10 min was allowed for the sample temperature to reach equilibrium. The heating rate used was 0.5 °C/min. Pure MQ water was used as a reference.

When determining the effect of different ions on the LCST, each salt solution at the concentration of 0.15 mol/L was used as a reference. Solutions were prepared by allowing the nanogel polymer to dissolve in purified water at 4 °C overnight. The LCST was determined at the inflection point of the figure plot of transmittance versus temperature. Measurements were performed at least three times for each nanogel polymer.

9.2.5.7 Scanning electron microscopy

Scanning electron microscope (Zeiss Sigma 300 VP-FESEM, Oberkochen, Germany) was used to determine the size and morphology of the dried synthesized nanogels. First, 10 µL of polymer nanogel solution with 1 wt% of aqueous polymer was dropped onto a glass slide and then oven dried at 40 °C for 2 h. Then, the dried samples were mounted on SEM specimen stubs with double-size conductive carbon tape and sputter-coated with carbon (Leica EM SCD005, Richmond Hill, ON, Canada) at 5 kV and 15 mA under low vacuum mode.

9.2.6 Antimicrobial activity measurement

The antimicrobial activity of nanogels loaded with thymol was determined using the *in vitro* agar well diffusion method based on the inhibition zone against two microorganisms. *Bacillus subtilis* FAD 110 and *Escherichia coli* AW 1.7 were kindly provided by Dr. Michael Ganzle's lab at University of Alberta (Edmonton, AB, Canada).

9.2.6.1 Endospores preparation

An endospore suspension of *B. subtilis* was prepared as described earlier (Margosch et al., 2006) with slight modifications. Briefly, *B. subtilis* was grown overnight on the ST1 broth under aerobic conditions. Aliquots of 100 μ L of the overnight culture were streaked onto the ST1 agar and supplemented with MnSO_4 (10 mg/mL). Plates were incubated at 37 $^\circ\text{C}$ and checked daily for the formation of endospores by light microscopy using Gram stain until over 90% of the population had sporulated. The surface of the agar was washed with a sterile saline solution (0.9%). The obtained solution was centrifuged at 2700 \times g for 20 min, and the precipitate was washed with sterile saline solution for 8-10 times to remove residual nutrients and lyse remaining vegetative cell. The concentration of the endospore suspension was adjusted to 10^6 endospores/mL. Endospores were then stored at 4 $^\circ\text{C}$ until further use.

9.2.6.2 Agar well diffusion method

The evaluation of antimicrobial activity of nanogels loaded with thymol against *B. subtilis* and *E. coli* was performed using the agar well diffusion method (Perez, Pauli & Bazerque, 1990; Vásconez, Flores, Campos, Alvarado & Gerschenson, 2009). Briefly, an inoculum of *E. coli* was prepared in LB broth (Becton, Dickinson and Company, Sparks, MD, USA) and incubated at 37 $^\circ\text{C}$ for 18 h. The 100 μ L of *E. coli* inoculum (10^6 CFU/mL) or *B. subtilis* spore suspension (10^6 endospores/mL) was added to 100 mL of temperate (approximately 50 $^\circ\text{C}$) LB agar, yielding an approximate final concentration of 10^4 CFU/mL for *E. coli* or 10^4 endospores/mL for *B. subtilis* endospore. After that, 15 mL of inoculated agar was poured into 9 cm diameter plates. Once the LB agar became solid, three wells of 8 mm diameter were punched into the agar medium by using sterilized cork borers. Wells were filled with 70 μ L of nanogel polymer suspensions loaded with thymol (same mass as the pure thymol solution),

controls of pure ethanol, thymol solution (pure antimicrobial agent, 5 mg/mL, MIC) and nanogel polymer suspensions without thymol. Loaded wells in the petri dishes were then incubated at 37 °C for 18 h. Antimicrobial activity was evaluated by measuring the clear inhibition zone diameters against the test microorganisms in triplicate.

9.3 Results and discussion

9.3.1 PNIPAM-co-PNDEA-co-PAA polymer nanogels

PNIPAM and PNDEA nanogels treated by KPS, an anionic initiator that provides negative charge to polymers, resulted in similar negative zeta potential values of approximately -25 mV. When AA was added to the KPS-treated copolymer nanogels, zeta potentials of PID100/0 to PID50/50 copolymers decreased to around -40 mV due to the deprotonation of carboxylic acid groups in AA. The negative charge of the resultant nanogels allowed self-assembly with the positively charged amino groups of chitosan films.

Fig. 9.1 shows the Fourier transform infrared spectra of the dried polymer nanogels. Characteristic peaks of PNIPAM, PNDEA, and PAA were observed in the different copolymers. In all nanogel polymers except PAA, the amide characteristic peaks at the wavenumbers of 1650 cm^{-1} and 1540 cm^{-1} can be assigned to C=O (amide I) and N-H bonding (amide II), respectively. In addition, a broad band for the NH secondary amide, which is assigned to H-bonded (NH stretching), could be observed at 3400-3100 cm^{-1} (Bajaj, Sreekumar & Sen, 2001; Okudan & Karasakal, 2013). The strong absorption at 1710 cm^{-1} belongs to carbonyl group of PAA. The spectra of copolymers showed the characteristic amide groups at 1650 and 1540 cm^{-1} of PNIPAM, where the carbonyl stretching bonds shifted from 1710 cm^{-1} (PAA) to 1720 cm^{-1} (copolymers). A shift of wavenumber values to higher wavenumber values on the carboxyl group in the copolymers was consistent with previously reported data for hydrogel and

microspheres of PNIPAM/PAA (Burillo, Briones & Adem, 2007; Lai, Wang, Wei, & Li 2016). The intensity of absorption at 1720 cm^{-1} was similar as the same AA concentration was used for the production of copolymer nanogels (PID100/0 to PID50/50). Furthermore, peaks observed at 1455 and 1380 cm^{-1} for copolymer nanogels suggested the presence of $-\text{CH}_2$ and $-\text{CH}_3$ groups in the resultant copolymers, respectively. Also, the characteristic peaks of PNDEA at 1636 and 1540 cm^{-1} assigned to $\text{C}=\text{O}$ were observed (Chen, Liu, Jin, & Liu, 2008; Chen et al., 2010).

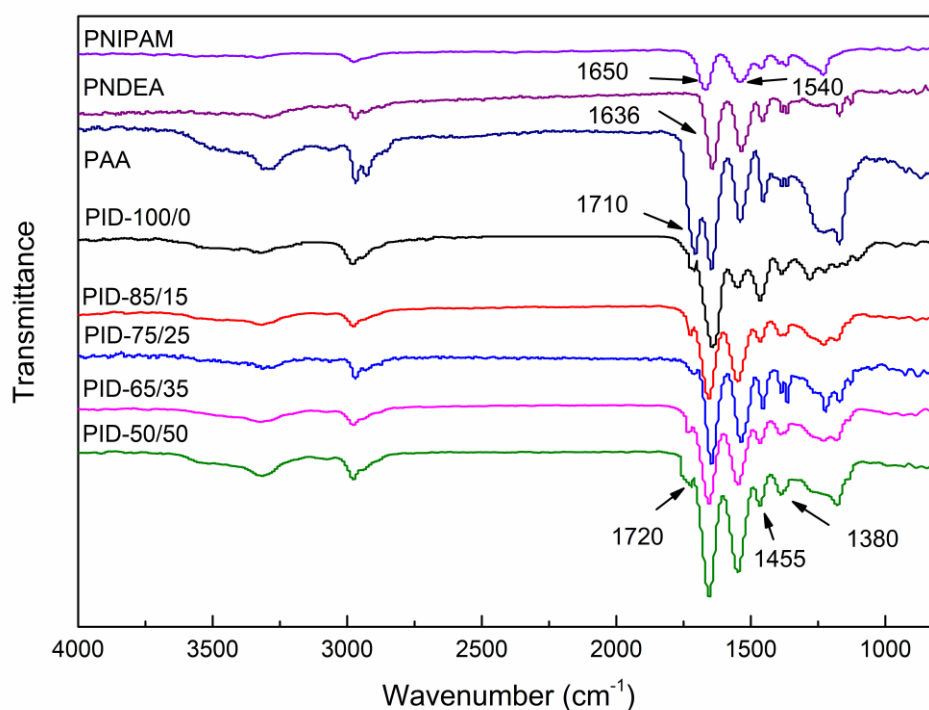


Fig. 9.1 FTIR spectra of polymer nanogels

Fig. 9.2 shows the thermal degradation behavior of nanogels studied in the range of 25–600 °C under nitrogen atmosphere. As observed, the weight loss for PNIPAM and PNDEA in stage one (33-105 °C) indicated the evaporation of adsorbed water. The second stage from 360 to 450°C corresponds to the effective degradation of the polymer due to random chain scission.

With the addition of PAA, PID 100/0 showed additional degradation at lower temperatures of 233-341 °C. The PAA had poor thermal stability, and its thermogravimetric curve exhibited a three-stage degradation process, as previously reported (McNeill & Sadeghi, 1990). The first degradation stage occurred at 180-260 °C that corresponded to the anhydration of the acid. In the second stage, the decomposition of the anhydride with loss of CO₂ was observed between 260 and 360 °C. Then, a significant weight loss was observed between 350 and 450 °C.

The temperatures of maximum degradation for copolymers of PID 85/15 and PID 50/50 were lower than the corresponding homopolymers of PNIPAM (357 °C) and PNDEA (426 °C) as a result of the acrylic acid addition. Similarly, Ruiz-Rubio et al. (2014) reported decreased degradation temperatures of 240 and 230 °C for PNIPAM/PAA and PNDEA/PAA copolymers, respectively. However, the degradation temperature increased from 348 to 355 °C with increasing PNDEA content in our study. This thermal stability is mainly attributed to an increase of the cross-linking. Similar results were reported by Bennour and Louzri (2014), where an increase of degradation temperature from 434 to 485 °C was observed with the increasing ratio of *N,N*-methylenebisacrylamide in poly (*N,N*-dimethylacrylamide-co-maleic acid-co-*N,N*-methylenebisacrylamide) due to the enhanced cross-linking. In addition, the residual weights of copolymers (15-20%) at the end temperature of degradation were higher than those of homopolymers (7-10%). The reason for incomplete degradation of copolymers is probably due to the thermal cross-linking induced by sample heating during thermogravimetric analysis.

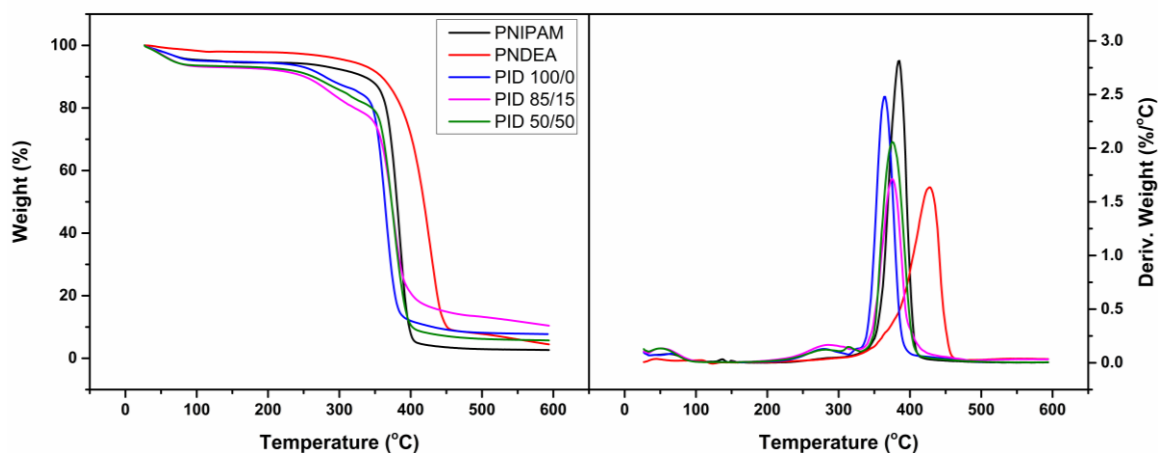


Fig. 9.2 Thermal gravity and derivation analysis (TG-DTG) of nanogel polymers.

Fig. 9.3 shows ^1H NMR spectra of PID 100/0 (a) and PID 50/50 (b) nanogels in D_2O measured at 25 °C. The strong signal at 4.69 ppm is a residual signal of water. In Fig. 9.3a, the peak of six protons of $-(\text{CH}_3)_2$ of PNIPAM appeared at 1.09 ppm (A). The backbone methylene ($-\text{CH}_2-$) and methine ($-\text{CH}-$) protons of the main-chain repeating units of NIPAM can be assigned at 1.51 ppm (B) and 1.95 ppm (C), respectively. The signal of $-\text{CH}-$ and $-\text{CH}_2-$ protons of the acrylic acid units overlapped with $-\text{CH}-$ and $-\text{CH}_2-$ signals of NIPAM units between 1 and 2 ppm. In addition, the characteristic signals of PNIPAM were found at 3.83 ppm (D) and 7.62 ppm (E), attributed to the methane ($-\text{CH}-$) proton of the isopropyl group and proton in $-\text{CONH}$, respectively. Similar findings were reported by Feng et al. (2009), where peaks of methyl ($-(\text{CH}_3)_2$) protons and ($-\text{CH}$) proton of the isopropyl group in PNIPAM block were observed at 1.14 and 4.01 ppm, respectively. Other characteristic peaks of the methyl (1 ppm) and $-\text{CH}$ (3.8 ppm) protons of the isopropyl group, backbone CH_2 (1.5 ppm) and $-\text{CH}$ (1.9 ppm) protons of the main-chain repeating units of NIPAM, and the NH proton (7.7 ppm) of the NIPAM unit were

also observed by Ray et al. (2004). After the addition of PNDEA (Fig. 9.3b), a new peak appeared at 3.28 ppm (F), which was ascribed to the protons in $-NCH_2$ of the NDEA repeating units. This peak was also reported by Spěváček et al. (2001) at 3.3 ppm, corresponding to $-CH_2$ -protons of ethyl groups in the NDEA side chains. The peak intensity (A-D) decreased in Fig. 9.3b due to the reduced PNIPAM portion in PID 50/50 nanogel, therefore, the plot was enlarged and a more evident signal of proton in $-CONH$ (F) can be observed.

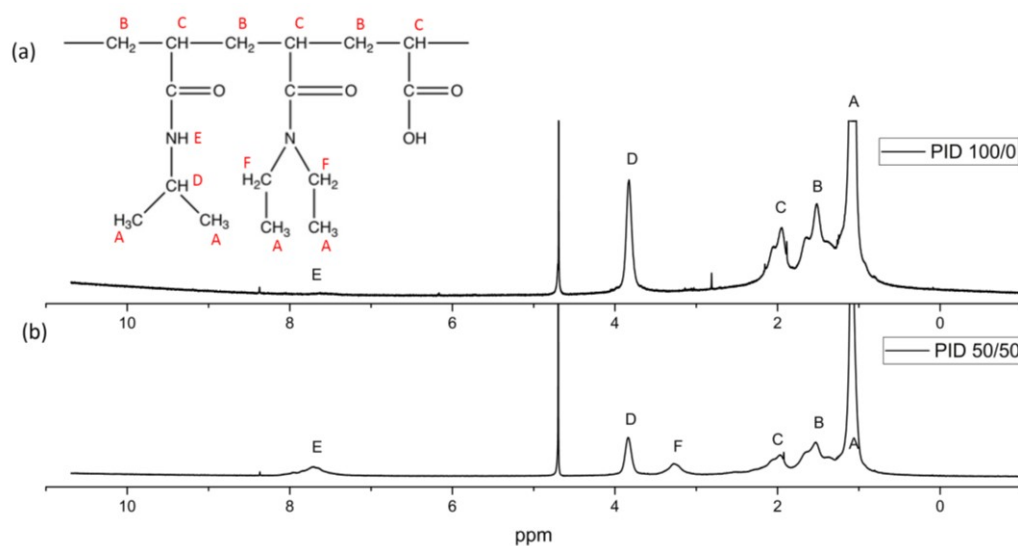


Fig. 9.3 ^1H NMR spectra of: (a) PID 100/0, and (b) PID 50/50 in D_2O . Hydrogen is indicated as “A-F” in the inset and spectra.

Fig. 9.4 shows SEM images of nanogel polymers, and copolymers, and their self-assembly onto the surface of chitosan films. Overall, spherical and uniformly distributed nanogels were observed in Fig. 9.4a-f, h. Besides, the boundary of single nanogel became less distinct morphology of SEM images observed in Fig. 9.4c-f changed due to the increasing content of PNDEA in copolymer nanogels, becoming more similar to the SEM image reported in Fig. 9.4b. Fig. 9.4g and h show the chitosan film before and after self-assembling with PID50/50

nanogels. Results indicated successful and stable self-assembly of nanogels after 3 times of water-washing of polymer nanogels from the chitosan film surface.

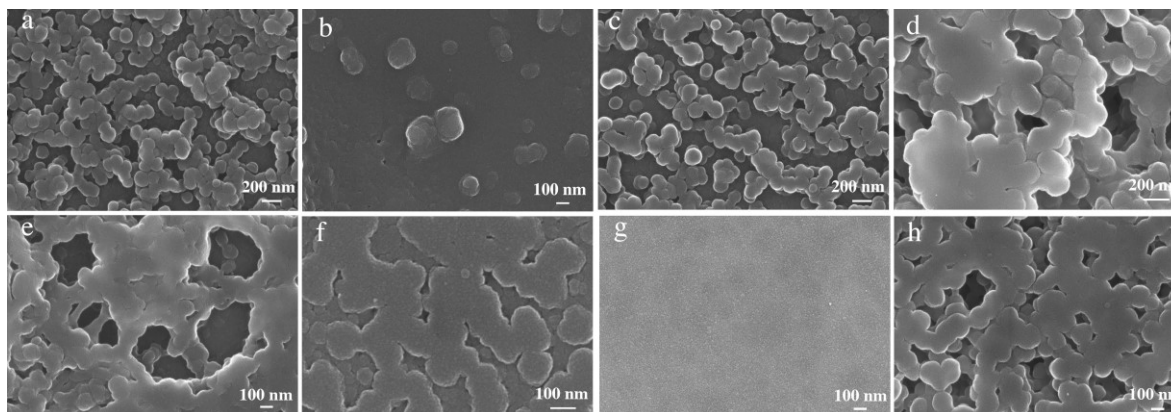


Fig. 9.4 SEM images of nanogels and their self-assembly onto chitosan films: (a) Dried PNIPAM nanogels, (b) Dried PNDEA nanogels, (c) Dried nanogels of PID85/15, (d) Dried nanogels of PID75/25, (e) Dried nanogels of PID65/35, (f) Dried nanogels of PID50/50, (g) Plain chitosan film, and (h) Self-assembled chitosan film with PID 50/50 nanogels

Fig. 9.5 shows the percentage transmittance (%T) measurements of aqueous solutions of polymer nanogels as a function of temperature and the LCST of nanogel copolymers (Table G.1, appendix G). A 100% transmittance was observed for the aqueous PNIPAM nanogels at temperatures below 32 °C (Fig. 9.5a). This result was in agreement with the obtained by Inal et al. (2013) where PNIPAM nanogels were dissolved in water at a temperature below 32 °C. When 10% AA was added to aqueous PNIPAM nanogels, the solution seemed clear without any phase transition, resulting in a 90% transmittance at 8-35 °C. There was no phase transition because PAA has various hydrophilic groups (-COOH) that form strong hydrogen bonding with water molecules. Meanwhile, other strong hydrogen bonds were formed by the PNIPAM amide groups and water molecules, enhancing hydrophilic interactions. PNDEA nanogels showed no sharp phase transition compared to PNIPAM nanogels because of the lack of amide hydrogen in

PNDEA nanogels. PNDEA can only form a single intermolecular hydrogen bond as proton acceptor with water. The structure difference makes the phase transition of PNIPAM nanogels occur abruptly, while that of PNDEA nanogels occurred continuously (Tirumala, Ilavsky & Ilavsky, 2006). With the increasing ratio of NDEA in the PNIPAM/PNDEA copolymers, the LCST range became wider (Fig. 5a). The LCST ranges of PID85/15, PID75/25, PID65/35, and PID50/50 were 20-25 °C, 18-24 °C, 16-23 °C and 8-23 °C, respectively. Interestingly, the LCST of copolymers was even lower than those of PNIPAM and PNDEA, agreeing with the same behaviour reported earlier (Keerl & Richtering, 2007). The highest reduction of LCST was observed at PID50/50 (Fig. 5b), which corresponded to 55 mole % NDEA that had the lowest LCST (McNeill & Sadeghi, 1990). The PID50/50 molar composition suggests strong hydrogen bonding between the PNIPAM and the PNDEA. As NDEA has a strong hydrogen-bonding acceptor group, the copolymerization with NIPAM led to the synergistic behaviour similar to a zipper model.

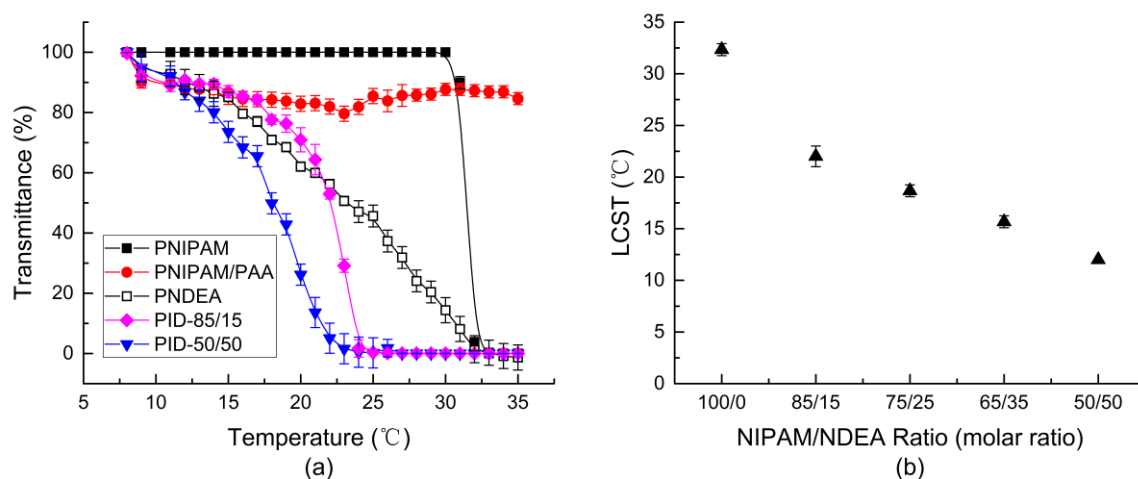


Fig. 9.5 The influence of polymer composition on nanogel transition temperature: (a) Transmittance of polymer nanogels in water as a function of temperature, and (b) LCST of polymer nanogels

Table 9.2 shows the hydrodynamic diameter of the nanogel polymers and copolymers as a function of temperature. The size of PID75/25, PID 65/35 and PID50/50 increased first from 10 to 20 °C followed by a decrease in size from 20 or 25 °C to 30 °C. Temperatures below the LCST had significant influence on the increase of nanogel size due to its swelling and absorption water capacity. After reaching the LCST, the polymer nanogels shrink. Sizes of PID100/0 and PID85/15 nanogels decreased when the temperature increased from 10 to 35 °C, and from 20 to 35 °C, respectively.

No significant change of copolymer particle size occurred in the temperature range of 30 to 35 °C with the exception of the PID85/15, which means that after phase transition (Fig. 9.5), all nanogels precipitated with no significant change in particle size. Phase transition of polymer nanogels is related to the transformation of structure from coil to globule, resulting in the release of antimicrobials from polymer nanogels.

Transparency of PID50/50 nanogels gradually reduced with the increase of temperature from 8 to 23 °C (Fig. 9.5a). This result indicated that PID50/50 had lower and wider LCST range of 8-23 °C. Therefore, the PID50/50 nanogels can be used during food transportation when temperature fluctuates in this range. In addition, the PID50/50 nanogels had high shrinking ability from 921 to 683 nm in water, providing the possibility to release hydrophobic antimicrobials. Polymer nanogels in water (700-1000 nm, Table 9.2) had swollen compared to dried nanogels (100-200 nm, Fig. 9.4), meaning that antimicrobials can be loaded.

Table 9.2 Hydrodynamic diameter of nanogels as a function of temperature (nm).

Polymers	10 °C	20 °C	25 °C	30 °C	35 °C
PNIPAM	492.7 ± 28.3 ^a	464.6 ± 17.0 ^a	421.3 ± 13.4 ^a	284.4 ± 23.8 ^b	152.8 ± 9.1 ^c
PNDEA	532.5 ± 24.2 ^a	418.0 ± 15.4 ^b	410.3 ± 14.3 ^b	310.3 ± 15.1 ^c	190.7 ± 17.1 ^d
PID100/0	849.7 ± 23.8 ^a	808.8 ± 10.3 ^{ab}	792.6 ± 19.7 ^{ab}	785.6 ± 7.2 ^{ab}	753.3 ± 25.9 ^b
PID85/15	874.8 ± 21.1 ^a	638.4 ± 17.1 ^b	552.1 ± 34.4 ^b	354.8 ± 32.2 ^c	238.3 ± 11.7 ^d
PID75/25	266.9 ± 16.3 ^a	1339.4 ± 56.7 ^b	478.6 ± 39.0 ^c	189.5 ± 21.9 ^c	186.6 ± 15.0 ^c
PID65/35	733.3 ± 49.8 ^a	1044.0 ± 82.7 ^a	1066.6 ± 81.6 ^{ab}	802.3 ± 31.5 ^b	852.1 ± 18.8 ^b
PID50/50	807.6 ± 29.6 ^a	921.7 ± 30.5 ^{ab}	920.0 ± 29.1 ^{bc}	704.9 ± 29.6 ^{cd}	678.1 ± 21.9 ^d

^{a-d} Different letters in the same row are statistically different from each other.

Fig. 9.6 shows the effect of different salts on the LCST of copolymer nanogels in aqueous solutions (Table G.2, appendix G). Salts of Na₂CO₃, Na₂SO₄, NaCl, CaCl₂, MgCl₂, KCl, and NH₄Cl at the same concentration of 0.15 mol/L of normal saline were used to investigate the effect of ions (K⁺, Na⁺, NH₄⁺, Ca²⁺, Mg²⁺; SO₄²⁻ and CO₃²⁻), commonly found in meat products, such as pork and beef. The LCST values of all copolymer nanogels were affected by the presence of ions, resulting in salting-out as the LCST value decreased. Overall, anions impacted the phase transition to a greater extent than cations; similar effect was observed when six anions and two cations were investigated to influence LCST of PNIPAM oligomers (Freitag & Garret-Flaudy, 2002). The salting-out effect of ions on copolymer solutions could be explained by two main interactions. First, the ions polarize adjacent water molecules, which are in turn involved in hydrogen bonding formation with amides. Second, the ions interfere with the hydrophobic hydration of polymers by increasing the surface tension around polymer chain backbones and isopropyl side chains. The salting-out effect of ions has been reported and related to the Hofmeister series (Pastoor & Rice, 2015; Zhang, Furyk, Bergbreiter & Cremer, 2005). The LCST values of copolymers changed according to the salt ions used, following the order of K⁺≈Na⁺< NH₄⁺< Ca²⁺≈Mg²⁺; Cl⁻<SO₄²⁻<CO₃²⁻.

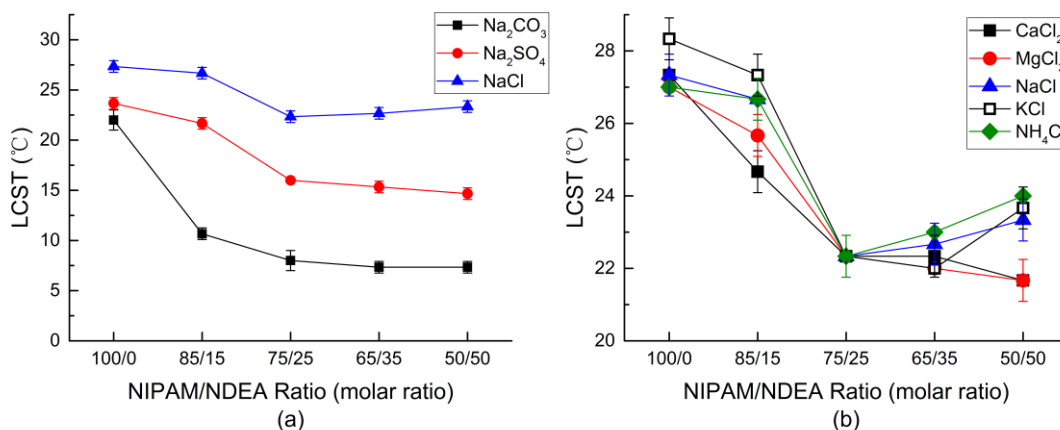


Fig. 9.6 Effect of different salt ions on the LCST of copolymer nanogels in aqueous solutions: (a) anions, and (b) cations

Fig. 9.7 shows the pH effect on the hydrodynamic diameter of polymer and copolymer nanogels. The pH ranges of 2, 6 and 8 were selected as most foods have the pH values varying from 2 to 8. Overall, sizes of polymer and copolymer nanogels were affected by pH. At near neutral pH range (6 to 8), particle sizes of all polymers distributed at approximately 600 to 800 nm, when pH value decreased from 8 to 2, shrink occurred to even around 200 nm, indicating possible antimicrobial release. This phenomenon might be explained as the pH polarizes the adjacent water molecules involved in hydrogen bonding with the polymer. At a lower pH value, more water molecule dissociation occurs, because the electrostatic repulsive force was vanished between the carboxyl groups, causing precipitation of nanogels. As can be observed from Fig. 9.7a and b, a significant shrinkage occurred to PNDEA (< 100nm) when pH value decreased to 2 due to hydrogen bond formation between PNDEA and H₃O⁺, creating enhanced crosslinked network within nanogels. In copolymer nanogels, the addition of PAA led to the formation of

hydrogen bonds between carboxylic acid groups of PAA and amide groups of PNDEA, which also resulted in the shrink of nanogels.

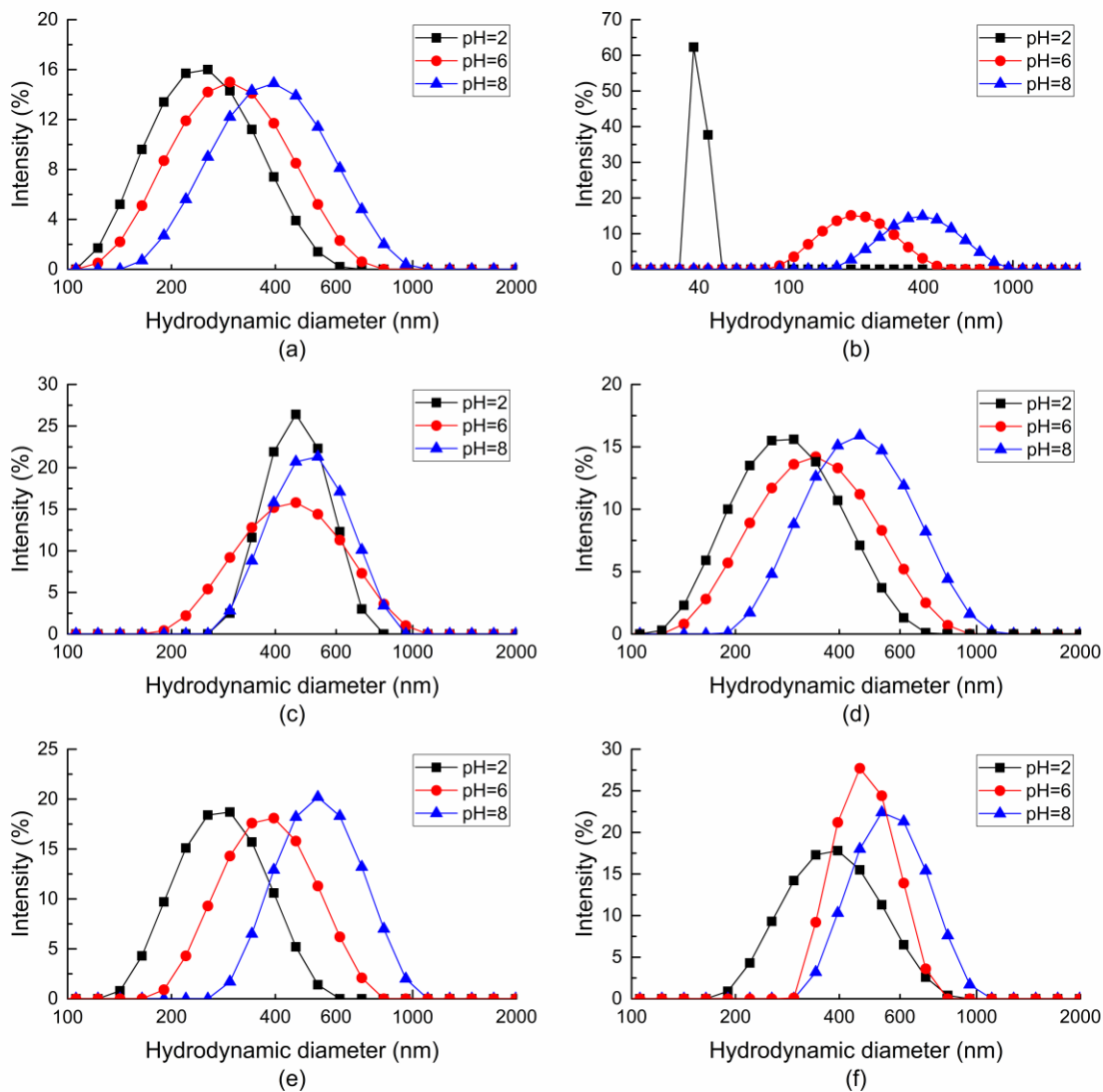


Fig. 9.7 Effect of pH on the diameter of polymer nanogels in aqueous solutions: (a) PNIPAM, (b) PNDEA, (c) PID85/15, (d) PID75/25, (e) PID65/35, and (f) PID50/50

9.3.2 Thymol loading and release from copolymer nanogels

Table 9.3 shows data on polymer nanogels loaded with thymol. Encapsulation efficiency and loading capacity determined using equations 9.1 and 9.2 showed that the PNIPAM polymer had lower encapsulation efficiency ($5.30 \pm 0.19\%$) compared to the copolymers used (5.91 ± 0.42 - $13.03 \pm 0.44\%$). Also, the encapsulation efficiency had a linear relationship with the loading capacity. The highest loading capacity was obtained by PID75/25 nanogels, as it has the highest swelling ratio in water as reported in Table 9.2. Thymol loading into polymer nanogels was significantly affected by the interactions between ethanol used with the thymol and ethanol with the polymer nanogels. Similar low loading capacity (5-10%) of hydrophilic 5-fluorouracil drug was reported using PNIPAM-based polymers as this drug was expelled from the hydrophobic inner core of the core-shell nanoparticles (Lo, Lin & Hsiue, 2005). Therefore, new strategies have been developed to improve drug loading by synthesizing PNIPAM with copolymers. For example, structure modification of PNIPAM-*co*-PAA microgels with unique hollow interior was employed to load doxorubicin hydrochloride. This modification promoted electrostatic interactions between the microgels and the drug molecules, improving drug-loading capacity up to 120% (Chen, Chen, Nan, Wang, & Chu, 2012). Therefore, to improve the loading capacity of thymol into polymer nanogels in our study, a strategy could be to load thymol at temperatures below the LCST of the polymer. The polymer chains could then be swollen in the solvent, allowing thymol to diffuse freely. As the room temperature used in this study was 23 °C, above the LCST, the polymer chains shrunk and formed a compact globule, preventing the loading of thymol.

Table 9.3 Encapsulation efficiency and loading capacity of thymol-loaded homopolymer and copolymer nanogels.

Nanogel	Encapsulation efficiency (%)	Loading capacity (%)
PNIPAM	5.30 ± 0.19 ^c	1.99 ± 0.07 ^c
PID100/0	6.31 ± 0.53 ^c	2.37 ± 0.20 ^c
PID85/15	5.91 ± 0.42 ^c	2.22 ± 0.16 ^c
PID75/25	13.03 ± 0.44 ^a	4.89 ± 0.17 ^a
PID65/35	8.43 ± 0.57 ^b	3.17 ± 0.21 ^b
PID50/50	11.91 ± 0.57 ^a	4.47 ± 0.22 ^b

^{a-c}Different letters in the same column are statistically different from each other.

Fig. 9.8 shows the effect of pH and temperature on thymol release behavior as a function of time (Table G.3, appendix G). Thymol release behavior was different for all polymer nanogels evaluated (data not shown). Fig. 9.8 shows only data for the PID50/50 nanogel due to its wider LCST range and high loading capacity. Thymol release rate from PID50/50 nanogels accelerated with the decrease of pH at the temperatures investigated (Fig. 9.8a and b), resulting in the fastest thymol release at pH of 2. The pH sensitivity of PID50/50 polymer nanogels is also consistent with the pH effect on particle size reported in Fig. 7f.

Nanogels of PID50/50 also showed strong temperature dependency (Fig. 9.8c). The PID50/50 nanogel had the longest thymol release time of more than 24 h at 4 °C. The fastest release at 25 °C occurred at around 4 h with 80% of thymol released due to the shrink of the polymer nanogel. Also, structure change occurred from coil to global form caused by the use of 25 °C, which is above the LCST results obtained earlier (Fig. 9.5a and b). Therefore, the copolymer nanogels loaded with thymol were sensitive to changes of temperature and pH. The

thymol releasing behavior from nanogels has an impact on food packaging applications as food deterioration usually undergoes an acidification process caused by microorganism spoilage, which are facilitated by temperature fluctuation, triggering the release of thymol.

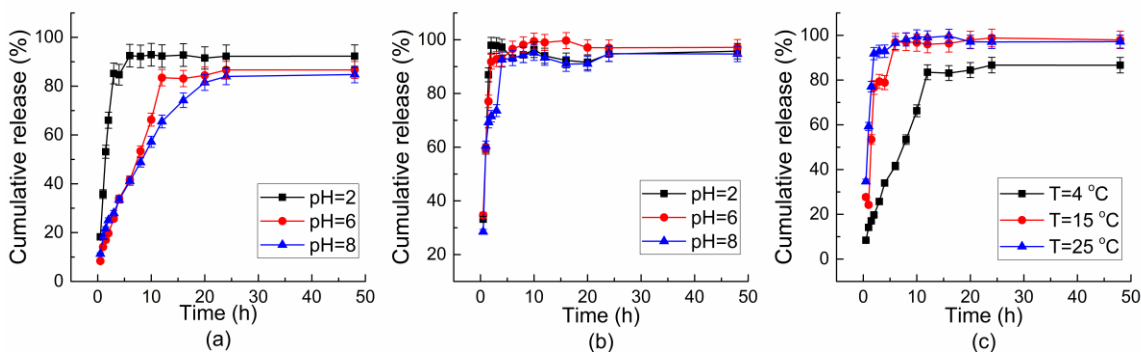


Fig. 9.8 Thymol release behavior of polymer nanogels: (a) PID50/50 at 4 °C, (b) PID50/50 at 25 °C, and (c) PID50/50 at pH 6

9.3.3 Antimicrobial activity of thymol loaded polymer nanogels

In the present study, the antimicrobial activity of pure thymol against *Bacillus subtilis* and *Escherichia coli* was determined before and after being loaded into nanogels (Table 9.4). Thymol-free nanogels were used as the control group. Thymol loaded nanogels exhibited significantly strong antimicrobial activity (12.8 ± 0.3 - 15.0 ± 1.0 mm) against both microorganisms evaluated, showing better activity against *Bacillus subtilis* (Gram-positive) than *Escherichia coli* (Gram-negative) bacteria, while no inhibition was found in the control, consisting of empty nanogels. The inhibition zone diameter of pure thymol in solution (16.1 ± 0.1 - 16.2 ± 0.5 mm) was bigger than the thymol loaded polymer nanogels (11.3 ± 0.2 - 15.0 ± 1.0 mm) as loaded polymer nanogels controlled the release of thymol. All thymol-loaded copolymers resulted in larger inhibition zone than thymol loaded in pure PNIPAM nanogels (Table 9.4).

Table 9.4 Antibacterial activity of thymol loaded nanogels, thymol and thymol-free nanogels against tested microorganisms

Microorganisms	Clear Zone (mm)							Thymol-free nanogels
	PNIPAM	PID 100/0	PID 85/15	PID 75/25	PID 65/35	PID 50/50	Thymol	
<i>E. coli</i>	11.3 ± 0.2 ^e	12.8 ± 0.3 ^d	14.1 ± 0.5 ^b	13.8 ± 0.3 ^{bc}	13.5 ± 0.1 ^{bcd}	13.0 ± 0.3 ^{cd}	16.1 ± 0.1 ^a	NG
<i>B. subtilis</i>	11.9 ± 0.2 ^e	13.5 ± 0.3 ^{cd}	15.0 ± 1.0 ^b	14.4 ± 0.2 ^b	14.0 ± 0.3 ^{bc}	13.7 ± 0.3 ^{cd}	16.2 ± 0.5 ^a	NG

Mean±standard deviation (n=3), NG = no antibacterial effect on visible growth.

Different letters in the same row are statistically different from each other.

After grafting thymol-loaded nanogels onto 8 mm in diameter of chitosan film, the diameter of the clear inhibition zone was the same size as the film alone (~8 mm). There was no expansion of the clear zone using the chitosan films grafted with thymol-loaded nanogels, possibly due to the low loading capacity of thymol nanogels that was not enough to inhibit the growth of the microorganisms evaluated. Another reason is that the diffusion of thymol is limited by the number of layers of nanogels formed onto the film (Fig 9.4h).

9.4. Conclusions

A new series of N-isopropylacrylamide-co-acrylic acid-co-*N,N*-diethylacrylamide nanogels were developed by free radical polymerization. By increasing the ratio of *N,N*-diethylacrylamide in the copolymers, a decrease in the lower critical solution temperature from 33 °C to 10 °C occurred. The synthesized nanogels in water solution exhibited unique thermal, pH and ionic responses. They were more sensitive within the LCST range, with shrinking occurring at pH of 2, and the addition of ions followed the Hofmeister series that influenced particle size of the nanogels. Uniform nanogels were formed within the range of 100 to 200 nm. Thymol successfully loaded into these nanogels was controlled released by changing temperature and pH conditions. The antimicrobial activity against *B. subtilis* and *E. coli* showed that thymol-loaded nanogels had the ability to delay the growth of both bacteria.

Chapter 10: Conclusions and Recommendations

10.1 Conclusions

In this thesis, pressurized hot water technology was explored to obtain bioactive starch-based films with enhanced mechanical and functional properties. Biopolymers of starch and chitosan, and agricultural residues [potato peel/cull and cellulose nanofiber (67.8% purity) from canola straw] were used to form the films. Bioactive compounds (gallic acid and carvacrol) were loaded into the films to tailor film functionality. The first study provided a better understanding of starch and chitosan behavior under pressurized hot water conditions, which set up the foundation of film forming mechanism and formulation. Then, the antimicrobial activity of films was tested on ready to-eat ham. Results showed that bioactive starch-based films obtained by pressurized hot water technology have a promising potential as antimicrobial packaging for food products. In addition, weight loss of bioactive starch-based films was determined as an indication of biodegradability. The major findings of this thesis are the following:

10.1.1 Pressurized hot water hydrolysis of starch and chitosan

The understanding of starch and chitosan behavior in pressurized hot water media is critical to develop starch films. As pressurized hot water media exhibits unique properties like increased ion products (H_3O^+/OH^-), it can hydrolyze and activate functional groups (-OH and NH_2) of starch and chitosan. Also, preserving the chain length of starch and chitosan in pressurized hot water media is essential for network formation. Therefore, the use of high temperatures above 150 °C should be avoided. The effect of pressure on molecular weight was less significant at temperatures above 100 °C especially for chitosan, as the role of pressure was mainly to maintain water in the liquid state. The increased short chain amylose production from cassava starch after pressurized hot water treatment enhanced the availability of amylose for cross-linking with

chitosan through hydrogen bonds, ester linkages and electrostatic interactions, forming starch-chitosan complexes using the cross-linker, gallic acid.

The formation of starch-chitosan complexes with gallic acid demonstrated the network building for complexes, which was crucial to understand starch film formation mechanism under pressurized hot water conditions. There is a need to control the starch/chitosan hydrolysis at a appropriate level to maintain the chain length for film network construction, while maximizing the reactivity of starch and chitosan at the same time. Based on that, potato cull based and cassava starch/chitosan films were developed using different bioactives (gallic acid and carvacrol essential oil).

10.1.2 Potato by-product film with(out) gallic acid

Potato by-products (peel and cull) are generated from the manufacture of potato-based food products in potato processing industry or whole potatoes not desired for human consumption or seed. The use of potato by-products in food packaging films may add value to this residue. Potato cull film loaded with potato peel had high tensile strength up to 9.0 MPa, due to the fiber content of potato peel, reducing free hydroxyl groups in starch by forming hydrogen bonds, thus further lowering film water activity, moisture content and water vapor permeability, however, the presence of fiber in potato peel also induced a poor film homogeneity that was observed by the increased opaqueness and reduced gloss. Even though potato peel is a rich source of phenolic compounds, the highest potato peel loading in our study could not provide enough antioxidant activity because of volume limitation of the reactor. To further improve film antioxidant activity, gallic acid was used. Significant higher antioxidant activity (500-1974 mg Trolox equivalent/g film) was obtained with gallic acid added (0.1-0.3 g/g cull starch) potato cull film compared to the film with potato peel (0.5-1.3 g/g cull, 1.5-93.2 mg Trolox equivalent/g film). Also, gallic

acid added to potato cull film promoted the formation of cross-linking through ester bonds and hydrogen bonds with starch. While due to the hydrophilic nature of gallic acid, the moisture content and film solubility in water increased, indicating less hydrophobic character compared to potato peel added films.

10.1.3 Cassava starch/chitosan film loaded with gallic acid

Even though gallic acid showed strong antioxidant activity, its low antimicrobial activity may not be sufficient enough to control the microbial contamination during food storage. Thus, chitosan, a biopolymer that exhibits high antimicrobial activity, was added to improve film functionality. The addition of gallic acid to cassava starch/chitosan films favored cross-linkings in pressurized hot water media by ester bonds between -COOH groups of gallic acid and $\text{-CH}_2\text{OH}$ groups of starch and chitosan as well as hydrogen bonds between NH_3^+ of the chitosan backbone and -OH of the starch, and electrostatic interactions between COO^- and NH_3^+ . These cross-linkings promoted film hydrophobicity by reducing the availability of -OH in starch and chitosan, as observed by the increase of contact angle and the decrease of water vapor permeability. Moreover, maximum film elongation value of 100% was obtained at 0.1 g chitosan/g starch but it decreased to 65.7% when additional chitosan was added (0.15 g/g starch) due to the cross-links that limited chain mobility.

10.1.4 Cassava starch/chitosan film loaded with carvacrol essential oil and biodegradability

In addition to chitosan, carvacrol essential oil also exhibits high antimicrobial activity. The starch/chitosan film with carvacrol incorporated can also benefit from the phenol structure of carvacrol, contributing to the antioxidant activity. More importantly, the incorporation of this hydrophobic compound may improve the film hydrophobicity. Therefore, the addition of

carvacrol (0-0.195 g/g starch) to cassava starch/chitosan film was investigated. Also, the weight loss as an indication of film biodegradability was confirmed using the compost burial method.

The pressurized hot water media acted as a catalyst, promoting cross-linkings through ester linkages of carvacrol essential oil and starch/chitosan. But, cross-linkings are influenced by the carvacrol concentration, which is hydrophobic. Hence, incorporation of carvacrol at a low concentration reduced the water vapor permeability of the film and film solubility in water, while high concentrations produced coarser film matrix structure, resulting in increase of water vapor permeability, moisture content, water activity and film solubility in water. The non-continuous film structure introduced by carvacrol addition also influenced film mechanical properties, lowering both film tensile strength and elongation.

For film biodegradability test, potato by-product films exhibited longer degradation time of 85 days compared to cassava starch-based films (45 days) due to the presence of fiber in potato peel, which is more resistance to microorganisms attack than starch.

10.1.5 Cassava starch/chitosan film loaded with gallic acid and cellulose nanofiber

Based on the above studies, all cassava starch-based films exhibited relatively low tensile strength (<1 MPa), thus to further enhance film mechanical strength, cellulose nanofibers (CNFs, 63.1% purity) was added to cassava starch/chitosan/gallic acid film. As expected, significant improvement of film tensile strength was obtained with the increasing CNFs content in films, due to the high crystallinity of cellulose and formation of hydrogen bonds between cassava starch and cellulose. These intensive cross-linkings also contributed to the reduced moisture content, water activity, film solubility in water and water vapor permeability. However, CNFs (63.1% purity) at concentrations above 0.05 g/g starch led to bumpy surfaces and less transparent

films with yellowish color due to the residual lignin content (20.0%) and hemicellulose content (7.7%).

10.1.6 Film antimicrobial activity against *Listeria monocytogenes* and reconstructed meat microbiota

The most commonly used *in vitro* experiment (e.g. disc diffusion) cannot provide comprehensive and accurate prediction of film antimicrobial efficiency due to the simplicity of agar media compared to food systems. Therefore, the antimicrobial activity of bioactive starch films was examined on RTE ham to mimic the real application.

Cassava starch-based films with either chitosan or carvacrol completely inhibited *L. monocytogenes* on ham to less than 100 cfu/cm² during storage up to 4 weeks at 4 °C, suggesting an elimination of food safety concerns caused by *L. monocytogenes* contamination and extending ham storage life using those natural bioactives. Even though gallic acid showed the least antimicrobial effect against both *L. monocytogenes* and reconstructed meat microbiota, with gallic acid in potato cull film, competitive meat microbiota prevented growth of *L. monocytogenes* by more than 2 log (cfu/cm²).

10.1.7 Nanoparticles loaded with essential oil for film grafting

The limited compatibility of hydrophobic essential oil to hydrophilic starch film matrix restricted the loading of essential oil, and to better preserve the essential oil from degradation due to its high reactivity and minimize the unpleasant sensorial impact caused by the strong flavor, the encapsulation of essential oil using thermosensitive poly(N-isopropylacrylamide) based nanogel was investigated.

The low critical solution temperature of poly(N-isopropylacrylamide) was tailored by copolymerization with poly *N,N*-diethylacrylamide and acrylic acid, exhibiting multi-response

with regards to temperature (10-33 °C), pH (2-8) and ions (K^+ , Na^+ , NH_4^+ , Ca^{2+} , Mg^{2+} ; SO_4^{2-} and CO_3^{2-}), which can trigger bioactive release at various food storage conditions. Using thymol essential oil as an example, the extended thymol releasing was achieved up to 24 h at 4°C. Further grafting of thymol-loaded nanogels onto chitosan films displayed the potential application of such nanogels in food packaging materials, preventing the direct addition in food products that may lead to safety concerns. Moreover, the agar diffusion test indicated potential antimicrobial activity of thymol loaded nanogels against *E. coli* and *B. subtilis*.

Overall, throughout research in this thesis, bioactive starch-based films were successfully developed using a green approach, pressurized hot water technology. The film properties were enhanced through cross-linking and modification by incorporating different bioactive compounds (gallic acid, chitosan and carvacrol). The weight loss as an indication of film biodegradability makes them promising packaging materials to replace non-biodegradable plastics and address increasing environmental concerns. Also, the antimicrobial tests on ham demonstrated the effectiveness of bioactive starch films, suggesting possible food packaging applications on various food products.

10.2 Recommendations

Further characterization of cassava starch and chitosan treated in pressurized hot water media at 75-150 °C and 50-155 bar with respect to molecular weight using size exclusion chromatography can provide molecular weight distribution, average degree of branching, average chain length and branching ratio of treated sample. Especially for starch, this information can provide better understanding of amylose-amylopectin interactions in pressurized hot water media and the influence of molecular weight and branching on composite formation, such as complex and film (Chapter 3).

Even though gallic acid has high antioxidant activity, it exhibited the lowest antimicrobial activity against both *Listeria* and reconstructed meat microbiota based on antimicrobial test performed in this thesis. Therefore, the use of other phenolic acid like cinnamic acid (MICs of 0.07-0.79 g/L) with stronger antimicrobial activity than gallic acid (MICs of 0.64-4.56 g/L) can be investigated (Chapter 4).

The essential oil used in this thesis was pure carvacrol (purity > 99%), which is the main compound after extraction and purification from essential oil mixtures of oregano. Thus, the use of oregano essential oil (~63-68% carvacrol, ~8-13% p-cymene and ~12% as main components) widely available on the market could be effective, avoiding the purification process. And, other components in oregano essential oil (thymoquinone and p-cymene), may lead to synergetic effect with carvacrol on inhibiting microorganism growth in food products. However, the heterogenous structure and phase separation of essential oil from the starch matrix during film drying is still a challenge when a high amount of essential oil (>0.098 g/g starch) was incorporated even in the presence of an emulsifier (20 w/w% lecithin), therefore, fast drying rates at temperatures above 40 °C should be investigated. To better understand the release of carvacrol from the film, a control release study of carvacrol as a function of time, temperature and pH is recommended.

Even though starch films are known to have low oxygen permeability (<1 cm³ μm/m² d kPa), further determination of film oxygen permeability is necessary for determining final film application, especially for fruit and vegetables that require gas exchange during storage. Oxygen permeability also influences the species of microorganisms (aerobic or an aerobic) predominant in meat product. In addition, thermogravimetric analysis is recommended to evaluate the thermal stability of starch-based films (Chapters 4, 5 and 6).

Perform biodegradability tests on cassava starch/chitosan/gallic acid films incorporated with CNFs and compare with the biodegradability of the other films. A more comprehensive study could be performed using controlled compost with a known formulation or known microorganisms. For example, a controlled compost following ISO 14855-2 standard has used wood blocks for growing mushrooms and chicken droppings composted for 7 months. Model microorganisms used in biodegradation are *Rhodococcus rhodochrous* (bacterium) and *Cladosporium cladosporoides* (fungus). Future study on O₂/CO₂ evolution tests, degradation products (glucose) or bacterial and fungal biomass in soil can reflect the activity of microorganisms, indicating the beginning and termination of biodegradation. Moreover, characterization of film structural properties (SEM, XRD and FT-IR) and mechanical properties by sampling every 10 days can provide data on film deterioration during biodegradation (Chapter 6).

In this thesis, cellulose nanofiber (63.1% purity) was added to starch-based films to improve film mechanical and water barrier properties. As cellulose nanofiber purity was 63.1% due to the use of PAE (20%) treatment, other components were lignin (20.0%) and hemicellulose (7.7%) that influenced film properties. More research should be performed to investigate the effect of lignin content using bleached cellulose nanofiber (>90% purity) (Chapter 7).

Atomic force microscopy is recommended for determining the film surface roughness.

The antimicrobial films developed can be used on different food products, like hot dogs that are currently coated with cellulose casings, which requires mechanical strength of < 10 MPa. The unique antimicrobial activity of starch-based films developed can further ensure food safety by extending shelf-life of these products. The regular shape of cheese or sausages ensures the sufficient surface contact with film, maximizing film antimicrobial efficiency. In addition, the

starch films developed can serve as a carrier for non-food applications of slow release of a fertilizer like urea to the crop field. The urea production of Canada reached 1021 metric tonnes in 2018, and typically canola and flax are fertilized with urea at 10-40 lb/ac depending on the soil moisture (8-50%). Current direct addition of urea to soil has only a plant uptake of urea below 50% due to the surface runoff, leaching and vaporization (Chapter 8).

To improve the essential oil loading capacity in nanogels, a polymer:essential oil of 1:1 w/w ratio can be used at a low temperature of 4 °C, as poly(N-isopropylacrylamide)/N,N-diethylacrylamide nanogels are in a coil structure with more space for loading. Due to the safety concern of breaking poly(N-isopropylacrylamide) and poly(N,N-diethylacrylamide) to acrylamide in food packaging, biopolymers such as chitosan can be used as the encapsulating material of essential oil. Then, comparison of both nanogels on encapsulation efficiency and releasing behavior can be performed. Additionally, the application of nanogel can be further investigated by surface grafting using plasma, limiting nanogel migration to food products (Chapter 9).

References

- Abreu, A. S., Oliveira, M., de Sá, A., Rodrigues, R. M., Cerqueira, M. A., Vicente, A. A., & Machado, A. (2015). Antimicrobial nanostructured starch based films for packaging. *Carbohydrate Polymers*, *129*, 127-134.
- Acioli-Moura, R., & Sun, X. S. (2008). Thermal degradation and physical aging of poly (lactic acid) and its blends with starch. *Polymer Engineering & Science*, *48*(4), 829-836.
- Acosta, S., Chiralt, A., Santamarina, P., Rosello, J., González-Martínez, C., & Cháfer, M. (2016). Antifungal films based on starch-gelatin blend, containing essential oils. *Food Hydrocolloids*, *61*, 233-240.
- Addis, M. (2015). Major causes of meat spoilage and preservation techniques: A review. *Food Science and Quality Management*, *41*, 101-114.
- Adnan, D. N. B. Pg. & Arshad, S. E. (2017). Effect of thermal treatment on mechanical properties rice husk ash filled tapioca starch composite. *Transactions on Science and Technology*, *4*(3-2), 286-291.
- Ahmad, N., Ahmad, I., Umar, S., Iqbal, Z., Samim, M., & Ahmad, F. J. (2016). PNIPAM nanoparticles for targeted and enhanced nose-to-brain delivery of curcuminoids: UPLC/ESI-Q-ToF-MS/MS-based pharmacokinetics and pharmacodynamic evaluation in cerebral ischemia model. *Drug Delivery*, *23*(7), 2095-2114.
- Ahmed, J., Tiwari, B. K., Imam, S. H., & Rao, M. (Eds.). (2012). *Starch-based polymeric materials and nanocomposites: Chemistry, processing, and applications* (1st ed.). New York: CRC Press.
- Aida, T. M., Oshima, K., Abe, C., Maruta, R., Iguchi, M., Watanabe, M., & Smith Jr, R. L. (2014). Dissolution of mechanically milled chitin in high temperature water. *Carbohydrate Polymers*, *106*, 172-178.
- Akiya, N., & Savage, P. E. (2002). Roles of water for chemical reactions in high-temperature water. *Chemical Reviews*, *102*(8), 2725-2750.
- Albarran, G., Boggess, W., Rassolov, V., & Schuler, R. H. (2010). Absorption spectrum, mass spectrometric properties, and electronic structure of 1, 2-benzoquinone. *The Journal of Physical Chemistry A*, *114*(28), 7470-7478.
- Alberta Agriculture and Forestry. (2017). Consumer Corner-updates from the Competitiveness and Market Analysis Section, [http://www1.agric.gov.ab.ca/\\$department/deptdocts.nsf/all/sis](http://www1.agric.gov.ab.ca/$department/deptdocts.nsf/all/sis).

- Alemdar, A., & Sain, M. (2008). Isolation and characterization of nanofibers from agricultural residues—Wheat straw and soy hulls. *Bioresource Technology*, *99*(6), 1664-1671.
- Al-Mariri, A., Swied, G., Oda, A., & Al Hallab, L. (2013). Antibacterial activity of thymus syriacus boiss essential oil and its components against some syrian gram-negative bacteria isolates. *Iranian Journal of Medical Sciences*, *38*(2), 180-186.
- Almeida, N., Rakesh, L., & Zhao, J. (2014). Phase behavior of concentrated hydroxypropyl methylcellulose solution in the presence of mono and divalent salt. *Carbohydrate Polymers*, *99*, 630-637.
- Alotaibi, S., & Tahergorabi, R. (2018). Development of a sweet potato starch-based coating and its effect on quality attributes of shrimp during refrigerated storage. *LWT-Food Science and Technology*, *88*, 203-209.
- Alvarez, V. H., Cahyadi, J., Xu, D., & Saldaña, M. D. A. (2014). Optimization of phytochemicals production from potato peel using subcritical water: Experimental and dynamic modeling. *The Journal of Supercritical Fluids*, *90*, 8-17.
- Andrade, M. M. P., de Oliveira, C. S., Colman, T. A. D., da Costa, F. J. O. G. & Schnitzler, E. (2014). Effects of heat–moisture treatment on organic cassava starch. *Journal of Thermal Analysis and Calorimetry*, *115*(3), 2115-2122.
- Andrews, B. (1993). Carbohydrates and carbohydrate polymers: Analysis, biotechnology, modification, antiviral, biomedical and other applications. In Y. Manssur (Ed.), *Frontiers in biomedicine and biotechnology*, Atl Pr Scientific Pub.
- Arismendi, C., Chillo, S., Conte, A., Del Nobile, M. A., Flores, S., & Gerschenson, L. N. (2013). Optimization of physical properties of xanthan gum/tapioca starch edible matrices containing potassium sorbate and evaluation of its antimicrobial effectiveness. *LWT-Food Science and Technology*, *53*(1), 290-296.
- Arrieta, M. P., Peltzer, M. A., del Carmen Garrigós, M., & Jiménez, A. (2013). Structure and mechanical properties of sodium and calcium caseinate edible active films with carvacrol. *Journal of Food Engineering*, *114*(4), 486-494.
- Arslan, B., & Soyer, A. (2018). Effects of chitosan as a surface fungus inhibitor on microbiological, physicochemical, oxidative and sensory characteristics of dry fermented sausages. *Meat Science*, *145*, 107-113.
- Arthur, C., Baker, J. E., & Bamford, H. A. (2009). Paper presented at the *Proceedings of the International Research Workshop on the Occurrence, Effects, and Fate of Microplastic Marine Debris*, University of Washington Tacoma, Tacoma, WA, USA.

- Atef, M., Rezaei, M., & Behrooz, R. (2015). Characterization of physical, mechanical, and antibacterial properties of agar-cellulose bionanocomposite films incorporated with savory essential oil. *Food Hydrocolloids*, 45, 150-157.
- Ayana, B., Suin, S., & Khatua, B. (2014). Highly exfoliated eco-friendly thermoplastic starch (TPS)/poly (lactic acid)(PLA)/clay nanocomposites using unmodified nanoclay. *Carbohydrate Polymers*, 110, 430-439.
- Azevedo, H. S., Gama, F. M., & Reis, R. L. (2003). *In vitro* assessment of the enzymatic degradation of several starch based biomaterials. *Biomacromolecules*, 4(6), 1703-1712.
- Babaei, M., Jonoobi, M., Hamzeh, Y., & Ashori, A. (2015). Biodegradability and mechanical properties of reinforced starch nanocomposites using cellulose nanofibers. *Carbohydrate Polymers*, 132, 1-8.
- Bajaj, P., Sreekumar, T., & Sen, K. (2001). Effect of reaction medium on radical copolymerization of acrylonitrile with vinyl acids. *Journal of Applied Polymer Science*, 79(9), 1640-1652.
- Balay, D. R., Dangeti, R. V., Kaur, K., & McMullen, L. M. (2017). Purification of leucocin A for use on wieners to inhibit listeria monocytogenes in the presence of spoilage organisms. *International Journal of Food Microbiology*, 255, 25-31.
- Bangyekan, C., Aht-Ong, D., & Srikulkit, K. (2006). Preparation and properties evaluation of chitosan-coated cassava starch films. *Carbohydrate Polymers*, 63(1), 61-71.
- Basiak, E., Lenart, A., & Debeaufort, F. (2017a). Effect of starch type on the physico-chemical properties of edible films. *International Journal of Biological Macromolecules*, 98, 348-356.
- Basiak, E., Lenart, A., & Debeaufort, F. (2017b). Effects of carbohydrate/protein ratio on the microstructure and the barrier and sorption properties of wheat starch–whey protein blend edible films. *Journal of the Science of Food and Agriculture*, 97(3), 858-867.
- Basiak, E., Linke, M., Debeaufort, F., Lenart, A., & Geyer, M. (2019). Dynamic behaviour of starch-based coatings on fruit surfaces. *Postharvest Biology and Technology*, 147, 166-173.
- Bellés, M., Alonso, V., Roncalés, P., & Beltrán, J. A. (2018). Sulfite-free lamb burger meat: Antimicrobial and antioxidant properties of green tea and carvacrol. *Journal of the Science of Food and Agriculture*, doi:10.1002/jsfa.9208
- Ben Arfa, A., Combes, S., Preziosi-Belloy, L., Gontard, N., & Chalier, P. (2006). Antimicrobial activity of carvacrol related to its chemical structure. *Letters in Applied Microbiology*, 43(2), 149-154.

- Bennour, S., & Louzri, F. (2014). Study of swelling properties and thermal behavior of poly (N, N-dimethylacrylamide-co-maleic acid) based hydrogels. *Advances in Chemistry*, 2014 doi:10.1155/2014/147398
- Benzie, I. F., & Strain, J. J. (1996). The ferric reducing ability of plasma (FRAP) as a measure of “antioxidant power”: The FRAP assay. *Analytical Biochemistry*, 239(1), 70-76.
- Bergueiro, J., & Calderón, M. (2015). Thermoresponsive nanodevices in biomedical applications. *Macromolecular Bioscience*, 15(2), 183-199.
- Beverly, R. L., Janes, M. E., Prinyawiwatkula, W., & No, H. K. (2008). Edible chitosan films on ready-to-eat roast beef for the control of *listeria monocytogenes*. *Food Microbiology*, 25(3), 534-537.
- Biji, K., Ravishankar, C., Mohan, C., & Gopal, T. S. (2015). Smart packaging systems for food applications: A review. *Journal of Food Science and Technology*, 52(10), 6125-6135.
- Biliarderis, C. (1992). Structure and phase transitions of starch in food system. *Food Technology*, 46, 98-109.
- Bof, M. J., Jiménez, A., Locaso, D. E., Garcia, M. A., & Chiralt, A. (2016). Grapefruit seed extract and lemon essential oil as active agents in corn starch–chitosan blend films. *Food and Bioprocess Technology*, 9(12), 2033-2045.
- Bonilla, J., Talón, E., Atarés, L., Vargas, M., & Chiralt, A. (2013). Effect of the incorporation of antioxidants on physicochemical and antioxidant properties of wheat starch–chitosan films. *Journal of Food Engineering*, 118(3), 271-278.
- Borah, P. P., Das, P., & Badwaik, L. S. (2017). Ultrasound treated potato peel and sweet lime pomace based biopolymer film development. *Ultrasonics Sonochemistry*, 36, 11-19.
- Borch, E., Kant-Muermans, M., & Blixt, Y. (1996). Bacterial spoilage of meat and cured meat products. *International Journal of Food Microbiology*, 33(1), 103-120.
- Bourtoom, T. (2008). Edible films and coatings: Characteristics and properties. *International Food Research Journal*, 15(3), 237-248.
- Bourtoom, T., & Chinnan, M. S. (2008). Preparation and properties of rice starch–chitosan blend biodegradable film. *LWT-Food Science and Technology*, 41(9), 1633-1641.
- Božič, M., Gorgieva, S., & Kokol, V. (2012). Laccase-mediated functionalization of chitosan by caffeic and gallic acids for modulating antioxidant and antimicrobial properties. *Carbohydrate Polymers*, 87(4), 2388-2398.

- Bredholt, S., Nesbakken, T., & Holck, A. (2001). Industrial application of an antilisterial strain of *lactobacillus sakei* as a protective culture and its effect on the sensory acceptability of cooked, sliced, vacuum-packaged meats. *International Journal of Food Microbiology*, 66(3), 191-196.
- Bröll, D., Kaul, C., Krämer, A., Krammer, P., Richter, T., Jung, M., . . . Zehner, P. (1999). Chemistry in supercritical water. *Angewandte Chemie International Edition*, 38(20), 2998-3014.
- Brun-Graepi, A. K. A. S., Richard, C., Bessodes, M., Scherman, D., Narita, T., Ducouret, G., & Merten, O. (2010). Study on the sol-gel transition of xyloglucan hydrogels. *Carbohydrate Polymers*, 80(2), 555-562.
- Brunner, G. (2009). Near critical and supercritical water. part I. hydrolytic and hydrothermal processes. *The Journal of Supercritical Fluids*, 47(3), 373-381.
- Burillo, G., Briones, M., & Adem, E. (2007). IPN's of acrylic acid and N-isopropylacrylamide by gamma and electron beam irradiation. *Nuclear Instruments and Methods in Physics Research Section B: Beam Interactions with Materials and Atoms*, 265(1), 104-108.
- Caetano, K. d. S., Hessel, C. T., Tondo, E. C., Flôres, S. H., & Cladera-Olivera, F. (2017). Application of active cassava starch films incorporated with oregano essential oil and pumpkin residue extract on ground beef. *Journal of Food Safety*, 37(4)
doi:10.1111/jfs.12355
- Carrero, M. G., Posada, J. J., & Sabino, M. A. (2018). Intelligent copolymers based on poly (N-isopropylacrylamide) PNIPAm with potential use in biomedical applications. part i: PNIPAm functionalization with 3-butenic acid and piperazine. *International Journal of Advances in Medical Biotechnology-IJAMB*, 1(1), 23-31.
- Caulfield, M. J., Hao, X., Qiao, G. G., & Solomon, D. H. (2003). Degradation on polyacrylamides. Part I. Linear polyacrylamide. *Polymer*, 44(5), 1331-1337.
- Chaillou, S., Christieans, S., Rivollier, M., Lucquin, I., Champomier-Verges, M., & Zagorec, M. (2014). Quantification and efficiency of *lactobacillus sakei* strain mixtures used as protective cultures in ground beef. *Meat Science*, 97(3), 332-338.
- Chan, C., Gan, R., Shah, N. P., & Corke, H. (2018). Polyphenols from selected dietary spices and medicinal herbs differentially affect common food-borne pathogenic bacteria and lactic acid bacteria. *Food Control*, 92, 437-443.
- Chang, Y., Karim, A. A., & Seow, C. (2006). Interactive plasticizing-antiplasticizing effects of water and glycerol on the tensile properties of tapioca starch films. *Food Hydrocolloids*, 20(1), 1-8.

- Charmley, E., Nelson, D., & Zvomuya, F. (2006). Nutrient cycling in the vegetable processing industry: Utilization of potato by-products. *Canadian Journal of Soil Science*, 86(4), 621-629.
- Che, L., Li, D., Wang, L., Özkan, N., Chen, X. D., & Mao, Z. (2007). Effect of high-pressure homogenization on the structure of cassava starch. *International Journal of Food Properties*, 10(4), 911-922.
- Cheetham, N. W., & Tao, L. (1998). Variation in crystalline type with amylose content in maize starch granules: An X-ray powder diffraction study. *Carbohydrate Polymers*, 36(4), 277-284.
- Cheigh, C., Yoo, S., Ko, M., Chang, P., & Chung, M. (2015). Extraction characteristics of subcritical water depending on the number of hydroxyl group in flavonols. *Food Chemistry*, 168, 21-26.
- Chen, C., Kuo, W., & Lai, L. (2009). Effect of surfactants on water barrier and physical properties of tapioca starch/decolorized hsian-tsaio leaf gum films. *Food Hydrocolloids*, 23(3), 714-721.
- Chen, D., Lawton, D., Thompson, M., & Liu, Q. (2012). Biocomposites reinforced with cellulose nanocrystals derived from potato peel waste. *Carbohydrate Polymers*, 90(1), 709-716.
- Chen, G., & Liu, B. (2016). Cellulose sulfate based film with slow-release antimicrobial properties prepared by incorporation of mustard essential oil and β -cyclodextrin. *Food Hydrocolloids*, 55, 100-107.
- Chen, H., Zhang, Y., & Zhong, Q. (2015). Physical and antimicrobial properties of spray-dried zein-casein nanocapsules with co-encapsulated eugenol and thymol. *Journal of Food Engineering*, 144, 93-102.
- Chen, J., Liu, M., Jin, S., & Liu, H. (2008). Synthesis and characterization of κ -carrageenan/poly (N, n-diethylacrylamide) semi-interpenetrating polymer network hydrogels with rapid response to temperature. *Polymers for Advanced Technologies*, 19(11), 1656-1663.
- Chen, J., Liu, M., Liu, H., Ma, L., Gao, C., Zhu, S., & Zhang, S. (2010). Synthesis and properties of thermo- and pH-sensitive poly (diallyldimethylammonium chloride)/poly (N, N-diethylacrylamide) semi-IPN hydrogel. *Chemical Engineering Journal*, 159(1), 247-256.
- Chen, W., Yu, H., Liu, Y., Chen, P., Zhang, M., & Hai, Y. (2011). Individualization of cellulose nanofibers from wood using high-intensity ultrasonication combined with chemical pretreatments. *Carbohydrate Polymers*, 83(4), 1804-1811.

- Chen, Y., Chen, Y., Nan, J., Wang, C., & Chu, F. (2012). Hollow poly (n-isopropylacrylamide)-co-poly (acrylic acid) microgels with high loading capacity for drugs. *Journal of Applied Polymer Science*, 124(6), 4678-4685.
- Chiumarelli, M., & Hubinger, M. D. (2012). Stability, solubility, mechanical and barrier properties of cassava starch–Carnauba wax edible coatings to preserve fresh-cut apples. *Food Hydrocolloids*, 28(1), 59-67.
- Ciftci, D., & Saldaña, M. D. A. (2015). Hydrolysis of sweet blue lupin hull using subcritical water technology. *Bioresource Technology*, 194, 75-82.
- Colivet, J., & Carvalho, R. (2017). Hydrophilicity and physicochemical properties of chemically modified cassava starch films. *Industrial Crops and Products*, 95, 599-607.
- Colussi, R., Pinto, V. Z., El Halal, S. L. M., Biduski, B., Prietto, L., Castilhos, D. D., da Rosa Zavareze, E. & Dias, A. R. G. (2017). Acetylated rice starches films with different levels of amylose: Mechanical, water vapor barrier, thermal, and biodegradability properties. *Food Chemistry*, 221, 1614-1620.
- Cornu, M., Billoir, E., Bergis, H., Beaufort, A., & Zuliani, V. (2011). Modeling microbial competition in food: Application to the behavior of *listeria monocytogenes* and lactic acid flora in pork meat products. *Food Microbiology*, 28(4), 639-647.
- Corti, A., Muniyasamy, S., Vitali, M., Imam, S. H., & Chiellini, E. (2010). Oxidation and biodegradation of polyethylene films containing pro-oxidant additives: Synergistic effects of sunlight exposure, thermal aging and fungal biodegradation. *Polymer Degradation and Stability*, 95(6), 1106-1114.
- Cruz-Gálvez, A., Castro-Rosas, J., Rodríguez-Marín, M., Cadena-Ramírez, A., Tellez-Jurado, A., Tovar-Jiménez, X., . . . Gómez-Aldapa, C. (2018). Antimicrobial activity and physicochemical characterization of a potato starch-based film containing acetic and methanolic extracts of hibiscus sabdariffa for use in sausage. *LWT- Food Science and Technology*, 93, 300-305.
- Cyras, V. P., Manfredi, L. B., Ton-That, M., & Vázquez, A. (2008). Physical and mechanical properties of thermoplastic starch/montmorillonite nanocomposite films. *Carbohydrate Polymers*, 73(1), 55-63.
- da Rosa, C. G., Borges, C. D., Zambiasi, R. C., Nunes, M. R., Benvenuti, E. V., da Luz, S. R., D'Avila, R. F. & Rutz, J. K. (2013). Microencapsulation of gallic acid in chitosan, β -cyclodextrin and xanthan. *Industrial Crops and Products*, 46, 138-146.
- Dang, K. M., & Yoksan, R. (2015). Development of thermoplastic starch blown film by incorporating plasticized chitosan. *Carbohydrate Polymers*, 115, 575-581.

- Dang, K. M., & Yoksan, R. (2016). Morphological characteristics and barrier properties of thermoplastic starch/chitosan blown film. *Carbohydrate Polymers*, *150*, 40-47.
- Das, D. K., Dutta, H., & Mahanta, C. L. (2013). Development of a rice starch-based coating with antioxidant and microbe-barrier properties and study of its effect on tomatoes stored at room temperature. *LWT-Food Science and Technology*, *50*(1), 272-278.
- Das, D., & Pal, S. (2015). Modified biopolymer-dextrin based crosslinked hydrogels: Application in controlled drug delivery. *RSC Advances*, *5*(32), 25014-25050.
- Das, K., Ray, D., Bandyopadhyay, N., Gupta, A., Sengupta, S., Sahoo, S., Mohanty, A. & Misra, M. (2010). Preparation and characterization of cross-linked starch/poly (vinyl alcohol) green films with low moisture absorption. *Industrial & Engineering Chemistry Research*, *49*(5), 2176-2185.
- Davoodi, M., Kavooosi, G., & Shakeri, R. (2017). Preparation and characterization of potato starch-thymol dispersion and film as potential antioxidant and antibacterial materials. *International Journal of Biological Macromolecules*, *104*, 173-179.
- de Aquino, A.B., Blank, A. F., & de Aquino Santana, L. C. L. (2015). Impact of edible chitosan–cassava starch coatings enriched with lippia gracilis schauer genotype mixtures on the shelf life of guavas (*psidium guajava L.*) during storage at room temperature. *Food Chemistry*, *171*, 108-116.
- de Araújo, Grace Kelly P, de Souza, S. J., da Silva, M. V., Yamashita, F., Gonçalves, O. H., Leimann, F. V., & Shirai, M. A. (2015). Physical, antimicrobial and antioxidant properties of starch-based film containing ethanolic propolis extract. *International Journal of Food Science & Technology*, *50*(9), 2080-2087.
- Delcour, J. A., Bruneel, C., Derde, L. J., Gomand, S. V., Pareyt, B., Putseys, J. A., . . . Lamberts, L. (2010). Fate of starch in food processing: From raw materials to final food products. *Annual Review of Food Science and Technology*, *1*, 87-111.
- Dias, A. B., Müller, C. M., Larotonda, F. D., & Laurindo, J. B. (2010). Biodegradable films based on rice starch and rice flour. *Journal of Cereal Science*, *51*(2), 213-219.
- Dincer, S., Rzaev, Z. M., & Piskin, E. (2006). Synthesis and characterization of stimuli-responsive poly (N-isopropylacrylamide-co-N-vinyl-2-pyrrolidone). *Journal of Polymer Research*, *13*(2), 121-131.
- Donsì, F., Annunziata, M., Sessa, M., & Ferrari, G. (2011). Nanoencapsulation of essential oils to enhance their antimicrobial activity in foods. *LWT-Food Science and Technology*, *44*(9), 1908-1914.

- Dorman, H., & Deans, S. G. (2000). Antimicrobial agents from plants: Antibacterial activity of plant volatile oils. *Journal of Applied Microbiology*, *88*(2), 308-316.
- Drider, D., Fimland, G., Hechard, Y., McMullen, L. M., & Prevost, H. (2006). The continuing story of class IIa bacteriocins. *Microbiology and Molecular Biology Reviews*, *70*(2), 564-582.
- Du, Y. L., Cao, Y., Lu, F., Li, F., Cao, Y., Wang, X. L., & Wang, Y. Z. (2008). Biodegradation behaviors of thermoplastic starch (TPS) and thermoplastic dialdehyde starch (TPDAS) under controlled composting conditions. *Polymer Testing*, *27*(8), 924-930.
- Duan, C., Zhang, D., Wang, F., Zheng, D., Jia, L., Feng, F., . . . Wang, F. (2011). Chitosan-g-poly (N-isopropylacrylamide) based nanogels for tumor extracellular targeting. *International Journal of Pharmaceutics*, *409*(1), 252-259.
- Durán, E., León, A., Barber, B., & de Barber, C. B. (2001). Effect of low molecular weight dextrans on gelatinization and retrogradation of starch. *European Food Research and Technology*, *212*(2), 203-207.
- Dutta, P., Tripathi, S., Mehrotra, G., & Dutta, J. (2009). Perspectives for chitosan based antimicrobial films in food applications. *Food Chemistry*, *114*(4), 1173-1182.
- Ebara, M., Yamato, M., Hirose, M., Aoyagi, T., Kikuchi, A., Sakai, K., & Okano, T. (2003). Copolymerization of 2-carboxyisopropylacrylamide with N-isopropylacrylamide accelerates cell detachment from grafted surfaces by reducing temperature. *Biomacromolecules*, *4*(2), 344-349.
- El Halal, S. L. M., Colussi, R., Deon, V. G., Pinto, V. Z., Villanova, F. A., Carreño, N. L. V., Dias, A.R.G & da Rosa Zavareze, E. (2015). Films based on oxidized starch and cellulose from barley. *Carbohydrate Polymers*, *133*, 644-653.
- El Halal, S. L., Bruni, G. P., do Evangelho, J. A., Biduski, B., Silva, F. T., Dias, A. R., da Rosa Zavareze, E. & de Mello Luvielmo, M. (2018). The properties of potato and cassava starch films combined with cellulose fibers and/or nanoclay. *Starch-Stärke*, *70*
doi:10.1002/star.201700115
- El Miri, N., Abdelouahdi, K., Barakat, A., Zahouily, M., Fihri, A., Solhy, A., & El Achaby, M. (2015). Bio-nanocomposite films reinforced with cellulose nanocrystals: Rheology of film-forming solutions, transparency, water vapor barrier and tensile properties of films. *Carbohydrate Polymers*, *129*, 156-167.
- Emiroğlu, Z. K., Yemiş, G. P., Coşkun, B. K., & Candoğan, K. (2010). Antimicrobial activity of soy edible films incorporated with thyme and oregano essential oils on fresh ground beef patties. *Meat Science*, *86*(2), 283-288.

- Esfanjani, A. F., & Jafari, S. M. (2016). Biopolymer nano-particles and natural nano-carriers for nano-encapsulation of phenolic compounds. *Colloids and Surfaces B: Biointerfaces*, *146*, 532-543.
- Esmaeili, A., & Asgari, A. (2015). *In vitro* release and biological activities of carum copticum essential oil (CEO) loaded chitosan nanoparticles. *International Journal of Biological Macromolecules*, *81*, 283-290.
- Espíndola-Cortés, A., Moreno-Tovar, R., Bucio, L., Gimeno, M., Ruvalcaba-Sil, J. L., & Shirai, K. (2017). Hydroxyapatite crystallization in shrimp cephalothorax wastes during subcritical water treatment for chitin extraction. *Carbohydrate Polymers*, *172*, 332-341.
- Fakhouri, F. M., Martelli, S. M., Caon, T., Velasco, J. I., & Mei, L. H. I. (2015). Edible films and coatings based on starch/gelatin: Film properties and effect of coatings on quality of refrigerated red crimson grapes. *Postharvest Biology and Technology*, *109*, 57-64.
- Farber, J. M., & Peterkin, P. I. (1991). *Listeria monocytogenes*, a food-borne pathogen. *Microbiological Reviews*, *55*(3), 476-511.
- Feil, H., Bae, Y. H., Feijen, J., & Kim, S. W. (1993). Effect of comonomer hydrophilicity and ionization on the lower critical solution temperature of N-isopropylacrylamide copolymers. *Macromolecules*, *26*(10), 2496-2500.
- Feng, C., Shen, Z., Li, Y., Gu, L., Zhang, Y., Lu, G., & Huang, X. (2009). PNIPAM-b-(PEA-g-PDMAEA) double-hydrophilic graft copolymer: Synthesis and its application for preparation of gold nanoparticles in aqueous media. *Journal of Polymer Science Part A: Polymer Chemistry*, *47*(7), 1811-1824.
- Fernandes, Regiane Victória de Barros, Guimarães, I. C., Ferreira, C. L. R., Botrel, D. A., Borges, S. V., & de Souza, A. U. (2017). Microencapsulated rosemary (*rosmarinus officinalis*) essential oil as a biopreservative in minas frescal cheese. *Journal of Food Processing and Preservation*, *41*(1), e12759.
- Flory, P. J. (1942). Thermodynamics of high polymer solutions. *The Journal of chemical physics*, *10*(1), 51-61.
- Fonseca, L. M., Gonçalves, J. R., El Halal, S. L. M., Pinto, V. Z., Dias, A. R. G., Jacques, A. C., & da Rosa Zavareze, E. (2015). Oxidation of potato starch with different sodium hypochlorite concentrations and its effect on biodegradable films. *LWT-Food Science and Technology*, *60*(2), 714-720.
- Forssell, P., Lahtinen, R., Lahelin, M., & Myllärinen, P. (2002). Oxygen permeability of amylose and amylopectin films. *Carbohydrate Polymers*, *47*(2), 125-129.

- Foulk, J. A., & Bunn, J. M. (2007). Factors influencing the duration of lag phase during in vitro biodegradation of compression-molded, acetylated biodegradable soy protein films. *Journal of Food Engineering*, 79(2), 438-444.
- Fourati, Y., Tarrés, Q., Mutjé, P., & Boufi, S. (2018). PBAT/thermoplastic starch blends: Effect of compatibilizers on the rheological, mechanical and morphological properties. *Carbohydrate Polymers*, 199, 51-57.
- Franco, M. J., Martin, A. A., Bonfim Jr, L. F., Caetano, J., Linde, G. A., & Dragunski, D. C. (2017). Effect of plasticizer and modified starch on biodegradable films for strawberry protection. *Journal of Food Processing and Preservation*, 41(4) doi:10.1111/jfpp.13063
- Freitag, R., & Garret-Flaudy, F. (2002). Salt effects on the thermoprecipitation of poly-(N-isopropylacrylamide) oligomers from aqueous solution. *Langmuir*, 18(9), 3434-3440.
- FSIS, USDA. (1989). Revised policy for controlling listeria monocytogenes. *Food Safety and Inspection Service, US Dept. of Agriculture, Washington, DC Federal Register*, 54, 22345-22346.
- Fuciños, C., Fuciños, P., Míguez, M., Katime, I., Pastrana, L. M., & Rúa, M. L. (2014). Temperature- and pH-sensitive nanohydrogels of poly (N-isopropylacrylamide) for food packaging applications: Modelling the swelling-collapse behaviour. *PLoS One*, 9(2) doi:10.1371/journal.pone.0087190
- Fugett, E., Fortes, E., Nnoka, C., & Wiedmann, M. (2006). International life sciences institute north america listeria monocytogenes strain collection: Development of standard listeria monocytogenes strain sets for research and validation studies. *Journal of Food Protection*, 69(12), 2929-2938.
- Fung, D. Y. C. (2009). Food spoilage, preservation and quality control. In: Schaechter, M. (Ed.), *Encyclopedia of microbiology*. 3rd edn. Elsevier, New York, pp. 54-79.
- Gao, Y., Ahiabu, A., & Serpe, M. J. (2014). Controlled drug release from the aggregation–disaggregation behavior of pH-responsive microgels. *ACS Applied Materials & Interfaces*, 6(16), 13749-13756.
- Garcia, P. S., Grossmann, M. V. E., Yamashita, F., Mali, S., Dall'Antonia, L. H., & Barreto, W. J. (2011). Citric acid as multifunctional agent in blowing films of starch/PBAT. *Química Nova*, 34(9), 1507-1510.
- Gattin, R., Copinet, A., Bertrand, C., & Couturier, Y. (2002). Biodegradation study of a starch and poly (lactic acid) co-extruded material in liquid, composting and inert mineral media. *International Biodeterioration & Biodegradation*, 50(1), 25-31.

- Gautam, N., & Kaur, I. (2013). Soil burial biodegradation studies of starch grafted polyethylene and identification of rhizobium meliloti therefrom. *Journal of Environmental Chemistry and Ecotoxicology*, 5(6), 147-158.
- Ghanbari, A., Tabarsa, T., Ashori, A., Shakeri, A., & Mashkour, M. (2018). Thermoplastic starch foamed composites reinforced with cellulose nanofibers; thermal and mechanical properties. *Carbohydrate Polymers*, 197, 305-311.
- Ghasemlou, M., Aliheidari, N., Fahmi, R., Shojaee-Aliabadi, S., Keshavarz, B., Cran, M. J., & Khaksar, R. (2013). Physical, mechanical and barrier properties of corn starch films incorporated with plant essential oils. *Carbohydrate Polymers*, 98(1), 1117-1126.
- Ghoreishi, S., & Shahrestani, R. G. (2009). Subcritical water extraction of mannitol from olive leaves. *Journal of Food Engineering*, 93(4), 474-481.
- Giello, M., La Stora, A., De Filippis, F., Ercolini, D., & Villani, F. (2018). Impact of *lactobacillus curvatus* 54M16 on microbiota composition and growth of *listeria monocytogenes* in fermented sausages. *Food Microbiology*, 72, 1-15.
- Gilbert-López, B., Plaza, M., Mendiola, J. A., Ibáñez, E., & Herrero, M. (2018). Subcritical water extraction and neoformation of antioxidants. *Water extraction of bioactive compounds* (pp. 109-130) Elsevier.
- Gómez-Estaca, J., De Lacey, A. L., López-Caballero, M., Gómez-Guillén, M., & Montero, P. (2010). Biodegradable gelatin–chitosan films incorporated with essential oils as antimicrobial agents for fish preservation. *Food Microbiology*, 27(7), 889-896.
- Guarda, A., Rubilar, J. F., Miltz, J., & Galotto, M. J. (2011). The antimicrobial activity of microencapsulated thymol and carvacrol. *International Journal of Food Microbiology*, 146(2), 144-150.
- Gunaratne, A., & Hoover, R. (2002). Effect of heat–moisture treatment on the structure and physicochemical properties of tuber and root starches. *Carbohydrate Polymers*, 49(4), 425-437.
- Guo, M., Jin, T. Z., Wang, L., Scullen, O. J., & Sommers, C. H. (2014). Antimicrobial films and coatings for inactivation of *listeria innocua* on ready-to-eat deli turkey meat. *Food Control*, 40, 64-70.
- Guohua, Z., Ya, L., Cuilan, F., Min, Z., Caiqiong, Z., & Zongdao, C. (2006). Water resistance, mechanical properties and biodegradability of methylated-cornstarch/poly (vinyl alcohol) blend film. *Polymer Degradation and Stability*, 91(4), 703-711.

- Gutiérrez, J., Rodríguez, G., Barry-Ryan, C., & Bourke, P. (2008). Efficacy of plant essential oils against foodborne pathogens and spoilage bacteria associated with ready-to-eat vegetables: Antimicrobial and sensory screening. *Journal of Food Protection*, 71(9), 1846-1854.
- Gutiérrez, T. J., Tapia, M. S., Pérez, E., & Famá, L. (2015). Structural and mechanical properties of edible films made from native and modified cush-cush yam and cassava starch. *Food Hydrocolloids*, 45, 211-217.
- Han, J. H., Patel, D., Kim, J. E., & Min, S. C. (2014). Retardation of *listeria monocytogenes* growth in mozzarella cheese using antimicrobial sachets containing rosemary oil and thyme oil. *Journal of Food Science*, 79(11), 2272-2278.
- Harini, K., Mohan, C. C., Ramya, K., Karthikeyan, S., & Sukumar, M. (2018a). Effect of *punica granatum* peel extracts on antimicrobial properties in walnut shell cellulose reinforced bi-thermoplastic starch films from cashew nut shells. *Carbohydrate Polymers*, 184, 231-242.
- Harini, K., Ramya, K., & Sukumar, M. (2018b). Extraction of nano cellulose fibers from the banana peel and bract for production of acetyl and lauroyl cellulose. *Carbohydrate Polymers*, 201, 329-339.
- Hebeish, A., Farag, S., Sharaf, S., & Shaheen, T. I. (2014). Thermal responsive hydrogels based on semi interpenetrating network of poly (NIPAm) and cellulose nanowhiskers. *Carbohydrate Polymers*, 102, 159-166.
- Hereu, A., Bover-Cid, S., Garriga, M., & Aymerich, T. (2012). High hydrostatic pressure and biopreservation of dry-cured ham to meet the food safety objectives for *listeria monocytogenes*. *International Journal of Food Microbiology*, 154(3), 107-112.
- Hietala, M., Mathew, A. P., & Oksman, K. (2013). Bionanocomposites of thermoplastic starch and cellulose nanofibers manufactured using twin-screw extrusion. *European Polymer Journal*, 49(4), 950-956.
- Homayouni, H., Kavooosi, G., & Nassiri, S. M. (2017). Physicochemical, antioxidant and antibacterial properties of dispersion made from tapioca and gelatinized tapioca starch incorporated with carvacrol. *LWT-Food Science and Technology*, 77, 503-509.
- Hoover, R., & Ratnayake, W. (2002). Starch characteristics of black bean, chick pea, lentil, navy bean and pinto bean cultivars grown in Canada. *Food Chemistry*, 78(4), 489-498.
- Hoover, R. (2001). Composition, molecular structure, and physicochemical properties of tuber and root starches: A review. *Carbohydrate Polymers*, 45(3), 253-267.
- Hoque, M. M., Bari, M., Juneja, V. K., & Kawamoto, S. (2008). Antimicrobial activity of cloves and cinnamon extracts against food borne pathogens and spoilage bacteria and inactivation

- of *listeria monocytogenes* in ground chicken meat with their essential oils. *Food Research International*, 72, 9-21.
- Horita, C. N., Baptista, R. C., Caturla, M. Y., Lorenzo, J. M., Barba, F. J., & Sant'Ana, A. S. (2018). Combining reformulation, active packaging and non-thermal post-packaging decontamination technologies to increase the microbiological quality and safety of cooked ready-to-eat meat products. *Trends in Food Science & Technology*, 72, 45-61.
- Horwitz, W. (2000). In Horwitz W. (Ed.), *Official methods of analysis of AOAC international* (17th ed.) Gaithersburg, Md. : AOAC International.
- Hosseini, S. F., Rezaei, M., Zandi, M., & Farahmandghavi, F. (2016). Development of bioactive fish gelatin/chitosan nanoparticles composite films with antimicrobial properties. *Food Chemistry*, 194, 1266-1274.
- Howland, R. D. (1981). The etiology of acrylamide neuropathy: enolase, phosphofructokinase, and glyceraldehyde-3-phosphate dehydrogenase activities in peripheral nerve, spinal cord, brain, and skeletal muscle of acrylamide-intoxicated cats. *Toxicology and applied pharmacology*, 60(2), 324-333.
- Huerta, R. R., & Saldaña, M. D. A. (2018a). Biorefining of canola straw using pressurized aqueous ethanol: Nanosized cellulose. In the proceeding of the 12th International Symposium on Supercritical Fluids, 8pp, France.
- Huerta, R. R., & Saldaña, M. D. (2018b). Pressurized fluid treatment of barley and canola straws to obtain carbohydrates and phenolics. *The Journal of Supercritical Fluids*, 141, 12-20.
- Huneault, M. A., & Li, H. (2007). Morphology and properties of compatibilized polylactide/thermoplastic starch blends. *Polymer*, 48(1), 270-280.
- Hunter, S. E., & Savage, P. E. (2004). Recent advances in acid-and base-catalyzed organic synthesis in high-temperature liquid water. *Chemical Engineering Science*, 59(22-23), 4903-4909.
- Iamareerat, B., Singh, M., Sadiq, M. B., & Anal, A. K. (2018). Reinforced cassava starch based edible film incorporated with essential oil and sodium bentonite nanoclay as food packaging material. *Journal of Food Science and Technology*, 55(5), 1953-1959.
- Imoto, T., & Yagishita, K. (1971). A simple activity measurement of lysozyme. *Agricultural and Biological Chemistry*, 35(7), 1154-1156.
- Inal, S., Kölsch, J. D., Sellrie, F., Schenk, J. A., Wischerhoff, E., Laschewsky, A., & Neher, D. (2013). A water soluble fluorescent polymer as a dual colour sensor for temperature and a specific protein. *Journal of Materials Chemistry B*, 1(46), 6373-6381.

- International Commission on Microbiological Specifications for Foods (ICMSF). (2018). *Listeria monocytogenes* in Ready-to-Eat Deli-Meats. *Microorganisms in Foods 7: Microbiological Testing in Food Safety Management*, 357-383.
- Issa, A., Ibrahim, S. A., & Tahergorabi, R. (2017). Impact of sweet potato starch-based nanocomposite films activated with thyme essential oil on the shelf-life of baby spinach leaves. *Foods*, 6(6), 43.
- Jain, S., Sandhu, P. S., Malvi, R., & Gupta, B. (2013). Cellulose derivatives as thermoresponsive polymer: An overview. *Journal of Applied Pharmaceutical Science*, 3(12), 139-144.
- Jamróz, E., Juszczak, L., & Kucharek, M. (2018). Investigation of the physical properties, antioxidant and antimicrobial activity of ternary potato starch-furcellaran-gelatin films incorporated with lavender essential oil. *International Journal of Biological Macromolecules*, 114, 1094-1101.
- Jane, J. L., Chen, Y. Y., Lee, L. F., McPherson, A. E., Wong, K. S., Radosavljevic, M., & Kasemsuwan, T. (1999). Effects of amylopectin branch chain length and amylose content on the gelatinization and pasting properties of starch. *Cereal chemistry*, 76(5), 629-637.
- Janssen, L., & Moscicki, L. (2006). Thermoplastic starch as packaging material. *Acta Scientiarum Polonorum Technica Agraria*, 5(1), 19-25.
- Jaramillo, C. M., Gutiérrez, T. J., Goyanes, S., Bernal, C., & Famá, L. (2016). Biodegradability and plasticizing effect of yerba mate extract on cassava starch edible films. *Carbohydrate Polymers*, 151, 150-159.
- Ji, N., Qin, Y., Xi, T., Xiong, L., & Sun, Q. (2017). Effect of chitosan on the antibacterial and physical properties of corn starch nanocomposite films. *Starch-Stärke*, 69(1-2)
- Jiang, T., Luo, Z., & Ying, T. (2015). Fumigation with essential oils improves sensory quality and enhanced antioxidant ability of shiitake mushroom (*lentinus edodes*). *Food Chemistry*, 172, 692-698.
- Jiménez, A., Fabra, M. J., Talens, P., & Chiralt, A. (2012a). Edible and biodegradable starch films: A review. *Food and Bioprocess Technology*, 5(6), 2058-2076.
- Jiménez, A., Fabra, M. J., Talens, P., & Chiralt, A. (2012b). Influence of hydroxypropylmethylcellulose addition and homogenization conditions on properties and ageing of corn starch based films. *Carbohydrate Polymers*, 89(2), 676-686.
- Jiménez, A., Fabra, M. J., Talens, P., & Chiralt, A. (2012c). Effect of re-crystallization on tensile, optical and water vapour barrier properties of corn starch films containing fatty acids. *Food Hydrocolloids*, 26(1), 302-310.

- Jin, F., & Enomoto, H. (2008). Application of hydrothermal reaction to conversion of plant-origin biomasses into acetic and lactic acids. *Journal of Materials Science*, 43(7), 2463-2471.
- Jones, C. D., & Steed, J. W. (2016). Gels with sense: Supramolecular materials that respond to heat, light and sound. *Chemical Society Reviews*, 45(23), 6546-6596.
- Jouki, M., Mortazavi, S. A., Yazdi, F. T., & Koocheki, A. (2014a). Characterization of antioxidant–antibacterial quince seed mucilage films containing thyme essential oil. *Carbohydrate Polymers*, 99, 537-546.
- Jouki, M., Yazdi, F. T., Mortazavi, S. A., & Koocheki, A. (2014b). Quince seed mucilage films incorporated with oregano essential oil: Physical, thermal, barrier, antioxidant and antibacterial properties. *Food Hydrocolloids*, 36, 9-19.
- Jovanović, G. D., Klaus, A. S., & Niksić, M. P. (2016). Antimicrobial activity of chitosan coatings and films against listeria monocytogenes on black radish. *Revista Argentina de Microbiología*, 48(2), 128-136.
- Kang, H. J., & Min, S. C. (2010). Potato peel-based biopolymer film development using high-pressure homogenization, irradiation, and ultrasound. *LWT-Food Science and Technology*, 43(6), 903-909.
- Kaushik, A., Singh, M., & Verma, G. (2010). Green nanocomposites based on thermoplastic starch and steam exploded cellulose nanofibrils from wheat straw. *Carbohydrate Polymers*, 82(2), 337-345.
- Keerl, M., & Richtering, W. (2007). Synergistic depression of volume phase transition temperature in copolymer microgels. *Colloid and Polymer Science*, 285(4), 471-474.
- Kettle, J., Lamminmäki, T., & Gane, P. (2010). A review of modified surfaces for high speed inkjet coating. *Surface and Coatings Technology*, 204(12-13), 2103-2109.
- Khalil, H., Tye, Y., Saurabh, C., Leh, C., Lai, T., Chong, E., Fazita, M.R., Hafidz, J.M., Banerjee, A. & Syakir, M. (2017). Biodegradable polymer films from seaweed polysaccharides: A review on cellulose as a reinforcement material. *Express Polymer Letters*, 11(4), 244-265.
- Khanoonkon, N., Yoksan, R., & Ogale, A. A. (2016). Effect of stearic acid-grafted starch compatibilizer on properties of linear low density polyethylene/thermoplastic starch blown film. *Carbohydrate Polymers*, 137, 165-173.
- Khuwijitjaru, P., Suaylam, B., & Adachi, S. (2014). Degradation of caffeic acid in subcritical water and online HPLC-DPPH assay of degradation products. *Journal of Agricultural and Food Chemistry*, 62(8), 1945-1949.

- Kim, S. R. B., Choi, Y., Kim, J., & Lim, S. (2015). Improvement of water solubility and humidity stability of tapioca starch film by incorporating various gums. *LWT-Food Science and Technology*, *64*(1), 475-482.
- Kim, S., Nishimoto, S. K., Bumgardner, J. D., Haggard, W. O., Gaber, M. W., & Yang, Y. (2010). A chitosan/ β -glycerophosphate thermo-sensitive gel for the delivery of ellagic acid for the treatment of brain cancer. *Biomaterials*, *31*(14), 4157-4166.
- Kong, M., Chen, X. G., Xing, K., & Park, H. J. (2010). Antimicrobial properties of chitosan and mode of action: A state of the art review. *International Journal of Food Microbiology*, *144*(1), 51-63.
- Konsula, Z., & Liakopoulou-Kyriakides, M. (2004). Hydrolysis of starches by the action of an α -amylase from bacillus subtilis. *Process Biochemistry*, *39*(11), 1745-1749.
- Kowalczyk, D., Kazimierczak, W., Zięba, E., Mężyńska, M., Basiura-Cembala, M., Lisiecki, S., . . . Baraniak, B. (2018). Ascorbic acid-and sodium ascorbate-loaded oxidized potato starch films: Comparative evaluation of physicochemical and antioxidant properties. *Carbohydrate Polymers*, *181*, 317-326.
- Kristo, E., & Biliaderis, C. G. (2007). Physical properties of starch nanocrystal-reinforced pullulan films. *Carbohydrate Polymers*, *68*(1), 146-158.
- Kruse, A., & Gawlik, A. (2003). Biomass conversion in water at 330– 410 C and 30– 50 MPa. identification of key compounds for indicating different chemical reaction pathways. *Industrial & Engineering Chemistry Research*, *42*(2), 267-279.
- Lachos-Perez, D., Tompsett, G., Guerra, P., Timko, M., Rostagno, M., Martínez, J., & Forster-Carneiro, T. (2017). Sugars and char formation on subcritical water hydrolysis of sugarcane straw. *Bioresource Technology*, *243*, 1069-1077.
- Lai, E., Wang, Y., Wei, Y., & Li, G. (2016). Preparation of uniform-sized and dual stimuli-responsive microspheres of poly (N-isopropylacrylamide)/poly (acrylic acid) with semi-IPN structure by one-step method. *Polymers*, *8*(3), 15 pp. doi:10.3390/polym8030090
- Lai, T., Chen, C., & Lai, L. (2013). Effects of tapioca starch/decolorized hsian-tsoa leaf gum-based active coatings on the quality of minimally processed carrots. *Food and Bioprocess Technology*, *6*(1), 249-258.
- Laohakunjit, N., & Noomhorm, A. (2004). Effect of plasticizers on mechanical and barrier properties of rice starch film. *Starch-Stärke*, *56*(8), 348-356.
- Leblanc, N., Saiah, R., Beucher, E., Gattin, R., Castandet, M., & Saiter, J. (2008). Structural investigation and thermal stability of new extruded wheat flour based polymeric materials. *Carbohydrate Polymers*, *73*(4), 548-557.

- Leceta, I., Guerrero, P., Ibarburu, I., Dueñas, M., & De la Caba, K. (2013). Characterization and antimicrobial analysis of chitosan-based films. *Journal of Food Engineering*, 116(4), 889-899.
- Lee, C. J., Shin, S. I., Kim, Y., Choi, H. J., & Moon, T. W. (2011). Structural characteristics and glucose response in mice of potato starch modified by hydrothermal treatments. *Carbohydrate Polymers*, 83(4), 1879-1886.
- Lee, H., Saravana, P. S., Cho, Y., Haq, M., & Chun, B. (2018). Extraction of bioactive compounds from oyster (*crassostrea gigas*) by pressurized hot water extraction. *The Journal of Supercritical Fluids*, 141, 120-127.
- Lenihan, P., Orozco, A., O'Neill, E., Ahmad, M., Rooney, D., & Walker, G. (2010). Dilute acid hydrolysis of lignocellulosic biomass. *Chemical Engineering Journal*, 156(2), 395-403.
- Li, J., Ye, F., Lei, L., & Zhao, G. (2018a). Combined effects of octenylsuccination and oregano essential oil on sweet potato starch films with an emphasis on water resistance. *International Journal of Biological Macromolecules*, 115, 547-553.
- Li, M., Tian, X., Jin, R., & Li, D. (2018b). Preparation and characterization of nanocomposite films containing starch and cellulose nanofibers. *Industrial Crops and Products*, 123, 654-660.
- Li, M., Liu, P., Zou, W., Yu, L., Xie, F., Pu, H., Liu, H. & Chen, L. (2011). Extrusion processing and characterization of edible starch films with different amylose contents. *Journal of Food Engineering*, 106(1), 95-101.
- Li, W., Tian, X., Liu, L., Wang, P., Wu, G., Zheng, J., Ouyang, S., Luo, Q. & Zhang, G. (2015). High pressure induced gelatinization of red adzuki bean starch and its effects on starch physicochemical and structural properties. *Food Hydrocolloids*, 45, 132-139.
- Li, Y., Lu, X., Yuan, L., & Liu, X. (2009). Fructose decomposition kinetics in organic acids-enriched high temperature liquid water. *Biomass and Bioenergy*, 33(9), 1182-1187.
- Lim, L., Khor, E., & Ling, C. (1999). Effects of dry heat and saturated steam on the physical properties of chitosan. *Journal of Biomedical Materials Research: An Official Journal of the Society for Biomaterials, the Japanese Society for Biomaterials, and the Australian Society for Biomaterials*, 48(2), 111-116.
- Liu, C., & Wyman, C. E. (2003). The effect of flow rate of compressed hot water on xylan, lignin, and total mass removal from corn stover. *Industrial & Engineering Chemistry Research*, 42(21), 5409-5416.

- Liu, C., & Wyman, C. E. (2005). Partial flow of compressed-hot water through corn stover to enhance hemicellulose sugar recovery and enzymatic digestibility of cellulose. *Bioresource Technology*, 96(18), 1978-1985.
- Liu, H., Xie, F., Yu, L., Chen, L., & Li, L. (2009). Thermal processing of starch-based polymers. *Progress in Polymer Science*, 34(12), 1348-1368.
- Liu, H., Du, Y., Wang, X., & Sun, L. (2004). Chitosan kills bacteria through cell membrane damage. *International Journal of Food Microbiology*, 95(2), 147-155.
- Liu, H., Adhikari, R., Guo, Q., & Adhikari, B. (2013). Preparation and characterization of glycerol plasticized (high-amylose) starch–chitosan films. *Journal of Food Engineering*, 116(2), 588-597.
- Liu, Z. (2005). Edible films and coatings from starches. In J. Han (Ed.), *Innovations in food packaging* (1st ed., pp. 318-337), Elsevier, New York, USA.
- Lo, C., Lin, K., & Hsiue, G. (2005). Preparation and characterization of intelligent core-shell nanoparticles based on poly (D, L-lactide)-g-poly (N-isopropyl acrylamide-co-methacrylic acid). *Journal of Controlled Release*, 104(3), 477-488.
- Lopez, O., Garcia, M., Villar, M., Gentili, A., Rodriguez, M., & Albertengo, L. (2014). Thermo-compression of biodegradable thermoplastic corn starch films containing chitin and chitosan. *LWT-Food Science and Technology*, 57(1), 106-115.
- Lu, Y., Weng, L., & Cao, X. (2005). Biocomposites of plasticized starch reinforced with cellulose crystallites from cottonseed linter. *Macromolecular Bioscience*, 5(11), 1101-1107.
- Luchese, C. L., Abdalla, V. F., Spada, J. C., & Tessaro, I. C. (2018). Evaluation of blueberry residue incorporated cassava starch film as pH indicator in different simulants and foodstuffs. *Food Hydrocolloids*, 82, 209-218.
- Ma, X., Chang, P. R., & Yu, J. (2008). Properties of biodegradable thermoplastic pea starch/carboxymethyl cellulose and pea starch/microcrystalline cellulose composites. *Carbohydrate Polymers*, 72(3), 369-375.
- Machmudah, S., Wahyudiono, Kanda, H., & Goto, M. (2017). Hydrolysis of biopolymers in near-critical and subcritical water. In H. Dominguez, & M. Munoz G. (Eds.), *Water extraction of bioactive compounds* (1st ed., pp. 69-107), Elsevier, New York, USA.
- Mahajan, H. S., Tyagi, V., Lohiya, G., & Nerkar, P. (2012). Thermally reversible xyloglucan gels as vehicles for nasal drug delivery. *Drug Delivery*, 19(5), 270-276.
- Maizura, M., Fazilah, A., Norziah, M., & Karim, A. (2007). Antibacterial activity and mechanical properties of partially hydrolyzed sago starch–alginate edible film containing

lemongrass oil. *Journal of Food Science*, 72(6), 7 pp. <https://doi.org/10.1111/j.1750-3841.2007.00427.x>

- Maksimovic, A. Z., Zunabovic-Pichler, M., Kos, I., Mayrhofer, S., Hulak, N., Domig, K. J., & Fuka, M. M. (2018). Microbiological hazards and potential of spontaneously fermented game meat sausages: A focus on lactic acid bacteria diversity. *LWT-Food Science and Technology*, 89, 418-426.
- Malhotra, B., Keshwani, A., & Kharkwal, H. (2015). Antimicrobial food packaging: Potential and pitfalls. *Frontiers in Microbiology*, 6, 7 pp. <https://doi.org/10.3389/fmicb.2015.00611>
- Manouras, T., & Vamvakaki, M. (2017). Field responsive materials: Photo-, electro-, magnetic- and ultrasound-sensitive polymers. *Polymer Chemistry*, 8(1), 74-96.
- Mansour, O. Y., Nagaty, A., & El-Zawawy, W. K. (1994). Variables affecting the methylation reactions of cellulose. *Journal of Applied Polymer Science*, 54(5), 519-524.
- Maran, J. P., Sivakumar, V., Thirugnanasambandham, K., & Sridhar, R. (2014). Degradation behavior of biocomposites based on cassava starch buried under indoor soil conditions. *Carbohydrate Polymers*, 101, 20-28.
- Margosch, D., Ehrmann, M. A., Buckow, R., Heinz, V., Vogel, R. F., & Ganzle, M. G. (2006). High-pressure-mediated survival of clostridium botulinum and bacillus amyloliquefaciens endospores at high temperature. *Applied and Environmental Microbiology*, 72(5), 3476-3481.
- Martins, A. B., & Santana, R. M. C. (2016). Effect of carboxylic acids as compatibilizer agent on mechanical properties of thermoplastic starch and polypropylene blends. *Carbohydrate Polymers*, 135, 79-85.
- Masina, N., Choonara, Y. E., Kumar, P., du Toit, L. C., Govender, M., Indermun, S., & Pillay, V. (2017). A review of the chemical modification techniques of starch. *Carbohydrate Polymers*, 157, 1226-1236.
- Mathew, S., & Abraham, T. E. (2008). Characterisation of ferulic acid incorporated starch-chitosan blend films. *Food Hydrocolloids*, 22(5), 826-835.
- Mathew, S., Brahmakumar, M., & Abraham, T. E. (2006). Microstructural imaging and characterization of the mechanical, chemical, thermal, and swelling properties of starch-chitosan blend films. *Biopolymers*, 82(2), 176-187.
- Matzinos, P., Tserki, V., Kontoyiannis, A., & Panayiotou, C. (2002). Processing and characterization of starch/polycaprolactone products. *Polymer Degradation and Stability*, 77(1), 17-24.

- Mayachiew, P., & Devahastin, S. (2010). Effects of drying methods and conditions on release characteristics of edible chitosan films enriched with indian gooseberry extract. *Food Chemistry*, *118*(3), 594-601.
- McNeill, I., & Sadeghi, S. (1990). Thermal stability and degradation mechanisms of poly (acrylic acid) and its salts: Part 1—Poly (acrylic acid). *Polymer Degradation and Stability*, *29*(2), 233-246.
- Mehdizadeh, T., Tajik, H., Razavi Rohani, S. M., & Oromiehie, A. R. (2012). Antibacterial, antioxidant and optical properties of edible starch-chitosan composite film containing thymus kotschyanus essential oil. *Veterinary Research Forum: An International Quarterly Journal*, *3*(3), 167-173.
- Mejlholm, O., Gunvig, A., Borggaard, C., Blom-Hanssen, J., Mellefont, L., Ross, T., Leroi, F., Else, T., Visser, D. & Dalgaard, P. (2010). Predicting growth rates and growth boundary of listeria monocytogenes—An international validation study with focus on processed and ready-to-eat meat and seafood. *International Journal of Food Microbiology*, *141*(3), 137-150.
- Mellegård, H., Strand, S., Christensen, B., Granum, P., & Hardy, S. (2011). Antibacterial activity of chemically defined chitosans: Influence of molecular weight, degree of acetylation and test organism. *International Journal of Food Microbiology*, *148*(1), 48-54.
- Mendes, J., Paschoalin, R., Carmona, V., Neto, A. R. S., Marques, A., Marconcini, J., Mattoso, L.H.C., Medeiros, E.S. & Oliveira, J. (2016). Biodegradable polymer blends based on corn starch and thermoplastic chitosan processed by extrusion. *Carbohydrate Polymers*, *137*, 452-458.
- Miles, M. J., Morris, V. J., & Ring, S. G. (1985). Gelation of amylose. *Carbohydrate Research*, *135*(2), 257-269.
- Miller, P., Liu, X., & McMullen, L. M. (2014). Microbiota of regular sodium and sodium-reduced ready-to-eat meat products obtained from the retail market. *Canadian Journal of Microbiology*, *61*(2), 150-154.
- Min, S., & Krochta, J. (2005). Antimicrobial films and coatings for fresh fruit and vegetables. In W. Jongen (Ed.), *Improving the safety of fresh fruit and vegetables* (pp. 454-492), Woodhead Publishing, Cambridge, UK.
- Miyague, L., Macedo, R. E., Meca, G., Holley, R. A., & Luciano, F. B. (2015). Combination of phenolic acids and essential oils against *Listeria monocytogenes*. *LWT-Food Science and Technology*, *64*(1), 333-336.
- Miyazaki, M., Van Hung, P., Maeda, T., & Morita, N. (2006). Recent advances in application of modified starches for breadmaking. *Trends in Food Science & Technology*, *17*(11), 591-599.

- Miyazawa, T., & Funazukuri, T. (2005). Polysaccharide hydrolysis accelerated by adding carbon dioxide under hydrothermal conditions. *Biotechnology Progress*, 21(6), 1782-1785.
- Mohammadi, A., Hashemi, M., & Hosseini, S. M. (2015). Chitosan nanoparticles loaded with cinnamomum zeylanicum essential oil enhance the shelf life of cucumber during cold storage. *Postharvest Biology and Technology*, 110, 203-213.
- Möller, M., Nilges, P., Harnisch, F., & Schröder, U. (2011). Subcritical water as reaction environment: Fundamentals of hydrothermal biomass transformation. *ChemSusChem*, 4(5), 566-579.
- Moradi, M., Tajik, H., No, H. K., Razavi Rohani, S., Oromiehie, A., & Ghasemi, S. (2010). Potential inherent properties of chitosan and its applications in preserving muscle food. *J Chitin Chitosan*, 15(1), 35-45.
- Moradi, M., Tajik, H., Rohani, S. M. R., Oromiehie, A. R., Malekinejad, H., Aliakbarlu, J., & Hadian, M. (2012). Characterization of antioxidant chitosan film incorporated with zataria multiflora boiss essential oil and grape seed extract. *LWT-Food Science and Technology*, 46(2), 477-484.
- Morán, J. I., Alvarez, V. A., Cyras, V. P., & Vázquez, A. (2008). Extraction of cellulose and preparation of nanocellulose from sisal fibers. *Cellulose*, 15(1), 149-159.
- Moreno, O., Atarés, L., & Chiralt, A. (2015). Effect of the incorporation of antimicrobial/antioxidant proteins on the properties of potato starch films. *Carbohydrate Polymers*, 133, 353-364.
- Moreschi, S. R., Petenate, A. J., & Meireles, M. A. A. (2004). Hydrolysis of ginger bagasse starch in subcritical water and carbon dioxide. *Journal of Agricultural and Food Chemistry*, 52(6), 1753-1758.
- Müller, C. M., Laurindo, J. B., & Yamashita, F. (2009). Effect of cellulose fibers addition on the mechanical properties and water vapor barrier of starch-based films. *Food Hydrocolloids*, 23(5), 1328-1333.
- Muller, J., González-Martínez, C., & Chiralt, A. (2017). Poly (lactic) acid (PLA) and starch bilayer films, containing cinnamaldehyde, obtained by compression moulding. *European Polymer Journal*, 95, 56-70.
- Murphy, R., Duncan, L., Driscoll, K., Beard, B., Berrang, M., & Marcy, J. (2003). Determination of thermal lethality of listeria monocytogenes in fully cooked chicken breast fillets and strips during postcook in-package pasteurization. *Journal of Food Protection*, 66(4), 578-583.

- Muscat, D., Adhikari, R., McKnight, S., Guo, Q., & Adhikari, B. (2013). The physicochemical characteristics and hydrophobicity of high amylose starch–glycerol films in the presence of three natural waxes. *Journal of Food Engineering*, 119(2), 205-219.
- Nagamori, M., & Funazukuri, T. (2004). Glucose production by hydrolysis of starch under hydrothermal conditions. *Journal of Chemical Technology and Biotechnology*, 79(3), 229-233.
- Naha, P. C., Casey, A., Tenuta, T., Lynch, I., Dawson, K. A., Byrne, H. J., & Davoren, M. (2009a). Preparation, characterization of NIPAM and NIPAM/BAM copolymer nanoparticles and their acute toxicity testing using an aquatic test battery. *Aquatic Toxicology*, 92(3), 146-154.
- Naha, P. C., Casey, A., Tenuta, T., Lynch, I., Dawson, K., Byrne, H., & Davoren, M. (2009b). Preparation, characterization and ecotoxicological evaluation of four environmentally relevant species of N-isopropylacrylamide and N-isopropylacrylamide-co-N-tert-butylacrylamide copolymer nanoparticles. *Aquatic Toxicology*, 92, 146-154.
- Nair, D. V., Kiess, A., Nannapaneni, R., Schilling, W., & Sharma, C. S. (2015). The combined efficacy of carvacrol and modified atmosphere packaging on the survival of salmonella, campylobacter jejuni and lactic acid bacteria on turkey breast cutlets. *Food Microbiology*, 49, 134-141.
- Najafi, M., Hebels, E., Hennink, W. E., & Vermonden, T. (2018). Poly (n-isopropylacrylamide): Physicochemical properties and biomedical applications. In V. Khutoryanskiy V., & T. Georgiou K. (Eds.), *Temperature-Responsive polymers: Chemistry, properties and applications* (1st ed., pp. 3-34) John Wiley & Sons Ltd, Hoboken, USA.
- Nandi, S., & Guha, P. (2018). Modelling the effect of guar gum on physical, optical, barrier and mechanical properties of potato starch based composite film. *Carbohydrate Polymers*, 200, 498-507.
- Neo, Y. P., Ray, S., Jin, J., Gizdavic-Nikolaidis, M., Nieuwoudt, M. K., Liu, D., & Quek, S. Y. (2013). Encapsulation of food grade antioxidant in natural biopolymer by electrospinning technique: A physicochemical study based on zein–gallic acid system. *Food Chemistry*, 136(2), 1013-1021.
- Nguyen, D. M., Do, T. V. V., Grillet, A., Thuc, H. H., & Thuc, C. N. H. (2016). Biodegradability of polymer film based on low density polyethylene and cassava starch. *International Biodeterioration & Biodegradation*, 115, 257-265.
- Nijs, A., Cartuyvels, R., Mewis, A., Peeters, V., Rummens, J. L., & Magerman, K. (2003). Comparison and evaluation of osiris and sirscan 2000 antimicrobial susceptibility systems in the clinical microbiology laboratory. *Journal of Clinical Microbiology*, 41(8), 3627-3630.

- Nilsson, L., Hansen, T. B., Garrido, P., Buchrieser, C., Glaser, P., Knöchel, S., Gram, L. & Gravesen, A. (2005). Growth inhibition of *listeria monocytogenes* by a nonbacteriocinogenic *carnobacterium piscicola*. *Journal of Applied Microbiology*, *98*(1), 172-183.
- Noshirvani, N., Hong, W., Ghanbarzadeh, B., Fasihi, H., & Montazami, R. (2017). Study of cellulose nanocrystal doped starch-polyvinyl alcohol bionanocomposite films. *International Journal of Biological Macromolecules*, *107*, 2065-2074.
- Nouri, L., & Nafchi, A. M. (2014). Antibacterial, mechanical, and barrier properties of sago starch film incorporated with betel leaves extract. *International Journal of Biological Macromolecules*, *66*, 254-259.
- Okudan, A., & Karasakal, A. (2013). The effect of H-bonding on radical copolymerization of maleic anhydride with N-tert-butylacrylamide and its characterization. *International Journal of Polymer Science*, 9 pp. doi:<http://dx.doi.org/10.1155/2013/842894>
- Oladzadabbasabadi, N., Ebadi, S., Nafchi, A. M., Karim, A., & Kiahosseini, S. R. (2017). Functional properties of dually modified sago starch/ κ -carrageenan films: An alternative to gelatin in pharmaceutical capsules. *Carbohydrate Polymers*, *160*, 43-51.
- Olivas, G., & Barbosa-Cánovas, G. (2005). Edible coatings for fresh-cut fruits. *Critical Reviews in Food Science and Nutrition*, *45*(7-8), 657-670.
- Olivato, J., Grossmann, M., Bilck, A., & Yamashita, F. (2012). Effect of organic acids as additives on the performance of thermoplastic starch/polyester blown films. *Carbohydrate Polymers*, *90*(1), 159-164.
- Orozco, R., Redwood, M., Leeke, G., Bahari, A., Santos, R., & Macaskie, L. (2012). Hydrothermal hydrolysis of starch with CO₂ and detoxification of the hydrolysates with activated carbon for bio-hydrogen fermentation. *International Journal of Hydrogen Energy*, *37*(8), 6545-6553.
- Ortega-Toro, R., Contreras, J., Talens, P., & Chiralt, A. (2015). Physical and structural properties and thermal behaviour of starch-poly (ϵ -caprolactone) blend films for food packaging. *Food Packaging and Shelf Life*, *5*, 10-20.
- Osada, M., Miura, C., Nakagawa, Y. S., Kaihara, M., Nikaido, M., & Totani, K. (2012). Effect of sub-and supercritical water pretreatment on enzymatic degradation of chitin. *Carbohydrate Polymers*, *88*(1), 308-312.
- Osada, M., Miura, C., Nakagawa, Y. S., Kaihara, M., Nikaido, M., & Totani, K. (2015). Effect of sub-and supercritical water treatments on the physicochemical properties of crab shell chitin and its enzymatic degradation. *Carbohydrate Polymers*, *134*, 718-725.

- Otake, K., Inomata, H., Konno, M., & Saito, S. (1990). Thermal analysis of the volume phase transition with N-isopropylacrylamide gels. *Macromolecules*, 23(1), 283-289.
- Othman, N., Azahari, N. A., & Ismail, H. (2011). Thermal properties of polyvinyl alcohol (PVOH)/corn starch blend film. *Malaysian Polymer Journal*, 6(6), 147-154.
- Otoni, C. G., Lodi, B. D., Lorevice, M. V., Leitão, R. C., Ferreira, M. D., de Moura, M. R., & Mattoso, L. H. (2018). Optimized and scaled-up production of cellulose-reinforced biodegradable composite films made up of carrot processing waste. *Industrial Crops and Products*, 121, 66-72.
- Oussalah, M., Caillet, S., Saucier, L., & Lacroix, M. (2007). Inhibitory effects of selected plant essential oils on the growth of four pathogenic bacteria: *E. coli* O157: H7, salmonella typhimurium, staphylococcus aureus and listeria monocytogenes. *Food Control*, 18(5), 414-420.
- Ozel, M. Z., Gogus, F., & Lewis, A. C. (2003). Subcritical water extraction of essential oils from thymra spicata. *Food Chemistry*, 82(3), 381-386.
- Paes, S. S., Yakimets, I., & Mitchell, J. R. (2008). Influence of gelatinization process on functional properties of cassava starch films. *Food Hydrocolloids*, 22(5), 788-797.
- Palma-Rodríguez, H. M., Berrios, J. D. J., Glenn, G., Salgado-Delgado, R., Aparicio-Saguilán, A., Rodríguez-Hernández, A. I., & Vargas-Torres, A. (2016). Effect of the storage conditions on mechanical properties and microstructure of biodegradable baked starch foams. *CyTA-Journal of Food*, 14(3), 415-422.
- Park, S., Marsh, K. S., & Dawson, P. (2010). Application of chitosan-incorporated LDPE film to sliced fresh red meats for shelf life extension. *Meat Science*, 85(3), 493-499.
- Parker, R., & Ring, S. (2001). Aspects of the physical chemistry of starch. *Journal of Cereal Science*, 34(1), 1-17.
- Parliament, E. (2004). Regulation (EC) no. 1935/2004 of the European parliament and of the council of 27 october 2004 on materials and articles intended to come into contact with food and repealing directives 80/590/EEC and 89/109/EEC. *Official Journal of the European Union*, 338(4), 456-493.
- Pasanphan, W., & Chirachanchai, S. (2008). Conjugation of gallic acid onto chitosan: An approach for green and water-based antioxidant. *Carbohydrate Polymers*, 72(1), 169-177.
- Pastoor, K. J., & Rice, C. V. (2015). Cation effects on the phase transition of n-isopropylacrylamide hydrogels. *Macromolecular Chemistry and Physics*, 216(9), 1024-1032.

- Pásztor, E., Makó, Á., Csóka, G., Fenyvesi, Z., Benko, R., Prosszer, M., Marton, S., Antal, I. & Klebovich, I. (2011). New formulation of in situ gelling metolose-based liquid suppository. *Drug Development and Industrial Pharmacy*, 37(1), 1-7.
- Peelman, N., Ragaert, P., De Meulenaer, B., Adons, D., Peeters, R., Cardon, L., Van Impe, F. & Devlieghere, F. (2013). Application of bioplastics for food packaging. *Trends in Food Science & Technology*, 32(2), 128-141.
- Pelissari, F. M., Grossmann, M. V., Yamashita, F., & Pineda, E. A. G. (2009). Antimicrobial, mechanical, and barrier properties of cassava starch– chitosan films incorporated with oregano essential oil. *Journal of Agricultural and Food Chemistry*, 57(16), 7499-7504.
- Pelissari, F. M., Yamashita, F., Garcia, M. A., Martino, M. N., Zaritzky, N. E., & Grossmann, M. V. E. (2012). Constrained mixture design applied to the development of cassava starch– chitosan blown films. *Journal of Food Engineering*, 108(2), 262-267.
- Perazzo, K. K. N. C. L., de Vasconcelos Conceição, A. C., dos Santos, J. C. P., de Jesus Assis, D., Souza, C. O., & Druzian, J. I. (2014). Properties and antioxidant action of actives cassava starch films incorporated with green tea and palm oil extracts. *PloS One*, 9(9) doi:<https://doi.org/10.1371/journal.pone.0105199>
- Pereda, M., Amica, G., & Marcovich, N. E. (2012). Development and characterization of edible chitosan/olive oil emulsion films. *Carbohydrate Polymers*, 87(2), 1318-1325.
- Peres, A. M., Pires, R. R., & Oréfice, R. L. (2016). Evaluation of the effect of reprocessing on the structure and properties of low density polyethylene/thermoplastic starch blends. *Carbohydrate Polymers*, 136, 210-215.
- Peressini, D., Bravin, B., Lapasin, R., Rizzotti, C., & Sensidoni, A. (2003). Starch– methylcellulose based edible films: Rheological properties of film-forming dispersions. *Journal of Food Engineering*, 59(1), 25-32.
- Perez, C., Pauli, M., & Bazerque, P. (1990). An antibiotic assay by the agar well diffusion method. *Acta Biologiae Et Medicinae Experimentalis*, 15, 113-115.
- Petri, D. F. (2015). Xanthan gum: A versatile biopolymer for biomedical and technological applications. *Journal of Applied Polymer Science*, 132(23), 13 pp. <https://doi.org/10.1002/app.42035>
- Piñeros-Hernandez, D., Medina-Jaramillo, C., López-Córdoba, A., & Goyanes, S. (2017). Edible cassava starch films carrying rosemary antioxidant extracts for potential use as active food packaging. *Food Hydrocolloids*, 63, 488-495.
- Plaza, M., & Turner, C. (2015). Pressurized hot water extraction of bioactives. *TrAC Trends in Analytical Chemistry*, 71, 39-54.

- Polo-Corrales, L., Ramirez-Vick, J. E., & Hernandez-Ramos, E. J. (2018). Thermosensitive hydrogels with nanofillers incorporated to use in food packaging applications. *International Journal of Applied Engineering Research*, 13(10), 7305-7308.
- Pothakos, V., Snauwaert, C., De Vos, P., Huys, G., & Devlieghere, F. (2014a). Psychrotrophic members of *Leuconostoc gasicomitatum*, *Leuconostoc gelidum* and *Lactococcus piscium* dominate at the end of shelf-life in packaged and chilled-stored food products in Belgium. *Food Microbiology*, 39, 61-67.
- Pothakos, V., Stellato, G., Ercolini, D., & Devlieghere, F. (2015). Processing environment and ingredients are both sources of *Leuconostoc gelidum*, which emerges as a major spoiler in ready-to-eat meals. *Applied and Environmental Microbiology*, 81(10), 3529-3541.
- Prabhat, S., Bhattacharyya, S., Vishal, V., Kalyan, R., Vijai, K., Pandey, K., & Singh, M. (2013). Studies on isolation and identification of active microorganisms during degradation of polyethylene/starch film. *International Research Journal of Environmental Sciences*, 2(9), 83-85.
- Prachayawarakorn, J., Chaiwatyothin, S., Mueangta, S., & Hanchana, A. (2013). Effect of jute and kapok fibers on properties of thermoplastic cassava starch composites. *Materials & Design*, 47, 309-315.
- Prado, J. M., Forster-Carneiro, T., Rostagno, M. A., Follegatti-Romero, L. A., Mauger Filho, F., & Meireles, M. A. A. (2014). Obtaining sugars from coconut husk, defatted grape seed, and pressed palm fiber by hydrolysis with subcritical water. *The Journal of Supercritical Fluids*, 89, 89-98.
- Prado, J. M., Vardanega, R., Nogueira, G. C., Forster-Carneiro, T., Rostagno, M. A., Mauger Filho, F., & Meireles, M. A. A. (2017). Valorization of residual biomasses from the agri-food industry by subcritical water hydrolysis assisted by CO₂. *Energy & Fuels*, 31(3), 2838-2846.
- Primarini, D., & Ohta, Y. (2000). Some enzyme properties of raw starch digesting amylases from *Streptomyces* sp. no. 4. *Starch-Stärke*, 52(1), 28-32.
- Priya, B., Gupta, V. K., Pathania, D., & Singha, A. S. (2014). Synthesis, characterization and antibacterial activity of biodegradable starch/PVA composite films reinforced with cellulosic fibre. *Carbohydrate Polymers*, 109, 171-179.
- Pushpadass, H. A., Bhandari, P., & Hanna, M. A. (2010). Effects of LDPE and glycerol contents and compounding on the microstructure and properties of starch composite films. *Carbohydrate Polymers*, 82(4), 1082-1089.

- Pyla, R., Kim, T., Silva, J. L., & Jung, Y. (2010). Enhanced antimicrobial activity of starch-based film impregnated with thermally processed tannic acid, a strong antioxidant. *International Journal of Food Microbiology*, 137(2-3), 154-160.
- Qian, J., & Wu, F. (2013). Thermosensitive PNIPAM semi-hollow spheres for controlled drug release. *Journal of Materials Chemistry B*, 1(28), 3464-3469.
- Quitain, A. T., Sato, N., Daimon, H., & Fujie, K. (2001). Production of valuable materials by hydrothermal treatment of shrimp shells. *Industrial & Engineering Chemistry Research*, 40(25), 5885-5888.
- Raafat, D., von Bargaen, K., Haas, A., & Sahl, H. G. (2008). Insights into the mode of action of chitosan as an antibacterial compound. *Applied and Environmental Microbiology*, 74(12), 3764-3773.
- Rachtanapun, P., & Tongdeesoontorn, W. (2009). Effect of antioxidants on properties of rice flour/cassava starch film blends plasticized with sorbitol. *Kasetsart Journal (Natural Science)*, 43, 252-258.
- Radha Krishnan, K., Babuskin, S., Rakhavan, K., Tharavin, R., Azhagu Saravana Babu, P., Sivarajan, M., & Sukumar, M. (2015). Potential application of corn starch edible films with spice essential oils for the shelf life extension of red meat. *Journal of Applied Microbiology*, 119(6), 1613-1623.
- Ramos, L., Kristenson, E., & Brinkman, U. T. (2002). Current use of pressurised liquid extraction and subcritical water extraction in environmental analysis. *Journal of Chromatography A*, 975(1), 3-29.
- Ramos, M., Jiménez, A., Peltzer, M., & Garrigós, M. C. (2012). Characterization and antimicrobial activity studies of polypropylene films with carvacrol and thymol for active packaging. *Journal of Food Engineering*, 109(3), 513-519.
- Ravishankar, S., Jaroni, D., Zhu, L., Olsen, C., McHugh, T., & Friedman, M. (2012). Inactivation of listeria monocytogenes on ham and bologna using pectin-based apple, carrot, and hibiscus edible films containing carvacrol and cinnamaldehyde. *Journal of Food Science*, 77(7), M377-M382.
- Ray, B., Isobe, Y., Habaue, S., Kamigaito, M., & Okamoto, Y. (2004). Novel initiating system for the stereocontrolled radical polymerization of acrylamides: Alkyl bromide/rare earth metal triflate system. *Polymer Journal*, 36(9), 728-736.
- Re, R., Pellegrini, N., Proteggente, A., Pannala, A., Yang, M., & Rice-Evans, C. (1999). Antioxidant activity applying an improved ABTS radical cation decolorization assay. *Free Radical Biology and Medicine*, 26(9-10), 1231-1237.

- Reddy, N., & Yang, Y. (2010). Citric acid cross-linking of starch films. *Food Chemistry*, *118*(3), 702-711.
- Reis, L. C. B., de Souza, C. O., da Silva, Jania Betânia Alves, Martins, A. C., Nunes, I. L., & Druzian, J. I. (2015). Active biocomposites of cassava starch: The effect of yerba mate extract and mango pulp as antioxidant additives on the properties and the stability of a packaged product. *Food and Bioproducts Processing*, *94*, 382-391.
- Reis, M. O., Zanela, J., Olivato, J., Garcia, P. S., Yamashita, F., & Grossmann, M. V. E. (2014). Microcrystalline cellulose as reinforcement in thermoplastic starch/poly (butylene adipate-co-terephthalate) films. *Journal of Polymers and the Environment*, *22*(4), 545-552.
- Reiter, W. (2002). Biosynthesis and properties of the plant cell wall. *Current Opinion in Plant Biology*, *5*(6), 536-542.
- Ren, L., Yan, X., Zhou, J., Tong, J., & Su, X. (2017). Influence of chitosan concentration on mechanical and barrier properties of corn starch/chitosan films. *International Journal of Biological Macromolecules*, *105*, 1636-1643.
- Requena, R., Vargas, M., & Chiralt, A. (2018). Obtaining antimicrobial bilayer starch and polyester-blend films with carvacrol. *Food Hydrocolloids*, *83*, 118-133.
- Resa, C. P. O., Gerschenson, L. N., & Jagus, R. J. (2014). Natamycin and nisin supported on starch edible films for controlling mixed culture growth on model systems and port salut cheese. *Food Control*, *44*, 146-151.
- Ritthidej, G. C., Phaechamud, T., & Koizumi, T. (2002). Moist heat treatment on physicochemical change of chitosan salt films. *International Journal of Pharmaceutics*, *232*(1), 11-22.
- Rivero, S., García, M., & Pinotti, A. (2010). Crosslinking capacity of tannic acid in plasticized chitosan films. *Carbohydrate Polymers*, *82*(2), 270-276.
- Rodríguez-Sandoval, E., Fernández-Quintero, A., Cuvelier, G., Relkin, P., & Bello-Pérez, L. A. (2008). Starch retrogradation in cassava flour from cooked parenchyma. *Starch-Stärke*, *60*(3-4), 174-180.
- Rogalinski, T., Liu, K., Albrecht, T., & Brunner, G. (2008). Hydrolysis kinetics of biopolymers in subcritical water. *The Journal of Supercritical Fluids*, *46*(3), 335-341.
- Roller, S., & Covill, N. (1999). The antifungal properties of chitosan in laboratory media and apple juice. *International Journal of Food Microbiology*, *47*(1-2), 67-77.

- Rommi, K., Rahikainen, J., Vartiainen, J., Holopainen, U., Lahtinen, P., Honkapää, K., & Lantto, R. (2016). Potato peeling costreams as raw materials for biopolymer film preparation. *Journal of Applied Polymer Science*, *133*(5), 11 pp. <https://doi.org/10.1002/app.42862>
- Roy, S. B., Ramaraj, B., Shit, S., & Nayak, S. K. (2011). Polypropylene and potato starch biocomposites: Physicomechanical and thermal properties. *Journal of Applied Polymer Science*, *120*(5), 3078-3086.
- Rubilar, J. F., Cruz, R. M., Silva, H. D., Vicente, A. A., Khmelinskii, I., & Vieira, M. C. (2013). Physico-mechanical properties of chitosan films with carvacrol and grape seed extract. *Journal of Food Engineering*, *115*(4), 466-474.
- Ruel-Gariepy, E., Chenite, A., Chaput, C., Guirguis, S., & Leroux, J. (2000). Characterization of thermosensitive chitosan gels for the sustained delivery of drugs. *International Journal of Pharmaceutics*, *203*(1-2), 89-98.
- Rui, L., Xie, M., Hu, B., Zhou, L., Yin, D., & Zeng, X. (2017). A comparative study on chitosan/gelatin composite films with conjugated or incorporated gallic acid. *Carbohydrate Polymers*, *173*, 473-481.
- Rujnić-Sokele, M., & Pilipović, A. (2017). Challenges and opportunities of biodegradable plastics: A mini review. *Waste Management & Research*, *35*(2), 132-140.
- Saberi, B., Vuong, Q. V., Chockchaisawasdee, S., Golding, J. B., Scarlett, C. J., & Stathopoulos, C. E. (2017). Physical, barrier, and antioxidant properties of pea starch-guar gum biocomposite edible films by incorporation of natural plant extracts. *Food and Bioprocess Technology*, *10*(12), 2240-2250.
- Sabetzadeh, M., Bagheri, R., & Masoomi, M. (2015). Study on ternary low density polyethylene/linear low density polyethylene/thermoplastic starch blend films. *Carbohydrate Polymers*, *119*, 126-133.
- Saïd Azizi Samir, M. A., Alloin, F., Paillet, M., & Dufresne, A. (2004). Tangling effect in fibrillated cellulose reinforced nanocomposites. *Macromolecules*, *37*(11), 4313-4316.
- Saito, T., Sasaki, M., Kawanabe, H., Yoshino, Y., & Goto, M. (2009). Subcritical water reaction behavior of d-Glucose as a model compound for biomass using two different Continuous-Flow reactor configurations. *Chemical Engineering & Technology: Industrial Chemistry-Plant Equipment-Process Engineering-Biotechnology*, *32*(4), 527-533.
- Salak Asghari, F., & Yoshida, H. (2006). Acid-catalyzed production of 5-hydroxymethyl furfural from D-fructose in subcritical water. *Industrial & Engineering Chemistry Research*, *45*(7), 2163-2173.

- Saldaña, M. D. A., & Valdivieso-Ramirez, C. S. (2015). Pressurized fluid systems: Phytochemical production from biomass. *The Journal of Supercritical Fluids*, 96, 228-244.
- Sánchez-Maldonado, A., Schieber, A., & Gänzle, M. (2011). Structure–function relationships of the antibacterial activity of phenolic acids and their metabolism by lactic acid bacteria. *Journal of Applied Microbiology*, 111(5), 1176-1184.
- Sánchez-González, L., Vargas, M., González-Martínez, C., Chiralt, A., & Cháfer, M. (2011). Use of essential oils in bioactive edible coatings: A review. *Food Engineering Reviews*, 3(1), 1-16.
- Santos, E. H., Kamimura, J. A., Hill, L. E., & Gomes, C. L. (2015). Characterization of carvacrol beta-cyclodextrin inclusion complexes as delivery systems for antibacterial and antioxidant applications. *LWT-Food Science and Technology*, 60(1), 583-592.
- Sanyang, M. L., Sapuan, S. M., Jawaid, M., Ishak, M. R., & Sahari, J. (2015). Effect of plasticizer type and concentration on tensile, thermal and barrier properties of biodegradable films based on sugar palm (*arenga pinnata*) starch. *Polymers*, 7(6), 1106-1124.
- Sapper, M., Wilcaso, P., Santamarina, M. P., Roselló, J., & Chiralt, A. (2018). Antifungal and functional properties of starch-gellan films containing thyme (*thymus zygis*) essential oil. *Food Control*, 92, 505-515.
- Saraiva, L. E. F., Naponucena, L. D. O. M., da Silva Santos, V., Silva, R. P. D., de Souza, C. O., Souza, I. E. G. L., de Oliveira Mamede, M.E. & Druzian, J. I. (2016). Development and application of edible film of active potato starch to extend mini panettone shelf life. *LWT-Food Science and Technology*, 73, 311-319.
- Saravana, P. S., Cho, Y., Woo, H., & Chun, B. (2018). Green and efficient extraction of polysaccharides from brown seaweed by adding deep eutectic solvent in subcritical water hydrolysis. *Journal of Cleaner Production*, 198, 1474-1484.
- Saravanan, S., Vimalraj, S., Thanikaivelan, P., Banudevi, S., & Manivasagam, G. (2019). A review on injectable chitosan/beta glycerophosphate hydrogels for bone tissue regeneration. *International Journal of Biological Macromolecules*, 121, 38-54.
- Sarkar, S., Alvarez, V. H., & Saldaña, M. D. A. (2014). Relevance of ions in pressurized fluid extraction of carbohydrates and phenolics from barley hull. *The Journal of Supercritical Fluids*, 93, 27-37.
- Sasaki, M., & Goto, M. (2011). Thermal decomposition of guaiacol in sub-and supercritical water and its kinetic analysis. *Journal of Material Cycles and Waste Management*, 13(1), 68-79.

- Savadekar, N., & Mhaske, S. (2012). Synthesis of nano cellulose fibers and effect on thermoplastics starch based films. *Carbohydrate Polymers*, 89(1), 146-151.
- Savitri, E., & Rosyadi, A. (2015). Degradation of chitosan by hydrothermal process in the presence of sonication Pre-Treatment with supercritical CO₂ as pressurized fluid. *Macromolecular Symposia*, 353(1), 212-219.
- Schillinger, U., Kaya, M., & Lücke, F. (1991). Behaviour of listeria monocytogenes in meat and its control by a bacteriocin-producing strain of lactobacillus sake. *Journal of Applied Bacteriology*, 70(6), 473-478.
- Seligra, P. G., Jaramillo, C. M., Famá, L., & Goyanes, S. (2016). Biodegradable and non-retrogradable eco-films based on starch–glycerol with citric acid as crosslinking agent. *Carbohydrate Polymers*, 138, 66-74.
- Seman, D., Borger, A., Meyer, J., Hall, P., & Milkowski, A. (2002). Modeling the growth of listeria monocytogenes in cured ready-to-eat processed meat products by manipulation of sodium chloride, sodium diacetate, potassium lactate, and product moisture content. *Journal of Food Protection*, 65(4), 651-658.
- Shah, U., Naqash, F., Gani, A., & Masoodi, F. (2016). Art and science behind modified starch edible films and coatings: A review. *Comprehensive Reviews in Food Science and Food Safety*, 15(3), 568-580.
- Shankar, S., & Rhim, J. (2016). Preparation of nanocellulose from micro-crystalline cellulose: The effect on the performance and properties of agar-based composite films. *Carbohydrate Polymers*, 135, 18-26.
- Shen, L., & Zhang, G. (2009). Formation of mesoglobules by poly (N, N-diethylacrylamide) chains in dilute solutions. *Chinese Journal of Polymer Science*, 27(04), 561-567.
- Shen, X. L., Wu, J. M., Chen, Y., & Zhao, G. (2010). Antimicrobial and physical properties of sweet potato starch films incorporated with potassium sorbate or chitosan. *Food Hydrocolloids*, 24(4), 285-290.
- Shen, Z., & Kamdem, D. P. (2015). Development and characterization of biodegradable chitosan films containing two essential oils. *International Journal of Biological Macromolecules*, 74, 289-296.
- Shirai, M., Grossmann, M., Mali, S., Yamashita, F., Garcia, P., & Müller, C. (2013). Development of biodegradable flexible films of starch and poly (lactic acid) plasticized with adipate or citrate esters. *Carbohydrate Polymers*, 92(1), 19-22.
- Shirakawa, M., Yamatoya, K., & Nishinari, K. (1998). Tailoring of xyloglucan properties using an enzyme. *Food Hydrocolloids*, 12(1), 25-28.

- Silva, D. F. P., Siqueira, D. L., Matias, R. G. P., Oliveira, S. P., Lins, Leila Cristina Rosa de, & Salomão, L. C. C. (2012). Performance of edible films in comparison to the polyvinyl chloride film in the post-harvest tangerines' Poncã'. *Ciência Rural*, *42*(10), 1770-1773.
- Silva-Weiss, A., Bifani, V., Ihl, M., Sobral, P., & Gómez-Guillén, M. (2013). Structural properties of films and rheology of film-forming solutions based on chitosan and chitosan-starch blend enriched with murta leaf extract. *Food Hydrocolloids*, *31*(2), 458-466.
- Singh, P. P., & Saldaña, M. D. A. (2011). Subcritical water extraction of phenolic compounds from potato peel. *Food Research International*, *44*(8), 2452-2458.
- Siripatrawan, U., & Harte, B. R. (2010). Physical properties and antioxidant activity of an active film from chitosan incorporated with green tea extract. *Food Hydrocolloids*, *24*(8), 770-775.
- Sirocchi, V., Devlieghere, F., Peelman, N., Sagratini, G., Maggi, F., Vittori, S., & Ragaert, P. (2017). Effect of *rosmarinus officinalis* L. essential oil combined with different packaging conditions to extend the shelf life of refrigerated beef meat. *Food Chemistry*, *221*, 1069-1076.
- Slavutsky, A. M., & Bertuzzi, M. A. (2014). Water barrier properties of starch films reinforced with cellulose nanocrystals obtained from sugarcane bagasse. *Carbohydrate Polymers*, *110*, 53-61.
- Sokolik, C. G., Ben-Shabat-Binyamini, R., Gedanken, A., & Lellouche, J. (2018). Proteinaceous microspheres as a delivery system for carvacrol and thymol in antibacterial applications. *Ultrasonics Sonochemistry*, *41*, 288-296.
- Soković, M., Glamočlija, J., Marin, P. D., Brkić, D., & van Griensven, L. J. (2010). Antibacterial effects of the essential oils of commonly consumed medicinal herbs using an *in vitro* model. *Molecules*, *15*(11), 7532-7546.
- Solomakos, N., Govaris, A., Koidis, P., & Botsoglou, N. (2008). The antimicrobial effect of thyme essential oil, nisin, and their combination against *listeria monocytogenes* in minced beef during refrigerated storage. *Food Microbiology*, *25*(1), 120-127.
- Song, X., Zuo, G., & Chen, F. (2018). Effect of essential oil and surfactant on the physical and antimicrobial properties of corn and wheat starch films. *International Journal of Biological Macromolecules*, *107*, 1302-1309.
- Souza, A., Goto, G., Mainardi, J., Coelho, A. C. V., & Tadini, C. C. (2013). Cassava starch composite films incorporated with cinnamon essential oil: Antimicrobial activity, microstructure, mechanical and barrier properties. *LWT-Food Science and Technology*, *54*(2), 346-352.

- Spěvák, J., Geschke, D., & Ilavský, M. (2001). ^1H NMR study of temperature collapse of linear and crosslinked poly (N, N-diethylacrylamide) in D_2O . *Polymer*, 42(2), 463-468.
- Starčević, K., Krstulović, L., Brozić, D., Maurić, M., Stojević, Z., Mikulec, Ž, . . . Mašek, T. (2015). Production performance, meat composition and oxidative susceptibility in broiler chicken fed with different phenolic compounds. *Journal of the Science of Food and Agriculture*, 95(6), 1172-1178.
- Stekelenburg, F., & Kant-Muermans, M. (2001). Effects of sodium lactate and other additives in a cooked ham product on sensory quality and development of a strain of *lactobacillus curvatus* and *listeria monocytogenes*. *International Journal of Food Microbiology*, 66(3), 197-203.
- Sun, F., Huang, Q., Hu, T., Xiong, S., & Zhao, S. (2014a). Effects and mechanism of modified starches on the gel properties of myofibrillar protein from grass carp. *International Journal of Biological Macromolecules*, 64, 17-24.
- Sun, Q., Sun, C., & Xiong, L. (2013). Mechanical, barrier and morphological properties of pea starch and peanut protein isolate blend films. *Carbohydrate Polymers*, 98(1), 630-637.
- Sun, S., Mitchell, J. R., MacNaughtan, W., Foster, T. J., Harabagiu, V., Song, Y., & Zheng, Q. (2009). Comparison of the mechanical properties of cellulose and starch films. *Biomacromolecules*, 11(1), 126-132.
- Sun, S., Liu, P., Ji, N., Hou, H., & Dong, H. (2018). Effects of various cross-linking agents on the physicochemical properties of starch/PHA composite films produced by extrusion blowing. *Food Hydrocolloids*, 77, 964-975.
- Sun, X., Wang, Z., Kadouh, H., & Zhou, K. (2014b). The antimicrobial, mechanical, physical and structural properties of chitosan-gallic acid films. *LWT-Food Science and Technology*, 57(1), 83-89.
- Šuput, D., Lazić, V., Pezo, L., Markov, S., Vaštag, Ž, Popović, L., Radulović, A., Ostojić, S., Zlatanović, S. & Popović, S. (2016). Characterization of starch edible films with different essential oils addition. *Polish Journal of Food and Nutrition Sciences*, 66(4), 277-286.
- Syafri, E., Kasim, A., Abral, H., Sulungbudi, G. T., Sanjay, M., & Sari, N. H. (2018). Synthesis and characterization of cellulose nanofibers (CNF) ramie reinforced cassava starch hybrid composites. *International Journal of Biological Macromolecules*, 120, 578-586.
- Tábi, T., & Kovács, J. (2007). Examination of injection moulded thermoplastic maize starch. *Express Polymer Letters*, 1(12), 804-809.

- Taghizadeh, M. T., & Bahadori, A. (2014). Ultrasonic degradation of N-di and trihydroxy benzoyl chitosans and its effects on antioxidant activity. *Ultrasonics Sonochemistry*, 21(3), 1140-1149.
- Takagi, H., & Asano, A. (2007). Characterization of “green” composites reinforced by cellulose nanofibers. Paper presented at the *Key Engineering Materials*, 334 389-392.
- Takahashi, K., Ogata, A., Yang, W., & Hattori, M. (2002). Increased hydrophobicity of carboxymethyl starch film by conjugation with zein. *Bioscience, Biotechnology, and Biochemistry*, 66(6), 1276-1280.
- Talón, E., Trifkovic, K. T., Vargas, M., Chiralt, A., & González-Martínez, C. (2017). Release of polyphenols from starch-chitosan based films containing thyme extract. *Carbohydrate Polymers*, 175, 122-130.
- Tassou, C., Koutsoumanis, K., & Nychas, G. (2000). Inhibition of *salmonella enteritidis* and *staphylococcus aureus* in nutrient broth by mint essential oil. *Food Research International*, 33(3-4), 273-280.
- Teacă, C., Bodîrlău, R., & Spiridon, I. (2013). Effect of cellulose reinforcement on the properties of organic acid modified starch microparticles/plasticized starch bio-composite films. *Carbohydrate Polymers*, 93(1), 307-315.
- Teixeira, E. d. M., De Campos, A., Marconcini, J., Bondancia, T., Wood, D., Klamczynski, A., . . . Glenn, G. (2014). Starch/fiber/poly (lactic acid) foam and compressed foam composites. *RSC Advances*, 4(13), 6616-6623.
- Teixeira, J. S., Maier, M. B., Miller, P., Gänzle, M. G., & McMullen, L. M. (2016). The effect of growth temperature, process temperature, and sodium chloride on the high-pressure inactivation of *listeria monocytogenes* on ham. *European Food Research and Technology*, 242(12), 2021-2029.
- Teixeira, J. S., Repková, L., Gänzle, M. G., & McMullen, L. M. (2018). Effect of pressure, reconstituted RTE meat microbiota, and antimicrobials on survival and post-pressure growth of *listeria monocytogenes* on ham. *Frontiers in Microbiology*, 9, doi:10.3389/fmicb.2018.01979
- Tharanathan, R. (2003). Biodegradable films and composite coatings: Past, present and future. *Trends in Food Science & Technology*, 14(3), 71-78.
- Thunwall, M., Kuthanova, V., Boldizar, A., & Rigdahl, M. (2008). Film blowing of thermoplastic starch. *Carbohydrate Polymers*, 71(4), 583-590.
- Tian, F., Liu, Y., Hu, K., & Zhao, B. (2004). Study of the depolymerization behavior of chitosan by hydrogen peroxide. *Carbohydrate Polymers*, 57(1), 31-37.

- Tian, H., Yan, J., Rajulu, A. V., Xiang, A., & Luo, X. (2017). Fabrication and properties of polyvinyl alcohol/starch blend films: Effect of composition and humidity. *International Journal of Biological Macromolecules*, *96*, 518-523.
- Tirumala, V. R., Ilavsky, J., & Ilavsky, M. (2006). Effect of chemical structure on the volume-phase transition in neutral and weakly charged poly (N-alkyl (meth) acrylamide) hydrogels studied by ultrasmall-angle x-ray scattering. *The Journal of Chemical Physics*, *124*(23), doi:https://doi.org/10.1063/1.2205364
- Tischer, P. C. F., Sierakowski, M. R., Westfahl Jr, H., & Tischer, C. A. (2010). Nanostructural reorganization of bacterial cellulose by ultrasonic treatment. *Biomacromolecules*, *11*(5), 1217-1224.
- Tiwari, B. K., Imam, S. H., Rao, M., & Ahmed, J. (2012). *Starch-based polymeric materials and nanocomposites: Chemistry, processing, and applications*. CRC Press, Boca Raton, USA.
- Tomasi, G., Scandola, M., Briese, B. H., & Jendrossek, D. (1996). Enzymatic degradation of bacterial poly (3-hydroxybutyrate) by a depolymerase from *pseudomonas lemoignei*. *Macromolecules*, *29*(2), 507-513.
- Toor, S. S., Rosendahl, L., & Rudolf, A. (2011). Hydrothermal liquefaction of biomass: A review of subcritical water technologies. *Energy*, *36*(5), 2328-2342.
- Torres, F., Troncoso, O., Torres, C., Díaz, D., & Amaya, E. (2011). Biodegradability and mechanical properties of starch films from andean crops. *International Journal of Biological Macromolecules*, *48*(4), 603-606.
- Tovar, L., Salafranca, J., Sánchez, C., & Nerín, C. (2005). Migration studies to assess the safety in use of a new antioxidant active packaging. *Journal of Agricultural and Food Chemistry*, *53*(13), 5270-5275.
- Uematsu, M., & Frank, E. (1980). Static dielectric constant of water and steam. *Journal of Physical and Chemical Reference Data*, *9*(4), 1291-1306.
- Ulloa, P. A., Guarda, A., Valenzuela, X., Rubilar, J. F., & Galotto, M. J. (2017). Modeling the release of antimicrobial agents (thymol and carvacrol) from two different encapsulation materials. *Food Science and Biotechnology*, *26*(6), 1763-1772.
- Urbanek, A. K., Rymowicz, W., Strzelecki, M. C., Kociuba, W., Franczak, Ł., & Mirończuk, A. M. (2017). Isolation and characterization of arctic microorganisms decomposing bioplastics. *AMB Express*, *7*(1), 148.
- Van der Sman, R. G. M. (2017). Predicting the solubility of mixtures of sugars and their replacers using the Flory–Huggins theory. *Food & function*, *8*(1), 360-371.

- Valencia-Sullca, C., Atarés, L., Vargas, M., & Chiralt, A. (2018a). Physical and antimicrobial properties of compression-molded cassava starch-chitosan films for meat preservation. *Food and Bioprocess Technology*, *11*(7), 1339-1349.
- Valencia-Sullca, C., Vargas, M., Atarés, L., & Chiralt, A. (2018b). Thermoplastic cassava starch-chitosan bilayer films containing essential oils. *Food Hydrocolloids*, *75*, 107-115.
- Van der Veen, M., Veelaert, S., Van der Goot, A., & Boom, R. (2006). Starch hydrolysis under low water conditions: A conceptual process design. *Journal of Food Engineering*, *75*(2), 178-186.
- Vårum, K., Ottøy, M., & Smidsrød, O. (2001). Acid hydrolysis of chitosans. *Carbohydrate Polymers*, *46*(1), 89-98.
- Vásconez, M. B., Flores, S. K., Campos, C. A., Alvarado, J., & Gerschenson, L. N. (2009). Antimicrobial activity and physical properties of chitosan-tapioca starch based edible films and coatings. *Food Research International*, *42*(7), 762-769.
- Veiga-Santos, P., Oliveira, L., Cereda, M., Alves, A., & Scamparini, A. (2005). Mechanical properties, hydrophilicity and water activity of starch-gum films: Effect of additives and deacetylated xanthan gum. *Food Hydrocolloids*, *19*(2), 341-349.
- Vermeiren, L., Devlieghere, F., De Graef, V., & Debevere, J. (2005). *In vitro* and *in situ* growth characteristics and behaviour of spoilage organisms associated with anaerobically stored cooked meat products. *Journal of Applied Microbiology*, *98*(1), 33-42.
- Vigneshwaran, N., Ammayappan, L., & Huang, Q. (2011). Effect of gum arabic on distribution behavior of nanocellulose fillers in starch film. *Applied Nanoscience*, *1*(3), 137-142.
- Villalobos, R., Chanona, J., Hernández, P., Gutiérrez, G., & Chiralt, A. (2005). Gloss and transparency of hydroxypropyl methylcellulose films containing surfactants as affected by their microstructure. *Food Hydrocolloids*, *19*(1), 53-61.
- Vilpoux, O., & Averous, L. (2004). Starch-based plastics. In Cereda M.P., & Vilpoux O. (Eds.), *Technology, use and potentialities of Latin American starchy tubers* (pp. 521-553). São Paulo, Brazil: NGO Raizes and Cargill Foundation.
- Volpert, E., Selb, J., & Candau, F. (1998). Associating behaviour of polyacrylamides hydrophobically modified with dihexylacrylamide. *Polymer*, *39*(5), 1025-1033.
- Walenta, E., Fink, H., Weigel, P., Ganster, J., & Schaaf, E. (2001). Structure-property relationships of extruded starch, 2 extrusion products from native starch. *Macromolecular Materials and Engineering*, *286*(8), 462-471.

- Wan, Y., Wu, H., Yu, A., & Wen, D. (2006). Biodegradable polylactide/chitosan blend membranes. *Biomacromolecules*, 7(4), 1362-1372.
- Wang, L., Dong, W., & Xu, Y. (2007). Synthesis and characterization of hydroxypropyl methylcellulose and ethyl acrylate graft copolymers. *Carbohydrate Polymers*, 68(4), 626-636.
- Wang, Q., Tian, F., Feng, Z., Fan, X., Pan, Z., & Zhou, J. (2015). Antioxidant activity and physicochemical properties of chitosan films incorporated with lycium barbarum fruit extract for active food packaging. *International Journal of Food Science & Technology*, 50(2), 458-464.
- Wang, S., Lu, A., & Zhang, L. (2016). Recent advances in regenerated cellulose materials. *Progress in Polymer Science*, 53, 169-206.
- Wang, W., Zhang, H., Jia, R., Dai, Y., Dong, H., Hou, H., & Guo, Q. (2018). High performance extrusion blown starch/polyvinyl alcohol/clay nanocomposite films. *Food Hydrocolloids*, 79, 534-543.
- Weiss, J., Loeffler, M., & Terjung, N. (2015). The antimicrobial paradox: Why preservatives lose activity in foods. *Current Opinion in Food Science*, 4, 69-75.
- Wen, P., Zhu, D., Wu, H., Zong, M., Jing, Y., & Han, S. (2016). Encapsulation of cinnamon essential oil in electrospun nanofibrous film for active food packaging. *Food Control*, 59, 366-376.
- Westacott, R. E., Johnston, K. P., & Rossky, P. J. (2001). Stability of ionic and radical molecular dissociation pathways for reaction in supercritical water. *The Journal of Physical Chemistry B*, 105(28), 6611-6619.
- WHO. (2004). Executive summary. *Risk assessment of Listeria monocytogenes in ready-to-eat foods: technical report. Microbiological risk assessment series; no. 5*. pp. xxv-xxxiii
- Woranuch, S., Yoksan, R., & Akashi, M. (2015). Ferulic acid-coupled chitosan: Thermal stability and utilization as an antioxidant for biodegradable active packaging film. *Carbohydrate Polymers*, 115, 744-751.
- Woraprayote, W., Malila, Y., Sorapukdee, S., Swetwivathana, A., Benjakul, S., & Visessanguan, W. (2016). Bacteriocins from lactic acid bacteria and their applications in meat and meat products. *Meat Science*, 120, 118-132.
- Xie, W., Xu, P., & Liu, Q. (2001). Antioxidant activity of water-soluble chitosan derivatives. *Bioorganic & Medicinal Chemistry Letters*, 11(13), 1699-1701.

- Xiong, B., Loss, R. D., Shields, D., Pawlik, T., Hochreiter, R., Zydney, A. L., & Kumar, M. (2018). Polyacrylamide degradation and its implications in environmental systems. *npj Clean Water*, 1(1), 17.
- Xiong, H., Tang, S., Tang, H., & Zou, P. (2008). The structure and properties of a starch-based biodegradable film. *Carbohydrate Polymers*, 71(2), 263-268.
- Xu, Y., Scales, A., Jordan, K., Kim, C., & Sismour, E. (2017). Starch nanocomposite films incorporating grape pomace extract and cellulose nanocrystal. *Journal of Applied Polymer Science*, 134(6), 9 pp. doi:<https://doi.org/10.1002/app.44438>
- Yan, Q., Hou, H., Guo, P., & Dong, H. (2012). Effects of extrusion and glycerol content on properties of oxidized and acetylated corn starch-based films. *Carbohydrate Polymers*, 87(1), 707-712.
- Yang, S., Cao, L., Kim, H., Beak, S., & Song, K. B. (2018a). Utilization of foxtail millet starch film incorporated with clove leaf oil for the packaging of queso blanco cheese as a model food. *Starch-Stärke*, 70(3-4), 7 pp. doi:<https://doi.org/10.1002/star.201700171>
- Yang, W., Wang, H., Zhou, J., & Wu, S. (2018b). Hydrolysis kinetics and mechanism of chitin in subcritical water. *The Journal of Supercritical Fluids*, 135, 254-262.
- Yang, Y., Zhao, Y., Liu, X., Ding, F., & Gu, X. (2007). The effect of different sterilization procedures on chitosan dried powder. *Journal of Applied Polymer Science*, 104(3), 1968-1972.
- Yang, Z., Fu, K., Yu, J., Zhou, P., & Cheng, Z. (2018c). "pH-triggered" drug release using shell cross-linked micelles from aqueous RAFT-synthesized PAPMA-b-PNIPAM copolymers. *Journal of Polymer Research*, 25(8), 7 pp. <https://doi.org/10.1007/s10965-018-1564-9>
- Yildirim, S., Röcker, B., Pettersen, M. K., Nilsen-Nygaard, J., Ayhan, Z., Rutkaite, R., . . . Coma, V. (2018). Active packaging applications for food. *Comprehensive Reviews in Food Science and Food Safety*, 17(1), 165-199.
- Yong, T. L., & Yukihiko, M. (2013). Kinetic analysis of guaiacol conversion in sub-and supercritical water. *Industrial & Engineering Chemistry Research*, 52(26), 9048-9059.
- Yousef, A. E., & Lou, Y. (1999). Characteristics of *listeria monocytogenes* important to food processors. In E. T. Ryser, & E. H. Marth (Eds.), *Listeria, listeriosis and food safety* (2nd ed., pp. 134-224). New York: Marcel Dekker, Inc. USA.
- Yu, L., & Christie, G. (2005). Microstructure and mechanical properties of orientated thermoplastic starches. *Journal of Materials Science*, 40(1), 111-116.

- Yu, S., Ma, Y., & Sun, D. (2009). Impact of amylose content on starch retrogradation and texture of cooked milled rice during storage. *Journal of Cereal Science*, 50(2), 139-144.
- Yu, S., Ma, Y., & Sun, D. (2010). Effects of freezing rates on starch retrogradation and textural properties of cooked rice during storage. *LWT-Food Science and Technology*, 43(7), 1138-1143.
- Yu, Y., & Wu, H. (2011). Kinetics and mechanism of glucose decomposition in hot-compressed water: Effect of initial glucose concentration. *Industrial & Engineering Chemistry Research*, 50(18), 10500-10508.
- Yun, Y., Wee, Y., Byun, H., & Yoon, S. (2008). Biodegradability of chemically modified starch (RS4)/PVA blend films: Part 2. *Journal of Polymers and the Environment*, 16(1), 12-18.
- Zhang, H., Kong, B., Xiong, Y. L., & Sun, X. (2009). Antimicrobial activities of spice extracts against pathogenic and spoilage bacteria in modified atmosphere packaged fresh pork and vacuum packaged ham slices stored at 4 °C. *Meat Science*, 81(4), 686-692.
- Zhang, J. (2015). *Bioactive films and hydrogels based on potato starch and phenolic acids using subcritical water technology*, Masters thesis, University of Alberta, Edmonton, AB, Canada, pp 97-172.
- Zhang, Y., Furyk, S., Bergbreiter, D. E., & Cremer, P. S. (2005). Specific ion effects on the water solubility of macromolecules: PNIPAM and the hofmeister series. *Journal of the American Chemical Society*, 127(41), 14505-14510.
- Zhao, Y., Lu, W., Wu, H., Liu, J., & Wang, H. (2012). Optimization of supercritical phase and combined supercritical/subcritical conversion of lignocellulose for hexose production by using a flow reaction system. *Bioresource Technology*, 126, 391-396.
- Zhao, Y., & Saldaña, M. D. A. (2019). Use of potato by-products and gallic acid for development of bioactive film packaging by subcritical water technology. *The Journal of Supercritical Fluids*, 143, 97-106.
- Zhao, Y., & Saldaña, M. D. (2018). Hydrolysis of cassava starch/chitosan and their mixtures in pressurized hot water media. *J. Supercrit. Fluid*. In press.
<https://doi.org/10.1016/j.supflu.2018.11.013>
- Zhao, Y., Teixeira, J. S., Gänzle, M. G., & Saldaña, M. D. A. (2018). Development of antimicrobial films based on cassava starch, chitosan and gallic acid using subcritical water technology. *The Journal of Supercritical Fluids*, 137, 101-110.
- Zhou, D., Wang, L., Chen, X., Wei, X., Liang, J., Zhang, D., & Ding, G. (2018). A novel acid catalyst based on super/subcritical CO₂-enriched water for the efficient esterification of rosin. *Royal Society Open Science*, 5(7), 8 pp. doi:<http://dx.doi.org/10.1098/rsos.171031>

- Zhou, G., Xu, X., & Liu, Y. (2010). Preservation technologies for fresh meat—A review. *Meat Science*, 86(1), 119-128.
- Zia-ud-Din, Xiong, H., & Fei, P. (2017). Physical and chemical modification of starches: A review. *Critical Reviews in Food Science and Nutrition*, 57(12), 2691-2705.
- Zivanovic, S., Chi, S., & Draughon, A. F. (2005). Antimicrobial activity of chitosan films enriched with essential oils. *Journal of Food Science*, 70(1), M45-M51.
- Zullo, R., & Iannace, S. (2009). The effects of different starch sources and plasticizers on film blowing of thermoplastic starch: Correlation among process, elongational properties and macromolecular structure. *Carbohydrate Polymers*, 77(2), 376-383.

Appendix A: Pressurized hot water hydrolysis of starch and chitosan

Table A.1 Amylose content of pure cassava starch after pressurized hot water treatment at 75-150 °C and 50-155 bar for 10 min.

Pressure (bar)	Temperature (°C)			
	75	100	125	150
50	13.37±0.20%	13.09±1.00%	11.40±2.19%	9.79±0.80%
85	21.96±1.00%	22.38±0.80%	17.03±1.97%	1.13±0.12%
120	25.20±1.99%	5.99±0.09%	2.10±0.30%	0.13±0.23%
155	27.11±2.39%	0.13±0.02%	0.31±0.03%	0.12±0.09%

Table A.2 Reducing end yield of pure cassava starch, and chitosan after pressurized hot water treatment at 75-150 °C and 50-155 bar for 10 min.

Pressure (bar)	Starch (mg glucose equivalent/g starch)			
	Temperature (°C)			
	75	100	125	150
50	3.38±0.21	4.00±0.34	8.20±0.13	17.59±1.12
85	5.36±0.12	6.39±0.45	13.67±0.24	23.46±0.56
120	5.19±0.23	16.71±0.51	21.08±0.76	26.39±0.85
155	5.94±0.15	23.37±0.65	27.03±1.01	38.59±2.56

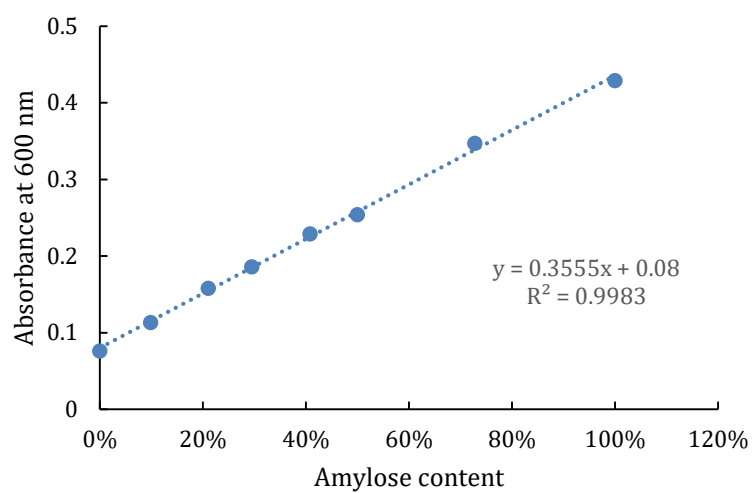
Pressure (bar)	Chitosan (mg N-acetyl-D-glucosamine equivalent/g chitosan)			
	Temperature (°C)			
	75	100	125	150
50	23.01±3.59	28.13±0.34	38.54±0.13	53.19±1.40
85	28.76±2.10	32.79±0.45	41.43±0.24	51.16±2.55
120	32.09±1.40	36.12±0.51	45.61±0.76	60.11±0.82
155	35.74±1.56	45.10±1.15	56.43±1.01	81.22±4.56

Table A.3a Molecular weight of pure cassava starch and chitosan after pressurized hot water treatment at 75-150 °C and 50-155 bar for 10 min.

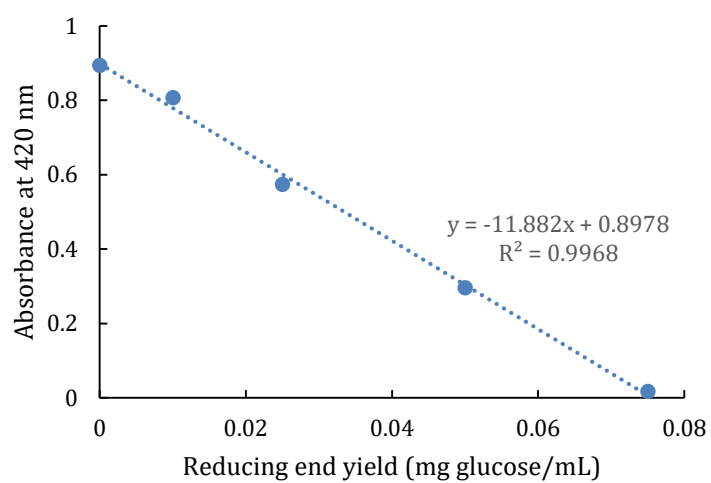
Starch (kDa)				
Pressure (bar)	Temperature (°C)			
	75	100	125	150
50	513.5±10.6	345.6±34.5	248.5±12.4	224.0±10.1
85	435.5±24.8	331.4±23.4	226.5±12.5	193.3±9.5
120	351.0±24.5	190.2±11.2	131.5±12.4	87.1±9.
155	172.5±13.5	130.7±9.4	120.5±4.5	79.9±9.4
Chitosan (kDa)				
Pressure (bar)	Temperature (°C)			
	75	100	125	150
50	180.5±6.4	79.9±0.7	42.9±2.4	36.6±1.8
85	167.5±7.8	65.3±1.1	47.1±2.1	34.1±2.3
120	142.0±4.2	61.2±1.3	54.2±3.5	30.4±1.3
155	77.0±1.1	52.3±1.6	49.3±1.1	24.7±1.5

Table A.3b Hydrodynamic diameter of chitosan after pressurized hot water treatment at 75-150 °C and 50-155 bar for 10 min.

Pressure (bar)	Temperature (°C)			
	75	100	125	150
50	2639.0±49.5	1691.5±40.3	1206.5±36.1	393.5±18.4
85	2510.5±77.7	1408.5±68.6	1132.5±112.4	377.3±31.3
120	2467.5±16.3	1267.5±31.8	953.3±70.0	344.4±24.4
155	2448.5±33.2	1214.0±28.3	1058.0±70.7	308.3±15.4



(a)



(b)

Fig A.1 Standard curves for: a) amylose content and b) reducing end yield.

Appendix B: Potato by-product film with(out) gallic acid

Table B.1 Tensile strength and elongation at break for bioactive films based on potato by-products.

Potato peel/cull ratio (g/g)	Tensile strength (MPa)	Elongation (%)
0:1	2.53±0.07 ^d	28.51±0.82 ^a
0.5:1	5.47±0.46 ^c	23.63±0.78 ^b
1:1	7.99±0.30 ^b	17.73±1.07 ^c
1.3:1	8.99±0.19 ^a	12.19±1.19 ^d
Glycerol/potato cull starch ratio (g/g)	Tensile strength (MPa)	Elongation (%)
0:1	7.90±0.36 ^a	13.35±0.41 ^b
0.5:1	2.58±0.09 ^b	30.78±1.77 ^a
1:1	1.44±0.09 ^c	28.69±1.98 ^a
2:1	0.88±0.05 ^c	28.00±1.31 ^a
GA/potato cull starch ratio (g/g)	Tensile strength (MPa)	Elongation (%)
0:1	3.03±0.12 ^a	18.91±0.56 ^d
0.1:1	1.93±0.15 ^b	24.45±1.13 ^{bc}
0.2:1	1.83±0.10 ^{bc}	28.23±1.67 ^a
0.3:1	1.55±0.13 ^c	25.54±0.71 ^{ab}

Bioactive films of potato peel/cull ratios (0-1.3 g/g) and glycerol/potato cull starch ratio (0.5 g/g), glycerol/potato cull starch ratios (0.5-2 g/g) and potato peel/cull ratios (1.3 g/g), and GA/potato cull starch ratios (0-0.3 g/g) and glycerol/potato cull starch ratio (1 g/g) produced at 120 bar and 125 °C.

^{a-d}Different lowercase letters in the same column indicate significant differences ($p < 0.05$).

Table B.2 Film solubility in water at 4, 25 and 50 °C, and top and bottom surfaces contact angle of bioactive films.

Potato peel/cull ratio (g/g)	Contact angle (°)		Film solubility in water (%)		
	Top	Bottom	4 °C	25 °C	50 °C
0:1	83.46±2.58 ^a	26.72±0.82 ^a	21.95±0.86 ^a	25.90±0.63 ^a	29.44±1.40 ^a
0.5:1	77.35±1.58 ^{ab}	26.34±3.01 ^a	20.84±0.86 ^a	22.05±0.99 ^b	27.56±1.38 ^b
1:1	71.42±2.17 ^b	21.12±2.01 ^{ab}	20.63±1.50 ^{ab}	21.50±1.32 ^b	26.10±0.47 ^{bc}
1.3:1	76.94±3.03 ^{ab}	16.75±1.53 ^b	18.72±1.16 ^b	20.06±0.55 ^b	25.28±0.71 ^c

GA/potato cull starch ratio (g/g)	Contact angle (°)		Film solubility in water (%)		
	Top	Bottom	4 °C	25 °C	50 °C
0:1	73.40±3.00 ^a	40.50±1.43 ^a	24.50±1.56 ^c	26.15±0.78 ^c	28.18±0.82 ^c
0.1:1	70.50±1.56 ^a	31.19±1.49 ^b	27.05±0.49 ^{bc}	27.75±0.21 ^{bc}	30.28±0.74 ^b
0.2:1	63.54±2.00 ^b	28.90±1.25 ^{bc}	29.35±0.78 ^b	29.15±0.78 ^b	31.91±0.83 ^b
0.3:1	58.79±3.97 ^b	23.68±2.40 ^c	32.10±0.56 ^a	31.10±0.56 ^a	35.50±0.29 ^a

Bioactive films based on potato by-products with different potato peel/cull ratios (0-1.3 g/g) and constant glycerol/potato cull starch ratio (0.5 g/g) or GA/potato cull starch ratios (0-0.3 g/g) and constant glycerol/potato cull starch ratio (1 g/g) at 120 bar and 125 °C. ^{a-c}Different lowercase letters in the same column indicate significant differences ($p < 0.05$).

Table B.3 Total phenolic content, and antioxidant activity by ABTS and FRAP methods of bioactive films.

Potato peel/cull ratio (g/g)	Total phenolics (mg gallic acid equivalent/g film)	FRAP (mg Trolox equivalent/g film)	ABTS (mg Trolox equivalent/g film)
0:1	0.34±0.02 ^d	1.13±0.24 ^d	1.55±0.06 ^d
0.5:1	2.24±0.06 ^c	34.47±0.52 ^c	40.57±0.97 ^c
1:1	3.45±0.11 ^b	50.05±3.88 ^b	63.56±4.52 ^b
1.3:1	6.13±0.17 ^a	93.08±2.47 ^a	105.36±2.92 ^a

GA/potato cull starch ratio (g/g)	Total phenolics (mg gallic acid equivalent/g film)	FRAP (mg Trolox equivalent/g film)	ABTS (mg Trolox equivalent/g film)
0:1	0.35±0.01 ^d	5.00±0.64 ^d	9.00±0.39 ^d
0.1:1	46.52±3.44 ^c	464.01±15.45 ^c	530.83±9.55 ^c
0.2:1	111.89±5.80 ^b	1343.17±6.63 ^b	1516.96±73.26 ^b
0.3:1	172.32±5.81 ^a	1811.30±19.10 ^a	2070.23±38.10 ^a

Bioactive films based on potato by-products with different potato peel/cull ratios (0-1.3 g/g) and constant glycerol/potato cull starch ratio of 0.5 g/g, and GA/potato cull starch ratios (0-0.3 g/g) and constant glycerol/potato cull starch ratio of 1 g/g produced at 120 bar and 125 °C.

^{a-d}Different lowercase letters in the same column indicate significant differences ($p < 0.05$).

Appendix C: Cassava starch/chitosan film loaded with gallic acid

Table C.1 Statistical analysis of fractional factorial design.

Source	DF	Adj SS	Adj MS	F-Value	P-Value
Temperature (°C)	3	9465.5	3155.15	66.34	0.000
Pressure (bar)	3	774.9	258.32	5.43	0.009
Gallic acid/starch ratio (g/g)	3	1513.3	504.42	10.61	0.000
Glycerol/starch ratio (g/g)	3	570.0	190.01	3.99	0.027
Chitosan/starch ratio (g/g)	3	531.8	177.28	3.73	0.033
Error	16	761.0	47.56		
S		R-sq	R-sq(adj)	R-sq(pred)	
6.89656		94.40%	89.16%	77.62%	

Table C.2 Mechanical properties of bioactive cassava starch films.

Chitosan/cassava starch ratio (g/g)	Tensile strength (MPa)	Elongation (%)
0:1	0.51±0.02 ^d	70.17±4.59 ^b
0.025:1	0.61±0.03 ^{cd}	94.7±8.83 ^a
0.05:1	0.63±0.02 ^{bcd}	100.15±4.77 ^a
0.075:1	0.66±0.04 ^{bc}	99.1±8.90 ^a
0.1:1	0.74±0.01 ^{ab}	93±1.73 ^a
0.15:1	0.83±0.13 ^a	65.7±9.95 ^b

Bioactive films with different chitosan/starch ratios of 0-0.15g/g, constant gallic acid/starch ratio of 0.1 g/g and glycerol/starch ratio of 0.5 g/g at 85 bar and 100 °C.

^{a-d}Different lowercase letters in the same column indicate significant differences ($p < 0.05$).

Table C.3 Film solubility in water at 4, 25 and 50°C, B) top and bottom surfaces contact angle of chitosan incorporated cassava starch/gallic acid films.

Chitosan/cassava starch ratio (g/g)	Contact angle (°)		Film solubility in water (%)		
	Top	Bottom	4 °C	25 °C	50 °C
0:1	36.71±1.02 ^d	55.15±1.15 ^f	26.30±1.80 ^a	36.71±1.40 ^a	40.00±1.88 ^a
0.025:1	37.20±3.16 ^d	59.00±1.11 ^e	22.60±0.92 ^{ab}	30.10±0.34 ^{ab}	33.60±2.35 ^{ab}
0.05:1	39.36±0.81 ^{cd}	69.00±1.36 ^d	18.00±0.64 ^{bc}	29.00±0.68 ^b	35.99±2.76 ^{abc}
0.075:1	44.13±0.41 ^c	74.00±0.10 ^c	17.10±2.57 ^{bc}	22.30±0.59 ^c	27.06±1.32 ^{bc}
0.1:1	55.97±2.37 ^b	78.00±1.90 ^b	16.73±0.73 ^c	19.87±2.68 ^c	27.55±0.75 ^{bc}
0.15:1	68.26±1.91 ^a	94.00±1.25 ^a	13.19±0.44 ^c	18.14±2.29 ^c	25.08±1.19 ^c

Bioactive cassava starch films with different chitosan/starch ratios of 0-0.15g/g, constant gallic acid/starch ratio of 0.1 g/g and glycerol/starch ratio of 0.5 g/g at 85 bar and 100 °C.

^{a-f} Different lowercase letters in the same column indicate significant differences.

Table C.4 Color performance (total color difference, whiteness index and yellowness index), transparency, and top and bottom surfaces gloss of chitosan incorporated cassava starch/gallic acid films.

Chitosan/cassava starch ratio (g/g)	Color performance			Transparency	Gloss (GU)	
	ΔE	YI	WI		Top	Bottom
0:1	4.87±0.38 ^b	3.66±0.03 ^c	97.2±0.08 ^a	2.17±0.09 ^a	8.05±0.07 ^d	10.75±0.07 ^e
0.025:1	5.25±0.19 ^b	3.77±0.09 ^c	96.7±0.10 ^{ab}	1.89±0.01 ^b	8.15±0.07 ^d	14.45±0.07 ^c
0.05:1	5.11±0.13 ^b	4.38±0.01 ^{bc}	96.5±0.10 ^{ab}	1.15±0.10 ^c	17.95±0.49 ^c	45.70±0.56 ^d
0.075:1	6.41±0.05 ^a	4.29±0.11 ^{bc}	95.9±0.27 ^{abc}	1.00±0.02 ^c	50.54±0.14 ^b	52.40±0.28 ^c
0.1:1	5.68±0.04 ^{ab}	5.04±0.59 ^{ab}	95.6±0.53 ^{bc}	0.90±0.02 ^{cd}	54.55±7.42 ^b	58.05±0.21 ^b
0.15:1	5.35±0.41 ^b	6.25±0.45 ^a	94.8±0.64 ^c	0.76±0.01 ^d	70.75±0.49 ^a	88.90±0.14 ^a

^{a-c} Different lowercase letters in the same column indicate significant differences.

Bioactive starch films with different chitosan/starch ratios of 0-0.15 g/g, constant gallic acid/starch ratio of 0.1 g/g and glycerol/starch ratio of 0.5 g/g at 85 bar and 100 °C.

Table C.5 Total phenolic content and antioxidant activity of chitosan incorporated cassava starch/gallic acid films.

Chitosan/cassava starch ratio (g/g)	Total phenolics (mg gallic acid equivalent/g film)	FRAP (mg Trolox equivalent/g film)	ABTS (mg Trolox equivalent/g film)
0:1	55.53±2.40 ^a	488.53±0.32 ^a	642.54±3.10 ^a
0.025:1	48.21±1.60 ^b	459.34±4.50 ^{ab}	606.58±11.93 ^b
0.05:1	44.33±1.45 ^{bc}	429.68±11.20 ^{bc}	549.91±44.32 ^c
0.075:1	41.84±0.31 ^c	402.48±4.66 ^c	485.46±41.75 ^d
0.1:1	40.41±0.68 ^{cd}	399.39±10.23 ^c	468.75±40.43 ^{de}
0.15:1	35.91±1.50 ^d	365.51±9.67 ^d	448.77±1.53 ^e

^{a-c} Different lowercase letters in the same column indicate significant differences.

Bioactive starch films with different chitosan/starch ratios of 0-0.15 g/g, constant gallic acid/starch ratio of 0.1 g/g and glycerol/starch ratio of 0.5 g/g at 85 bar and 100 °C.

Appendix D: Cassava starch/chitosan film loaded with carvacrol essential oil and biodegradability

Table D.1 Statistical analysis of fractional factorial design.

Analysis of Variance					
Source	DF	Adj SS	Adj MS	F-Value	P-Value
Temperature (°C)	2	16674	8336.8	44.96	0.000
Pressure (bar)	2	15337	7668.6	41.35	0.000
Chitosan/starch ratio (g/g)	2	34327	17163.6	92.56	0.000
Carvacrol/starch ratio (g/g)	2	6630	3315.1	17.88	0.001
Error	9	1669	185.4		
Total	17	80475			
S		R-sq	R-sq(adj)	R-sq(pred)	
13.6176		97.93%	96.08%	91.70%	

Table D.1 Mechanical properties of carvacrol incorporated cassava starch/chitosan films.

Carvacrol/cassava starch ratio (g/g)	Tensile strength (MPa)	Elongation (%)
0:1	0.56±0.04 ^a	231.80±15.98 ^a
0.049:1	0.48±0.04 ^a	126.85±9.69 ^b
0.098:1	0.46±0.07 ^{ab}	56.50±8.34 ^c
0.147:1	0.29±0.03 ^{bc}	54.35±1.34 ^c
0.196:1	0.19±0.02 ^c	70.55±7.28 ^c

Bioactive starch films produced at different carvacrol/starch ratios of 0-0.195 g/g, constant chitosan/starch ratio of 0.025 g/g and glycerol/starch ratio of 0.5 g/g produced at 75 °C and 120 bar.

^{a-c} Different lowercase letters in the same column indicate significant differences.

Table D.2 Total phenolics content and total antioxidant activity of carvacrol incorporated cassava starch/chitosan films.

Carvacrol/cassava starch ratio (g/g)	Total phenolics (mg gallic acid equivalent/g film)	FRAP (mg Trolox equivalent/g film)	ABTS (mg Trolox equivalent/g film)
0:1	0±0 ^d	1.33±0.12 ^d	3.49±0.31 ^e
0.049:1	0.34±0.06 ^d	12.25±0.67 ^c	16.87±0.62 ^d
0.098:1	1.82±0.03 ^c	26.62±1.34 ^b	33.23±2.15 ^c
0.147:1	4.79±0.38 ^b	54.33±1.90 ^a	65.93±2.77 ^b
0.196:1	6.62±0.44 ^a	61.00±3.48 ^a	84.91±6.78 ^a

Bioactive starch films with different carvacrol/starch ratios of 0-0.195 g/g, constant chitosan/starch ratio of 0.025 g/g and glycerol/starch ratio of 0.5 g/g produced at 75 °C and 120 bar.

^{a-c} Different lowercase letters in the same column indicate significant differences.

Table D.3 Weight loss curves of potato peel/cull films, potato cull/gallic acid films, cassava starch/gallic acid/chitosan films, and cassava starch/chitosan/carvacrol films during biodegradation in compost as a function of time.

Weight loss (%) - potato peel/cull films				
Time (days)	0 g peel/g cull	0.5 g peel/g cull	1.0 g peel/g cull	1.3 g peel/g cull
0	0±0	0±0	0±0	0±0
3	4.23±0.86	2.80±0.19	0.99±0.21	0.81±0.06
5	12.25±0.80	9.40±1.67	4.81±0.75	2.52±0.49
10	17.44±1.53	14.32±0.73	10.38±1.15	7.85±2.85
15	23.35±0.88	18.80±2.09	16.44±0.44	10.25±2.79
20	40.12±3.62	31.77±0.39	27.14±3.27	23.44±1.52
25	61.88±2.20	53.43±2.91	45.80±2.97	41.28±5.52
35	83.47±1.14	77.59±3.86	72.54±1.80	65.86±3.15
45	85.88±2.25	84.12±6.23	77.54±1.60	75.54±6.71
55	89.20±2.13	86.60±3.23	82.30±2.45	78.60±3.10
65	93.10±4.20	90.50±2.34	86.50±1.23	80.30±2.73
75	96.40±3.10	92.40±1.75	89.10±1.56	83.20±2.60
85	99.10±2.20	95.60±1.59	93.30±2.12	93.10±2.63

Weight loss (%) - potato cull/gallic acid films				
Time (days)	0 g GA/g cull starch	0.1 g GA/g cull starch	0.2 g GA/g cull starch	0.3 g GA/g cull starch
0	0±0	0±0	0±0	0±0
3	3.40±2.25	0.16±0.03	2.47±0.27	4.74±0.38
5	9.41±1.83	4.55±0.75	0.44±0.34	28.37±5.50
10	20.30±0.76	5.19±1.23	2.18±2.57	36.61±0.87
15	30.90±3.47	10.52±3.16	7.34±2.19	45.05±5.75
20	49.83±2.03	31.28±3.08	22.50±6.09	72.54±7.94
25	72.30±1.32	60.34±2.58	38.40±1.17	84.43±5.49
35	85.06±5.96	73.00±4.73	75.09±1.42	92.17±6.52
45	91.23±4.32	82.48±1.71	85.43±5.98	91.63±3.13
55	93.40±2.34	87.90±2.51	88.40±1.42	93.10±2.58
65	98.10±2.45	93.30±3.41	93.40±3.24	96.70±2.67

Weight loss (%) -cassava starch/gallic acid/chitosan films						
Time (days)	0 g chitosan/ g starch	0.025g chitosan/ g starch	0.05 g chitosan/ g starch	0.075g chitosan/ g starch	0.1 g chitosan/ g starch	0.15 g chitosan/ g starch
0	0±0	0±0	0±0	0±0	0±0	0±0
3	6.91±1.34	1.71±0.12	1.14±1.00	1.43±0.28	0.45±0.60	2.37±0.43
5	34.15±2.79	20.22±0.00	7.26±0.33	7.75±0.89	6.11±2.90	16.78±0.61
10	60.20±3.31	63.31±4.24	41.58±8.56	49.40±5.85	56.88±3.62	57.83±1.64
15	78.39±7.16	71.63±2.22	57.65±4.41	63.68±4.30	69.60±2.61	77.04±2.48
20	94.05±5.16	79.16±2.13	76.28±3.54	76.30±2.30	78.97±3.74	84.04±0.21
25	95.54±4.02	97.59±2.84	86.09±2.78	89.72±2.10	86.22±3.00	90.72±5.06
35	100.44±6.02	99.75±0.67	97.62±0.65	94.42±3.27	92.63±3.94	93.25±3.00
45	100.00±0.00	100.00±0.00	99.21±0.50	100.00±0.00	100.00±0.00	100.00±0.00

Weight loss (%) -cassava starch/chitosan/carvacrol films					
Time (days)	0 g carvacrol/ g starch	0.049 g carvacrol/ g starch	0.098 g carvacrol/ g starch	0.147 g carvacrol/ g starch	0.195 g carvacrol/ g starch
0	0±0	0±0	0±0	0±0	0±0
3	3.58±0.69	4.01±0.27	2.35±1.51	2.29±1.67	10.89±3.51
5	18.94±0.01	6.46±0.17	21.92±3.47	13.26±1.74	28.46±6.77
10	62.72±4.31	56.57±10.22	55.89±7.08	41.06±5.82	51.49±9.68
15	71.18±2.25	77.49±2.09	67.70±1.01	64.93±5.69	72.05±5.09
20	78.82±2.17	87.52±0.18	76.65±1.65	81.66±3.23	77.44±1.94
25	97.55±2.89	92.69±2.05	84.17±4.16	89.36±2.74	87.94±5.01
35	99.75±0.68	95.69±1.59	92.63±0.54	95.17±1.84	91.24±1.72
45	100.79±0.00	97.83±1.10	98.40±0.83	97.60±0.45	99.00±0.00

Appendix E: Cassava starch/chitosan film loaded with gallic acid and cellulose nanofiber

Table E.1 Statistical analysis of fractional factorial design.

Analysis of Variance					
Source	DF	Adj SS	Adj MS	F-Value	P-Value
Model	15	316.686	21.1124	86.48	0.000
Blocks	1	0.107	0.1068	0.44	0.519
Linear	6	295.589	49.2648	201.81	0.000
Temperature (°C)	2	74.204	37.1022	151.99	0.000
CNF/starch ratio (g/g)	4	221.385	55.3461	226.72	0.000
2-Way Interactions	8	20.990	2.6237	10.75	0.000
Temperature (°C)*CNF/starch ratio (g/g)	8	20.990	2.6237	10.75	0.000
Error	14	3.418	0.2441		
Total	29	320.103			
S	R-sq	R-sq(adj)	R-sq(pred)		
0.494083	98.93%	97.79%	95.10%		

Table E.2 Total phenolic content, and total antioxidant activity of CNFs reinforced cassava starch/chitosan/gallic acid films.

CNFs/cassava starch ratio (g/g)	Total phenolics (mg gallic acid equivalent/g film)	FRAP (mg Trolox equivalent/g film)	ABTS (mg Trolox equivalent/g film)
0:1	35.12±1.40 ^c	365.34±9.40 ^c	448.49±6.20 ^c
0.025:1	52.46±0.63 ^a	711.45±32.43 ^a	614.30±28.43 ^a
0.05:1	41.72±2.96 ^b	518.49±16.03 ^b	535.45±6.09 ^b
0.075:1	39.84±0.55 ^{bc}	514.03±4.70 ^b	464.84±13.56 ^c
0.1:1	41.09±0.66 ^{bc}	428.45±35.40 ^{bc}	480.43±3.10 ^{bc}

Bioactive films with different CNFs/starch ratios, constant chitosan/starch ratio (0.15 g/g) and gallic acid/starch ratio (0.1 g/g) produced at 100 °C and 85 bar.

^{a-c} Different lowercase letters in the same column indicate significant differences.

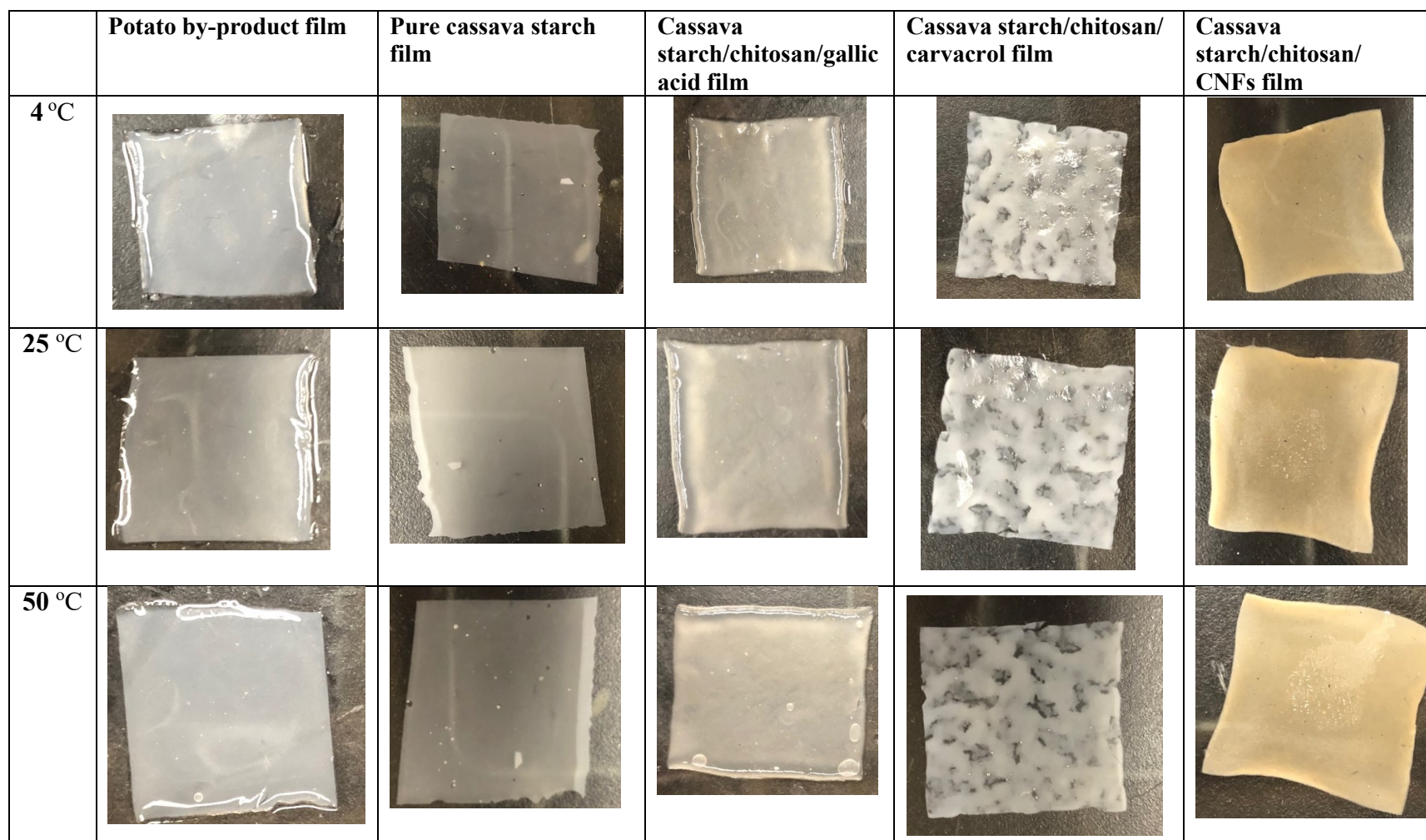


Fig. E.1 Swelling of bioactive films in water at 4, 25 and 50 °C after 24 h immersion.

Potato by-product film at 0.3 g gallic acid/g cull starch and 1 g glycerol/g cull starch; pure cassava starch film at 1 g glycerol/g starch; cassava starch/chitosan/gallic acid film at 0.15 g chitosan/g starch, 0.1 g gallic acid/g starch and 0.5 g glycerol/g starch; cassava starch/chitosan/ carvacrol film 0.195 g carvacrol/g starch, 0.025 g chitosan/g starch ratio and 0.5 g glycerol/g starch; cassava starch/chitosan/ CNFs film at 0.1 g CNFs/g starch 0.15 g chitosan/g starch and 0.1 g gallic acid/g starch.

Appendix F: Film antimicrobial activity against *Listeria monocytogenes* and reconstructed meat microbiota

Table F.1 Minimal inhibitory concentration (g/L) of gallic acid and carvacrol as a function of chitosan concentration (g/L) for *L. monocytogenes* strains.

Carvacrol (g/L)					
Chitosan (g/L)	FSL J1-177	FSL R2-499	FSL C1-056	FSL N1-227	FSL N3-013
0	0.61±0	0.61±0	0.61±0	0.61±0	0.61±0
0.08	--	--	--	--	0.305±0.07
0.12	0.305±0	0.305±0	0.305±0	0.305±0	--
0.47	--	0.15±0	0.15±0		0.15±0
0.55	0.15±0.06				--
0.94	--	0.077±0	0.077±0	--	0.077±0
1.095	--	--	--	0.15±0.72	--
1.875	0±0	0±0	0±0	0±0	0±0

Gallic acid (g/L)					
Chitosan (g/L)	FSL J1-177	FSL R2-499	FSL C1-056	FSL N1-227	FSL N3-013
0	15±0	15±0	15±0	15±0	15±0
0.47	7.5±0	--	4.92±2.24	7.5±0	7.5±0
0.94	0±0	3.75±3.75	0.86±0.89	1.875±0	0.781±0.95
1.875	0±0	0±0	0±0	0±0	0±0

--: No inhibition observed.

Table F.2 Minimal inhibitory concentration (g/L) of gallic acid and carvacrol as a function of chitosan concentration (g/L) for reconstituted meat microbiota.

Gallic acid (g/L)					
Chitosan (g/L)	<i>Brochothrix thermosphacta</i> FUA3558	<i>Carnobacterium maltaromaticum</i> FUA3559	<i>Leuconostoc gelidum</i> FUA3560	<i>Leuconostoc gelidum</i> FUA3561	<i>Lactobacillus sakei</i> FUA3562
0		--	--	--	--
1.875	15±0	--	15±0		15±0
3.75	0±0	15±0	1.25±2.16	15±0	11.25±2.3
3.75	--	--	--	7.5±0	--
7.5	--	0	0	0	0

Carvacrol (g/L)					
Chitosan (g/L)	<i>Brochothrix thermosphacta</i> FUA3558	<i>Carnobacterium maltaromaticum</i> FUA3559	<i>Leuconostoc gelidum</i> FUA3560	<i>Leuconostoc gelidum</i> FUA3561	<i>Lactobacillus sakei</i> FUA3562
0	0.61±0	1.22±0.11	0.61±0.26	0.61±0	0.61±0
1.875	--	0.61±0.12	--	0.305±0.12	0.305±0
2.18	--	--	0.305±0	--	--
3.75	0.305±0.15	--	0.15±0.15	0.15±0.23	0.15±0
5	0	--			--
7.5	--	0	0	0	0

--: No inhibition observed.

Table F.3 Growth of a 5 strain cocktail of *L. monocytogenes* strains on the surface of cooked ham during storage at 4 °C.

Cell counts on PALCAM agar [(Log (cfu/cm ²))]								
Time (days)	Potato control	Cassava control	0.1 g gallic acid	0.3 g gallic acid	0.025 g chitosan	0.15 g chitosan	0.048 g carvacrol	0.195 g carvacrol
0	2.76±0.01	2.61±0.04	2.62±0.01	2.60±0.07	2.68±0.01	2.46±0.04	2.35±0.04	1.80±0.16
7	4.71±0.02	3.02±0.04	2.47±0.31	4.49±0.44	1.75±0.35	1.67±0.23	2.01±0.30	0.82±0.75
14	6.87±0.03	5.42±0.56	5.12±0.15	6.76±0.32	1.64±0.21	1.12±0.50	2.19±0.18	1.90±0.29
21	8.36±0.26	6.26±0.01	5.70±0.29	8.15±0.17	1.67±0.44	0.52±0.45	1.73±0.19	1.12±0.50
28	8.99±0.07	7.48±0.36	6.08±0.37	9.02±0.02	1.52±0.30	1.37±0.21	2.59±0.16	1.56±0.14

Cell counts on TSA [(Log (cfu/cm ²))]								
Time (days)	Potato control	Cassava control	0.1 g gallic acid	0.3 g gallic acid	0.025 g chitosan	0.15 g chitosan	0.048 g carvacrol	0.195 g carvacrol
0	2.67±0.04	2.64±0.03	2.73±0.16	2.67±0.05	2.66±0.28	2.43±0.08	2.29±0.11	1.88±0.07
7	4.66±0.34	3.01±0.06	2.51±0.41	4.69±0.29	1.67±0.54	1.30±0.22	1.60±0.11	0.82±0.55
14	6.91±0.04	5.43±0.17	5.20±0.27	6.29±0.03	1.70±0.38	1.37±0.39	2.18±0.08	1.92±0.11
21	8.33±0.02	6.25±0.21	5.79±0.13	8.27±0.20	1.64±0.42	1.00±0.43	1.78±0.13	1.43±0.09
28	9.00±0.03	7.53±0.31	5.76±0.51	9.02±0.13	1.52±0.30	1.37±0.21	2.63±0.30	1.70±0.17

5 strain cocktail of *L. monocytogenes* strains: FSL J1-177, FSL C1-056, FSL N3-013, FSL R2-499, and FSL N1-227.

Table F.4 Growth of a 5 strain cocktail of reconstituted meat microbiota on the surface of cooked ham during storage at 4 °C.

Cell counts on APT agar [(Log (cfu/cm ²))]								
Time (days)	Potato control	Cassava control	0.1 g gallic acid	0.3 g gallic acid	0.025 g chitosan	0.15 g chitosan	0.048 g carvacrol	0.195 g carvacrol
0	3.76±0.22	3.66±0.13	3.51±0.27	3.51±0.66	3.00±0.42	2.04±0.25	2.35±0.12	2.03±0.03
7	7.04±0.11	6.88±0.45	5.14±0.69	6.77±0.31	4.52±0.23	3.99±0.41	4.26±0.31	3.98±0.27
14	8.48±0.05	7.92±0.44	7.01±0.77	8.23±0.21	6.09±0.34	6.16±0.87	6.84±0.75	5.56±0.25
21	8.60±0.08	8.35±0.25	7.38±0.73	8.66±0.08	6.81±0.48	7.47±0.60	7.06±0.14	6.58±0.17
28	8.72±0.21	8.48±0.21	7.52±0.76	8.56±0.17	7.77±0.71	7.91±0.01	7.81±0.44	6.35±0.36

5 strain cocktail of reconstituted meat microbiota: *Brochothrix thermosphacta* FUA3558, *Carnobacterium maltaromaticum* FUA3559, *Leuconostoc gelidum* FUA3560 and FUA3561, and *Lactobacillus sakei* FUA3562 .

Table F.5 Growth of the mixture of a 5 strain cocktail of reconstituted meat microbiota and a 5 strain cocktail of *L. monocytogenes* strains on the surface of cooked ham during storage at 4 °C.

Cell counts on APT agar [Log (cfu/cm ²)]																
Time (days)	Potato control		Cassava control		0.1 g gallic acid		0.3 g gallic acid		0.025 g chitosan		0.15 g chitosan		0.048 g carvacrol		0.195 g carvacrol	
	Avg	SD	Avg	SD	Avg	SD	Avg	SD	Avg	SD	Avg	SD	Avg	SD	Avg	SD
0	4.16	0.29	4.05	0.04	3.83	0.06	4.16	0.06	2.63	0.27	2.43	0.04	2.65	0.12	2.63	0.03
7	8.12	0.06	6.22	0.29	6.12	0.03	7.96	0.62	5.82	0.04	5.72	0.36	5.26	0.31	4.98	0.27
14	9.05	0.42	8.93	0.19	7.96	0.17	9.12	0.26	7.65	0.03	7.48	0.09	7.74	0.75	6.56	0.25
21	9.04	0.09	8.97	0.37	8.10	0.68	9.03	0.25	8.00	0.26	7.52	0.26	7.26	0.14	7.08	0.17
28	9.02	0.15	8.95	0.57	8.47	0.16	9.02	0.33	7.83	0.44	7.53	0.23	8.10	0.44	6.65	0.36

Cell counts on PALCAM agar [Log (cfu/cm ²)]																
Time (days)	Potato control		Cassava control		0.1 g gallic acid		0.3 g gallic acid		0.025 g chitosan		0.15 g chitosan		0.048 g carvacrol		0.195 g carvacrol	
	Avg	SD	Avg	SD	Avg	SD	Avg	SD	Avg	SD	Avg	SD	Avg	SD	Avg	SD
0	2.75	0.26	2.72	0.05	2.66	0.01	2.72	0.06	2.08	0.10	2.10	0.52	2.14	0.05	1.80	0.40
7	4.20	0.16	3.83	0.09	2.19	0.13	4.58	0.46	2.07	0.25	1.64	0.12	2.32	0.07	1.90	0.27
14	4.74	0.09	3.66	0.55	2.37	0.29	4.92	0.31	1.70	0.30	1.37	0.47	1.78	0.13	1.52	0.20
21	4.37	0.33	3.38	0.38	1.73	0.12	4.42	0.24	2.07	0.41	1.70	0.31	2.24	0.31	2.10	0.40
28	3.99	0.04	4.22	0.49	1.52	0.64	4.17	0.06	1.43	0.38	1.88	0.35	1.94	0.16	2.12	0.44

5 strain cocktail of reconstituted meat microbiota: *Brochothrix thermosphacta* FUA3558, *Carnobacterium maltaromaticum* FUA3559, *Leuconostoc gelidum* FUA3560 and FUA3561, and *Lactobacillus sakei* FUA3562 and a 5 strain cocktail of *L. monocytogenes* strains: FSL J1-177, FSL C1-056, FSL N3-013, FSL R2-499, and FSL N1-227.

Appendix G: Nanogels loaded with essential oil for film grafting

Table G.1 The influence of polymer composition on nanogel transition temperature:

Temperature (°C)	Transmittance (%)									
	PNIPAM		PNIPAM/ PAA		PNDEA		PID 85/15		PID 50/50	
	Avg	SD	Avg	SD	Avg	SD	Avg	SD	Avg	SD
8	100.0	4.3	100.0	5.0	100.0	5.0	99.1	5.0	100.0	7.2
9	100.0	5.3	90.1	4.5	95.6	4.8	91.6	4.6	95.3	6.4
11	100.0	2.5	90.4	4.5	94.1	4.7	91.1	4.6	91.7	9.3
12	100.0	6.4	88.4	4.4	91.5	4.6	91.4	4.6	87.2	2.8
13	100.0	4.7	88.5	4.4	89.8	4.5	89.5	4.5	84.8	8.6
14	100.0	5.3	87.8	4.4	87.6	4.4	89.5	4.5	80.4	5.9
15	100.0	3.8	87.5	4.4	83.5	4.2	86.8	4.3	73.9	7.4
16	100.0	2.6	86.8	4.3	77.9	6.9	84.2	4.2	68.7	7.2
17	100.0	2.6	86.7	4.3	75.9	5.8	83.6	4.2	65.8	6.9
18	100.0	3.8	86.6	4.3	69.2	9.5	77.8	3.9	50.2	9.5
19	100.0	4.4	86.1	4.3	66.8	10.3	77.9	3.9	43.2	11.5
20	100.0	3.6	85.2	4.3	60.4	6.0	70.8	3.5	26.5	12.5
21	100.0	4.1	85.4	4.3	58.3	5.9	65.1	3.3	13.6	13.6
22	100.0	2.7	84.3	4.2	54.6	8.7	53.9	2.7	5.1	10.3
23	100.0	5.4	81.9	4.1	49.0	5.4	31.4	1.6	1.6	5.6
24	100.0	2.1	84.2	4.2	48.1	6.4	5.0	2.3	0.4	2.7
25	100.0	1.4	87.8	4.4	46.6	6.3	1.2	1.1	0.2	1.3
26	100.0	1.6	86.8	4.3	38.3	7.9	0.3	1.0	0.2	5.2
27	100.0	1.9	88.6	4.4	32.9	11.6	0.2	0.6	0.1	6.1
28	100.0	2.1	87.8	1.4	25.1	10.3	0.1	1.6	0.1	3.4
29	100.0	3.6	88.1	2.2	21.4	10.1	0.1	4.3	0.1	3.5
30	100.0	3.5	89.7	1.5	15.7	6.8	0.0	0.5	0.0	5.7
31	89.7	2.2	89.7	2.5	9.5	7.5	0.0	0.4	0.0	6.3
32	3.2	1.6	89.2	1.9	2.4	3.1	0.0	0.3	0.0	9.5
33	0.0	1.9	88.8	1.7	1.6	7.1	0.0	0.5	0.0	3.6
34	0.0	1.0	88.9	4.4	0.5	7.0	0.0	0.6	0.0	7.9
35	0.0	0.2	86.6	4.3	0.0	0.0	0.0	0.9	0.0	8.1

Avg: average; SD: standard deviation.

Table G.2 Effect of different salt ions on the LCST of copolymer nanogels in aqueous solutions: anions, and cations.

LCST (°C)							
NIPAM/NDEA molar ratio	Na ₂ CO ₃	Na ₂ SO ₄	NaCl	CaCl ₂	MgCl ₂	KCl	NH ₄ Cl
100/0	22.00±1.00	23.67±0.58	27.33±0.52	27.33±0.43	27.00±0.47	28.33±0.43	27.00±0.12
85/15	10.67±0.58	21.67±0.58	26.67±0.23	24.67±0.52	25.67±0.84	27.33±0.66	26.67±0.43
75/25	8.00±1.00	16.00±0.00	22.33±0.34	22.33±0.12	22.33±0.59	22.33±0.57	22.33±0.53
65/35	7.33±0.58	15.33±0.58	22.67±0.55	22.33±0.34	22.00±0.51	22.00±0.38	23.00±0.49
50/50	7.33±0.58	14.67±0.58	23.33±0.76	21.67±0.98	21.67±0.58	23.67±0.29	24.00±0.58

Table G.3 Thymol release behavior of polymer nanogels.

Accumulative release (%) -PID50/50 at 4 °C						
	pH=2		pH=6		pH=8	
Time (h)	Average	SD	Average	SD	Average	SD
0.5	18.23	0.91	8.39	0.34	11.27	0.45
1	35.76	1.79	14.13	0.57	18.22	0.73
1.5	53.11	2.66	17.03	0.68	21.56	0.86
2	66.03	3.30	19.70	0.79	25.05	1.00
3	85.18	4.26	25.70	1.03	27.93	1.12
4	84.67	4.23	33.95	1.36	33.45	1.34
6	92.48	4.62	41.56	1.66	41.03	1.64
8	92.18	4.61	53.37	2.13	48.78	1.95
10	92.86	4.64	66.26	2.65	57.19	2.29
12	92.30	4.61	83.46	3.34	65.51	2.62
16	92.74	4.64	83.11	3.32	74.20	2.97
20	91.53	4.58	84.44	3.38	81.50	3.26
24	92.24	4.61	86.66	3.47	83.96	3.36
48	92.28	4.61	86.65	3.47	84.76	3.39

Accumulative release (%) -PID50/50 at 25 °C						
	pH=2		pH=6		pH=8	
Time (h)	Average	SD	Average	SD	Average	SD
0.5	8.39	0.34	27.67	1.11	34.67	1.04
1	14.13	0.57	24.24	0.97	59.28	1.78
1.5	17.03	0.68	53.42	2.14	77.04	2.31
2	19.70	0.79	76.66	3.07	91.81	2.75
3	25.70	1.03	79.34	3.17	92.79	2.78
4	33.95	1.36	78.84	3.15	92.89	2.79
6	41.56	1.66	96.94	3.88	96.58	2.90
8	53.37	2.13	97.04	3.88	98.15	2.94
10	66.26	2.65	96.72	3.87	99.46	2.98
12	83.46	3.34	96.00	3.84	99.01	2.97
16	83.11	3.32	96.36	3.85	99.69	2.99
20	84.44	3.38	97.92	3.92	97.10	2.91
24	86.66	3.47	98.79	3.95	97.02	2.91
48	86.65	3.47	97.94	3.92	97.18	2.92

Avg: average; SD: standard deviation.

Accumulative release (%)-PID50/50 at pH 6						
Time (h)	T=4 °C		T=15 °C		T=25 °C	
	Average	SD	Average	SD	Average	SD
0.5	33.17	1.00	34.67	1.04	28.51	0.86
1	59.17	1.78	59.28	1.78	60.48	1.81
1.5	86.94	2.61	77.04	2.31	69.25	2.08
2	97.96	2.94	91.81	2.75	71.51	2.15
3	97.84	2.94	92.79	2.78	73.59	2.21
4	97.24	2.92	92.89	2.79	92.60	2.78
6	93.15	2.79	96.58	2.90	93.15	2.79
8	94.35	2.83	98.15	2.94	94.31	2.83
10	96.29	2.89	99.46	2.98	95.17	2.86
12	94.03	2.82	99.01	2.97	93.30	2.80
16	92.29	2.77	99.69	2.99	90.95	2.73
20	91.64	2.75	97.10	2.91	91.06	2.73
24	94.69	2.84	97.02	2.91	94.83	2.84
48	95.74	2.87	97.18	2.92	94.72	2.84

Avg: average; SD: standard deviation.